

学位論文

Geometrical approaches to defect operators in
the class S theories

(クラスS理論における欠陥演算子への幾
何学的アプローチ)

平成28年12月博士（理学）申請

東京大学大学院理学系研究科

物理学専攻 渡辺 伯陽

Abstract

In the context of class S theories and 4D/2D duality relations there, we discuss the skein relations of general topological defects on the 2D side which are expected to be counterparts of composite surface-line operators in 4D class S theory. Such defects are geometrically interpreted as networks in a three dimensional space. We also propose a conjectural computational procedure for such defects in two dimensional $SU(N)$ topological q -deformed Yang-Mills theory by interpreting it as a statistical mechanical system associated with ideal triangulations.

Contents

1	Defects in QFTs	10
1.1	The brief taxonomy of defects	10
1.2	Wilson-'t Hooft loops	15
2	Class S description	27
2.1	5D Super Yang-Mills viewpoint	29
2.2	Codimension two defects	33
2.3	Branch dimension analysis	41
2.4	Examples of class S theories	42
3	Superconformal index and 2D q-deformed Yang-Mills	50
3.1	State-operator correspondence	50
3.2	General definition	53
3.3	Reduced SCIs	59
3.4	4D $\mathcal{N}=2$ superconformal indices	61
3.5	4D/2D duality : class S Schur indices and 2D q -deformed Yang-Mills correlators	70
3.6	Concrete computations from 2D q -deformed Yang-Mills theory	73
3.7	Defect indices	78
3.8	2D topological q -deformed Yang-Mills theory	78
4	Geometrical Eyes on Class S Defects	82
4.1	Loop operators in 4d and skein relations in 2d	84
4.2	Networks and skein relations in 2d	86
4.3	Wilson punctured network defects in 2D and composite surface-line systems in 4D	100
4.4	Coexistence of closed networks and isolated punctures	109
4.5	Proposal of conjectural formula for Wilson punctured network defects in 2D q -deformed Yang-Mills	113
5	Return to SCIs and skein relations	123
5.1	Schur indices with line defects	123
5.2	New kinds of skein relations	132

5.3	Networks for $\mathcal{N}=4$ Yang-Mills	137
5.4	Examples of OPE and charge/network dictionary	147
5.5	General charge/network correspondence	153
6	Conclusion : summary and discussions	156
A	Lie algebra convention	160
A.1	A-type Lie algebra convention	160
A.2	$\mathfrak{so}(8)$ convention	162
A.3	$\mathfrak{so}(4)$ convention : the four vector and spinors	164
B	Superconformal algebra	165
B.1	4D SCA	165
C	Formulae for SCI	176
C.1	Symbols used in SCI	176
D	Orbit of simple Lie algebra	179
D.1	Semi-simple orbit	180
D.2	Nilpotent orbit	181
D.3	Induced orbit	182
E	More mathematics on the dual model	185
E.1	Definitions	185
E.2	Convenient formulae	187
E.3	Derivation of several skein relations	188
F	Seiberg-Witten curve and Gaiotto duality	191
F.1	Gaiotto duality	191
F.2	Gaiotto curve from the Seiberg-Witten curve	195
F.3	Classification of punctures	205
F.4	Class S construction	214
G	Drukker-Morrison-Okuda's correspondence	217
G.1	Possible set of loop operators	217
G.2	Construction of the one-to-one map	218

Introduction

The quantum field theory [1–3] has long history and has made great successes not only in the particle physics but also in the condensed matter physics, for example. Among several kinds of field theories, in particular, conformal field theories (CFTs) [4] and gauge theories are so powerful to make themselves predictive based on their symmetry constraints. Even recently, there are many progresses in them such as conformal bootstraps [5,6] and reformulations of gauge theory scattering amplitudes [7–10]. One of the motivations of these researches is the new reformulation of the old style QFTs based on Lagrangians or path integrals. Actually, CFTs can be defined with only the flavor symmetry and the operator product expansions (OPEs), namely, three points correlators of primary fields. In gauge theory, the computations of amplitudes are very hard tasks compared to their simplicities of final results [11].

From the purely theoretical viewpoint, topological field theories (TQFTs) and supersymmetric theories [12] are more powerful and, indeed, have provided us many ways to understand what “quantum field theories” are and many aspects of them, such as anomaly, non-perturbative effects (confinement, chiral symmetry breaking) and dualities although they are less phenomenological. Notice that the dualities of (supersymmetric) gauge theories are marvellous phenomena that two different Lagrangians describe the same physics, in many cases, in the infra-red (IR) fixed point. Furthermore, the combination of supersymmetries and conformal symmetry produces more interesting class called superconformal field theories (SCFTs). These theories naturally appear in superstring theories. For examples, the world sheet theories are superconformal. In the original and simplest example of the AdS/CFT correspondences [13], the 4D field theory (CFT side) is a SCFT known as 4D $\mathcal{N}=4$ super Yang-Mills theory. In this thesis, SCFTs are main targets and, in particular, we focus on a part of 4D $\mathcal{N}=2$ SCFTs called class S theories [14–16].¹⁾ In many case, they have no known Lagrangian descriptions but several properties of these theories are determined by using string dualities and symmetry constraints. Surprisingly, some other types of QFTs, that is to say, non-SUSY 2D CFTs or 2D TQFTs show up in this context and these totally different theories describe the (BPS) observables of the 4D SCFTs. We refer to this phenomenon as the 4D/2D duality relation [17,18]. The details of this marvellous duality relation are remarked later.

Although this relation is limited, this offers new approaches to these Lagrangian un-

¹⁾The letter “S” comes from “Six-dimension” because they are defined as the dimensional reduction of special 6D theories usually referred to as 6D $\mathcal{N}=(2,0)$ SCFTs.

known theories. Furthermore, this relation is still relevant for gauge theories with Lagrangians. Some string theory's brane constructions of gauge theories [19, 20] make both reasons clear. The most important observation in these constructions is that several non-trivial dualities of some gauge theories are explained as some geometrical equivalences in the stringy set-ups. For example, the famous Montonen-Olive duality ($\mathcal{N}=4$ S-duality) [21] which exchanges the role of electric particles and that of magnetic particles is geometrically understood as the exchange of two different cycles of a 2-torus [22]. This suggests that the dualities of gauge theories maybe beyond the QFT frameworks at this stage can be naturally understood in terms of geometrical viewpoints. In addition, this viewpoint is independent of the existences of the Lagrangians. And these geometrical realizations are directly encoded in these 2D theories of the above 4D/2D duality relation. That is why we consider this 4D/2D duality relation as some clues to discuss Lagrangian unknown theories and still a valid method to understand gauge theory dualities.

However, there are another relevant objects in this thesis : defects. Although we have no unified definitions of defects and, instead, discuss the characterization of them in Chapter 1, we give a concept for them here. Roughly speaking, defects are some regions in space-time where the physics is different from that at bulk to some extent. The terminology also means the physics there. For example, the boundaries of the space and boundary conditions there are defects in this sense. As you see from this simple example, defects are not minor but seems to be common objects in physics. Other interesting aspects of defects not discussed in this thesis are the roles of order parameters of phases. The most famous examples are Wilson loop operators [23]. Intuitively speaking, they just insert a non-dynamical electric particles, namely, heavy quarks and see their responses in the free energy, for example. Their behaviours at a large loop limit measure the force or the potential energy between two heavy quarks and, in some cases, determine the gauge theory phase (Coulomb, Higgs and confinement).

Defects are common and important concepts in the string theory, in particular ,branes too. Recall that the branes have the following aspects. They can arise as the boundaries of fundamental strings or other branes and also naturally show up as the dynamical solitons in string theory [24]. And the effective theories of the (BPS-)branes are (supersymmetric) gauge theories in the simple set-ups. Therefore, the natural objects can be described by the boundaries of those effective theories. In other words, the sting theory offers several viewpoints on the defects of gauge theories and, conversely, the field theories describe the dynamics of branes in the string theory. They play the role of a bridge between these totally different theories.

Now that we see that the defects are important in understanding the frameworks of QFTs and the string theory. The works discussed in this dissertation are motivated by the following questions:

- In general, QFTs allow the existence of defects but how can we characterize them ?
In particular, how can we study the defects in the Lagrangian unknown theories ?
- If they are defined once, how can we compute the spectrum ?

Here recall the previous idea : some aspects of special field theories, regardless of whether or not they have some Lagrangians, are geometrically described. This relation is expected to be also applied to the defects without exceptions and, indeed, turned out to hold true based on several observations [25–28] for examples. This is the starting point to answer the above questions.

Let us review the developments of the defects in the context of class S theories and 4D/2D duality relations there.

First of all, see the above story in detail. The field theories we would like to analyze are interacting superconformal field theories called “class S theory” which are obtained as twisted compactifications of the 6d $\mathcal{N}=(2,0)$ SCFTs on Riemann surfaces C with punctures.²⁾ Interestingly, even though almost all of the SCFTs have no definition based on the Lagrangians, some of their BPS observables have been evaluated assuming the dualities following their geometrical constructions. In particular, for theories with $\mathcal{N}=2$ Lagrangian descriptions, their partition functions on the squashed four-sphere S_b^4 [29, 30] and the superconformal indices (SCIs) [31] (in the Schur limit) or equivalently partition functions on $S^1 \times_q S^3$ [32] were computed. Based on their explicit expressions, it was recently suggested that many class S theories beyond the Lagrangian definition³⁾ have alternative effective descriptions by some 2D theories : Liouville/Toda CFTs for S_b^4 case [17, 38] and 2D topological q -deformed Yang-Mills for $S^1 \times_q S^3$ case [18, 39, 40]. In particular, the conjectural SCI expression of the (non-Lagrangian) Argyres-Seiberg dual theory [41] for $SU(3)$ $N_f = 6$ superconformal QCD was obtained using the inversion formula [18]. Indeed, in addition to the partition functions, these 4D/2D dualities also offer new geometrical descriptions of supersymmetric defects in such SCFTs, which are main subjects of this thesis.

Let us focus on the 4D gauge theory at first. As basic objects, there are supersymmetric Wilson-’t Hooft line operators [23, 42–49].⁴⁾ They are one-dimensional objects, *loops* in 4D and the natural extensions of Wilson loop operators by replacing the electrically charged particles (quarks) by both electrically and magnetically charged heavy probes (dyons). As another generalization of loop operators, there are half-BPS surface operators [50–56]. They are two-dimensional objects in 4D. They correspond to the insertions of heavy string-like objects (for instance, cosmic strings [57]) or some non-dynamical vortex. Here we quote a fact that 6D $\mathcal{N}=(2,0)$ SCFTs have codimension-two defects and codimension-four defects. Then, before the dimensional reduction via C (a punctured Riemann surface), both loops and surface operators are expected to be some codimension four defects.⁵⁾ Equivalently speaking, both defects come from codimension-four defects

²⁾The punctures correspond to the codimension two defects in 6D as explained in Chapter. 2 and Appendix. F.

³⁾In this thesis, we focus on the Riemann surface compactifications with more than two regular punctures and no irregular ones. There are generalized proposals for non-SCFTs and Argyres-Douglas theories which need such irregular punctures [15, 33–37].

⁴⁾Throughout this thesis, we use the words *defects* and *operators* interchangeably. We also use *loops* and *lines* interchangeably although there are subtle differences.

⁵⁾Precisely speaking, some surface operators can also come from codimension-two defects in the 6D

appearing in 6D $\mathcal{N}=(2,0)$ SCFTs and both have the same origin in 6D. Notice that 4D loop defects and 4D surface defects look like codimension-one defects and local defects on the 2D side, respectively. Their appearances in those 2D theories on C look totally different. See Fig. 1.

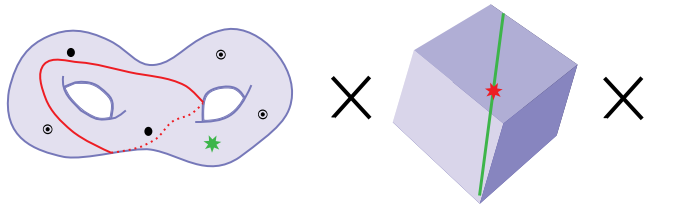


Figure 1: By starting the 6D $\mathcal{N}=(2,0)$ SCFT, after the twisted compactification by C , we have some 4D $\mathcal{N}=2$ theory according to the choice of C and types of punctures on it. On the other hand, reduced onto C , some 2D theory lives on C . We have a decomposition $6 = 4 + 2$. Strictly speaking, they capture only BPS sectors of the 4D theory. In this set-up, we can add codimension four defects in 6D (= two dimensional surfaces). There are at least two ways of reductions: $2 = 1 + 1$ (red) or $2 = 2 + 0$ (green). The first case is 4D loop defects and the latter is 4D surface defects.

Let us focus on the 2D theory. The 4D loop operators correspond to Verlinde network operators/Wilson network operators in the Liouville-Toda CFTs/ q -deformed Yang-Mills theories, see [25, 62–64] for the geometrical viewpoint, [26–28, 65–68] for the Verlinde network and [69–75] for the Wilson network. On the other hand, the 4D surface operators are mapped into (fully degenerate) vertex operators/difference operators in the CFTs/Yang-Mills theories, see [26, 28, 76] and [55, 77–81]. Geometrically, they can be represented as special punctures on the Riemann surface in both the set-ups. These works seem to give the answers to the above questions. However, they are far from the complete answer. One of the reasons is that they discuss only $SU(2)$ gauge theories and some special cases of $SU(3)$ type theories at most. Our work [75] provided the extension to general $SU(N)$ -type theory.

The key concept in this work is the class S skein relation. To explain that, we regard the above 4D/2D duality relation as follows. This duality relates the charge of 4D loops and the network geometry in 2D and, naïvely, it is expected that this correspondence is one-to-one. However, this is not true actually and the map is many-to-one, that is to say, there are infinitely many networks to give the same 4D loop operators. In this thesis, we view the skein relations as the equivalence relations. See Chapter. 4 as for the more precise definition and their concrete examples. Among the skein relations, there is a special class of skein relations called crossing resolutions. This relation connects the OPEs of loop operators in 4D and the resolutions of all crossings between networks in 2D. We found that these relations naturally coincide with those already well-known in mathematics. We do many consistency checks that this conjecture is true in Chapter. 4 and 5.

theory [58–61]. However, we do not pay attentions to them in this thesis.

At this stage, there appear no surface defects. Let us consider a situation in which both line operators and surface operators coexist [82]. A key observation to describe their skein relations on the geometrical side as follows. On both the Liouville/Toda CFT and the q -deformed Yang-Mills theory, the concept of crossings of networks exists and, in fact, they correspond to the ordering of corresponding half-BPS line operators in one space direction determined by the unbroken supersymmetry in 4D gauge theory [48, 49, 75, 83]. Then, the existence of crossings among several networks suggests that there is a hidden direction which is exactly identified with one of physical directions on the 4D gauge theory side. ⁶⁾ In other words, there appears a three dimensional geometry combined with the 2D space C and one of 4D directions which is determined by the unbroken supersymmetry for the half-BPS loop operators. This is the more familiar story in RCFTs whose conformal blocks are the wave functions of the corresponding 3D Chern-Simon theories [84, 85]. See also [86, 87] as for Verlinde loop operators in the Liouville CFT. We must note that the closer story exists for q -deformed Yang-Mills theory [74, 88, 89] but we do not know the precise relation between two systems. When we recall that the expectation values of BPS loops are independent of the positions on that direction [30, 48, 49, 83], it is natural to speculate that the networks are still topological in the new geometry. In this new three dimensional geometry, codimension four defects are expressed as knot with junctions and both surface defects and line defects are on the same ground. We refer the corresponding defects in the q -deformed Yang-Mills theory to as “punctured networks”. This discussion is the half story of our paper [90] and shown in Chapter. 4.

Once we have understood the geometrical relations on the 2D side, we go to the second question before : How to compute the correlators for the given general network defects in the 2D q -deformed Yang-Mills theories ? ⁷⁾ Naively speaking, it seems to be enough to replace ordinary Lie groups by “quantum group” as gauge groups at mathematical level. Indeed, the rigorous definition of Wilson loops without junctions in that case was given in [73] based on quantum groups, but its extension to any networks is not obvious yet for several reasons. Furthermore, even if it can be well-defined, it is not useful for the actual computations because it needs the general invariant tensors in the quantum group sense. Instead of giving rigorous definitions, we will propose the direct procedure to obtain the conjectural expressions in Chapter. 4 and apply them to many examples in 5. This is based on the other half of the paper [90] mainly.

Finally, we make a few comments on the applications of the skein relations. The first concerns the dyonic loop operators of $\mathcal{N}=4$ $SU(N)$ Yang-Mills theory. From the 4d gauge theory perspective, their classification was performed in [44]. When the electric charge and the magnetic charge of a dyonic loop are parallel in the weight system, there is an obvious realization of such dyonic loop in the class S language as a loop wrapping the torus. When they are not parallel, it was expected that they are represented by networks on the torus. We will give a complete description in the case of $SU(3)$. Later,

⁶⁾If we replace the 4-manifold on which the gauge theory is defined by the squashed 4-sphere S_b^4 , there are locally two such directions which are exchanged under the flip from b to b^{-1} [30]. Here we focus on either direction.

⁷⁾See [68] for the Verlinde networks.

we discuss the extension to general $SU(N)$ cases. The other is proposals of new kinds of skein relations. This work is based on [91].

The organization of this dissertation is following: In the chapter. 1, we see what defects are and their examples briefly. In Sec. 1.1, we summarize the author's viewpoint on the notion of defects. In Sec. 1.2, we introduce the 4D Wilson-'t Hooft loop operators which are important class of loop operators if we have some gauge theory Lagrangian description. In the chapter. 2, we review the main set-ups called the class S theories which are 4D $\mathcal{N}=2$ theories obtained by the 6D $\mathcal{N}=(2,0)$ theory compactifications. Notice that Appendix. F is the complement of this chapter. In Sec. 2.1, we provide another approach to analyze the class S theories. In Sec. 2.2, we discuss the analysis on the 6D codimension two defects and see their important consequences about the dimensions of moduli spaces are shown in Sec. 2.3. In 2.4, we see the several class S theory examples needed for later arguments. Notice that there is a bit argument not explicitly discussed before as we know

After the set-ups are explained, we move on to the observables called the superconformal indices (SCI) and its relations to TQFTs in the chapter. 3. In Sec. 3.1, we discuss the state-operator correspondence and then in Sec. 3.2, we define the SCI and explain their properties. In Sec. 3.3, we make a brief comment on the poles of SCI. In Sec. 3.5, we state the 4D/2D duality relations between the class S Schur indices and 2D topological q -deformed Yang-Mills theory and check them for free hypermultiplets in Sec. 3.6 which includes a discussion explicitly written nowhere before. In Sec. 3.7, we briefly comments on the SCI in the presence of defects. Finally, we briefly review the necessary facts about 2D q -deformed Yang-Mills in Sec. 3.8.

The central works done by author originally are written in chapter 4 and 5 mainly. The chapter. 4 is main subject in this thesis. The first two chapters are based on [75] and all sequent sections on [90]. In Sec. 4.1, we review the 4D physical interpretation of crossings of networks on the 2D side and make the dictionary between 4D and 2D. In Sec. 4.2, we discuss the geometrical descriptions, namely, skein relations. We see there they are equivalent to those already known in mathematics. In Sec. 4.3, we introduce the new definitions of defects in the 2D topological q -deformed Yang-Mills theory, what we call, Wilson punctured network defects. We explain their 6D viewpoint. Sequentially, in Sec. 4.4, we translate these results into the language of q -defomred Yang-Mills correlators or their operator actions. In Sec. 4.5, finally, we propose the new conjectural formula to compute their correlators.

The sequent chapter. 5 focus on the applications of the results in the previous chapter. Sec. 5.1 includes both the result in [90] and unpublished results. There we exhibit many computations of Schur indices based on the conjectural formula and see the results support it conversely. In Sec. 5.2, we propose the new kinds of skein relations which means that they include 6D codimension two defects. In Sec. 5.3 and Sec. 5.5, we apply the skein relations to see the charge/netwrok correspondence which is the 4D/2D duality relation for 4D loop operators and 2D networks, in particular, when some gauge theory Lagrangian exists. In Sec. 5.4, we exhibit several examples in the 4D $\mathcal{N}=4$ $SU(N)$ super Yang-Mills theory.

Throughout this thesis, we use several conventions on the expressions of irreducible representations. In particular, we summarize several basis of weight vectors and some formulae about them in Appendix. A.

Chapter 1

Defects in QFTs

In this chapter, we give our perspectives on defects in QFTs. In Sec. 1.1, we classify the defects from the dimensional viewpoint at first and in terms of the characterizations. In many cases, these characterizations are related each other but we do not discuss this point in this thesis. Notice also that these viewpoints are far from complete classifications. In Sec. 1.2, we focus on the special well-known defects called 4D Wilson-'t Hooft loops which we will use in the later chapters.

1.1 The brief taxonomy of defects

In this section, we use some examples of defects without detail definitions. See Sec. 1.2 as for Wilson-'t Hooft loops.

1.1.1 Dimensional viewpoint

First of all, defects can be categorized according to the dimensions or the codimensions of their locus. Let us consider four cases below.

The dimension zero defect are just local operators. We usually compute the correlation functions of these local operators. The dimension one defects are loop / line operators. The 4D Wilson-'t Hooft loop operators are such examples. In 3D, there are Wilson loops and vortex loops [92]. The dimension two defects are called surface defects [50]. If we have a two-form Abelian gauge field, they can couple to surfaces as the extension of Wilson loops. These are sometimes called Wilson surface operators. The dimension three defects are volume defects.

The other characterization is the codimension. The codimension four defects are realized as non-dynamical instanton [93]. The codimension three defect includes the monopole operator for example. The above Wilson-'t Hooft loops are such examples in 4D. The codimension two are some vortex like operators. In 4D, these are just the surface operators. In this thesis, we focus on this type of operators in Appendix. 2. The codimension one defects are domain walls [94–96]. Formally, we can consider codimension zero, namely, “full filling” defects. These defects just induce the new matters in the bulk.

If some Lagrangian descriptions, they just add some new Lagrangian to the original Lagrangian. The codimension two defects in 6D localized at the 2D Riemann surface in the class S story are such defects for the 4D theories after the compactification.

More precisely, defects with different dimensions can couple each other. In particular, some d -dimensional defects with some boundaries can be attached to by some $(d - 1)$ -dimensional defects. The first examples are open Wilson lines. When a Wilson open line operator in the representation R is put on, to make it gauge invariant, we must attach some local operators $q_R(x)$ at the ends like

$$W_R([b, a]) = q_R^*(b)P \exp \left[\int_a^b \rho_R(A) ds \right] q_R(a) \quad (1.1.1)$$

where ρ_R is the representation map from \mathfrak{g} to the endomorphism of the dim R representation vector space and q_R transforms as the representation R .

The second examples are open surface operators.

$$\exp \left[\int_S B \right] \exp \left[\oint_{\partial S} A \right] \quad (1.1.2)$$

where S is an open surface and B and A are some 2-form and 1-form gauge fields, respectively. A TQFT called BF theory has this kind of operators [97, 98].

The third examples are the interfaces between different defects. The composite surface-line system we consider in Chapter. 4.3 is such an example. This system is expected to be realized as the surface defect on which some interface exists. It is possible to consider two kinds of surface defects glued along their boundaries. As briefly remarked later, we can view this as two 2D systems with different gauge groups or matters coupled through an interface. The S-duality wall in 4D $\mathcal{N}=4$ SYM is also such an example [28, 95, 96].

1.1.2 Characterization of defects

The important and interesting properties of defects are that they can be characterized in several ways. We briefly see this below. Notice that they are sometimes equivalent in the sense that they flow to the same object in the IR.

In particular, we focus on the (super)conformal theories because any defect is expected to be introduced at the UV CFT. We assume that the bulk β function (at least far away from the defects inserted regions) is free from defects insertions except full filling defects. In other words, the systems still remain conformal. We call such defects conformal defects. If the system enjoys supersymmetry, the defects break it because the supersymmetry generators lead to the space-time translational generators some of which are broken in the presence of defects. However, in many cases, it is possible to consider the defects preserving some of supersymmetry generators. We also call such defects BPS defects. In this thesis, we only treat the maximally supersymmetric ones in 4D $\mathcal{N}=2$ systems and they are usually called half-BPS defects.

defects as general boundary condition

The original definition of defects introduced by 't Hooft [42] is the imposition of singular boundary conditions on dynamical fields. We show two important examples in this thesis : Gukov-Witten type surface defects [50], namely, codimension two defects and 't Hooft loop defects. See Sec. 1.2.2 for the definition of Wilson-'t Hooft loops.

The UV 't Hooft loops [44] are defined by requiring the boundary condition

$$F \sim Bd\Omega_{S^2} \quad (1.1.3)$$

around a locus at which the loop inserted.¹⁾ $d\Omega_{S^2}$ is a volume two-form on S^2 linking the loop by one. Notice that the magnetic charge arising from the loop $\int_{S^2} F$ is quantized. At the topological level, this charge corresponds to the first Chern class of the gauge bundle or an element of $\pi_1(G)$ [42].

In the case of the Gukov-Witten type surface defects, we require the boundary condition like

$$A \sim \alpha\theta \quad (1.1.4)$$

where θ is the coordinate of S^1 which links with the surface defect locus. The holonomy around the surface defect is given by $\oint_{S^1} A = 2\pi\alpha$ where α is not quantized. And the topological charge is given by $\pi_0(G)$ which is trivial in usual cases.

defects as coupled theory

The second definition is the most practical one, at least, in the many supersymmetric gauge theories, where their partition functions can be computed by the localization methods.

This concept is well-discussed in [94, 95], [50] for example. Let us consider a theory with defects on which some lower dimensional field theory lives. The formal computation of partition function of the composite system is given by

$$Z_{\text{coupled}}[x_{\text{others}}^{\text{bg}}] = \int \mathcal{D}X Z_{\text{bulk}}[X] \mathcal{D}Y_M Z_{\text{defect}}[Y_M] \delta(X|_M - Y_M) \quad (1.1.5)$$

where X represents some bulk fields and Y_M does all fields on defects M . After the coupling, they are gauged if they are background gauge fields on the defects.

Notice that the delta function comes from the integration over some auxiliary field \mathcal{J} coupled to both X as

$$\delta(X|_M - X_M) \sim \int \mathcal{D}\mathcal{J} e^{\int d^D x \delta(M) \mathcal{J} \cdot (X|_M - X_M^{\text{bg}})}. \quad (1.1.6)$$

¹⁾We ignore the regularization or counter terms in this thesis. In the localization computation, they are needed [46].

More generally speaking, when we have D -dimensional (S)CFT with the global symmetry G_{bulk} and p -dimensional (S)CFT with the global symmetry G_{defect} , by gauging some H satisfying $G_{\text{bulk}} \supset H \subset G_{\text{defect}}$ and being non-anomalous, we have new system with flavor symmetry $F_{\text{bulk}}^{Dd} \times F_{\text{defect}}^{pd}$ where each F is the commutant group of H in each G . We call such set-ups Dd - pd coupled systems.

In particular,

$$Z_{\text{coupled}} = \int \mathcal{D}V Z_{\text{bulk}}[V] Z_{\text{defect}}[V_M] \delta(V|_M - V_M) \quad (1.1.7)$$

where Z_{bulk} includes the contribution of the gauge field or the vector multiplet V . This perspective is natural in terms of D-brane construction, see [99, 100] for example.

The concrete examples of this kind of systems are following : 4d-2d system [54, 55, 76, 101] ($\mathcal{N}=2$ and $\mathcal{N}=(2, 2)$) [102] ($\mathcal{N}=1$ and $\mathcal{N}=(2, 0)$), 4d-3d system [94, 95] ($\mathcal{N}=4$ and $\mathcal{N}=4$), 4d-2d-0d system [103] (In 4d $\mathcal{N}=2$, there are two kinds of 2d $\mathcal{N}=(2, 2)$ systems and 0d $\mathcal{N}=4$ QM appears at their intersection), 3d-1d system [104] ($\mathcal{N}=4$ and two kinds of $\mathcal{N}=4$), 5d-3d system [105–107] ($\mathcal{N}=1$ and $\mathcal{N}=4$), 5d-3d-1d system [108] (strictly speaking, not analyzed as coupled systems), 5d-1d [93].

defects as varying parameters

The third characterisation of defects is valid in some IR theories into which some UV theory flows after relevant perturbations. The idea is simple as follows [26, 50].

Let us consider a space-varying classical background of a field with characteristic scale ℓ at UV CFT. After flowing at the energy scale $\frac{1}{L} \ll \frac{1}{\ell}$, we have the lower dimensional region where the background field dramatically changes. In the deep IR, we may identify this as some defects. By regarding a physical parameter as the vacuum expectation value of a dynamical field, it is possible to replace it by the physical parameter in the above discussion.

Let \mathcal{P} be a parameter space or a classical vacuum manifold. Now, we have a map

$$\text{Map}(M \rightarrow \mathcal{P}) \quad (1.1.8)$$

where M be some space-time manifold. In the long distance limit, the map may have some dramatically changed regions which are identified as defects. Recall that the disconnected part of the space of maps corresponds to the topological sector of field configurations. Therefore, in some cases, we can regard some defects as the IR limit of heavy topological solitons.

These viewpoints sometimes provide new ways of computations of the corresponding correlators. The most successful story was did in [77] and they add a bi-fundamental hypermultiplet and, by giving variant VEVs to it, construct a $\mathcal{N}=(2, 2)$ vortex in 4D $\mathcal{N}=2$ systems which flows to an IR surface defect. They found this operations results in the actions of difference operators on the superconformal indices.

In this thesis, in particular, in Sec. 4.3, we view 4D line defect coupled to the 2D surface defect as the 2D interface. Let us discuss this perspective. There, \mathcal{P} is a Riemann

surface C in the class S theory. By recalling that the brane construction of the $\mathcal{N}=(2,2)$ surface defects [26] on which some 2D $\mathcal{N}=(2,2)$ system lives [109], we can expect the local coordinate is identified with the 2D complexified FI parameters. It is considered that \mathcal{P} is some parameter space of surface defects in the corresponding 4D $\mathcal{N}=2$ systems determined by C . M is the 2D surface defect in this case (not \mathbb{R}^4) because we would like to consider the interface on it. Furthermore, we may reduce one of directions along the interface will extend. Now, a map from \mathbb{R} or S^1 (one of 4D directions) to C (2D space) appears and we can view this as an orbit in $\mathbb{R} \times C$ or $S^1 \times C$. This is the background idea in Sec. 4.3 where S^1 is just the Hopf fiber direction there.

The related simple example is the Abelian Wilson loop in two dimension. Let η be a 2D FI parameter and varies as one direction denoted by x^1 as follows;

$$\eta(x^1) = \pi \left[1 + \tanh \left(\frac{x^1 - a}{\ell} \right) \right]. \quad (1.1.9)$$

If we take the IR limit $\ell \rightarrow 0$,

$$\eta(x^1) \longrightarrow 2\pi\theta(x^1 - a). \quad (1.1.10)$$

Now, we have the FI coupling

$$\frac{1}{2\pi} \int \eta F = -\frac{1}{2\pi} \int dx^0 \int dx^1 \partial_1 \eta(x^1) A_0 = - \int dx^0 A_0(x^1 = a). \quad (1.1.11)$$

where we assumed $A(x^0 = \pm\infty) = A(x^1 = \pm\infty) = 0$. This is exactly the 2D Wilson loop. The higher dimensional extension is also possible by introducing the electric surface operator.

The other example is the Abelian Higgs model just discussed above in the construction of the 2D surface defects in the 4D.

defects as probe

The fourth definition is also related to the previous viewpoints : just addition of some probes. For example, the Wilson-'t Hooft loops are abstractly viewed as non-dynamical (heavy) dyonic particles. At least, for the Abelian Wilson loops, this is realized by adding the interaction terms $j(x)A(x)$ to the Lagrangian where $j(x) = \delta(\gamma)$ is a $(D-1)$ -form which is Poincaré dual to the loop γ .

defects as representation of symmetries

The final viewpoint is just characterization by the representations of the conformal symmetry and the flavor symmetry. This is powerful in the sense that the form of correlation functions are constrained. Any local operator in CFT is such example.

The flat D -dimensional Euclidean CFT has $SO(D+1,1)$ conformal symmetry and global symmetry F and any local operator belongs to a unitary representation of $SO(d+$

$1, 1) \times F$. In 2D CFT, the boundary conditions in RCFT are determined [110, 111]. Some recent progresses have been done in the conformal bootstrap developments. In particular, by analysing the conformal quadratic Casimir equation, they discuss the conformal block in the presence of defects [112, 113].

1.2 Wilson-'t Hooft loops

In this section, we define the Wilson-'t Hooft (or dyonic) loop defects following [44].

1.2.1 Wilson network defects

First of all, let us define the Wilson loop operator. This just inserts the factor

$$W_R(\gamma) := \text{Tr}_R \left[P \exp \left(i \oint_{\gamma} A \right) \right] \quad (1.2.1)$$

for the real gauge field A and the closed path γ .

Next, we extend these Wilson loops to networks. To see that these objects are also physically natural, let us interpret the ordinary Wilson loop cases in terms of the probe descriptions.

In the Abelian gauge theory, the insertion of the q charged Wilson loop along φ corresponds to the addition of the following term to the Lagrangian

$$q \int_{\varphi} ds A_{\varphi} = q \int d^d x \delta(\varphi) A \quad (1.2.2)$$

where s is one parameter coordinate along φ and A_{φ} is the pull-back of A onto φ . In the non-Abelian case, this probe looks like a heavy quark.

Now, let us take φ to be the trajectory of a pair of quarks in a creation-annihilation process. T and L are the process time interval and the average of space separation length respectively. Roughly, the logarithm corresponds to the potential energy between quarks

$$\frac{1}{T} \log(\langle W_R(\gamma) \rangle) \sim V_{M_{RR^*}}(L). \quad (1.2.3)$$

Since the Wilson loop measures an effective potential energy of a meson, it is possible to define the counterpart for hadrons. The trajectory of three bound quarks is a graph consisting of three open edges $\varphi_1, \varphi_2, \varphi_3$ and two trivalent junctions (Fig. 1.1):

$$W(\{\varphi_1, R_1; \varphi_2, R_2; \varphi_3, R_3\}) = \text{Inv}_{\mathbf{1}_i: R_1 \otimes R_2 \otimes R_3} [U(\varphi_1)U(\varphi_2)U(\varphi_3)] \quad (1.2.4)$$

where R_1, R_2 and R_3 are representations of \tilde{G} satisfying that $R_1 \otimes R_2 \otimes R_3$ includes trivial one $\mathbf{1}$.²⁾

²⁾If there is multiplicity, we must attach the information of the choice of the invariant tensors or the projections to each junction.

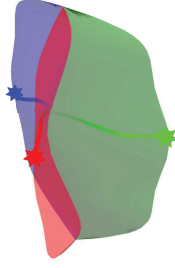


Figure 1.1: The Wilson network operators.

1.2.2 Wilson-'t Hooft loop

Although the original definition of 't Hooft operators was given in [42], we adopt a more refined definition following [44]. Their supersymmetric cases are discussed in [45] and some following papers.³⁾ In this section, we do not require any supersymmetry but introduce scalars which will be a complex scalar in a ($\mathcal{N}=2$) vector multiplet.

Especially, we consider maximal symmetric class of the loop operators. This means that the loop defects break the full conformal isometry into the stabilizer subgroup maximally preserving their locus, namely, $SO(3) \times SL(2, \mathbb{R})$. This is the same for the boundary in 2d CFTs. In fact, we can conformally map this geometry $\mathbb{R} \times \mathbb{R}_{\geq 0} \times S^2$ into $\mathbb{H} \times S^2$ which have the common isometry group.

Monopole background

Let us first analyse what boundary condition preserving the maximal isometry is allowed in the Abelian case. Then, we generalize this result to non-Abelian case.

For a field strength $F \in \Omega^2(\mathbb{R}^{1,3} \setminus (\mathbb{R} \times \{0\}))$ where $\mathbb{R} \times \{0\}$ is the loop/line operator locus the $SO(3)$ -invariance requires

$$\mathcal{L}_{L_i} F = 0 \quad \text{for } i = 1, 2, 3 \quad \longrightarrow \quad F = \frac{1}{2} (B(t, r) d\Omega_{S^2} + E(t, r) dt \wedge dr)$$

$L_{i=1,2,3}$ is the $SO(3)$ Killing vector *i.e.* satisfying $\mathfrak{su}(2)$ algebra.

Imposing the maximal conformal symmetry ($SO(3) \times SL(2, \mathbb{R})$ here) further, we gain the result as follow :

$$\mathcal{L}_{r\partial_r + t\partial_t} F = \mathcal{L}_{\partial_t} F = 0 \quad \longrightarrow \quad F = \frac{1}{2} \left(B d\Omega_{S^2} + E \frac{dr}{r^2} \wedge dt \right)$$

Note that the above solutions satisfy the Bianchi identity $dF = Q_m \delta(r) d^3x$ and the equation of motion $d \star F = Q_e \delta(r) d^3x$ and the electric and magnetic charge is given as $Q_e = \int_{S^2} \star F = 2\pi E$ and $Q_m = \int_{S^2} F = 2\pi B$.

³⁾For the supersymmetric Wilson loops in $\mathcal{N}=4$ SYM, this had been already defined in [114] for example.

The Abelian gauge field is represented as

$$A = \frac{B}{2}(1 - \cos \theta)d\phi - \frac{E}{2} \frac{dt}{r} \quad (1.2.5)$$

which is not globally defined on even $\mathbb{R}^{1,3} \setminus (\mathbb{R} \times \{0\})$. The undefined region is $\mathbb{R} \times \mathbb{R}_{\geq 0} = \{(r, \theta, \phi) | \theta = 0\}$ and this is the exactly famous *Dirac string*.

It is straightforward to generalize from the Abelian case to the non-Abelian case. There is a new constraint that $[B, E] = 0$ *i.e.*

$$E \in \mathfrak{g}_B := \{X \in \mathfrak{g} | [X, B] = 0\} \quad (1.2.6)$$

where \mathfrak{g}_B is called the stabilizer of B in \mathfrak{g} and also turn out to be a Lie subalgebra using the Jacobi identity. For simplicity, we set E to be zero *i.e.* consider no electric charge background at first. We consider B to be an element of \mathfrak{g} however. The consistency with the equations of motion depends on the details of the system and we will make a comment on it later.

Recalling that any element in \mathfrak{g} can be in the Cartan subalgebra \mathfrak{h} of \mathfrak{g} , it is possible to regard B as an element of \mathfrak{h} . Notice also that the above boundary condition makes sense when the gauge fixing is specified like this.

Quantization condition and magnetic charge

The existence of the Dirac string says that it is impossible to define a global and non-trivial connection (gauge fields with topological charges) without any singularities over S^2 or $\mathbb{R}^3 \setminus \{0\}$ and it is necessary to have at least two patches $U_N (0 < \theta \leq \pi)$ and $U_S (0 \leq \theta < \pi)$. The non-Abelian version of (1.2.5) in $E = 0$ are defined on U_N and we need the gauge field expression on U_S . This can be obtained by changing $\theta \rightarrow \pi - \theta$ and $\phi \rightarrow -\phi$.⁴⁾

$$A_N = \frac{B}{2}(1 - \cos \theta)d\phi \quad \text{over } U_N \quad (1.2.7)$$

$$A_S = \frac{B}{2}(-1 - \cos \theta)d\phi \quad \text{over } U_S \quad (1.2.8)$$

The common region is $U_{NS} := U_N \cap U_S = S^2 \setminus \{p_N, p_S\} \simeq S^1 \times \mathbb{R}$ where p_N and p_S are the north pole and south pole respectively. The transition function over U_{NS} should be given by

$$g_{NS}(\theta, \phi) = \exp(iB\phi) \in \mathbb{T}_{\tilde{G}} \subset \tilde{G} \quad \text{for } (\theta, \phi) \in U_{NS}. \quad (1.2.9)$$

Naively, the single valued condition for g_{NS} can be written

$$\exp(2\pi iB) = Id_{\tilde{G}}. \quad (1.2.10)$$

⁴⁾This is not a coordinate transformation in the same patch but a transformation between two patches. The latter one is needed to preserve the orientation on S^2 .

However, in the case that there are only adjoint matters for example, we can weaken the above condition. In that case, if we choose $g_{NS}(\phi = 2\pi) \neq Id_{\tilde{G}}$ but satisfying $Ad(g_{NS}(\phi = 2\pi)) = Id_{Ad, \tilde{G}}$, this transition function acts on all the wave functions appropriately in the sense that it is single valued.

To be precise and to avoid confusions, we cautiously redefine the ordinarily used term “gauge group” at this stage [83,115]. Denote the theory we consider by X and its universal gauge group by \tilde{G} which is uniquely determined. There is also a unique maximal subgroup \mathcal{Z}_X of $\tilde{\mathcal{Z}}_{\tilde{G}}$ such that all purely electrically charged dynamical matters are invariant under \mathcal{Z}_X action. Now, we define “unframed electric gauge group” as $G_X := \tilde{G}/\mathcal{Z}_X$.

Next, let us choose a discrete group Γ satisfying

$$\mathcal{Z}_X \subset \Gamma \subset \tilde{\mathcal{Z}}_{\tilde{G}} \quad (1.2.11)$$

and define a “framed electric gauge group” as $\hat{G} = \hat{G}^\Gamma := \tilde{G}/\Gamma$. This depends on the choice of Γ and is not unique unlike G_X . When we say that the framed electric gauge group of the theory is \hat{G}^Γ , we do not allow the Wilson loops charged for Γ .

Hereafter, we use simply $G = \tilde{G}/\Gamma_G$ for G_X or \hat{G} .

When there are only matters neutral to \mathcal{Z}_G -charge, we may relax (1.2.10) to

$$R_G(\exp(2\pi i B)) = Id_{R_G} \quad \text{for } \forall R_G \in \text{Rep}(G) \quad (1.2.12)$$

where R_G is the unitary irreducible representation set of G not \tilde{G} . This expression is equivalent to

$$R_G(B) \in \mathbb{Z} \cdot Id_{R_G} \quad (1.2.13)$$

and, after setting $B \in \mathbb{T}_G$, this reduces to

$$\lambda_{R_G}(B) \in \mathbb{Z} \quad (1.2.14)$$

where λ_{R_G} is the highest weight of R_G .

Now, the condition (1.2.12) is simply expressed as

$$\lambda(B) \in \mathbb{Z} \quad \text{for } \lambda \in \Lambda_{\text{ch}}^G \quad (1.2.15)$$

where Λ_{ch}^G is the character lattice of G which is defined by the integral linear combinations of the highest weights of G . See Fig. 1.2 for the $A_2 = \mathfrak{su}(3)$ example. This is the non-Abelian version of Dirac quantization condition derived in [116] and called Goddard-Nuyts-Olive quantization condition named after it. Notice also that the cocharacter lattice Λ_{cc}^G is defined as the set of B satisfying this quantization condition which form the lattice structure.

This result suggests an important and expected fact. Recalling that Λ_{cc}^G equals to the character lattice of the dual group G^\vee i.e. $\Lambda_{\text{cc}}^G \simeq \Lambda_{\text{ch}}^{G^\vee}$ and that the Weyl equivalent elements are also gauge-equivalent by definition, we can conclude that possible magnetic charges B or 't Hooft loops are classified by the irreducible representation of G^\vee .

$$B \in \Lambda_{\text{ch}}^{G^\vee}/\mathcal{W}_{\mathfrak{g}} \simeq \Lambda_{\text{cc}}^G/\mathcal{W}_{\mathfrak{g}} \quad (1.2.16)$$

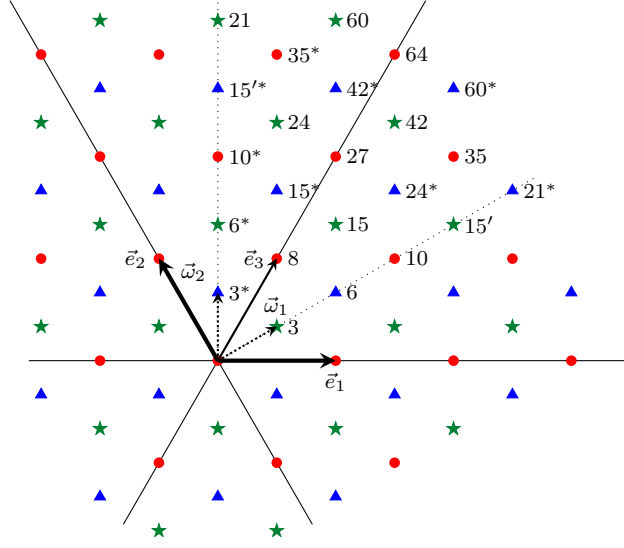


Figure 1.2: For example, A_2 or $SU(3)$ charge lattice. Each number shows the dimension of the representation which corresponds to the highest weight. \bullet , \star and \blacktriangle mean that the center charges of $\mathcal{Z}(SU(3)) = \mathbb{Z}_3$ are 0,1 and 2 respectively.

In this framework, the original classification of the 't Hooft loops in [42] referred to as the “topological charge” is given by

$$\Lambda_{\text{cc}}^G / \Lambda_{\text{cr}}^G \simeq \pi_1(G) \simeq \mathcal{Z}_{G^\vee} \simeq \mathcal{Z}_{\tilde{G}} / \mathcal{Z}_G. \quad (1.2.17)$$

This is because the topological charge corresponds to the center element of $g_{NS}(0)^{-1}g_{NS}(2\pi)$ in \tilde{G} where \mathcal{Z}_G acts on the wave function trivially by the physical definition. Mathematically, this is the isotopy class of glue transition function or the topology class of an associated vector bundle specified by $(G, \rho_{\text{matter}})$. They are related via $\pi_0(\text{Map}(S^1 \rightarrow G)) = \pi_1(G)$.

When $G = G_X = G_{\text{ad}} := \tilde{G} / \mathcal{Z}_{\tilde{G}}$, Λ_{cc} equals to Λ_{mw} . This is the case for $\mathcal{N}=4$ Super Yang-Mills or pure Yang-Mills and the magnetic charges are classified by $\pi(G_{\text{ad}}) \simeq \mathcal{Z}_{\tilde{G}}$. Note that if the dual fundamental quarks (monopoles for the original gauge theory) exist, any magnetic charge are screened by them and 't Hooft loops have no information in the deep IR (N-ality). On the other hand, if $G = G_X = \tilde{G}$, Λ_{cc} equals to Λ_{cr} . This is the case for general QCDs with fundamental quarks. In this case, there are no non-trivial topological charge by nature.

In the compact Abelian case $G = G_X = U(1)$, we can define the minimum electric charge as e and (1.2.10) reduces to the simple condition

$$\exp(2\pi i e B) = 1 \quad \text{i.e.} \quad B = \frac{m}{e} \quad \text{for } m \in \mathbb{Z}. \quad (1.2.18)$$

The magnetic charge $Q_m = 2\pi B = m \frac{2\pi}{e}$ is quantized where the minimal magnetic charge is $\frac{2\pi}{e}$ and this is the exactly Dirac quantization condition. Mathematically, the topological

charge m is the element of $\pi_1(U(1)) \simeq \mathbb{Z}$. This is the infinite choice whereas the set of topological charges is a finite set in any non-Abelian groups.

1.2.3 The classification of Wilson-'t Hooft loops

The classification of possible charged loop defects in gauge theory has some subtle problems. They seem to be labelled by pairs of representation of G and G^\vee , namely (R_G, R_{G^\vee}) , but the correct answer is not so simple. As explained, we must specify G for the possible set of loop operators. However, for the purpose of the classification, we should not specify the detail of dynamical matters neither.

Now, let us define the Wilson-'t Hooft loops following [44]. This is defined by inserting a non-dynamical monopole at first and then adding the Wilson loop on it. At $\mathbb{R}_t \times \{0\}$ which is the boundary or the orbit of the charged non-dynamical probe particle, the gauge symmetry G is (classically) broken to G_B which is the stabilizer subgroup of $B \in \Lambda_{cc}^G = \Lambda_{mw}^g$ with the adjoint action. Now, we can introduce a Wilson loop for \tilde{G}_B . In conclusion, the Wilson-'t Hooft loops are classified by pairs (B, R_B) where R_B is an irreducible representation of \tilde{G}_B .

Notice that different B which are mapped into each other by a Weyl reflection gives distinct G_B but $G_{B_1} \simeq G_{B_2}$ for any B_1 and B_2 mapped via a Weyl reflection action each other, that is to say, $\exists w B_1 = w^{-1} B_2 w$. This is natural and consistent with the previous result (1.2.6) on the boundary condition analysis.

Kapustin also show that the possible pair (B, R_B) is also specified by the set

$$(\Lambda_{mw}^g \times \Lambda_{wt}^g) / \mathcal{W}_g \tag{1.2.19}$$

where the quotient means that there exists a $w \in \mathcal{W}_g$ such that $(B, \mu) \sim (w \cdot B, w \cdot \mu)$. Here we have written the element as (B, μ) .⁵⁾

Two types of Wilson-'t Hooft loops There are two types of dyonic loop operators. We define these in $\mathcal{N}=4$ super Yang-Mills theory in order to make use of the $SL(2, \mathbb{Z})$ duality and then extend them to the other CFTs.

One type is parallelizable Wilson-'t Hooft loops which can be mapped into Wilson loops without no magnetic charge in some appropriate duality frames. We call this charge ‘‘pure dyonic charge’’ and the other one ‘‘complex dyonic charge’’. For the simplest example, see fig.1.3.

Quantum definition using path integral

Now that we know the possible boundary conditions, we define the expectation values or correlators by the path integrals under the boundary condition and with the Wilson loops

⁵⁾Be aware that the ordering of the electric charge and magnetic charge depends on the literatures. We adopt magnetic-electric order because the magnetic charge is first determined in the definition.

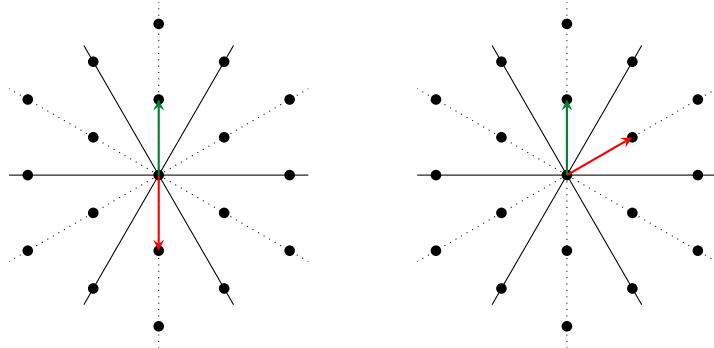


Figure 1.3: Consider the case that the electric and magnetic charges correspond to ω_1 and ω_2 respectively. We do map the magnetic charge into the highest weight (in the closure of the fundamental Weyl chamber) using the Weyl action. In this rule, the electric charge is a weight ω_1 of the fundamental representation and the magnetic charge is the highest weight of the anti-fundamental representation. There are three choices for the weights of the electric charge which are exchanged each other under the Weyl action. One is a weight $-\omega_1 - \omega_2$. This can be mapped into the fundamental Wilson loop using sequent duality transformations $ST \rightsquigarrow$. (left) This becomes a pure charge. The other two ω_1 and $\omega_2 - \omega_1$ are Weyl equivalent even when they are paired into dyonic charge with the magnetic one ω_2 . (right) This can not be mapped into any purely Wilson loops.

as follows.

$$\langle D_{(B,\mu)}(\gamma) \rangle \sim \int_{\frac{1}{2\pi} \int_{S^2} F=B} \mathcal{D}A \mathcal{D}\vec{\Phi} W_R(\gamma) e^{iS[A,\vec{\Phi}]} \quad (1.2.20)$$

where $\vec{\Phi}$ stands for the other fields. Notice that it is necessary to consider the gauge fixing terms (ghosts) and the counter terms exactly.

Half-BPS Wilson-'t Hooft loop operator

To have a benefit of the localization techniques, we must have Q -closed operators where Q is a nilpotent twisted supercharge. In order to be Q -invariant, it is necessary to modify the definition because the supersymmetric transformation of A include a gluino. To cancel the gluino, we have to add the complex scalar in the gauge multiplet. For the Wilson loops ([117] for $\mathcal{N}=4$ for instance),

$$W_R^S(\gamma) = \text{Tr}_R \left[P \exp \left(\int_{\gamma} iA_{\gamma} + \phi \cdot \theta |dx^{\mu}| \right) \right] \quad (1.2.21)$$

where ϕ are the scalars which is the adjoint representation of G and the vector representation of R -symmetry and θ is a constant vector with the same component as the number

of the adjoint scalars. Note that θ determine the unbroken algebra. ⁶⁾

$$\delta_\epsilon W_R^S(\gamma) = \text{Tr}_R \left[P \int_\gamma ds \bar{\lambda} \left(i\Gamma_\mu \frac{dx^\mu}{ds} + \Gamma_a \theta^a \left| \frac{dx^\mu}{ds} \right| \right) \epsilon \cdot \exp \left(\int_\gamma iA_\gamma + \phi \cdot \theta |dx^\mu| \right) \right] \quad (1.2.22)$$

where a runs over $5, 6, \dots, 10$ for $\mathcal{N}=4$ or $5, 6$ for $\mathcal{N}=2$. Then we attain the half-BPS condition for ϵ

$$\left(i\Gamma_\mu \frac{dx^\mu}{ds} + \Gamma_a \theta^a \left| \frac{dx^\mu}{ds} \right| \right) \epsilon = 0 \quad (1.2.23)$$

For the 't Hooft loops, we also require the singular boundary condition of ϕ determined by the supersymmetric transformation. ([44] [45]) Notice that we must use the same ϵ for the half-BPS Wilson loop if considering the half-BPS Wilson-'t Hooft loop. The concrete form is unnecessary because we do not calculate the expectation values directly using the localization method or the gauge/gravity setup.

Operator product expansion and ring structure

We comments on the OPE structure briefly. At first we ignore the divergence in the OPE. By the definition $W_{\mathbf{1}} = 1$ and Wilson loops form a representation ring of G whose additive $+$ and product \cdot correspond to the direct sum \oplus and the tensor product \otimes respectively.

$$\langle W_{R_a} W_{R_b} \rangle = \langle W_{R_a \otimes R_b} \rangle = \sum_i N_{ab}^i \langle W_{R_i} \rangle \quad (1.2.24)$$

$$\text{for } R_a \otimes R_b = \oplus_i N_{ab}^i R_i \quad (1.2.25)$$

where N_{ab}^i is the Littlewood-Richardson coefficient.

The same structure is conjectured to be hold true for the 't Hooft loop operators. ([45])

$$\langle T_{R_a^\vee} T_{R_b^\vee} \rangle = \langle T_{R_a^\vee \otimes R_b^\vee} \rangle = \sum_i N_{ab}^{\vee i} \langle T_{R_i^\vee} \rangle \quad (1.2.26)$$

$$\text{for } R_a^\vee \otimes R_b^\vee = \oplus_i N_{ab}^{\vee i} R_i^\vee \quad (1.2.27)$$

Therefore the loop/line operators form some algebra. ⁷⁾

Note that for $\mathcal{N}=2$ supersymmetric gauge theories the half-BPS fully time-like loop operators are topological. There are two given supercharges that annihilates the half-BPS loop operators and the anticommutator gives the spatial translational generators. ⁸⁾ This says that no divergence appears in the OPE of the half-BPS loop operators.

⁶⁾In [15], θ is written as ζ and plays an important role by analytically continuation and the Stokes phenomena on the plane.

⁷⁾Rigorously speaking, the line defect operators form a semiring because there should be a (monoid) homomorphism from the $\mathbb{Z}_{\geq 0}$ coefficient group semiring of the charge lattice (as an additive group) to the semiring of the Hilbert space.

⁸⁾Precisely speaking, there is a continuous parameter determining the type of half-BPS loops (= how to break the SUSY by half) and this is not true for loops with the different types.

It is natural to ask the following question : what types of dyonic loop operators appear when two general dyonic operators approach each other ? The satisfactory answer has not been given and this is the future problem.

It is necessary to note that for space-like loop operators it is followed from the definition of the 't Hooft operator in operator formalism that

$$\hat{W}_{R_e}(\gamma_e)\hat{T}_{R_m^\vee}(\gamma_m) = \exp [2\pi i \langle \lambda_{R_e}, \lambda_{R_m^\vee} \rangle_{\mathfrak{g}} \cdot L(\gamma_e, \gamma_m)] \hat{T}_{R_m^\vee}(\gamma_m)\hat{W}_{R_e}(\gamma_e) \quad (1.2.28)$$

where $\langle \lambda_1, \lambda_2 \rangle_{\mathfrak{g}}$ is the metric defined on the lattice and $L(\gamma_1, \gamma_2)$ is the linking number of loops γ_1 and γ_2 . This says that the OPE is ill-defined for the Wilson-'t Hooft loop operators whose charge $\langle \lambda_{R_e}, \lambda_{R_m^\vee} \rangle_{\mathfrak{g}} \cdot L(\gamma_e, \gamma_m) \in \mathbb{Z}$. The same relation may be true for (fully) time-like ones too because it is just the quantization condition itself.⁹⁾

1.2.4 Abelian duality for loop operators

Are 't Hooft loops dual objects for Wilson loops ? In the $U(1)$ case, we can check it using ‘‘Abelian S-duality’’ proposed in [118] in terms of path integral. Assume that there is no charged matter (the Maxwell theory).

Let us evaluate a Wilson loop $W_q(\gamma) = \exp \left[iq \int_{\gamma} A \right]$. Define the Abelian holomorphic coupling as $\tau := \frac{\theta}{\pi} + \frac{2\pi i}{e^2}$ and introduce the dual gauge field B , an auxiliary field G and a new gauge-invariant field strength $\mathcal{F} := F - G$.

$$\begin{aligned} \langle W_q(\gamma) \rangle_{\tau} &= \int \mathcal{D}A W_q(\gamma) e^{-\frac{1}{4\pi i} \int (\tau F_+ \wedge F_+ - \bar{\tau} F_- \wedge F_-)} \\ &= \int \mathcal{D}A \mathcal{D}B \mathcal{D}G e^{-\frac{1}{4\pi i} \int (\tau F_+ \wedge F_+ - \bar{\tau} F_- \wedge F_-) + \frac{i}{2\pi} \int G \wedge F_B + iq \int_D (F_A - G)} \\ &= \int \mathcal{D}B \mathcal{D}G e^{-\frac{1}{4\pi i} \int (\tau G_+ \wedge G_+ - \bar{\tau} G_- \wedge G_-) + \frac{i}{2\pi} \int G \wedge (F_B - 2\pi q [D])} \\ &= \int \mathcal{D}B e^{-\frac{1}{4\pi i} \int (\tau^\vee \tilde{F}_{B+} \wedge \tilde{F}_{B+} - \bar{\tau}^\vee \tilde{F}_{B-} \wedge \tilde{F}_{B-})} = \langle T_q(\gamma) \rangle_{\tau^\vee} \end{aligned} \quad (1.2.29)$$

where $\tilde{F}_B := F_B - 2\pi q [D]$ and $\tau^\vee := -\frac{1}{\tau}$. We also omit the volume factor. D is a surface satisfying $C = \partial D$ and $[D]$ is the Poincaré dual δ 2-form of D . In this case for $\forall p \in C$, $\int_{S_p^2} \tilde{F}_B = 2\pi q$ ensures that there exists a monopole and a magnetic current through C .

Since this exchanges the Wilson loop as the order parameter and the 't Hooft loop as the disorder parameter, this duality is also called ‘‘Kramers-Wannier’’ duality. Notice that it is possible to consider this duality over general manifolds and with general actions as formally shown as

$$\int [\mathcal{D}A/\text{Vol}] e^{-I[dA]} = \int \mathcal{D}F \delta(dF) e^{-I[F]} = \int \mathcal{D}F e^{-I[F]} \int [\mathcal{D}B/\text{Vol}] e^{i \int dF \wedge B}$$

⁹⁾The linking number is not defined in that case. It is unnecessary.

$$= \int [\mathcal{D}B/\text{Vol}] e^{-I^\vee[dB]} = \int \mathcal{D}H \delta(dH) e^{-I^\vee[H]} \quad (1.2.30)$$

where

$$A \in \Omega^{p-1}(M) \quad F = dA \in \Omega^p(M) \quad B \in \Omega^{d-p-1}(M) \quad H = dB \in \Omega^{d-p}(M) \quad (1.2.31)$$

and $\int [\mathcal{D}A/\text{Vol}] \cdots$ represents the path integral over the gauge inequivalent configuration.

1.2.5 Duality action on Wilson-'t Hooft loop operators

We see the S-duality action on the loop operators in the non-Abelian gauge group G in the 4D $\mathcal{N}=4$ SYM. The full S-duality group $SL(2, \mathbb{Z})$ are generated by S , T and it is enough to investigate the action of S , T only.¹⁰⁾ However, in addition, we consider the charge conjugation $C = S^2$.

As it is discussed before, the loop operators are classified by the Kapustin's charge lattice (up to the simultaneous Weyl action) of the gauge group G . Therefore, each duality action acts on the charge lattice. For the action to be well-defined, it is necessary to be compatible with the actions of the Weyl reflection group \mathcal{W}_g . In other words,

$$\forall w \exists w' \quad wX = Xw' \quad (1.2.32)$$

where $w, w' \in \mathcal{W}_g$.

Witten effect

Recalling that T corresponds to the Witten effect, we expect¹¹⁾ that this shifts the electric charge by a charge proportional to the magnetic charge as follows:

$$T : (B, \mu) \mapsto (B, \mu + B^\vee) \quad (1.2.33)$$

and see fig.1.4 for example. See also [119].

Charge conjugation

The charge conjugation is simple. This corresponds to taking the complex conjugation and for non-Abelian charges

$$C : (B, \mu) \mapsto (-B, -\mu) \quad (1.2.34)$$

and see fig.1.5 for example.

¹⁰⁾The S-duality for non-simply laced is a subgroup of this and is included automatically.

¹¹⁾See [44] for the proof.

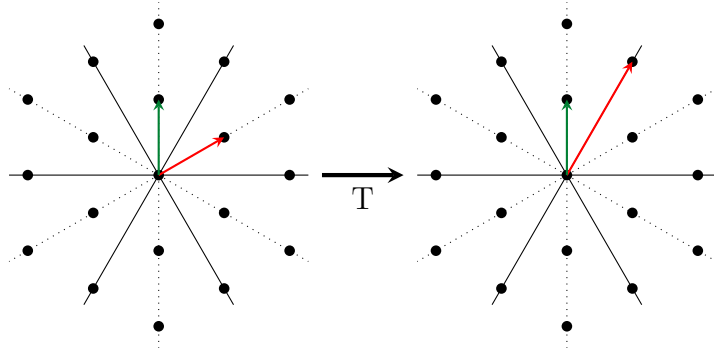


Figure 1.4: The θ -shift action on (ω_2, ω_1)

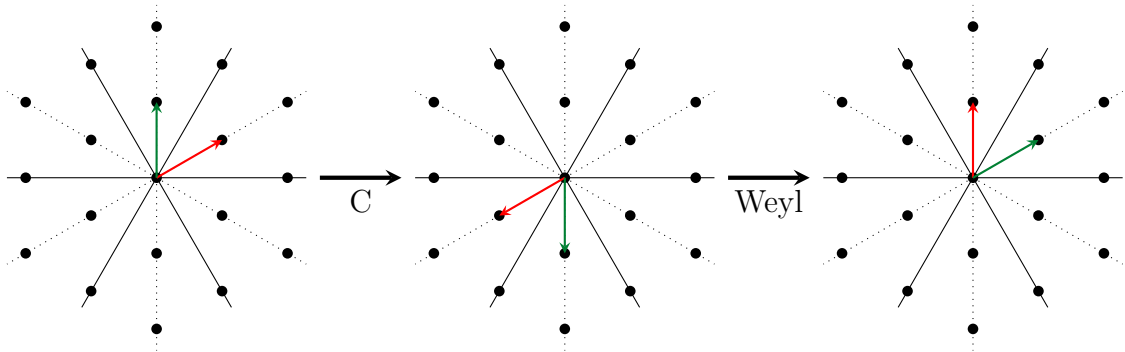


Figure 1.5: The charge conjugation action on (ω_2, ω_1)

Montonen-Olive duality

The most interesting action on loop operators is the S-duality map. This is expected to exchange the electric charge and the magnetic charge but they belong to the different lattice. Taking $S^2 = C$ into consideration, we can naturally expect

$$S : (B, \mu) \mapsto (\mu^\vee, -B^\vee) \tag{1.2.35}$$

and see fig.1.6 for example.

For non-simply-laced case, T action is modified to

$$ST^qS : (B, \mu) \mapsto (q\mu^\vee - B, -\mu). \tag{1.2.36}$$

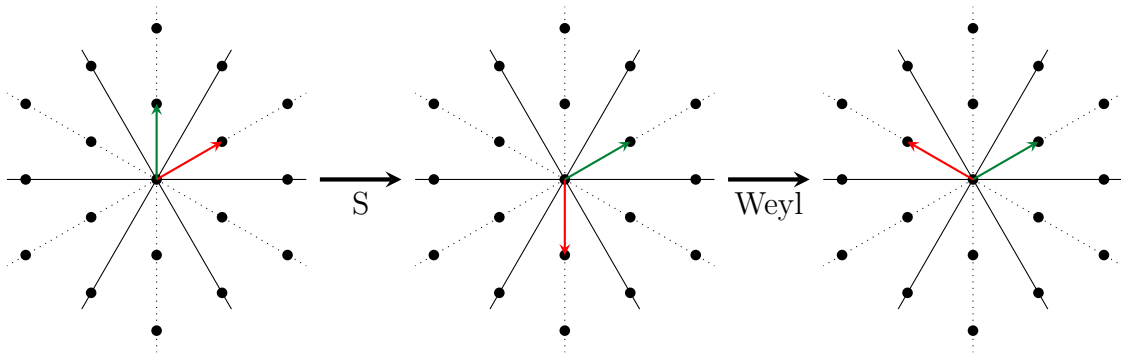


Figure 1.6: The S-dual action on (ω_2, ω_1)

Chapter 2

Class S description

In this chapter, we review several aspects of the class S theory in terms of codimension two defects. In particular, we explain the classification of codimension two defects in Sec. 2.2, the local contributions of the defects to the Coulomb branch and the Higgs branch in Sec. 2.3 and relevant examples of the class S theory in Sec. 2.4. Since other aspects of the class S theory are necessary to understand the 4D physics and 4D/2D duality relation in detail but less important to the later discussions, we review several of them, in particular, the Seiberg-Witten curve approach, brane constructions in string theory and the dualities of class S theories in Appendix. F. We use the following important facts of the class S theory (observations, conjectures) :

- The choice of a duality frame corresponds to that of a pants decomposition of the punctured Riemann surface.
- The 4D holomorphic gauge couplings is specified by the complex moduli of punctured Riemann surface (Teichmüller space).
- The exact dualities in 4D are realized by changing the decompositions and holomorphic coordinates on the moduli.

The other results will be introduced when necessary.

For the purpose to derive the necessary results for later, we explain the background story (relations to the M-theory and 6D SCFTs viewpoint) of Sec. 2.1. The following overview is summarized in Fig.2.1 to some extent. In the gravity decoupling limit, the effective theories of the spatially coincident M5-branes are expected to be non-trivial SCFTs called type A ($\mathfrak{g} = \mathfrak{su}$) 6D $\mathcal{N}=(2, 0)$ SCFT. On M5-branes, there lives a self-dual 2-form gauge field. Since the proper Lagrangians of self-dual forms are unknown yet, these theories are sometimes referred to as non-Lagrangian theories. However, these theories satisfy several properties following the string properties. One of the important properties is that, after the S^1 compactification, these theories flow to 5D maximally supersymmetric Yang-Mills (MSYM) theories in the IR. On the string theory side, this corresponds to the fact that the S^1 reduction of M5-branes lead to D4-branes.

The 6D $\mathcal{N}=(2,0)$ superconformal algebra (SCA) indicates the existence of the two types of defects : codimension two and codimension four defects. In terms of M-theory (the 11D supersymmetry algebra), this corresponds to the existence of BPS M2-branes and M5-branes. On the S^1 compactification, there are two ways to reduce each codimension two and four defects and, at first, we focus on the cases that these defects extend along the reduced S^1 direction at first. This reduction helps us find the classification of defects of 6D $\mathcal{N}=(2,0)$ SCFTs once we assume that there is some one-to-one correspondence between the UV defects and IR ones. For the codimension four defects, they are loop operators coupled to the gauge field in 5D and they are expected to be Wilson loops. This fact suggests that the codimension four defects may be labelled by the irreducible representations of the Lie algebra type \mathfrak{su} of 6D $\mathcal{N}=(2,0)$ SCFTs.¹⁾ This can be understood in terms of the string theory. Because M2-branes reduce to F1-strings and their end points look electrically charged particles, namely, Wilson loops. Correspondingly, the two-form gauge field B reduces to one-form gauge field A . On the other hand, the codimension two defects become vortex like defects. This means that the classification of the codimension two defects is equivalent to the analysis of some BPS solutions with a specified monodromy. This BPS equation is called Hitchin equation as we will discuss in Sec. 2.2.

Next, let us consider the other type of the reduction in which the defects are localized at S^1 -direction. In this case, the codimension four defects become surface defects in 5D which are expected to be non-dynamical monopole strings and the codimension two defects become domain walls or boundaries of the 5D theories. Therefore, the classification of the codimension two defects is replaced by that of the half-BPS boundary conditions of 5D MSYM whose BPS equation is called Nahm equation. We will see this analysis later in Sec. 2.2.

In both systems, we can characterize the codimension two defects by the classification of the half-BPS (codimension two and one) boundary conditions. This analysis is reviewed in Sec. 2.2. The stringy approach is reviewed in Appendix.F.3.

Keep in mind that, in this chapter, all the general punctures on the punctured Riemann surface correspond to the codimension two defects extending along the whole directions of 4D but that there are cases that the codimension four defects are some of punctures and extend along two directions in 4D in later chapters. See also 4.3.

Now, let us unify the above story and 4D $\mathcal{N}=2$ theories called class S theories. Several 4D $\mathcal{N}=2$ superconformal field theories can be obtained by the compactification of 6D $\mathcal{N}=(2,0)$ SCFTs on some punctured Riemann surfaces C . For this purpose, let us further compactify the 4D theory into the 3D $\mathcal{N}=4$ theory in the IR. This analysis was done in [122], for example. This relates the moduli spaces of 4D theories with those of 3D theories. Concretely speaking, each 3D Coulomb branch is the torus fibration of the corresponding 4D Coulomb branch and its dimension is doubled. Therefore, if we know

¹⁾Strictly speaking, we use the fact that the reduction without any twist leads to the gauge symmetry G which is a compact Lie group of \mathfrak{g} . In this thesis, we focus on $\mathfrak{g} = \mathfrak{su}(N) = A_{N-1}$ case with trivial outer morphism, namely, no twisted punctures [120, 121]. In string theory language, this corresponds to the absence of orientifolds.

the dimensions of moduli spaces in 3D, we can also compute those of both 4D branches. On the other hand, each 3D Higgs branch is equivalent to the corresponding 4D Higgs branch.²⁾ However, in general, this 3D theory is some non-Lagrangian theory because the original 4D theory is so and this does not help us analyse the 4D theories.

Next, let us exchange the order of compactifications, namely, S^1 at first and then on C . In this operation, we have the 5D MSYM at first and we can apply the above story. Further compactification on C gives a 3D theory which is expected to be the mirror theory [123] to the above 3D theory as explained in Sec. 2.1. Here, a nice thing happens. Since the 5D MSYM has a Lagrangian description, the reduced theory to 3D is expected to have some Lagrangian description too [124]. In turn, this can help us search several properties of the original non-Lagrangian 3D theory via the 3D mirror symmetry.

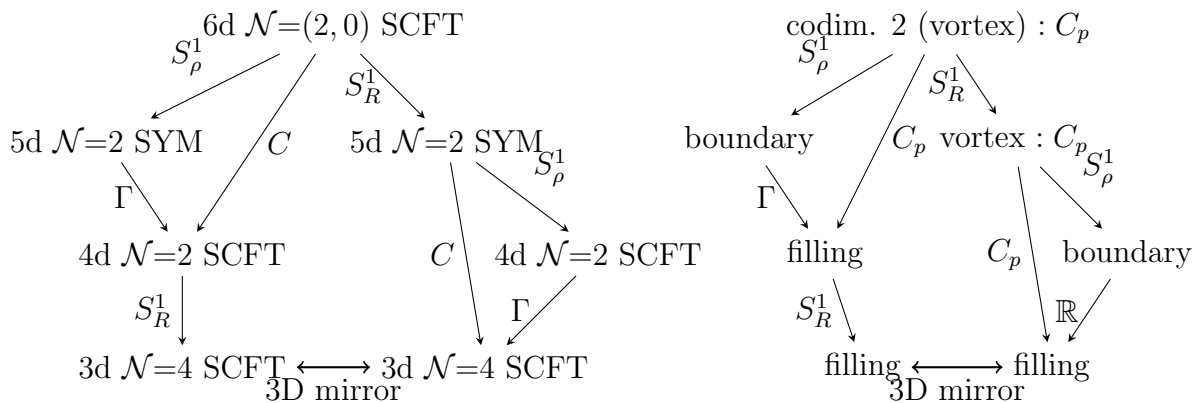


Figure 2.1: The 6D $\mathcal{N}=(2,0)$ SCFT and its descendant theories at each dimension. Here we approximate the Riemann surface C as $S^1 \times \Gamma$ where Γ is the trivalent graph according to the given pants decomposition of C . That is the meaning of the gauge theory on the graph Γ .

2.1 5D Super Yang-Mills viewpoint

This section is mainly based on [15,94,95,124,125]. The starting set-up is the 6D $\mathcal{N}=(2,0)$ SCFT on $\mathbb{R}^3 \times S_R^1 \times C$ where C is punctured Riemann surface and R is the radius of S_R^1 . Instead of considering the punctured Riemann surface C , we locally analyse the physics near one of punctures.

To this end, let us consider the open patch around the given puncture p as a cigar geometry, which is a S^1 -fibration over a half-open line. Hereafter we write this open

²⁾In the former case, the real scalar coming from the compactified component the 4D gauge field and its dual photon form the torus at the generic point of the 4D Coulomb branch. In the latter case, this holds true because of the hyperKähler structure to prevent the moduli from the quantum corrections.

region near the puncture as $S^1_\rho \times \mathbb{R}_{\geq 0}$ where \times is not the direct product in the rigorous sense. Notice that ρ is the typical scale of tubes of C .

Now, we have a 2-torus fibration over $\mathbb{R}_{\geq 0}$ and consider the torus compactification of the 6D $\mathcal{N}=(2, 0)$ SCFT. The low-energy effective theory at generic bulk point locally is well-known to be the 4D maximally super Yang-Mills (MSYM). However, upon the order of compactifications, the effective Lagrangians looks different although they describe the same physics. This phenomenon is called S-duality originally found in [21]. See Fig.2.2 In the following, we take a look at this in the presence of the boundary at $0 \in \mathbb{R}_{\geq 0}$.

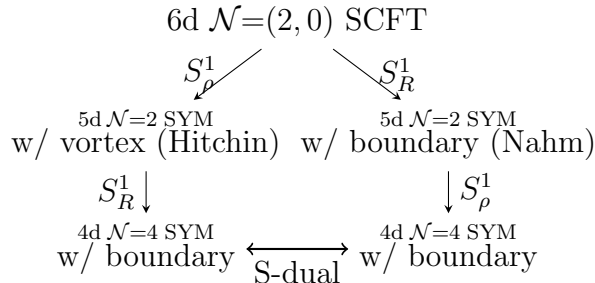


Figure 2.2: The S-duality of the 4D MSYM from the exchange of the order on the torus compactification of the 6D $\mathcal{N}=(2, 0)$ SCFT. We can rephrase this change as the $SL(2, \mathbb{Z})$ modular transformation or the mapping class group of the 2-torus in the geometrical language. Notice also that this slightly differs from the situation in Fig. 2.1.

Before analysing the reductions, we refer to the multiplet of the 6D $\mathcal{N}=(2, 0)$ SCFT. It consists of the self-dual 2-form B , two symplectic Majorana fermions and five real scalars which correspond to the NG modes for the translation symmetry of transverse directions to M5-branes. φ denotes the complex scalar for the fiber direction in T^*C and χ does three scalars for the other transverse directions along \mathbb{R}^3 .

S^1_R reduction

When the S^1_R is reduced at first, we have 5D MSYM with gauge group $G_1 = SU(N)$ ³⁾ defined on $\mathbb{R}^3 \times S^1_r \times \mathbb{R}_{\geq 0}$.

Let us look at bulk physics at first. Classically, the gauge coupling g^2 is proportional to the radius $g^2_{5D} \sim R$.⁴⁾ Further reduction on S^1_ρ of this theory gives the 4D $\mathcal{N}=4$ Super

³⁾Here, we do not pay attention to the topological structure, that is to say, do not distinguish between $SU(N)$ and $PSU(N) = SU(N)/\mathbb{Z}$ for example. See also a recent reference [115] on this point.

⁴⁾The rough derivation is following. When the M-theory is reduced into the type IIA string theory, the string coupling g_s is proportional to its radius because D0-branes with tension $\sim \frac{1}{g_s \ell_s}$ are identified with the KK momentum $\frac{1}{R}$. Then, we use the relation between the D4-brane tension and the string coupling like $T_{Dp} \sim \frac{1}{\ell_s^p g_s}$ where ℓ_s is the string scale. Notice that the classical Yang-Mills coupling appears in the overall factor of the DBI action as $\frac{1}{g^2_{(p+1)DYM}}$. See [126] for these facts.

Yang-Mills (SYM) with $SU(N)$ and the gauge coupling is given as

$$g_{4D,(1)}^2 \sim \frac{R}{\rho}. \quad (2.1.1)$$

On approaching to the boundary, this coupling becomes stronger because $\rho \rightarrow 0$. We explain what happens at the boundary in this framework later.

Next, to see the global structure of C , consider the direct compactification from the 5D SYM theory over $C \times \mathbb{R}^3$ to 3D $\mathcal{N}=4$ theories living on \mathbb{R}^3 . In order to keep the half of the supersymmetry, we must consider the 3d Poincaré invariant vacuum, namely, translational invariant BPS configuration. In other words, we have the self-dual Yang-Mills equation reduced on C as the BPS equation, which is known as the Hitchin equation [127]. This is the equation for $(A_C, \varphi, \bar{\varphi})$.

In the string set-up, φ and $\bar{\varphi}$ correspond to the NG modes along the fiber direction (or Seiberg-Witten 1-form differential) and they parametrize the Coulomb branch in the 4D theory. Therefore, the Coulomb branch is described by the moduli space of the Hitchin equation.

In summary,

$$\mathcal{M}_{3D \text{ Coulomb}} = \mathcal{M}_{\text{Hitchin}} \quad (2.1.2)$$

$$\dim_{\mathbb{C}} \mathcal{B}_{4D \text{ Coulomb}} = 2 \dim_{\mathbb{C}} \mathcal{M}_{3D \text{ Coulomb}} = \dim_{\mathbb{H}} \mathcal{M}_{3D \text{ Coulomb}} \quad (2.1.3)$$

where $\mathcal{B}_{4D \text{ Coulomb}}$, $\mathcal{M}_{3D \text{ Coulomb}}$ and $\mathcal{M}_{\text{Hitchin}}$ are the 4D Coulomb branch, the 3D Coulomb branch and the Hitchin moduli space respectively.

S^1_ρ reduction

Let us repeat the above story by exchanging the reduction order. We have 5D MSYM with G_2 defined on $\mathbb{R}^3 \times S^1_R \times \mathbb{R}_{\geq 0}$ with $g_{5D}^2 \sim \rho$. The sequent reduction with S^1_R gives 4D $\mathcal{N}=4$ SYM with the gauge coupling

$$g_{4D,(2)}^2 \sim \frac{\rho}{R}. \quad (2.1.4)$$

By comparing this to (2.1.1), we get a relation

$$g_{4D,(2)}^2 \sim \frac{1}{g_{4D,(1)}^2} \quad (2.1.5)$$

which suggests the two bulk 4D $\mathcal{N}=4$ SYM are S-dual [21] (See [22] as for the derivation without punctures). In contrast to the former case, at the boundary, the theory is weakly coupled.

To analyse the boundary condition, go back to the brane construction. As explained in Appendix. F, any regular puncture comes from some D4-D6 brane system. ⁵⁾ The

⁵⁾Of course, NS5-branes exist but they are identified with simple punctures in the weak coupling.

M-theory on $S^1_\rho \times S^1_R$ reduces to the effective 9D string theory with $(g_s^{9D})^2 \sim (g_s^{10D})^2 \frac{1}{R} \sim \frac{\rho^2}{\ell_s^2 R}$ (we focus on the closed string sector, namely, the gravity sector although we see the brane action in the former case) and M5-branes and the codimension two defect (puncture) reduce to D4-branes and D6-branes, respectively. Both D-branes wind S^1_R -direction. Using T-duality, we have type IIB realization of this 9D string theory, namely, type IIB string theory with $S^1_{\ell_s^2/R}$ and $g_s^{10D} \sim g_s^{9D} \frac{\ell_s}{R^{1/2}} \sim \frac{\rho}{R}$. Now, D4- and D6-branes are realized as D3- and D5-branes, respectively. In this set-up, the boundary condition for D5-branes, namely, Dirichlet-type boundary condition appears and they were studied in [94]. There, it turned out that the moduli of the supersymmetric vacua in 4D $\mathcal{N}=4$ SYM in the presence of this boundary is described by the Nahm equations. They are equations for $\vec{\chi}$ which correspond to the NG modes in the \mathbb{R}^3 directions in the original M-theory. This is dictated by the Higgs branch in the 4D theory. Since there are some five branes in each picture, it is expected that there exists some flavor symmetry associated with each codimension two defect, namely, the boundary or the puncture.

Recalling that the former system is S-dual of this system (indeed, the gauge coupling relation is reproduced here), the former strongly coupled boundary is realized as D3-NS5 systems or Hanany-Witten systems [19]. In other words, there lives the degrees of freedom at the boundary. This is the story of [95], which claims the S-duality map the Dirichlet boundary to the boundary with some 3D theory on it. The 4D $\mathcal{N}=4$ S-duality is identified with the type IIB string S-duality and it also acts on the five-three brane systems as 3D mirror symmetry [19, 123]. After the total reduction of $C \times S^1_R$ to 3D, the former theory is expected to be a 3D $\mathcal{N}=4$ non-Lagrangian theory and the latter becomes collections of 3D theories living at the 4D boundary in each local analysis. Indeed, in [124], they claim that all the 3D theory are $SU(N)$ diagonally gauged since each has $SU(N)$ flavor symmetry. Notice also that this exchanges the Coulomb branch and the Higgs branch, namely, the moduli of Hitchin systems and that of Nahm systems.

In summary,

$$\mathcal{M}_{3\text{D Higgs}} = \mathcal{M}_{\text{Nahm}} \tag{2.1.6}$$

$$\dim_{\mathbb{H}} \mathcal{M}_{4\text{D Higgs}} = \dim_{\mathbb{H}} \mathcal{M}_{3\text{D Higgs}} \tag{2.1.7}$$

where $\mathcal{M}_{4\text{D Higgs}}$, $\mathcal{M}_{3\text{D Higgs}}$ and $\mathcal{M}_{\text{Nahm}}$ are the 4D Higgs branch, the 3D Higgs branch and the Nahm moduli space respectively.

2D topological q -deformed Yang-Mills from 5D SYM

We make brief comments on the appearance of 2D q -deformed Yang-Mills theory in terms of 5D SYM. Historically, it appeared in [74] where they studied the theory living on the topological D4-branes on a line bundle in a two line bundle over C . Since the effective theory of D4-branes is the 5D MSYM, they reduce them to the 2D topological q -deformed Yang-Mills with chemical potentials (D2 and D0-branes inclusion effects) after some topo-

logical twist.

The direct derivation from the Lagrangian based on the localization technique is discussed in [128, 129].⁶⁾

Codimension four defects

In this section, we discuss the Abelian free 6D $\mathcal{N}=(2,0)$ theory which is the effective theory of a single M5-brane. Let x^0 and θ be the coordinates of S_R^1 and S_ρ^1 respectively.

⁷⁾ Now, the 5D $U(1)$ gauge field has both components denoted by

$$A_\theta^{(H)} \sim RB_{\theta 0} \quad A_\theta^{(N)} \sim \rho B_{0\theta} \quad (2.1.8)$$

where only the zero modes of $B_{\theta 0}$ are considered. This relation implies that two holonomies along the circles coincide:

$$\oint_{S_\rho^1} A^{(H)} \sim - \oint_{S_R^1} A^{(N)} \sim R\rho B_{\theta 0} \sim \int_{S_R^1 \times S_\rho^1} B. \quad (2.1.9)$$

In other words, classically, if the B field is a constant two-form along $S_\rho^1 \times S_\theta^1$ directions, this says that the holonomy around punctures on C and the holonomy around S_R^1 coincide up to sign.

In terms of 6D viewpoint, the (BPS) codimension four operators in 6D $\mathcal{N}=(2,0)$ SCFT which are surface operators coupled to the B -field may be described by two different ways : the Wilson loops around punctures on C or the Wilson loops winding S_R^1 .

If we go to the 4D/2D duality relations as discussed in Sec. 4, this naive expectation is translated into the conjecture of equivalence between the partition function with a 4D Wilson loop in a representation R associated with a flavor symmetry F at a puncture p and the partition function with a 2D Wilson loop in the same R encircling the puncture p . This conjecture is the essential start point of our analysis later.

2.2 Codimension two defects

We see that the some new BPS equations appear when codimension two defects are inserted. The sequent task is the analysis of this moduli space and their classifications. See also the Seiberg-Witten curves and type IIA string approach reviewed in Appendix. F. The physics references on these moduli spaces are [45] and [50, 51] for the Hitchin system, [94] for the Nahm system and [131] for its relations to the spectral curves and so on. Keep in mind that \mathfrak{g} is real simple Lie algebra, in particular, $\mathfrak{su}(N)$ in this section.

⁶⁾In [130], the (4D $\mathcal{N}=1$) SCIs was realized as partition functions on the primary Hopf surface where p, q are complex moduli. The fugacity of a flavor symmetry is realized as holomorphic line bundle structure.

⁷⁾The normalizations, that is to say, $\oint_{S_R^1} dx^0$ and $\oint_{S_\rho^1} d\theta$ are not fixed here because we ignore the constant ambiguity.

Hitchin system

The Hitchin equation [127] naturally appears when the 4D instanton equation (or the BPS equation called Kapustin-Witten equation [45]) is reduced into 2D and can be defined on Riemann surfaces C . In particular, punctures play a role of the boundary condition of fields [132].

Let A and φ be a gauge field (connection) on C and a holomorphic 1-form field valued in \mathfrak{g} , *i.e.* the adjoint representation. Mathematically speaking, $\varphi \in K_C \otimes_{\mathbb{R}} \text{Ad}(\mathfrak{g})$ where K_C is the canonical complex line bundle over C . The Hitchin equation without any punctures, or some singular boundary conditions, is given as

$$\begin{aligned}\Omega_0 &:= F - [\varphi, \bar{\varphi}]dz \wedge d\bar{z} = 0 \\ \Omega_+ &:= -\bar{D}\varphi dz = (\bar{\partial}\varphi + [A_{\bar{z}}, \varphi]) dz \wedge d\bar{z} = 0 \\ \Omega_- &:= D\bar{\varphi}d\bar{z} = (\partial\bar{\varphi} + [A_z, \bar{\varphi}]) dz \wedge d\bar{z} = 0\end{aligned}\tag{2.2.1}$$

or, equivalently,

$$\mathcal{F} := d\mathcal{A} + \mathcal{A} \wedge \mathcal{A} = 0 \quad \tilde{\mathcal{F}} := d\tilde{\mathcal{A}} + \tilde{\mathcal{A}} \wedge \tilde{\mathcal{A}} = 0\tag{2.2.2}$$

where the relation between two is given as

$$\mathcal{A} = A + i\varphi dz + i\bar{\varphi}d\bar{z} \quad \tilde{\mathcal{A}} = A + \varphi dz - \bar{\varphi}d\bar{z}.\tag{2.2.3}$$

The second equation is the flatness condition for the complexified gauge connection but the gauge transformation is not complexified at this stage. However, notice that this condition is invariant under the complex valued gauge transformations.

Nahm system

The Nahm equation is introduced to construct monopoles satisfying the Bogomol'nyi equation [133]. In terms of branes, this equation appears in the D(p+2) of D(p+2)-Dp-branes systems. For the Dp -brane, this is exactly the equation for the boundary condition. As performed in [94], this also naturally appears in the analysis of half-BPS boundary conditions in 4D $\mathcal{N}=4$ SYM without the string theory.

Let $T_a = T_a(s)$ ($a = 1, 2, 3$) and A be real scalars valued in \mathfrak{g} and gauge field defined on $s \in \mathbb{R}_{\geq 0}$. The Nahm equation is given as

$$\Omega_a := \frac{DT_a}{Ds} - \sum_{b,c=1,2,3} \epsilon_{abc} T_b T_c = 0 \quad \text{for } a = 1, 2, 3\tag{2.2.4}$$

where ϵ_{abc} is the antisymmetric tensor with $\epsilon_{123} = 1$ or the structure constant of $\mathfrak{su}(2)$ and $\frac{D}{Ds} = \frac{d}{ds} - \text{Ad}_A$. We will analyze the solutions later.

There is an equivalent equation by introducing the complex fields $\mathcal{A} = A + iT_3$ and $\mathcal{X} = T_1 + iT_2$ ($\bar{\mathcal{A}} = A - iT_3$ and $\bar{\mathcal{X}} = T_1 - iT_2$),

$$\Omega_+ := D_{\mathcal{A}}\mathcal{X} = \frac{d\mathcal{X}}{ds} - [\mathcal{A}, \mathcal{X}] = 0\tag{2.2.5}$$

$$\Omega_0 := \frac{d}{ds} (\mathcal{A} - \overline{\mathcal{A}}) + [\mathcal{A}, \overline{\mathcal{A}}] + [\mathcal{X}, \overline{\mathcal{X}}] = 0.$$

and $\Omega_- := (\Omega_+)^*$. Notice that this equation is invariant under the complexified gauge transformation. In addition, the gauge transformation at the boundary is the large gauge transformation and we fix the value there to be the identity element, namely, $g(0) = e$ (the identity element). We also require $\mathcal{X}(\infty)$ is regular, namely, the commutant $\mathcal{Z}_{\mathcal{G}_{\mathbb{C}}}(\mathcal{X}(\infty))$ is the maximal torus $\mathbb{T}_{\mathbb{C}}$. Any non-regular element is defined as the limit of some regular element to keep the moduli space smooth. Indeed, the set of the regular elements are dense and the unbroken gauge symmetry become larger on top of it discontinuously.

HyperKähler construction

Here, our aim is to know the moduli space or solutions of equations (2.2.4) and (2.2.1) and they have a hyperKähler quotient construction. Although we focus on the Hitchin system here, its application to the Nahm system is straightforward. The moment map is given as

$$\mu_a(\theta_G; \mathcal{A}, \varphi) \sim \int_C \text{Tr} [\theta_G \Omega_a] \quad \text{for } a = +, 0, - \quad (2.2.6)$$

where θ_G is an element of the Lie algebra of the gauge transformation group $\mathcal{G} = \text{Map}(C \rightarrow G)$. When \mathcal{W} denotes the infinite dimensional space of the possible field configuration (\mathcal{A}, φ) , $\vec{\mu} := (\mu_0, \Re(\mu_+) = \Re(\mu_-), \Im(\mu_+) = -\Im(\mu_-))$ is the function over \mathcal{W} valued on $(\text{Lie}(\mathcal{G}))^* \otimes \mathbb{R}^3$ where $*$ means the dual operation as vector spaces.⁸⁾ Since \mathcal{G} naturally acts on \mathcal{W} , we can formally define the quotient of \mathcal{W} by \mathcal{G} identified with the Hitchin moduli space $\mathcal{M}_{\text{Hitchin}} \simeq \mathcal{W}/\mathcal{G}$. This is just infinite dimensional extension of the ordinary hyperKähler quotient construction.

Precisely speaking, the moduli space also depends on the boundary conditions at infinity but we ignore it here because they depends on the global gluing conditions.

As discussed in [134], we have the following equivalence :

$$\begin{array}{ccc} \mathcal{W} // \mathcal{G} := \vec{\mu}^{-1}(0) / \mathcal{G} & \sim & (\mathcal{W} \cap \mu_{\mathbb{R}}^{-1}(0)) // \mathcal{G} := \mu_{\mathbb{C}}^{-1}(0) / \mathcal{G} \sim \mu_{\mathbb{C}}^{-1}(0) / \mathcal{G}_{\mathbb{C}} \\ \text{hyperKähler quotient} & & \text{symplectic quotient} \end{array} \quad (2.2.7)$$

where $\mu_{\mathbb{R}} := \mu_0$, $\mu_{\mathbb{C}} := \mu_+$ and $\mathcal{G}_{\mathbb{C}}$ is the complexified gauge transformation group. Here the complex “gauge group” shows up. The benefit of this equality is the reduction of three equations to one simple equation written by the action of the covariant derivative. Later, we see this relevance.

Finally, let us remark the effects of some boundary conditions [15, 132]. The addition of some $\delta(z_P)$ -like singularity to the holomorphic scalar field over C is equivalent to the addition of $\text{Tr}_{\mathfrak{g}} [\theta_P \zeta]$ to $\mu_{\mathbb{C}}$ where θ_P is the chosen generator at the puncture and $\zeta \in \mathfrak{g}_{\mathbb{C}}$ is determined by the boundary condition.

⁸⁾To define the dual vector space, we need an inner product and it is defined by $(\theta_1, \theta_2) = \pm \int_C \text{Tr}_{\mathfrak{g}} [\theta_1 \theta_2]$ where the overall sign \pm depends on the convention but is chosen such that the inner product is positive definite.

2.2.1 Moduli space of Hitchin equation with Hitchin pole

From Hitchin to Nahm on boundary conditions

As remarked in Sec. 2.1, the Hitchin system can describe the codimension two defect and the Nahm system can describe the codimension one defect in 5D MSYM. However, their 6D origin is the same, that is to say, both come from the codimension two defects in the 6D $\mathcal{N}=(2,0)$ SCFT. How are these two systems related? The answer is simple. At the neighbourhood around the codimension two boundary, the reduction along the angular direction in the Hitchin system gives the Nahm system as expected.

The boundary condition for which such a relation exists is called the regular singularity. Before defining it, notice that the Hitchin equation (2.2.1), after gauging away the $A_{\bar{z}}$, claims that φ is holomorphic in the z coordinate. This assures the axial symmetric behaviour with the following form

$$A \sim a(r)d\theta = \frac{a(r)}{2i} \left(\frac{dz}{z} - \frac{d\bar{z}}{\bar{z}} \right) \quad (2.2.8)$$

$$\varphi dz \sim \frac{b(r) + ic(r)}{2z} dz \quad (2.2.9)$$

where $z = re^{i\theta}$ the A_r component has been gauged away.

Now, for the boundary condition, the Hitchin equations (2.2.1) are equivalent to the Nahm equations (2.2.4)

$$\frac{da}{ds} = [b, c] \quad \frac{dc}{ds} = [a, b] \quad \frac{db}{ds} = [c, a] \quad (2.2.10)$$

where $s := -\log r$. The elimination of the gauge connection in the covariant derivative corresponds to that of A_r .

Semi-simple type

At least, there are two types of conditions. One is given by any triple of commuting elements in \mathfrak{g} . Since we can put each triple into the same Cartan subalgebra and, furthermore, we can identify different a 's related by the large gauge transformations around the singularity, they are labelled by $(\mathbb{T} \times \mathfrak{h} \times \mathfrak{h})/\mathcal{W} = (\mathfrak{h} \times \mathfrak{h} \times \mathfrak{h})/\mathcal{W}_{\text{aff}}$ [50] where the corresponding Lie group is simply-laced.

Nilpotent type

The conditions of the other type are labelled by the embedding homomorphism $\rho : \mathfrak{su}(2) \rightarrow \mathfrak{g}$. Using $t_i := -\frac{i}{2}\rho(\sigma_i)$ where σ_i are the Pauli matrices,

$$a(r) = -\frac{t_2}{s + 1/f} \quad b(r) = -\frac{t_3}{s + 1/f} \quad c(r) = -\frac{t_1}{s + 1/f} \quad (2.2.11)$$

where $f \in \mathbb{R}_{\geq 0}$. Notice that this solution is valid for $0 \leq r < e^{1/f}$ and we should modify the solutions for large r .

The classification of the embedding of $\mathfrak{su}(2) \rightarrow \mathfrak{g} = \mathfrak{su}(N)$ is equivalent to the decomposition ways of the $\mathfrak{su}(N)$ define representation \mathbf{N} into the irreducible representations of $\mathfrak{su}(2)$. In other words, they are classified by the partition of N . In particular, for the partition $[n_1, n_2, \dots, n_k] = \{s_1, s_2, \dots, s_r\}$ where the sequent n and s is related as the transposition of the Young diagram (See D), we can assign the Jordan block

$$J_{\{s_1, s_2, \dots, s_r\}} := J_{s_1} \oplus J_{s_2} \oplus \dots \oplus J_{s_r} \quad J_d := \overbrace{\begin{pmatrix} 0 & 1 & 0 & & 0 \\ 0 & 0 & 1 & \dots & 0 \\ \vdots & \ddots & \ddots & & \vdots \\ \vdots & & & 0 & 1 \\ 0 & 0 & \dots & 0 & 0 \end{pmatrix}}^{d \text{ components}} \quad (2.2.12)$$

because the restriction of $\rho(\sigma^+)$ on the representation vector space of \mathfrak{s}_i is expressed by $J_{\{s_i\}}$.

Once we have the boundary behaviours of the Nahm equation, we can go back to the Hitchin system. The complexified connection is

$$\mathcal{A}_\theta = a(r) - ic(r) = \begin{cases} \text{1st. type} & : \xi \quad \text{for } \xi := \alpha - i\gamma \in \mathfrak{h}_{\mathbb{C}} \\ \text{2nd. type} & : \frac{it^+}{s + 1/f} \quad \text{for } t^+ := t_1 + it_2 = -i\rho(\sigma^+) \end{cases} \quad (2.2.13)$$

and the related monodromy is

$$U_R := U(\Gamma_R) := P \exp \left(- \oint_{\Gamma} \mathcal{A} \right) \quad (2.2.14)$$

where $\Gamma_R := \{Re^{i\theta} \mid \theta \in [0, 2\pi)\}$. Since the gauge connection \mathcal{A} is valued in $\mathfrak{g}_{\mathbb{C}}$, this monodromy for fixed s is an element of $G_{\mathbb{C}}$ and the gauge transformation is complexified.

The flatness condition (2.2.2) says that the conjugacy class of this monodromy depends only on the homotopy class of the loop Γ_R and then is independent of R . The first type is clearly independent of R . For the second type, the independence is a bit non-trivial. In this case, the monodromy is given as

$$U_R = \exp \left(-2\pi i \frac{t^+}{-\log(R) + 1/f} \right) \quad (2.2.15)$$

and it is enough to show that the conjugacy class of λt^+ is independent of λ , in other words, there exists $V_\lambda \in G_{\mathbb{C}}$ such that $V_\lambda^{-1}(\lambda t^+)V_\lambda = t^+$ for any $\lambda \in \mathbb{C}^\times$. Indeed, $V_\lambda = \exp \left[-\frac{1}{2} \log(\lambda) \rho(\sigma^3) \right] \in G_{\mathbb{C}}$ is such a solution. Now we can directly see that the conjugacy class is independent of R for fixed ρ .

In mathematical terminology, the first type is labelled by the semi-simple orbit and the latter is by the nilpotent orbit. Indeed, it is known that the nilpotent orbit is classified

by the above embedding ρ in $\text{Hom}^\times(\mathfrak{sl}(2), \mathfrak{g}_C)/\text{Ad}_{G_C}$ where Ad_{G_C} represents the conjugacy action. See [135] and Appendix.D on these subjects.

Notice that, as $f \rightarrow \infty$, the boundary condition approaches to the trivial one and this implies the moduli is the form of a cone. Indeed, the closure of the nilpotent orbit is known to be the hyperKähler cone [136].

HyperKähler quotient

Consider a new complex coordinate $\omega := \log(z)$. In this coordinate,

$$\mathcal{A} = \frac{a - ic}{2i}(d\omega - d\bar{\omega}) + \frac{-b}{2i}(d\omega + d\bar{\omega}) \quad (2.2.16)$$

where we used

$$\mathcal{A}_z = A_z + i\varphi \quad \mathcal{A}_{\bar{z}} = A_{\bar{z}} + i\bar{\varphi}. \quad (2.2.17)$$

Let us consider the second-type solution case

$$a = -\frac{t_3}{s+1/f} \quad b = -\frac{t_1}{s+1/f} \quad c = -\frac{t_2}{s+1/f}. \quad (2.2.18)$$

Notice that, when ρ is of $[1^N]$ -type, they have the following matrix form

$$(t_3)_{ab} = -i \left(\frac{N}{2} - a \right) \delta_{ab} \quad (t^+)_{ab} = -i \sqrt{a(N-a)} \delta_{a,b-1}. \quad (2.2.19)$$

Using a different basis of $SU(2)_R$ from the previous one, we have

$$A = -\frac{it_3}{\omega + \bar{\omega} + \kappa}(d\omega - d\bar{\omega}) \quad \varphi dz = \frac{t^+}{\omega + \bar{\omega} + \kappa} d\omega \quad (2.2.20)$$

where $\kappa := -2/f$.

Now, let us consider the trivialization by using the gauge transformation

$$U := U(\omega, \bar{\omega}) = u^{it^3} \quad (2.2.21)$$

where $u := \frac{\omega + \bar{\omega} + \kappa}{\omega}$. Notice that

$$\rho \text{ is of } [1^N]\text{-type} : \quad U = \text{diag}(u^{\frac{N}{2}-1}, u^{\frac{N}{2}-2}, \dots, u^{1-\frac{N}{2}}, u^{-\frac{N}{2}}). \quad (2.2.22)$$

The covariant derivative $\overline{D}_\omega = \partial_{\bar{\omega}} + A_{\bar{\omega}}$ is transformed into

$$\begin{aligned} \overline{D}_\omega^U &= U \overline{D}_\omega U^{-1} = \overline{\partial}_\omega \\ \varphi^U &= U \varphi dz U^{-1} = u \varphi dz = \frac{t^+ d\omega}{\omega} \end{aligned} \quad (2.2.23)$$

because $u^{-\alpha} \overline{\partial}_\omega u^\alpha = \frac{\alpha}{\omega + \overline{\omega} + \kappa}$.

In the ω coordinate and after this gauge transformation, \overline{A} is locally trivialized and φ has a simple pole at the origin whose residue is a nilpotent. By using the mathematical argument in D.3 and the fact that mass deformations correspond to a semi-simple element in the residue, we can expect that the possible mass deformation is restricted. If we have a nilpotent orbit specified by $Y = [n] = \{s\}$, the corresponding semi-simple orbit has the orbit of $\text{diag}(\underbrace{m_1, \dots, m_1}_{n_1}, \underbrace{m_2, \dots, m_2}_{n_2}, \dots, \underbrace{m_k, \dots, m_k}_{n_k})$ with $\sum_{i=1}^k n_i m_i = 0$. Therefore, we can read off the associated flavor symmetry as $S(\prod_a U(f_a))$ where f_a is the number of the appearance of a in $[n]$.

It is expected that the degree of freedom at puncture is given by the choice of the nilpotent orbit, namely, $\mathcal{O}_{J_{\{s\}}}$. Its complex dimension is given by

$$N^2 - \sum_{i=1}^k n_i^2. \quad (2.2.24)$$

There are two special punctures. One is specified by $[1^N] = \{N\}$ called full or maximal. In this case, we have $N - 1$ independent mass parameters and $SU(N)$ flavor symmetry. The other is specified by $[N - 1, 1] = \{2, 1^{N-2}\}$ called simple or minimal. In this case, we have only one independent mass parameter and $U(1)$ flavor symmetry.

2.2.2 Moduli space of Nahm equation with Nahm pole

At first, let us consider the case \mathcal{A} is non-singular at $s = 0$. By using the complexified gauge transformation with $g(0) = e$, we can set $\mathcal{A}^g = g\mathcal{A}g^{-1} + \frac{dg}{ds}g^{-1} = 0$.⁹⁾ The degree of freedom of \mathcal{A} is encoded in the Wilson line

$$g(\infty) = \exp \left[- \int_{\mathbb{R}_{\geq 0}} \mathcal{A} \right] \quad (2.2.25)$$

modulo by the complexified gauge transformation at infinity $\mathbb{T}_{\mathbb{C}}$. $\mathcal{X}^g(s) := g\mathcal{X}(s)g^{-1}$ after the gauge transformation satisfies the complex Nahm equation $\Omega^+ = 0$ with $\mathcal{A} = 0$, namely, $\frac{d\mathcal{X}^g}{ds} = 0$ and $\mathcal{X}^g(s)$ is constant : $\mathcal{X}^g(s) = \mathcal{X}^g(0) = \mathcal{X}(0) = \mathcal{X}^g(\infty) = g(\infty)\mathcal{X}(\infty)g(\infty)^{-1}$. In other words, if we fix $g(\infty)$, \mathcal{X} is also fixed. Conversely, if we fix $\mathcal{X}(0)$, $g(\infty)$ is determined up to $\mathbb{T}_{\mathbb{C}}$.

Using the discussion in Sec. D.1, when \mathcal{X}_∞ is a regular semi-simple element, the left moduli is given by

$$\mathcal{O}_{\mathcal{X}(\infty)} \sim G_{\mathbb{C}}/\mathbb{T}_{\mathbb{C}}. \quad (2.2.26)$$

⁹⁾Such a g is unique : $g(s) = \exp \left[- \int_0^s \mathcal{A} \right]$.

In the limit $\mathcal{X}(\infty) \rightarrow 0$, this approaches to the nilpotent cone $\mathcal{N}_{\mathfrak{g}}$ as discussed in Appendix. D.3. This corresponds to the Higgs branch associated to the full puncture ($[1^N]$ type) in the Hitchin system.

Now, we come to the solutions with the following singular boundary condition called Nahm pole.

$$\mathcal{X} \rightarrow \frac{t^+}{s} \quad \mathcal{A} \rightarrow \frac{it_3}{s} \quad \text{as } s \rightarrow 0 \quad (2.2.27)$$

In this case, we cannot completely gauge away the singularity of \mathcal{A} at the boundary but can fix $\mathcal{A} = \frac{it_3}{s}$. Notice that there are left some gauge transformation to preserve this gauge fixing. The problem is to solve the equation (2.2.5). Let us perturb \mathcal{X} around $\frac{t^+}{s}$, namely, $\delta\mathcal{X} = \mathcal{X} - \frac{t^+}{s}$ satisfies the condition that $\delta\mathcal{X}(0)$ is finite. Then, $\delta\mathcal{X}$ obeys

$$\frac{d}{ds}\delta\mathcal{X} = [it_3, \delta\mathcal{X}] \quad (2.2.28)$$

and, by using the basis of the parabolic subalgebra of $\mathfrak{g}_{\mathbb{C}}$

$$\mathfrak{p} = \{X_{\alpha} \in \mathfrak{g} \mid [it_3, X_{\alpha}] = m_{\alpha}X_{\alpha}, m_{\alpha} \geq 0\}, \quad (2.2.29)$$

we can expand $\delta\mathcal{X}$ as

$$\delta\mathcal{X}(s) = \sum_{\alpha \in \text{Basis}(\mathfrak{p})} c_{\alpha} X_{\alpha} s^{m_{\alpha}}. \quad (2.2.30)$$

In particular, the left gauge transformation can gauge away the zero modes, namely, the components generated by the commutant of it_3 which is the Cartan part. Finally, $\delta\mathcal{X}$ is generated by the basis of this unipotent radical of the parabolic subgroup.

The set of Lie algebra element $t^+ + \bigoplus_{\alpha} \mathbb{C}X_{\alpha}$ in the nilpotent cone is called Slodowy slice mathematically, and, the δX is labelled by this slice. It is known that this is transverse to \mathcal{O}_{t^+} at t^+ . The Nahm moduli space is given this and its complex dimension is given by

$$\dim_{\mathbb{C}} \mathcal{N}_{\mathfrak{g}} - \dim_{\mathbb{C}} \mathcal{O}_{t^+} = \sum_a s_a^2 - N. \quad (2.2.31)$$

To see the relations to the classification in Hitchin system, we need the mirror symmetry analysis but, intuitively speaking, the S-duality acts on transposed operation on the Young diagram representation as seen in F.3.1. Therefore, the embedding ρ_{H} appearing in the Hitchin system and that ρ_{N} in this Nahm system differ but related by the transposition.

2.3 Branch dimension analysis

Now, we know the moduli space coming from each puncture locally. They are independent and there is an internal moduli coming from the degree of freedom after we fix the boundary conditions at punctures.

We expect that the dimensions of the 4D Coulomb branch and the 4D Higgs branch are given by the following formula

$$\dim_{\mathbb{C}} \mathcal{B}_{\text{Coulomb}} = \sum_A \dim_{\mathbb{C}} \mathcal{B}_{\text{Coulomb}}(Y_A) - \frac{1}{2} \chi_C \dim_{\mathbb{R}} \mathfrak{g} \quad (2.3.1)$$

$$\dim_{\mathbb{H}} \mathcal{M}_{\text{Higgs}} = \sum_A \dim_{\mathbb{H}} \mathcal{M}_{\text{Higgs}}(Y_A) + \text{rk} \mathfrak{g} \quad (2.3.2)$$

where χ_C is the Euler number of the Riemann surface ignoring the punctures. Keep in mind that the analysis up to now are locally and do not give any global information.

Higgs branch

The degree of freedom not from punctures is given by $\text{rk} \mathfrak{g}$. If we have two full punctures, there is $SU(N) \times SU(N)$ symmetry and can be diagonally gauged. Since there is the moduli equivalent to the nilpotent cone $\mathcal{N}_{\mathfrak{g}}$ at each full puncture, after the quotient of the gauge transformation, the difference of the complex dimension of the moduli between before and after the gauging operation is given by

$$\dim_{\mathbb{C}} \mathcal{N}_{\mathfrak{g}} - \dim_{\mathbb{C}} G_{\mathbb{C}} = -\text{rk} \mathfrak{g}. \quad (2.3.3)$$

This suggests that the internal degree of freedom is independent of the genus of C . Now, comparing the results in the Lagrangian case, we see that this degree is given by $\text{rk} \mathfrak{g} = N - 1$.

Coulomb branch

For the 4D Coulomb branch, we use the fact that the 3D Coulomb branch is the Hitchin fibration over the 4D branch and is expected to be the moduli space of Hitchin equation (2.2.1).

$$\dim_{\mathbb{C}} \mathcal{B}_{\text{Coulomb}}(Y = [n] = \{s\}) = \dim_{\mathbb{H}} \mathcal{M}_{\text{3D Coulomb}}(Y = [n] = \{s\}) = \frac{1}{2} \dim_{\mathbb{C}} \mathcal{O}_{m_Y} \quad (2.3.4)$$

Since the Hitchin equation is equivalent to the flat condition for the complex connection,

$$\mathcal{M}_{\text{Coulomb}} \sim \text{Map}(\pi_1(C), G_{\mathbb{C}}) \sim \langle U_{\alpha,i}, U_{\beta,i} \mid \prod_{i=1}^g [U_{\alpha,i}, U_{\beta,i}] = e_{G_{\mathbb{C}}} \rangle / \sim_{\text{Conjugate}} \quad (2.3.5)$$

where $U_{\alpha/\beta,i}$ is the G_C holonomy around the i -th α/β cycle and e_{G_C} is the identity element. $\sim_{\text{Conjugate}}$ is the common conjugate action of G_C to all holonomies. Therefore, the dimension of the Hitchin moduli without any punctures is given by $2g \dim_{\mathbb{C}} G_C - \dim_{\mathbb{C}} G_C - \dim_{\mathbb{C}} G_C = -\chi_C \dim_{\mathbb{R}} \mathfrak{g}$.

When $\mathfrak{g} = \mathfrak{su}(N)$, the above local contributions to each dimension are given as

$$d_C^Y := \dim_{\mathbb{C}} \mathcal{B}_{\text{Coulomb}}(Y = [n] = \{s\}) = \frac{1}{2} \left(N^2 - \sum_i n_i^2 \right) \quad (2.3.6)$$

$$d_H^Y := \dim_{\mathbb{H}} \mathcal{M}_{\text{Higgs}}(Y = [n] = \{s\}) = \frac{1}{2} \left(\sum_i s_i^2 - N \right) \quad (2.3.7)$$

However, the 4D Coulomb branch has more information about the scaling dimension of the Coulomb branch operators. This approach cannot derive the result about the number of the Coulomb branch operators at each scaling dimension.¹⁰⁾ We quote (F.3.18) in Appendix. F.3. That is

$$d_{C,k}^Y = p_k^Y = k - H_k = k - \min\{a \mid \sum_{b=1}^a s_b \geq k\} \quad \text{for } k = 2, 3, \dots, N \quad (2.3.8)$$

where $Y = \{s\}$ and see Appendix. F.3 as for the definition of H_k . Indeed, the sum over $k = 2, 3, \dots, N$ reproduces the above result

$$\sum_{k=2}^N d_{C,k}^Y = \frac{1}{2} N(N+1) - \sum_{k=1}^N H_k = \frac{1}{2} N(N+1) - \sum_{i=1}^{s_1} \sum_{j=1}^{n_i} j = d_C^Y \quad (2.3.9)$$

where we use $d_{C,k=1}^Y = 0$ and (D.0.10).

By quoting the result in Appendix. F.3 again, we find that the Coulomb branch of the theory is given by

$$\dim_{\mathbb{C}} \mathcal{B}_{\text{Coulomb}}^{(k)} = \sum_A d_{C,k}^Y - (2k-1) \quad (2.3.10)$$

for $k = 2, 3, \dots, N$.

2.4 Examples of class S theories

In this section, we introduce three kinds of non-gauge theory examples : T_N -theory, the free hypermultiplets and rank 1 SCFTs. All are obtained by some three punctured spheres.¹¹⁾

¹⁰⁾We assume that all the scaling dimensions are integer. This assumption is true for all the class S theories with regular punctures. The counterexamples are Argyres-Douglas theories, for instance, but they are constructed with irregular singularities (fractional power singularities).

¹¹⁾Although, in [121, 137], they studied SCFTs from the three punctured spheres allowing the formal irregular punctures and twisted ones and classified them up to $\mathfrak{g} = A_4$, we restrict ourselves to cases with only untwisted regular singularities but for general A -type.

In this thesis,

$$T_{\mathfrak{g}=\mathfrak{su}(N)}^{\mathcal{S}}[C(Y_1, Y_2, \dots, Y_n)] \quad (2.4.1)$$

denotes the resulting 4D $\mathcal{N}=2$ theory in the IR after the compactification on the punctured Riemann surface C with punctures whose types are specified by Y_1, Y_2, \dots, Y_n .

In the first subsection of the T_N -theory, we also explain the two important procedures in the class S theory : “gauging” and “partially closing/Higgsing”.

2.4.1 T_N -theory

First class is the parent theory in the sense that other theories are obtained by two operations called gauging (gluing) and partially closing (Higgsing). See Appendix. F.4.1 as for the construction from the Lagrangian theories.

The T_N -theory is the 4D $\mathcal{N}=2$ theory specified by

$$T^{\mathcal{S}}[C([1^N], [1^N], [1^N])] \quad (2.4.2)$$

namely a sphere with three full punctures.

By applying the previous formula (2.3.2), the dimensions of each branch are given by

$$\dim_{\mathbb{H}} \mathcal{M}_{\text{Higgs}} = \frac{1}{2}(3N + 2)(N - 1) \quad (2.4.3)$$

$$\dim_{\mathbb{C}} \mathcal{B}_{\text{Coulomb}}^{(k)} = k - 2 \quad (2.4.4)$$

In the simplest case $N = 2$, there is no Coulomb branch and the quaternionic dimension of the Higgs branch is 4. We have three $SU(2)$ -symmetry. This theory is expected as 4 free hypermultiplets Q_{abc} in the representation $\mathbf{2}_A \otimes \mathbf{2}_B \otimes \mathbf{2}_C$. Then, this theory is also referred to as the tri-fundamental hypermultiplet.

$N = 3$ is the next simplest case. In this case, there is a one dimensional Coulomb branch whose scaling dimension is three and the Higgs branch is eleven dimensional. The important point is that this theory has no gauge multiplet or holomorphic gauge coupling and is not a gauge theory although it has a non-trivial Coulomb branch. Since we do not know such a theory described by Lagrangian yet up to now, this theory is sometimes called no Lagrangian theory.¹²⁾

Gauging

First of all, we use the relation between the one-loop β function of holomorphic gauge couplings and central charge of the gauge symmetry currents [139].¹³⁾The coefficient of

¹²⁾In the IR after relevant deformations or moving to a generic point at the branch, this theory has an effective Lagrangian of one $U(1)$ vector multiplet as usual. It was also proposed that an UV $\mathcal{N}=1$ Lagrangian theory flows to this theory with the supersymmetry and the R-symmetry enhancement [138].

¹³⁾The flavor central charge k_F^{4D} which is the normalization of the OPE of currents or the two point correlation functions of flavor currents associated with F . We count the contribution of the half-hypermultiplet (one 4D $\mathcal{N}=1$ chiral multiplet) in the representation R as $T(R)$ ($T(\square) = 1$. See Appendix. A.1). This is the same notation used in [140] for instance. In the trace anomaly, k_F appears as the coefficient of quadratic term of the field strength [141].

the one-loop β function is proportional to sum of all the flavor central charges of matters and the vector multiplet. The contribution of vector multiplet is $-4h^\vee$.

Let us remark the computation of k_F associated to each puncture with a flavor symmetry F . For that purpose, we use the results reviewed in Appendix. F.3. Recall that, for the regular puncture specified by $[n] = \{s\}$, the flavor symmetry is given by $S(\prod_{a=1}^h U(d_a))$ where $d_a = s_a - s_{a+1}$. Each flavor symmetry $U(d_a)$ acts on the d_a fundamental hypermultiplets of $SU(k_a)$ as the d_a -dimensional representation where $k_a = \sum_{b=1}^a s_b$.

Now, we know $k_{SU(N)} = 2N$ for $SU(N)$ symmetry associated to the full puncture. The β -function for holomorphic gauge coupling vanishes when two $SU(N)$ symmetry associated with two full punctures are identified and gauged.

On the other hand, when we have a four fully-punctured sphere, in a degeneration limit associated to a pants decomposition (= choice of one-cycle in this case), they decompose into two different spheres with three full punctures one of which is new and weakly gauged. We represent this as

$$T^{\mathcal{S}}[C([1^N]_A, [1^N]_B, [1^N]_C, [1^N]_D)] \rightarrow T^{\mathcal{S}}[C([1^N]_A, [1^N]_B, [1^N]_E)]_{SU(N)_E} + T^{\mathcal{S}}[C([1^N]_E, [1^N]_C, [1^N]_D)] \quad (2.4.5)$$

and see Fig. 2.3.

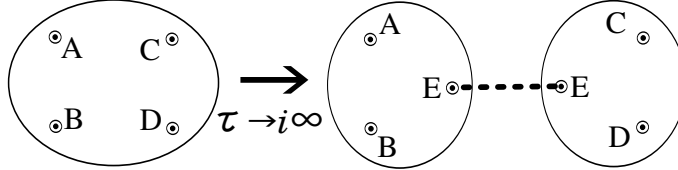


Figure 2.3: The sphere with four full punctures is decomposed into two sphere with three full punctures at the weak coupling limit in a duality frame.

The other decomposition corresponds to the weak coupling limit in other duality frame.

$$T^{\mathcal{S}}[C([1^N]_A, [1^N]_B, [1^N]_C, [1^N]_D)] \rightarrow T^{\mathcal{S}}[C([1^N]_A, [1^N]_C, [1^N]_F)]_{SU(N)_F} + T^{\mathcal{S}}[C([1^N]_F, [1^N]_A, [1^N]_D)] \quad (2.4.6)$$

Higgsing / Partially closing

Although we discuss the Nahm system, we translate it into the 4D language [142].

If we have global $SU(N)$ symmetry in 4D $\mathcal{N}=2$ SCFTs, there are BPS primary operators in the same supermultiplet as the flavor current belongs to. They are the triplet of $SU(2)_R$ R-symmetry and the adjoint representation of $SU(N)$ global symmetry. By giving a nilpotent VEV to the highest weight of those operators at UV point, we have

another SCFTs in the IR. This is called partially Higgsing/closure operation [125, 142]. The nilpotent orbit of $SL(N, \mathbb{C})$ can be always uniquely mapped to the Jordan normal forms $J_Y = \oplus_i J_{n_i}$ whose all eigenvalues vanish and they are classified by the partition $Y = [n_1, n_2, \dots, n_d]$ of N . Now that $SU(2)_R \times SU(N)$ global symmetry is spontaneously broken into a subgroup $U(1) \times G_Y$. In particular, this $U(1)$ is generated by

$$I_{IR}^3 := I_{UV}^3 \otimes 1 - 1 \otimes \frac{1}{2} \rho_Y^3 \quad (2.4.7)$$

where ρ_Y is the unique embedding homomorphism from $\mathfrak{su}(2)$ into $\mathfrak{su}(N)$ satisfying $J_Y = \rho_Y \left[\begin{pmatrix} 0 & 1 \\ 0 & 0 \end{pmatrix} \right]$, $\rho_Y^3 := \rho_Y \left[\begin{pmatrix} 1 & 0 \\ 0 & -1 \end{pmatrix} \right]$ and I_{UV}^3 is a diagonal R -symmetry generator of $SU(2)_R$. This R -symmetry generator in new IR SCFT is enhanced to $SU(2)_R^{IR}$ and the SCI can be also defined there.

Hereafter, we use the transpose of Y to specify the type of punctures. For example, $[1^N]$ represents the full (maximal) puncture and $[N-1, 1]$ does the simple (minimum) puncture.

2.4.2 Free hypermultiplet

In our analysis, we assume that all the SCFTs without any Coulomb branch are free hypermultiplets specified by the representation of the flavor symmetry. Under the condition that only untwisted regular punctures are allowed, we can classify them. Using the formula (2.3.8) and the condition $(d_C)_k = 0$ leads to the constraint $p_k^A + p_k^B + p_k^C = 2k - 1$ for $k = 2, 3, \dots, N$. We use the property that the regular punctures must satisfy $p_{k+1} - p_k = 0$ or 1 in addition. These constraints determine all the possibility of $p_k^{A,B,C}$ and all the three punctures combinations are listed in Table. 2.1. We categorize them into four classes. From the analysis later, we call each Bi-fundamental type, Second rank anti-symmetric type and two exceptional types.

To determine what representations of the explicit global symmetry associated to three punctures, we use the information about the dimension of the Higgs branch and flavor central charges for non-Abelian simple group.

theory	explicit flavor symmetry	d_H	flavor central charges
$T^S[C([1^N], [1^N], [N-1, 1])]$	$SU(N)_1 \times SU(N)_2 \times U(1)$	N^2	$k_{SU(N)_1} = k_{SU(N)_2} = 2N$
$T^S[C([1^N], [n^2], [n, n-1, 1])]$ ($N = 2n \geq 4$) $T^S[C([1^N], [n^2, 1], [n+1, n])]$ ($N = 2n+1 \geq 5$)	$SU(N) \times SU(2) \times U(1)^2$	$\frac{1}{2}N(N+3)$	$k_{SU(N)} = N, k_{SU(2)} = 2N$
$T^S[C([1^6], [2^3], [4, 2])]$	$SU(6) \times SU(3) \times U(1)$	28	$k_{SU(6)} = 12, k_{SU(3)} = 12$
$T^S[C([2, 1^4], [2^3], [3^2])]$	$SU(4) \times SU(3) \times SU(2) \times U(1)$	24	$k_{SU(4)} = 10, k_{SU(3)} = 12, k_{SU(2)} = 12$

Table 2.1: Classification of the class S free hypermultiplets and their data

Half-hypermultiplet

If we have an $\mathcal{N}=2$ supersymmetry (not superconformal), we can diagonalize the anti-commutators for physical states like $\{A_a^\dagger, A_b\} = \delta_{ab}(M \pm Z)$ ($a, b = 1, 2, 3, 4$). The irreducible representations are annihilated by A for example. In addition, the BPS representation consists of the states annihilated by half of these combined supercharges A^\dagger . Therefore, the dimension of that representation is four formed by $|\Omega\rangle, A_1^\dagger|\Omega\rangle, A_2^\dagger|\Omega\rangle$ and $A_1^\dagger A_2^\dagger|\Omega\rangle$. $|\Omega\rangle$ belongs to a representation R of the gauge/flavor group. This multiplet is usually not CPT invariant (R is mapped into R^*) and the physical multiplet is doubled to make them CPT invariant. But when R is pseudo-real, namely, an antisymmetric map $\epsilon : R \otimes R \rightarrow \mathbf{1}$ exists, this multiplet is CPT self-conjugate and physically allowed. This is called half-hypermultiplet. Notice that $\wedge^k \square$ is the pseudo-real representation when $k = N/2$ is odd.

As is well-known (see, for example, [143]), the fourth homotopy groups $\pi_4 G$ of simple groups are \mathbb{Z}_2 when $G = Sp(N), Sp(N)/\mathbb{Z}_2$ ($N = 1, 2, 3, \dots$) and trivial otherwise.

In [144], the global anomaly exists when there exists the odd number of even dimensional representations of $SU(2)$. To avoid that, we need the even number of half-hypermultiplets and this is why only hypermultiplets are allowed in the $SU(2)$ gauge theory.

Bi-fundamental type

The first case $T^{\mathcal{S}}[C([1^N], [1^N], [N-1, 1])]$ is well-known to be the bi-fundamental free hypermultiplet [14]. In fact, the bi-fundamental free hypermultiplets has $SU(N)_1 \times SU(N)_2 \times U(1)$ -symmetry where $U(1)$ is the baryon symmetry.

In them of $\mathcal{N}=1$ chiral multiplets, the representation is given as $(\mathbf{N}, \mathbf{N}, 1) \oplus (\overline{\mathbf{N}}, \overline{\mathbf{N}}, -1)$ and this means $k_{SU(N)_i} = 2N \times T(\square) = 2N$ ($i = 1, 2$). The degree of freedom in \mathbb{H} also equals to $d_H = N^2$.

We can also see this fact from the associated Seiberg-Witten curves.

Second rank anti-symmetric type

Although the class S realizations of the even and odd cases look different, we discuss both cases at the same time because the 4D physical properties are uniformly treated.

We have two cases. In the case that $N = 2n$ ($N \geq 4$ or $n \geq 2$) is even, the theory $T^{\mathcal{S}}[C([1^N], [n^2], [n, n-1, 1])]$ is rank 0. In the case that $N = 2n+1$ ($N \geq 5$ or $n \geq 2$) is odd, the theory $T^{\mathcal{S}}[C([1^N], [n^2, 1], [n+1, n])]$ is also rank 0.

However, the following arguments are independent from the even-odd property of N . Indeed, we can read off explicit flavor symmetry as $SU(N) \times SU(2) \times U(1)^2$ for $N \geq 5$ and $SU(N) \times SU(2)^2 \times U(1)$ when $N = 4$. In both cases, $k_{SU(N)} = 2N$ and $k_{SU(2)} = 2N$ ($k_{SU(2)_1} = 8$ and $k_{SU(2)_2} = 6$ when $N = 4$) holds true. The dimension of Higgs branch is given by $d_H = \frac{1}{2}N(N+3)$.

The matter content, namely, the representation in terms of the chiral multiplets, satisfying these conditions is following :

$$(\mathbf{N}, \mathbf{2}, *) \oplus (\overline{\mathbf{N}}, \mathbf{2}, *) \oplus (\wedge^2 \mathbf{N}, \mathbf{1}, *) \oplus (\wedge^2 \overline{\mathbf{N}}, \mathbf{1}, *) \quad (2.4.8)$$

where $*$ represents an undetermined $U(1)$ charge. When $N = 4$,

$$(\mathbf{4}, \mathbf{2}, \mathbf{1}, *) \oplus (\overline{\mathbf{4}}, \mathbf{2}, \mathbf{1}, *) \oplus (\wedge^2 \mathbf{6}, \mathbf{1}, \mathbf{2}, *) \quad (2.4.9)$$

We can see in Sec. 3.6 that this conjecture is consistent with the 4D/2D duality relation conjecture by deriving the SCI expression.

Exceptional case 1 : $\mathbf{T}^S[\mathbf{C}([\mathbf{1}^6], [\mathbf{2}^3], [\mathbf{4}, \mathbf{2}])]$

In this case, the flavor symmetry is $SU(6) \times SU(3) \times U(1)$, the flavor central charges are $k_{SU(6)} = 12$ and $k_{SU(3)} = 12$ and the Higgs branch dimension is $d_H = 28$.

The candidates satisfying the above conditions are the following two cases:

$$(\wedge^3 \mathbf{6} = \mathbf{20}, \mathbf{1}, *) \oplus (\mathbf{6}, \mathbf{3}, *) \oplus (\overline{\mathbf{6}}, \overline{\mathbf{3}}, *) \quad (2.4.10)$$

or

$$(\wedge^3 \mathbf{6} = \mathbf{20}, \mathbf{1}, *) \oplus (\wedge^3 \overline{\mathbf{6}} = \mathbf{20}, \mathbf{1}, *) \oplus (\mathbf{1}, \mathbf{Adj} = \mathbf{8}, *) \oplus (\mathbf{1}, \overline{\mathbf{Adj}} = \mathbf{8}, *) \quad (2.4.11)$$

In the author's knowledge, we cannot determine which candidate is actually true. However, we will see that the former case is true by the SCI computation.¹⁴⁾

Exceptional case 2 : $\mathbf{T}^S[\mathbf{C}([\mathbf{2}, \mathbf{1}^4], [\mathbf{2}^3], [\mathbf{3}^2])]$

In this case, the flavor symmetry is $SU(4) \times SU(3) \times SU(2) \times U(1)$, the flavor central charges are $k_{SU(4)} = 10$, $k_{SU(3)} = 12$ and $k_{SU(2)} = 12$ and the Higgs branch dimension is $d_H = 24$.

The candidate of the matter content is given by

$$(\wedge^2 \mathbf{4} = \mathbf{6}, \mathbf{1}, \mathbf{2}, *) \oplus (\mathbf{4}, \overline{\mathbf{3}}, \mathbf{1}, *) \oplus (\overline{\mathbf{4}}, \mathbf{3}, \mathbf{1}, *) \oplus (\mathbf{1}, \mathbf{3}, \mathbf{2}, *) \oplus (\mathbf{1}, \overline{\mathbf{3}}, \mathbf{2}, *) \quad (2.4.12)$$

and this is reproduced by computing the corresponding SCI in Sec. 3.6.

2.4.3 Rank 1 SCFT

Among the rank 1 SCFTs, we focus on the special rank 1 SCFTs with larger global symmetries. See [14, 41, 145, 146].

¹⁴⁾Naively speaking, if the latter case is true, there may exist a $SU(2)$ symmetry but such symmetry does not appear.

E_6 SCFT in A_2 -type

The first example of rank 1 SCFT we consider is the the E_6 theory of Minahan and Nemeschansky theory [147] or T_3 -theory which appeared at the strong coupling limit of the $SU(3)$ $N_f = 6$ superconformal QCD [41]. The corresponding punctured Riemann surface is the 2-sphere with three maximal/full punctures and the 4D theory is represented by $T^S[C([1^3], [1^3], [1^3])]$ as we see above. Although it was found in the analysis of the $SU(3)$ $N_f = 6$ Seiberg-Witten curve originally [147], we rephrase them from the punctured Riemann surface [14].

It can be also realized as a seven-three branes system in the type IIB string theory [145, 148]. In that set-up, the flavor symmetry and the Higgs branch of the theory on the D3-branes are the gauge symmetry and the instanton moduli of the theory on the seven branes respectively. Indeed, the dimension of the one-instanton moduli of E_6 after removing the center mode is given by $h_{E_6}^\vee - 1 = 11$. This is another evidence.

Let us start from the $SU(3)$ $N_f = 6$ SCFT. This is constructed from two bi-fundamental hypermultiplets $T^S[C([1^3], [1^3], [2, 1])]$ by gauging each $SU(3)$ flavor symmetry and then specified by $T^S[C([1^3], [1^3], [2, 1], [2, 1])]$. Now, we have other duality frame corresponding to different pants decomposition like

$$T^S[C([1^3], [1^3], [2, 1], [2, 1])] \rightarrow T^S[C([1^3], [1^3], [1^3])] + T^S[C([1^3], [2, 1], [2, 1])]. \quad (2.4.13)$$

$T^S[C([1^3], [1^3], [1^3])]$ is exactly the T_3 theory. However, a subtle problem happens. To see this, let us consider the remnant theory $T^S[C([1^3], [2, 1], [2, 1])]$. On computing the dimension of Coulomb branch, the formal number of the Coulomb branch operators whose scaling dimension is 3 is negative, namely, -1 . This implies that the total theory has not $SU(3)$ symmetry but only subgroup. Indeed, this is true and $SU(3)$ is broken to $SU(2)$. In terms of the Higgs branch, the formal Higgs branch dimension is 7 but, at a generic point, $SU(3)$ cannot be completely Higgsed after gauging. If there remains $SU(2)$ gauge symmetry in the reduction from 6D to 4D, five NG hypermultiplets are eaten by gauge bosons and there remains only two which charged under $SU(2)$. Indeed, the flavor central charge $k_{SU(2)}$ contributing from this and T_N theory is given by 2 and 6 respectively, and the β -function of this $SU(2)$ gauge coupling vanishes. These theories with different flavor symmetries between at UV and at IR are called bad [149].

E_7 SCFT in A_3 -type

The next SCFT is expected to have E_7 symmetry and given by $T^S[C([1^4], [1^4], [2, 2])]$. There is one Coulomb branch operator with the scaling dimension 4 and the Higgs branch dimension is 17. With the same reason before, this coincides with the dimension of the instanton moduli space $h_{E_7}^\vee - 1 = 17$.

Let us remark the class S construction from some Lagrangian theory. Using the previous results in free hypermultiplets, the theory $T^S[C([1^4], [3, 1], [2, 2], [2, 1, 1])]$ is realized as $SU(4)$ gauge theory with three fundamental hypermultiplet and single third-rank an-

tisymmetric half-hypermultiplet like

$$T^{\mathcal{S}}[C([1^4], [3, 1], [2, 2], [2, 1, 1])] = T^{\mathcal{S}}[C([1^4]_G, [1^4], [3, 1])] +_G T^{\mathcal{S}}[C([1^4]_G, [2, 2], [2, 1, 1])]. \quad (2.4.14)$$

Now let us consider another decomposition like

$$T^{\mathcal{S}}[C([1^4], [3, 1], [2, 2], [2, 1, 1])] = T^{\mathcal{S}}[C([1^4]_H, [1^4], [2, 2])] +_H T^{\mathcal{S}}[C([1^4]_H, [3, 1], [2, 1, 1])]. \quad (2.4.15)$$

In the same reason as before, $SU(4)$ gauge symmetry is broken to its subgroup, actually, $SU(3)$ gauge symmetry. The formal Higgs branch dimension of the theory $T^{\mathcal{S}}[C([1^4]_H, [3, 1], [2, 1, 1])]$ is 13. After the gauging process, there remain 6 hypermultiplets in the IR. If they forms the fundamental representations of $SU(3)$, there are two such hypermultiplets whose central charges is given by $k_{SU(3)} = 4$. The sum of central charges is 12 which assures that this is conformally gauged.

E_8 SCFT in A_5 -type

The final rank 1 SCFT is given by $T^{\mathcal{S}}[C([1^6], [2^3], [3^2])]$. There is one Coulomb branch operator with the scaling dimension 6 and the Higgs branch dimension is $29 = h_{E_8}^{\vee} - 1$.

The class S construction from some Lagrangian theory is following. We can construct $SU(6)$ conformal gauge theory with five fundamental hypermultiplets, single second-rank anti-fundamental hypermultiplets and single third-rank anti-fundamental hypermultiplets. That is to say, $(\square \oplus \bar{\square})^{\oplus 5} \oplus (\wedge^2 \square \oplus \wedge^2 \bar{\square}) \oplus (\wedge^3 \square)$. That SQCD corresponds to $T^{\mathcal{S}}[C([2^3], [3^2], [4, 2], [3, 2, 1])]$ in the class S language.

$$T^{\mathcal{S}}[C([2^3], [3^2], [4, 2], [3, 2, 1])] = T^{\mathcal{S}}[C([1^6]_G, [3^2], [3, 2, 1])] +_G T^{\mathcal{S}}[C([1^6]_G, [2^3], [4, 2])]. \quad (2.4.16)$$

Other decomposition we consider is given by

$$T^{\mathcal{S}}[C([2^3], [3^2], [4, 2], [3, 2, 1])] = T^{\mathcal{S}}[C([1^6]_H, [2^3], [3^2])] +_H T^{\mathcal{S}}[C([1^6]_H, [3, 2, 1], [4, 2])]. \quad (2.4.17)$$

In this case, the additional coupling theory is $T^{\mathcal{S}}[C([1^6]_H, [3, 2, 1], [4, 2])]$. The formal Higgs branch dimension is given by 26 and the number of the formal Coulomb branch operator with the scaling dimension 6 is -1 . It is expected that $SU(6)$ is broken into $SU(5)$ in this case. In this case, if we assume that all belong to the fundamental representation of $SU(5)$, $SU(5)$ symmetry is not conformally gauged. To make it conformally coupled, the remaining 15 hypermultiplets should be the sum of single fundamental hypermultiplet and single second-rank anti-symmetric hypermultiplet. Indeed, the flavor central charge for these matters is given by $2 + 6 = 8$ and that from the rank 1 SCFT sector is 12. The sum cancels the contribution -20 from the $SU(5)$ vector multiplet.

Chapter 3

Superconformal index and 2D q -deformed Yang-Mills

First of all, let us define the full superconformal indices (SCIs) in the absence of any defects. [31]. When we add several conformal BPS-defects, the original superconformal symmetry is partially broken. However, using this general definition, we can define the superconformal indices in the presence of these defects in the same way.

In particular, in 4D $\mathcal{N}=2$ superconformal case, they are formal power series of three variables each coefficient of which is a polynomial of flavor fugacities. ¹⁾Furthermore, there are many special limits : Macdonald limits, Schur limit, Hall-Littlewood limit Coulomb limit. In this thesis, we mainly focus on the Schur limit ²⁾ and, in this limit, the SCIs are usually called Schur indices. Only this limit allow the loop operators (and domain walls) although the surface operators are allowed in any cases. In this special case, there are two other approaches to Schur indices : the vacuum characters of hidden chiral algebras [140] and the trace of Kontsevich-Soibelman quantum monodromy operators associated to their IR BPS quivers [36, 150, 151].

3.1 State-operator correspondence

One of the most important properties (but assumption) of CFT is the state-operator correspondence. Consider any d -dimensional connected open region with a local operator inserted at a point inside it. After removing the point, it has a non-trivial topology like $\mathbb{R} \times S^{d-1}$ which allows us to reinterpret the first \mathbb{R} -component as a new time direction. In other words, we view some $d - 1$ dimensional surfaces surrounding that point as the time slice. If we have an exact symmetry which generates the translation along the radial direction, we have the new Hamiltonian which equals to the dilatation operator in the

¹⁾I do not know the proof for general 4D $\mathcal{N}=2$ SC theories but this claim holds true for free hypermultiplets and vector multiplets.

²⁾There are two Schur limits, $q = t$ and $p = t$, which are exchanged under a $SO(4)$ rotational symmetry $(z, w \rightarrow w, -z)$.

flat Euclidean space. This happens for CFTs or, TQFTs which are more symmetric and where there are many candidates for the new Hamiltonian.

$\mathcal{H}_{S_r^{d-1}}$ denotes the Hilbert space over the S_r^{d-1} which is the $d - 1$ dimensional sphere with the radius r . The scaling symmetry suggests the isomorphism between the Hilbert space with different radii

$$\mathcal{H}_{S_{r_1}^{d-1}} \simeq \mathcal{H}_{S_{r_2}^{d-1}} \quad (3.1.1)$$

and, hereafter, we denote the representative space $\mathcal{H}_{S^{d-1}}$.

In this set-up, the state-operator correspondence claims that there is a natural isomorphism³⁾ between the local operators and the states of $\mathcal{H}_{S^{d-1}}$. In particular, in the unitary theory, the vacuum state $|\Omega\rangle$ have zero eigenvalue which is minimum for the scaling operator D . Therefore, the identity operator corresponds to the vacuum state. Now, the general map from operators into states is simple:

$$|\phi\rangle := \phi(0)|\Omega\rangle = \lim_{x \rightarrow 0} \phi(x)|\Omega\rangle \quad (3.1.2)$$

and this means that the eigenvalues of each generators of the symmetry for $|\psi\rangle$ if diagonalized equal to that of local operators.

Conversely, if we specify all the weights of the symmetry group, the corresponding local operators are expected to be almost unique, at least, we have no general way to distinguish them. Here we assume that the inverse map from any state into local operators exists.

In the discussion of superconformal theories, there is an important class of local operators called superconformal primary (or chiral primary). In $d = 4$, we use this terminology for the operators $\mathcal{O}(x)$ satisfying the condition $[\mathcal{S}, \mathcal{O}(0)] = [\tilde{\mathcal{S}}, \mathcal{O}(0)] = 0$. See the notation in Appendix. B. In the state language, this means that the states are annihilated by $\mathcal{S}, \tilde{\mathcal{S}}$. The superconformal primary property automatically assures the primary condition $[K_\mu, \mathcal{O}(0)] = 0$ and $\mathcal{O}(x)$ is called a primary operator.

Conformal mapping

Next, we show that $\mathbb{R}^d \setminus \{0\}$ and $S^{d-1} \times \mathbb{R}$ are conformally equivalent. In the above discussion, we do not need this mapping at all. However, this map naturally introduces the supersymmetry on S^{d-1} . In other words, we can discuss the defects configurations in the original flat space and the unbroken symmetry algebra associated to them.

Let us consider a following conformal map

$$\begin{aligned} \varphi : \mathbb{R}^d \setminus \{0\} &\longrightarrow S^{d-1} \times \mathbb{R} \\ \Downarrow &\qquad \qquad \qquad \Downarrow \\ (x^a) &\longmapsto (\Omega_{S^{d-1}}, \tau := \log(r)) \end{aligned} \quad (3.1.3)$$

³⁾Here, we ignore the structures other than additions and symmetry actions, namely, the operator product expansion (OPE), for example.

where the Euclidean \mathbb{R}^d is equipped with a natural Descartes coordinate $\{x^a\}$, $\{0\}$ is its origin and $r := \sqrt{x^a x_a}$.⁴⁾ These two geometries with natural metrics are conformally equivalent because of

$$ds_{\mathbb{R}^d}^2 = dx^a dx_a = dr^2 + r^2 d\Omega_{S^{d-1}} = r^2 \left(\frac{dr^2}{r^2} + d\Omega_{S^{d-1}} \right) = e^{2\tau} (d\tau^2 + d\Omega_{S^{d-1}}) = e^{2\tau} ds_{\mathbb{R} \times S^{d-1}}^2. \quad (3.1.4)$$

When $d = 4$, notice that the natural $U(1)^2$ action on \mathbb{C}^2 are identified with the Cartan $U(1)^2$ in $SO(4)$ acting on S^3 if we take a complex structure and identify \mathbb{R}^4 as \mathbb{C}^2 following it.

The S^1 compactification does not break neither supersymmetry and conformal symmetry, and after this conformal mapping, we usually perform this reduction. This implies the equivalence between the superconformal indices and $S^{d-1} \times S^1$ partition functions [32]. In fact, this is true in some sense, however, when $d = 4$ at least, there is a subtle difference usually called supersymmetric Casimir energies, or some anomaly not removed by finite supersymmetric counter terms [152–155], finally related to the central charges a, c . In this thesis, we ignore this subtle quantity.

Conjugation

In the ordinary canonical quantization, the Hilbert space consists of the set of normalized functions over \mathbb{R}^{d-1} and the Hamiltonian $H = P^0$ acts on it. Any wave function is a functional over such configuration space. Similarly, in the radial quantization, the normalized functions over S^{d-1} give the new Hilbert space $\mathcal{H}_{S^{d-1}}$ on which the new Hamiltonian D (dilatation/scaling operator) acts. The state-operator correspondence says that any element of $\mathcal{H}_{S^{d-1}}$ is generated by a local operator insertion.

Hereafter, unless we refer to, we use the symbol \dagger as the conjugation in the radial quantization sometimes called *BPZ* conjugation. Roughly speaking, this operation corresponds to $\tau \rightarrow -\tau$ (inversion). An in-state identified as a local operator at the origin is mapped into an out-state identified as that at the infinity. In the original conjugation on $\mathbb{R}^3 \times \mathbb{R}$, the translation generators P_μ are mapped into themselves. However, in this conjugation, they are mapped into the special conformal translation generator K_μ . See also the BPZ conjugation part in Appendix. B.

Conformal defect

Let us consider non-local defects not breaking the scaling symmetry. Such defects must pass through the origin at least.⁵⁾ Among them, we consider defect locus preserving the

⁴⁾In the Minkowski metric, this space is conformally equivalent to $AdS_2 \times S^2$ which do not have any global time. Therefore, SCIs are defined only in the Euclidean CFT in this thesis.

⁵⁾We can map such defects into others not passing through the origin with the broken symmetry generators. Such generators change the defects locus by definition. Strictly speaking, in the context of SCIs, we only allow the generators commuting the supercharges to define the SCIs.

maximal symmetry as possible. The natural choice of such locus of the codimension q conformal defects in \mathbb{R}^d is the hyperplane \mathbb{R}^{d-q} . Since they extend along the radian direction, after the conformal mapping, the defect locus is S^{d-q-1} in S^{d-1} .

In these cases, the Hilbert space is the wave functional satisfying some boundary conditions, for example. In the operator language, it is expected that the corresponding operators are the defect local operators induced by $4D$ local operators.

More precisely, we have two interpretations at least in gauge theories. One interpretation is natural in the line operators, namely, codimension one defects, of gauge theories. They are bulk local operators which can be line changing operators or junction operators in general [151]. The other interpretation is also natural in coupled systems in gauge theories with gauge symmetry G . If we have a bulk local operator $\phi_A(0)$ in a representation R for G and a defect local operator $\tilde{\phi}^A(0)$ in R^* for G which may be the flavor symmetry for defect theories, after gauging, there is a composite gauge-singlet operator like

$$(\phi_A \tilde{\phi}^A)(0) \tag{3.1.5}$$

and, in the SCI languages, it counts such composite operators satisfying some BPS conditions as discussed later.

3.2 General definition

Let \mathfrak{sc} be the superconformal algebra. In the important case $d = 4$, $\mathfrak{sc} = \mathfrak{su}(2, 2|\mathcal{N})$ ($\mathcal{N}=1, 2, 3$) or $\mathfrak{psu}(2, 2|4)$ ($\mathcal{N}=4$). See Appendix. B.

By the definition of the super Lie algebra, \mathfrak{sc} is decomposed into two parts as follows:

$$\mathfrak{sc}^B := \{X \in \mathfrak{sc} \mid (-1)^F X = X(-1)^F\} \tag{3.2.1}$$

$$\mathfrak{sc}^F := \{X \in \mathfrak{sc} \mid (-1)^F X = -X(-1)^F\} \tag{3.2.2}$$

where $(-1)^F$ is the operator giving the \mathbb{Z}_2 grading structure in \mathfrak{sc} . Notice that \mathfrak{sc}^B is closed under the Lie bracket but \mathfrak{sc}^F is not so, that is to say, $\{\mathfrak{sc}^F, \mathfrak{sc}^F\} \subset \mathfrak{sc}^B$ where $\{, \}$ is the super Lie bracket. Let \mathfrak{h} be the Cartan subalgebra of \mathfrak{sc}^B including $\mathfrak{so}(1, 1)$.⁶⁾ In addition to the super Lie algebra structure, there is a involution called the conjugation in the canonical quantization. As remarked before, the \dagger operation depends on the time axis and we also use \dagger associated to the radial quantization.

⁶⁾In general, some Lie algebras over \mathbb{R} has several Cartan subalgebras which are non-conjugate each other. However, in the d dimensional Euclidean conformal theory, \mathfrak{sc}^B is considered to consist of the conformal algebra $\mathfrak{so}(d+1, 1)$ and the R-symmetry algebra which may be a compact Lie algebra. The later algebra has the unique Cartan subalgebra. The former one also has the unique one when d is even but two different ones when d is odd [156]. There, we choose the Cartan subalgebra whose Lie group has a non-compact direction. Notice also that, in the Minkowski CFT cases, the above statement does not hold true for all d .

Comments on choices of \mathcal{Q}

Now, let us pick up a supercharge denoted \mathcal{Q} which is an element of $\mathbb{C}^* \backslash (\mathfrak{sc}^F \setminus \{0\})$ (scaling is not irrelevant). Then, we can define a superconformal index for each choice of \mathcal{Q} . However, in usual, we have several essentially different SCIs. Let us discuss this briefly before defining SCIs. First of all, we can divide \dagger operation as we easily see from the definition remarked later. Next, let us consider $SC^B = \text{Exp}(\mathfrak{sc}^B)$ -orbit of \mathcal{Q} denoted $SC^B(\mathcal{Q}) := \{\rho(g)\mathcal{Q} \mid g \in SC^B\}$ where ρ is the representation to which the supercharges belong. Any supercharge in $SC^B(\mathcal{Q})$ may give the same SCI.⁷⁾ In 4D $\mathcal{N}=2$ case, as vector spaces, $\mathfrak{sc}^F \simeq (\mathbf{4}, \mathbf{2}) \oplus (\bar{\mathbf{4}}, \bar{\mathbf{2}})$ under $SO(5, 1)_C \times U(2)_R$. There, we identify this as a pair of 2×4 matrices $\mathcal{Q} = (\mathcal{Q}, \tilde{\mathcal{S}})$ and $\tilde{\mathcal{Q}} = (\tilde{\mathcal{Q}}, \mathcal{S})$. To have the maximal bosonic symmetry, it is expected that \mathcal{Q} must belong to either representation of $SO(5, 1)_C \times U(2)_R$, that is to say, either $C = 0$ or $\tilde{C} = 0$ for $\mathcal{Q} = \text{Tr}[C\mathcal{Q}] + \text{Tr}[\tilde{C}\tilde{\mathcal{Q}}]$ where C, \tilde{C} are 4×2 matrices. Then, the choice of C after the quotient by $SO(5, 1) \times U(2)$ is expected to be classified by the rank, namely, 1 or 2. The first case is $\tilde{\mathcal{Q}}_1^\dagger$ and the latter case is $\tilde{\mathcal{Q}}_1^\dagger + \tilde{\mathcal{Q}}_2^\dagger$ which corresponds to the $pq = t$ limit (See Sec. B.1.1). When the bosonic symmetry is allowed to be smaller, we can take linear combinations of elements both from \mathcal{Q} and from $\tilde{\mathcal{Q}}$. This includes the Schur limit we will focus on later.

Weights for the commutant group of \mathcal{Q}

As it is well believed in quantum mechanics, any state is specified by the eigenvalues of all generators (sometimes called weights) which commute each other up to the label of finite degeneracy. To see such generators, let us define the commutant of \mathcal{Q} and \mathcal{Q}^\dagger at first.

$$\mathfrak{z} := \mathfrak{z}_{\text{sc}}(\mathcal{Q}, \mathcal{Q}^\dagger) := \{X \in \mathfrak{sc} \mid [X, \mathcal{Q}] = [X, \mathcal{Q}^\dagger] = 0\} \quad (3.2.3)$$

Next, let \mathfrak{h} be a maximal and commutative subalgebra in $\mathfrak{sc}^B \cap \mathfrak{z}$. Since $\mathcal{E} := \{\mathcal{Q}, \mathcal{Q}^\dagger\} \in \mathfrak{z}$ and $[\{\mathcal{Q}, \mathcal{Q}^\dagger\}, Y] = 0$ for $\forall Y \in \mathfrak{h}$ by definition, $\mathcal{E} = \{\mathcal{Q}, \mathcal{Q}^\dagger\} \in \mathfrak{h}$ always holds true. Furthermore, $\{\mathcal{Q}, \mathcal{Q}^\dagger\}$ includes D which is a generator of non-compact algebra, namely, \mathbb{R} . Then, in general, $\text{Lie}(\mathfrak{h}) \simeq U(1)^\ell \times \mathbb{R}$ when the R-symmetry is compact group. We assume that this subalgebra is unique up to the conjugacy action of $\mathfrak{sc}^B \cap \mathfrak{z}$ after we fix \mathcal{Q} .

Suppose $\{Y_\alpha\}_\alpha$ generate \mathfrak{h} and are linearly independent each other. G_F and \mathfrak{f} denote the global symmetry and its Cartan subalgebra which is unique up to the conjugacy action. $\{F_i\}_i$ are their basis of \mathfrak{f} .

In summary, the Cartan subalgebra which commutes with \mathcal{Q} is generated by

$$\mathcal{E}, \quad Y_{\alpha=1,2,\dots,\ell}, \quad F_{i=1,2,\dots,\text{rk}G_F} \quad (3.2.4)$$

⁷⁾Here we assume that for any $\mathcal{Q}' \in SC^B(\mathcal{Q})$, there exists $g \in SC^B$ such that $\mathcal{Q}' = g\mathcal{Q}g^{-1}$. Then, $\mathfrak{h}' = g\mathfrak{h}g^{-1}$ in the above definition.

Fermion number

The super Lie algebra is graded by $(-1)^F$ called ‘‘Fermion number’’. Indeed, to define the SCI, we must specify the action of $(-1)^F$ on the Hilbert space. Rigorously speaking, $(-1)^F$ is not an element of the superconformal algebra and we want to express it in terms of the algebra, actually, its Lie group of \mathfrak{sc}^B .⁸⁾

For that purpose, recall the property $(-1)^F \mathcal{Q} = -\mathcal{Q}(-1)^F$ and $(-1)^F \mathcal{Q}^\dagger = -\mathcal{Q}^\dagger(-1)^F$. If we take L satisfying

$$[L, \mathcal{Q}] = \frac{1}{2} \mathcal{Q} \pmod{\mathbb{Z}\mathcal{Q}}, \quad (3.2.5)$$

it is possible to define it as

$$(-1)^F := \exp(2\pi i L). \quad (3.2.6)$$

Furthermore, we need the condition $[(-1)^F, Y_\alpha] = 0$. When \mathfrak{h} is a Cartan subalgebra including \mathfrak{h} , $L \in \mathfrak{h}$ is sufficient condition for this and we take L from \mathfrak{h} . Notice that there is ambiguity of the choice because of the addition of \mathfrak{h} .

In the 4D theory, we have one choice $L = j_1 + j_2$, namely, $(-1)^F = e^{2\pi i(j_1 + j_2)}$ where j_1 and j_2 are the Cartan of $SO(4)$ isometry. This choice is maybe natural by recalling the spin-statistical theorem where F is exactly the fermion number. In the case of 4D $\mathcal{N}=2$ systems, this can be also true for $L = -I$, namely, $(-1)^F = e^{2\pi i I}$ where I is the Cartan of $SU(2)_R$ symmetry or for $L = r$ which is the Cartan of the $U(1)_r$ -symmetry. We will see this ambiguity of choice later.

If we define \mathcal{Q} to be a natural basis, namely, the eigenstate of the action of \mathfrak{h} , we can always say

$$\mathfrak{h} = \mathfrak{h} \oplus \mathfrak{h}^\perp \quad (3.2.7)$$

where

$$\mathfrak{h}^\perp = \mathbb{R}L \quad \mathfrak{h} = \mathbb{R}\mathcal{E} \oplus \bigoplus_{\alpha} \mathbb{R}Y_\alpha. \quad (3.2.8)$$

In this discussion, when we choose \mathcal{Q} be the above simple one, the maximal number of fugacities associated to the superconformal symmetry is given by $\dim \mathfrak{h} - 2$.

Superconformal index

Now, we can define the fully refined superconformal indices by

$$\mathcal{I}(a; b, y) := \text{Tr}_{\mathcal{H}_{S^{d-1}}} \left[(-1)^F b^{\mathcal{E}} \prod_{\alpha} y_{\alpha}^{Y_{\alpha}} \prod_i a_i^{F_i} \right]. \quad (3.2.9)$$

⁸⁾Strictly speaking, we cannot identify $(-1)^F$ for \mathfrak{sc} and $(-1)^F$ in the SCI in general. Instead, we have a weaker condition that $(-1)^F$ plays a role of \mathbb{Z}_2 -grading operator for \mathfrak{h} . In fact, only the property to define SCI is $\{(-1)^F, \mathcal{Q}\} = 0$, $((-1)^F)^\dagger = (-1)^F$ and $[(-1)^F, Y_\alpha] = [(-1)^F, F_i] = 0$. However, through this thesis, we use the same symbols both for \mathfrak{sc} and for the SCIs.

where the action of $(-1)^F$ on the Hilbert space is defined later. Notice that the SCIs depends on the choice of \mathcal{Q} up to the inner automorphism $\text{Inn}(\mathfrak{sc})$ as seen before. Therefore, if the duality acts on the supercharge non-trivially (map to the different SC^B -orbit) such as the 3D $\mathcal{N}=4$ mirror symmetry, we care about the supercharge choice in the duality check. However, in 4D with any supercharges, since it is believed that there is no non-trivial actions up to phase (See a footnote in [45] for $\mathcal{N}=4$), we have no troubles in the later discussion.

Next, we discuss several properties about this quantities.

3.2.1 b -independence

Grading

To this end, let us decompose Hilbert space according to its weights discussed above. First of all, it decomposes into the bosonic sector and the fermionic sector following $(-1)^F$ as

$$\mathcal{H}_{S^{d-1}} = \mathcal{H}_{S^{d-1}}^B \oplus \mathcal{H}_{S^{d-1}}^F. \quad (3.2.10)$$

⁹⁾ On the other hand, we have the weights (other than \mathcal{E} here) decomposition as

$$\mathcal{H}_{S^{d-1}} = \bigoplus_{y_\alpha, f_i} \mathcal{H}_{S^{d-1}}^{(y_\alpha, f_i)}. \quad (3.2.11)$$

Non-BPS cancellations

Here we see that the contributions from the Hilbert space with $\mathcal{E} > 0$ cancels.

There are two important properties to show this. One is the unitarity implying that there is no zero norm in the physical Hilbert space except zero itself. The other is that, in the quantum mechanical description, the Hamiltonian \mathcal{E} (either in the radial or in the ordinary quantization) is generated by odd charges \mathcal{Q} in the algebra of symmetry.

Let us take one of states $|v\rangle := |E, y_\alpha, f_i; \alpha\rangle \in \text{Ker}(\mathcal{Q})$ with definite charges for Y_α and F_i and positive E (the eigenvalue of \mathcal{E}) where α is other labels if exists. ¹⁰⁾ Then, $\mathcal{Q}^\dagger|v\rangle$ has the same charges. $(\mathcal{Q}^\dagger)^2 = 0$ and $\mathcal{Q}(\mathcal{Q}^\dagger|v\rangle) = E|v\rangle$ mean that $|v\rangle$ and $\mathcal{Q}^\dagger|v\rangle$ forms an irreducible representation of the super algebra $\langle \mathcal{Q}, \mathcal{Q}^\dagger, \mathcal{E} \mid \{\mathcal{Q}, \mathcal{Q}^\dagger\} = \mathcal{E} \rangle$ when $E \neq 0$. This also means

$$\mathcal{H}_{S^{d-1}}^{(E>0, y, f), B} \simeq \mathcal{H}_{S^{d-1}}^{(E>0, y, f), F}. \quad (3.2.12)$$

Furthermore, the unitarity implies

$$\| \mathcal{Q}^\dagger|v\rangle \|^2 = \langle v | \{\mathcal{Q}, \mathcal{Q}^\dagger\} | v \rangle = E \geq 0. \quad (3.2.13)$$

⁹⁾We do not discuss other possibilities like $(-1)^F$ acts on the state as the non-real phase.

¹⁰⁾We can always take the state in $\text{Ker}(\mathcal{Q})$ because \mathcal{Q} commutes with the charges and $\mathcal{Q}^2 = 0$ means $\text{Im}(\mathcal{Q}) \subset \text{Ker}(\mathcal{Q})$.

and $E = 0$ is equivalent to $|v\rangle \in \text{Ker}(\mathcal{Q}^\dagger)$.

In summary,

$$\mathcal{H}_{S^{d-1}}^{BPS} := \mathcal{H}_{S^{d-1}}^{E=0} \simeq \text{Ker}(\mathcal{Q}) \cap \text{Ker}(\mathcal{Q}^\dagger) \quad (3.2.14)$$

$$\mathcal{H}_{S^{d-1}}^{E>0} = \mathbf{2}_{\text{pair}} \otimes V \quad (3.2.15)$$

where $\mathbf{2}_{\text{pair}}$ is the above irreducible representation and V is the vector space for the label α .

Since $\text{Tr}_{\mathbf{2}_{\text{pair}}} [(-1)^F] = 0$, it is enough to take the trace over $\mathcal{H}_{S^{d-1}}^{BPS}$. So, the index has the form like

$$\mathcal{I}(a; y) = \sum_{y,f} \prod_{\alpha,i} y_\alpha^{x_\alpha} a_i^{f_i} \text{Tr}_{\mathcal{H}_{S^{d-1}}^{BPS,(y_\alpha,f_i)}} [(-1)^F] \quad (3.2.16)$$

where we assumed that the eigenvalues are discrete. Now, the SCI is clearly b -independent and we can drop off the b in the expressions. ¹¹⁾

3.2.2 A few comments

Constant series over conformal manifolds

The SCIs are expected to be invariant under any exactly marginal deformation. ¹²⁾ In 4D $\mathcal{N}=2$ SCFTs, the holomorphic gauge couplings are such parameters and it is believed that they are only possible deformations. Since the SCIs just count the BPS local operators with \mathbb{Z}_2 -grading, and each coefficient is always integer. Therefore, there are two possibilities : discontinuous changes of the coefficients and continuous changes of the exponents of fugacities. The former case does not happen because we focus on the Hilbert space on the compact space and the long multiplets do not contribute to the SCI.

Let us remark on the latter case. Since the weights of compact Lie groups are discrete, only the scaling dimensions and r -charges of BPS operators can be continuous. However, in all the known examples, they are discretized, namely, valued in the integer multiples of some fractional number. Moreover, according to [157], we can restrict the form of the exactly marginal operators¹³⁾ which ensures the vanishing of three points correlators of two chiral operators and any single exactly marginal operator.

The independence of SCIs from the holomorphic couplings enables us to evaluate them at any point of the conformal manifold. As seen in Sec. 3.4.1 in the 4D $\mathcal{N}=2$ SCFTs, we can evaluate them at the weakly coupled region where some almost free Lagrangian descriptions may exist. In other words, we can compute the SCIs in the near free limit if exists. In such regions, the Lagrangian consist of those of hypermultiplets and vector multiplets and it is enough to evaluate it for each multiplet and finally to couple them.

¹¹⁾We also assume that each BPS Hilbert space over S^{d-1} is finite dimensional.

¹²⁾As commented in [31], all the deformation operators commuting with the chosen supercharge to define the SCI are allowed.

¹³⁾We greatly thank Y.Tachikawa for telling us this fact and K.Yonekura for proving the invariance of SCI based on this fact.

In the class S cases, by construction, the conformal manifolds are identified with the Teichmüller spaces which are moduli spaces of punctured Riemann surfaces C .

Let $\mathcal{C}, \mathcal{T}_{\mathfrak{g}}^{\mathcal{S}}$ and $\mathcal{I}_{p,q,t}$ be the set of all the punctured Riemann surface with the holonomies data at punctures and with the complex moduli, a map from \mathcal{C} to the set of 4D $\mathcal{N}=2$ SCFTs $\mathcal{T}_{4\text{D } \mathcal{N}=2 \text{ SCFT}}$ and the SCI map from $\mathcal{T}_{4\text{D } \mathcal{N}=2 \text{ SCFT}}$ to $C_{p,q,t,\{a\}} = \mathbb{Z}[[p^{1/2}, q^{1/2}, t^{\pm 1/2}]] \otimes \mathbb{Z}((a))$ where p, q and t are fugacities for \mathfrak{h} as introduced later in Sec. 3.4 and $\mathbb{Z}((a))$ (a is the set of flavor fugacities) depends on the theory respectively.¹⁴⁾ After the choice of C other than the complex moduli, the composition $\mathcal{Z}_{\mathfrak{g},p,q,t} := \mathcal{I}_{p,q,t} \circ \mathcal{T}_{\mathfrak{g}}^{\mathcal{S}}|_{\mathcal{C}(C)}$ is the map from the moduli space \mathcal{M}_C of C to $C_{p,q,t,\{a\}}$ but constant from the above discussion. The important point is that $\mathcal{Z}_{\mathfrak{g},p,q,t}$ can be regarded as a TQFT correlator on C . In Sec. 3.5, we see that $\mathcal{Z}_{\mathfrak{g},p,q,t}$ in some special limit ($q = t$) is essentially same as the 2D topological q -deformed Yang-Mills correlators.

At the most singular point of \mathcal{M}_C , C fully degenerate to a trivalent graph Γ and we can evaluate the above map. Let \mathcal{I}_{Γ} be the integral expression of it based on the gauging operations (discussed below) where there is an integral over a subgroup of H in G at each internal edge. Therefore, when we have two different degenerations Γ_1 and Γ_2 , there should be the equality $\mathcal{I}_{\Gamma_1} = \mathcal{I}_{\Gamma_2} \in C_{p,q,t,\{a\}}$ which is highly non-trivial. Notice that these infinitely many non-trivial equalities becomes trivial, however, after the identification as the q -deformed Yang-Mills correlators.

Unitarity bound

First of all, recall that we have the degree of freedom to change the basis $\{Y_{\alpha}\}_{\alpha}$ of \mathfrak{h} . If we have the special basis written as $\hat{Y}_{\beta} := \{\hat{Q}_{\beta}^{\dagger}, \hat{Q}_{\beta}\}$ by using \hat{Q} for some β 's, the eigenvalues of \hat{Y}_{β} are non-negative on $\mathcal{H}_{S^{d-1}}$. This is because, in unitary theories, the squared norm of any physical state is positive and \hat{Q}_{β} map any physical state to other physical state or 0. \hat{y}_{α} is uniquely defined by

$$\prod_{\alpha} y_{\alpha}^{Y_{\alpha}} = \prod_{\alpha} \hat{y}_{\alpha}^{\hat{Y}_{\alpha}}. \quad (3.2.17)$$

One way to find the above \hat{Q} 's is to take them from

$$\mathfrak{r} := \mathfrak{z} \cap \mathfrak{sc}^F \quad (3.2.18)$$

where $\{\mathfrak{r}, \mathfrak{r}\} \subset \mathfrak{h}$.

When we view the SCIs as the formal polynomial of \tilde{y}_{β} where β may not run over all indices of the new basis of \mathfrak{h} , their exponents are always non-negative.

Gauging process

The final comment is on the ‘‘gauging’’ of flavor symmetries.

¹⁴⁾Here we ignore the rigorous mathematical treatments and do not insert any defects.

Consider several superconformal theories with a simple flavor symmetry G at least denoted by $T_i = T_i[G]$ ($i = 1, 2, \dots, s$) and assume that they are conformally gauged together, that is to say, the sum of the flavor symmetry central charge $k_{G,i}$ associated to G equals to $4h_G^\vee$. Then, the SCI of the resulting theory denoted by \hat{T} is given by

$$\mathcal{I}_{\hat{T}}(\{z_A\}_A) = \oint_{\mathbb{T}_G} [d\mathbf{a}] \Delta_{\text{Haar}}(a) \mathcal{I}_{\text{vector}}(a) \prod_{i=1}^s \mathcal{I}_{T_i}(a, \{z_{i,\alpha_i}\}_{\alpha_i}) \quad (3.2.19)$$

where $\{z_{i,\alpha_i}\}_{\alpha_i}$ is the other fugacities set of the i -th theory T_i and $\{z_A\}_A$ represents the total set of them. Here we use the Weyl's integration formula stating

$$\int_G [dU] f(U) = \oint_{\mathbb{T}^{\text{rk} \mathfrak{g}}} [da] \Delta_{\text{Haar}}(a) f(a) \quad (3.2.20)$$

where $a \in \mathbb{T}^{\text{rk} \mathfrak{g}}$, f is the class function over G which means $f(U) = f^g(U) := f(gUg^{-1})$ for $\forall g \in G$. $\Delta(a)_{\text{Haar}}$ is the Haar measure coming from the fiber (or the adjoint orbit) integration. In the case $\mathfrak{g} = \mathfrak{su}(N)$,

$$\int_{SU(N)} [dU] f(U) = \frac{1}{N!} \oint_{T^{N-1}} \prod_{i=1}^{N-1} \frac{da_i}{2\pi i a_i} \Delta(a) \Delta(a^{-1}) f(a) \Big|_{a_N = \prod_{i=1}^{N-1} a_i^{-1}} \quad (3.2.21)$$

where we also introduced new symbols

$$\oint_{T^{N-1}} \prod_{i=1}^{N-1} \frac{da_i}{2\pi i a_i} =: \oint [d\mathbf{a}] \quad \oint [da] \Delta_{\text{Haar}}(a) =: \oint [da]_{\text{Haar}} \quad (3.2.22)$$

$$\Delta_{\text{Haar}}(a) = \frac{1}{N!} \Delta(a) \Delta(a^{-1}) = \frac{1}{N!} \prod_i a_i^{-(N-1)} \prod_{i \neq j} (a_i - a_j) = \frac{1}{N!} \prod_{i \neq j} \left(1 - \frac{a_i}{a_j}\right) \quad (3.2.23)$$

$$\Delta(a) := \prod_{i < j} (a_i - a_j) \quad \text{discriminant} \quad (3.2.24)$$

with the constraint $a_0 := \prod_{i=1}^N a_i = 1$.¹⁵⁾

3.3 Reduced SCIs

In many cases, the fully refined SCIs (= the number of fugacities is maximal) are hard to treat although we can compute them if we have a Lagrangian description in some duality frame. To simplify them, we can reduce the number of fugacities as long as the dimension of each BPS Hilbert space is finite.

¹⁵⁾This corresponds to $U(N)/U(1) \simeq PSU(N) = SU(N)/\mathbb{Z}_N$ case not $SU(N)$ strictly speaking [98,158]. If $A_i := a_i/a_0^{1/N}$, A_i corresponds to the $SU(N)$ fugacity. The above formula differs by $|\mathbb{Z}_N| = N$ with respect to this difference but we ignore this subtlety.

More generally speaking, we may define the new indices by removing the divergent part like

$$\tilde{\mathcal{I}}(\tilde{a}; \tilde{y}) = \lim_{\{a,y\} \rightarrow \{\tilde{y}, \tilde{a}\}} \frac{1}{\mathcal{J}(y; a)} \mathcal{I}(y; a) \quad (3.3.1)$$

where $\mathcal{J}(y; a)$ is some zero modes contributions which diverges at $(a, y) = (\tilde{a}, \tilde{y})$.

3.3.1 Poles of the index

The superconformal indices have infinitely many poles in the fugacity plane. Are there any physical meanings for them? To answer the questions, we explain the idea discussed in [77].

For that purpose, let us go back to the flat space formulation. Let a be the fugacity which we focus on and b be all others, namely, $b^g = \prod_i b_i^{g_i}$.

$$\mathcal{I}(a, b) = \text{Tr}_{\mathcal{H}^{\text{BPS}}} [(-1)^F a^f b^g] \quad (3.3.2)$$

Now, we assume that we have the singular structure like

$$\mathcal{I} = \frac{\tilde{\mathcal{I}}(a, b)}{1 - a^{f_{\mathcal{O}}} b^{g_{\mathcal{O}}}} \quad (3.3.3)$$

where we assume that $f_{\mathcal{O}}$ is an integer.¹⁶⁾ It is expected that the singular part $\frac{1}{1 - a^{f_{\mathcal{O}}} b^{g_{\mathcal{O}}}}$ comes from a bosonic chiral operator \mathcal{O} with charges $f = f_{\mathcal{O}}, g = g_{\mathcal{O}}$. The divergence comes from the equal contributions of the sequence of operators

$$\{\mathcal{O}, \mathcal{O}^2, \mathcal{O}^3, \dots\} \quad (3.3.4)$$

which are powers of \mathcal{O} . In other words, there is a zero mode at the special fugacities choice.

Taking the residues corresponds to the removal of this zero mode and the set of a to the special values consisting of b . The latter means that

$$\text{Tr} [(-1)^F b^{f^{new}}] \quad (3.3.5)$$

where $f^{new} = f - \frac{f_{\mathcal{O}}}{g_{\mathcal{O}}} g$. Since \mathcal{O} is uncharged under f^{new} , this new charge is preserved when \mathcal{O} has some VEV. This fact implies that the zero mode is the NG mode associated to the symmetry breaking by a VEV of \mathcal{O} and taking the residue corresponds to the SCI in the IR after the RG flow triggered by the giving VEV to \mathcal{O} .

When we apply this discussion to the free hypermultiplets and to the pole in the $U(1)_B$ symmetry, it is expected that the multiplets produce a vortex at the UV and flows

¹⁶⁾At least, this is always possible when all the symmetry groups associated with a are compact.

to a surface defect in the IR. In particular, we couple the free hypermultiplets to the original theory at the UV and then, in the IR, we expect that the original theory with the surface defect. Interestingly, this procedure results in the difference operator action on the would-be gauged fugacity of the original theory.

Instead of performing the full computation, we see the simplest mathematical toy model. The divergence comes from the contour pinch of the integral, namely, the pole inside the contour and that outside collide in the limit corresponding to the residue.

For some function $f(z)$ of z , consider

$$F(a, b) := \oint_{|z|=1-\epsilon} \frac{dz}{2\pi i} \frac{f(z)}{(z - ab^\pm)(z - q\frac{b^\pm}{a})} \quad (3.3.6)$$

where $|a| = |b|$, $|q| < 1$ and $(x - ya^\pm) := (x - ya)(x - ya^{-1})$. Using the residue theorem, we have

$$F(a, b) = \frac{a^3 b f(q\frac{b}{a})}{q(a - q^{1/2})(a + q^{1/2})(a - q^{1/2}b)(a + q^{1/2}b)(b^2 - 1)} + (b \rightarrow b^{-1}) \quad (3.3.7)$$

$$+ \sum_{z_i} \frac{f(z_i)}{(z_i - ab^\pm)(z_i - q\frac{b^\pm}{a})} \quad (3.3.8)$$

where $z_i (\neq q^{1/2}b^\pm)$ are simple poles of $f(z)$ inside the contour. $F(a, b)$ have some poles in the a -plane and we focus on one pole $a = q^{1/2}$. Indeed, two simple poles $z = ab^\pm$ and $z = q\frac{b^\pm}{a}$ in the original integrand coincide for each \pm . Then, the residue is

$$\text{Res}_{a=q^{1/2}} F(a, b) = -\frac{b}{2q(1 - b^2)^2} f(q^{1/2}b) + (b \rightarrow b^{-1}) \quad (3.3.9)$$

and the result can be written as the difference operator actions on z when we identify z and b again. Notice that this is not just the change of the variable by multiplying $q^{1/2}$.

3.4 4D $\mathcal{N}=2$ superconformal indices

In this section, we focus on the 4D $\mathcal{N}=2$ superconformal systems.

First of all, the superconformal algebra is given by

$$\mathfrak{sc} = \mathfrak{su}(2, 2|2) \quad \mathfrak{sc}^B = \mathfrak{su}(2, 2) \oplus \mathfrak{su}(2)_R \oplus \mathfrak{u}(1)_r \quad (3.4.1)$$

and there are 16 supercharges : eight super Poincaré supercharges \mathcal{Q} and eight superconformal supercharges \mathcal{S} . See Appendix. B. To use the recent standard notation in the 4D $\mathcal{N}=2$ SCIs, we quote the results in [40].

For $\mathcal{Q}_{\alpha A}$ and $\tilde{\mathcal{Q}}_{\dot{\alpha} A}$, A, α and $\dot{\alpha}$ denote the indices of $SU(2)_R$, $SU(2)_1$ and $SU(2)_2$ symmetry, respectively. The relation between \mathcal{Q} and \mathcal{S} is given by

$$(\mathcal{Q}_{\alpha A})^\dagger = \mathcal{S}^{\alpha A} \quad (\tilde{\mathcal{Q}}_{\dot{\alpha} A})^\dagger = -\tilde{\mathcal{S}}^{\dot{\alpha} A} \quad (3.4.2)$$

where \dagger is the BPZ conjugate.

The supercharge to define the SCI is usually chosen as

$$\mathcal{Q} = \tilde{\mathcal{Q}}_{1-}. \quad (3.4.3)$$

and the anti-commutator with $\mathcal{Q}^\dagger = \tilde{\mathcal{S}}_{2+}$ is

$$\mathcal{E} = 2\tilde{Y}_0 := \{\mathcal{Q}, \mathcal{Q}^\dagger\} = \Delta + r - 2j_2 - 2I \geq 0. \quad (3.4.4)$$

The Hilbert space over S^3 with $\mathcal{E} = 0$ is given by

$$\text{Ker}(\mathcal{Q}) \cap \text{Ker}(\mathcal{Q}^\dagger) = \mathcal{H}_{S^3}^{(\Delta=2j_2+2I-r, j_1, j_2, I, r)} \quad (3.4.5)$$

where other fugacities ignored here.

Notice that all choices of \mathcal{Q} from the supercharges with definite weights for the fixed Cartan are equivalent under some involutions as follows.

$$\begin{array}{lll} z \longleftrightarrow w & SU(2)_1 \longleftrightarrow SU(2)_2 & \mathcal{Q} \longleftrightarrow \tilde{\mathcal{Q}} \\ I \rightarrow -I & \pi\text{-rotation in } SU(2)_R & 1 \longleftrightarrow 2 \\ j_1 \rightarrow -j_1 & \pi\text{-rotation in } SU(2)_1 & + \longleftrightarrow - \\ j_2 \rightarrow -j_2 & \pi\text{-rotation in } SU(2)_2 & \dot{+} \longleftrightarrow \dot{-} \\ \tau \rightarrow -\tau & \text{inversion in } SO(1,1)_D & \mathcal{Q} \longleftrightarrow \mathcal{S} \end{array}$$

We do not consider linear combinations of these supercharges although some appear in the limit of fugacities. The above choice of \mathcal{Q} is the case with the maximal fugacities of superconformal symmetry. Since $\text{rk}\mathfrak{h} = 4$, $\text{rk}\mathfrak{g} = 3$ is expected. Indeed,

$$\mathfrak{k} = \langle \mathcal{Q}_{1-}, \mathcal{Q}_{1+}, \tilde{\mathcal{Q}}_{2+} \rangle \quad (3.4.6)$$

and

$$\mathfrak{g} = \langle \delta(\mathcal{Q}_{1-}), \delta(\mathcal{Q}_{1+}), \delta(\tilde{\mathcal{Q}}_{2+}) \rangle \quad (3.4.7)$$

holds true where we have introduced the new symbol $\delta(\mathcal{Q}') := 2\{\mathcal{Q}'^\dagger, \mathcal{Q}'\}$. The discussion in the unitarity bound part in 3.2.2 gives

$$2\hat{Y}_1 = \delta(\mathcal{Q}_{1-}) = \Delta - 2j_1 - 2I - r = 2\hat{Y}_0 + 2(I + j_2) \quad (3.4.8)$$

$$2\hat{Y}_2 = \delta(\mathcal{Q}_{1+}) = \Delta + 2j_1 - 2I - r = 2\hat{Y}_0 + (j_2 - j_1 - r) \quad (3.4.9)$$

$$2\hat{Y}_3 = \delta(\tilde{\mathcal{Q}}_{2+}) = \Delta + 2j_2 + 2I + r = 2\hat{Y}_0 + (j_2 + j_1 - r) \quad (3.4.10)$$

and

$$\hat{y}_1 =: \rho \quad \hat{y}_2 =: \sigma \quad \hat{y}_3 =: \tau. \quad (3.4.11)$$

Using this basis of fugacities,

$$\mathcal{I}(a; b, \rho, \sigma, \tau) = \text{Tr} \left[(-1)^F \rho^{\hat{Y}_1} \sigma^{\hat{Y}_2} \tau^{\hat{Y}_3} e^{-\beta \mathcal{E} a} \right] \quad (3.4.12)$$

where $b = e^{-\beta}$

Several choices of fugacities are used in [18, 39, 40] and they are related as follows:

$$\begin{cases} \rho = t'v^{1/2}y = q/\sqrt{t} \\ \sigma = t'v^{1/2}y^{-1} = p/\sqrt{t} \\ \tau = t'^2v^{-1/2} = t^{1/2} \end{cases} \quad \begin{cases} t' = (\rho\sigma\tau^2)^{1/6} = (pq)^{1/6} \\ y = \rho^{-1/2}\sigma^{1/2} = \sqrt{p/q} \\ v = (\rho\sigma/\tau)^{2/3} = (pq)^{2/3}/t \end{cases} \quad \begin{cases} p = \sigma\tau = t'^3y \\ q = \rho\tau = t'^3y^{-1} \\ t = \tau^2 = t'^4/v \end{cases} \quad (3.4.13)$$

Obeying the more recent convention, we use the (p, q, t) parameter representation. In this basis of fugacities, the corresponding generators of \mathfrak{h} up to \mathcal{E} are¹⁷⁾

$$Y_1 = j_2 - j_1 - r \quad Y_2 = j_2 + j_1 - r \quad Y_3 = I + r \quad (3.4.14)$$

$$y_1 = q \quad y_2 = p \quad y_3 = t. \quad (3.4.15)$$

Fermion number convention

As discussed in 3.2, we have several choices of the Fermion number operator $(-1)^F$. One natural choice is

$$L_j = j_1 + j_2 \quad (3.4.16)$$

and we use this choice through this thesis. However, other convention sometimes used [151] is

$$L_R = -I. \quad (3.4.17)$$

However, the difference between two is in \mathfrak{h} and, indeed,

$$L_j - L_R = j_1 + j_2 + I = Y_2 + Y_3 \in \mathfrak{h}. \quad (3.4.18)$$

In terms of fugacity, this is just replacement of p, t by $e^{2\pi i}p, e^{2\pi i}t$. In the Schur limit, this is the map from $q^{1/2}$ to $-q^{1/2}$. This difference of conventions is equivalent to that of the conventions introduced in Sec. 4.2.

The other possible simple choice is

$$L_r = r \quad (3.4.19)$$

and the difference between this and L_j is

$$L_j - L_r = j_1 + j_2 - r = Y_2 \in \mathfrak{h}. \quad (3.4.20)$$

¹⁷⁾Some references like [140] use the a bit different conventions where p and q are exchanged, or equivalently, j_1 is flipped $-j_1$.

Various limitation and index contribution from the short multiples of SCA

There are special important limitations : Macdonald limit ($p \rightarrow 0$), Schur limit ($q = t$), Hall-Littlewood (HL) limit ($p, q \rightarrow 0$) and Coulomb limit ($p, q, t \rightarrow 0$ for fixed $T := \frac{pq}{t}$).¹⁸⁾

Following the notations introduced in [159], we list which short multiplets contribute to each index from [40].

At the index level,

$$\begin{aligned} \hat{\mathcal{B}}_I &= \hat{\mathcal{C}}_{I-1(-1/2, -1/2)} & \mathcal{D}_{I(0, j_2)} &= \hat{\mathcal{C}}_{I-1/2(-1/2, j_2)} \\ \mathcal{D}_{I(j_1, 0)} &= \hat{\mathcal{C}}_{I-1/2(j_1, -1/2)} & \bar{\mathcal{B}}_{I, r, (j_1, 0)} &= \bar{\mathcal{C}}_{I-1/2, r+1/2(j_1, -1/2)} \end{aligned} \quad (3.4.21)$$

and types \mathcal{B} , \mathcal{C} and \mathcal{E} vanish.

First of all, for the full index,

$$\bar{\mathcal{C}}_{I, r(j_1, j_2)} : -(-1)^{F_j} (pq)^{j_2-r} t^{I+r} \frac{(1 - \frac{pq}{t})(t-p)(t-q)(p^{j_1+1}q^{-j_1} - p^{-j_1}q^{j_1+1})}{(1-p)(1-q)(p-q)} \quad (3.4.22)$$

$$\hat{\mathcal{C}}_{I(j_1, j_2)} : (pq)^{j_1+1} t^{J_2-j_1+I+1} \frac{(1 - \frac{pq}{t})}{(1-p)(1-q)(p-q)} \left[\left(\frac{p}{q}\right)^{j_1} p \left(\frac{1}{q} - \frac{1}{t}\right) - \left(\frac{q}{p}\right)^{j_1} q \left(\frac{1}{p} - \frac{1}{t}\right) \right] \quad (3.4.23)$$

$$\overline{\mathcal{E}}_{r(j_1, 0)} : (-1)^{2j_1} \left(\frac{t}{pq}\right)^{r+1} \frac{(t-p)(t-q)(p^{j_1+1}q^{-j_1} - p^{-j_1}q^{j_1+1})}{t(1-p)(1-q)(p-q)} \quad (3.4.24)$$

$$\begin{aligned} \overline{\mathcal{D}}_{0(j_1, 0)} &: (-1)^{2j_1} \left(\frac{t}{pq}\right)^{j_1+1} \frac{1}{(1-p)(1-q)(p-q)} \\ &\times \left[\left(\frac{p}{q}\right)^{j_1} p \left(1 + t - q - \frac{1}{q}\right) - \left(\frac{q}{p}\right)^{j_1} q \left(1 + t - p - \frac{1}{p}\right) \right] \end{aligned} \quad (3.4.25)$$

$$\mathcal{D}_{0(0, j_2)} : (-1)^{2j_2+1} \frac{t^{j_2+1}(1 - \frac{pq}{t})}{(1-p)(1-q)} \quad (3.4.26)$$

For the Macdonald index ($p \rightarrow 0$),

$$\hat{\mathcal{C}}_{I(j_1, j_2)} : (-1)^{F_j} \frac{q^{2j_1+1} t^{j_2-j_1+I+1}}{1-q} \quad \bar{\mathcal{D}}_{0(j_1, 0)} : (-1)^{2j_1+1} \frac{q^{2j_1+1} t^{-j_1}}{1-q} \quad \mathcal{D}_{0(0, j_2)} = (-1)^{2j_2+1} \frac{t^{j_2+1}}{1-q}. \quad (3.4.27)$$

For the Schur index ($t \rightarrow q$ in the Macdonald index),

$$\hat{\mathcal{C}}_{I(j_1, j_2)} : (-1)^{F_j} \frac{q^{j_1+j_2+I+2}}{1-q} \quad \bar{\mathcal{D}}_{0(j_1, 0)} : (-1)^{2j_1+1} \frac{q^{j_1+1}}{1-q} \quad \mathcal{D}_{0(0, j_2)} = (-1)^{2j_2+1} \frac{q^{j_2+1}}{1-q}. \quad (3.4.28)$$

¹⁸⁾For computational convenience, we define q-Coulomb limit $p, t \rightarrow 0$. The Coulomb limit is obtained with the further limit $q \rightarrow 0$.

For the Hall-Littlewood index ($q \rightarrow 0$ in the Macdonald limit),

$$\hat{\mathcal{C}}_{I(-\frac{1}{2}, j_2)} : -(-1)^{2j_2} t^{j_2 + I + \frac{3}{2}} \quad \mathcal{D}_{0(0, j_2)} = (-1)^{2j_2 + 1} t^{j_2 + 1}. \quad (3.4.29)$$

It is known that this index is equivalent to the Hilbert series on the Higgs branch [160].

Th examples are $\hat{\mathcal{C}}_{0(0,0)}$: stress-energy tensor multiple, $\hat{\mathcal{B}}_{1/2}$: free hypermultiplet, $\hat{\mathcal{B}}_1$: flavor current multiplet and $\mathcal{D}_{0(0,0)} \oplus \overline{\mathcal{D}}_{0(0,0)}$: vector multiplet. We can easily check that the corresponding single letter satisfies the above expressions.

Unitarity bound

The non-negativity condition of physical norms

$$2\tilde{Y}_1 = \delta(\mathcal{Q}_{1-}) \geq 0 \quad 2\tilde{Y}_2 = \delta(\mathcal{Q}_{1+}) \geq 0 \quad 2\tilde{Y}_3 = \delta(\tilde{\mathcal{Q}}_{2+}) \geq 0 \quad (3.4.30)$$

with the constraint $2\tilde{Y}_0 = \delta(\tilde{\mathcal{Q}}_{2+}) = 0$ (3.4.10) claim that

$$I + j_2 \geq 0, j_2 \pm j_1 - r \geq 0. \quad (3.4.31)$$

Notice also

$$\Delta + r \Big|_{\tilde{Y}_0=0} = 2(I + j_2) \geq 0. \quad (3.4.32)$$

When j_2 linearly depends on the others, we have the constraints

$$\Delta \geq 2|j_1| + 2I + r \quad \Delta \geq -r. \quad (3.4.33)$$

When Δ linearly depends on the others, we have

$$j_2 - |j_1| - r \geq 0 \quad j_2 + R \geq 0. \quad (3.4.34)$$

For the (ρ, σ, τ) parameter representation of SCIs, their exponents are always non-negative by definition. For the (p, q, t) parameter representation, we can say that the exponents of p, q are always non-negative and half-integers when r is integer.

Finally, let us discuss the unitarity bound in the particular limits. In the Macdonald limit $p \rightarrow 0$, the condition $j_2 + j_1 - r \geq 0$ becomes $j_2 + j_1 = r$. Using $j_2 - j_1 \geq r$, $j_1 \leq 0$. Combining the other bound $I + j_2 \geq 0$, $I + j_2 - j_1 \geq 0$ holds true. In the Hall-Littlewood limit $p, q \rightarrow 0$, we have $j_1 = 0$ and $j_2 = r$. The left unitary bound is $I + r = I + j_2 \geq 0$.

On the other hand, in the Schur limit $t \rightarrow q$, there left two bosonic generators $j_2 + j_1 - r$ and $j_2 - j_1 + I$ and the supercharge \mathcal{Q}^{2-} accidentally commutes with both, that is to say, there happens the "supersymmetry enhancement". This means that only the state belonging to $\text{Ker}(\mathcal{Q}^{2-})$ contribute the SCIs. Since $2\delta(\mathcal{Q}^{2-}) \Big|_{\tilde{Y}_0=0} = j_1 + j_2 - r$, there happens the additional constraint $j_1 + j_2 = r$ for the contributing states. This is exactly the same as the Macdonald limit and we have the condition $\Delta - I = I + j_2 - j_1 \geq 0$.¹⁹⁾ In conclusion, the exponent of q in the Schur limit is always non-negative.

¹⁹⁾The corresponding supercharge is given by $\sqrt{2}\tilde{\mathcal{Q}}_2^- + \mathcal{Q}^{2+}$.

Single letter functions

As discussed in Sec.3.2.2, we can evaluate the SCI at the almost zero coupling region, namely , at the free limit. The free fields contributing to SCIs, that is to say, satisfying the condition $E = 0$ are listed in Table. 3.1.

	Letters	full	Macdonald	Schur	HL	q-Coulomb
vector multiplet	ϕ	$\frac{pq}{t}$	0	$0 \leftarrow (p)$	0	T
	λ_{1+}	$-p$	0	$0 \leftarrow (-p)$	0	0
	λ_{1-}	$-q$	$-q$	$-q$	0	$-q \rightarrow 0$
	$\bar{\lambda}_{1+}$	$-t$	$-t$	$-q$	$-t$	0
	\bar{F}_{++}	pq	0	$0 \leftarrow (pq)$	0	0
half-hyper-multiplet	$\partial_{-+}\lambda_{1+} + \partial_{++}\lambda_{1-} = 0$	pq	0	$0 \leftarrow (pq)$	0	0
half-hyper-multiplet	Q	$t^{\frac{1}{2}}$	$t^{\frac{1}{2}}$	$q^{\frac{1}{2}}$	$t^{\frac{1}{2}}$	0
	$\bar{\psi}_+$	$-\frac{pq}{t^{\frac{1}{2}}}$	0	$0 \leftarrow (-pq^{\frac{1}{2}})$	0	0
descendant	∂_{++}	p	0	$0 \leftarrow (p)$	0	0
	∂_{-+}	q	q	q	0	0

Table 3.1: Single letter and their associated fugacities in each limit.

Because of the Dirac equation (the on-shell condition) $\partial_{-+}\lambda_{1+} + \partial_{++}\lambda_{1-} = 0$ (recall that we must discuss the operators on the “physical” Hilbert space), two letters $\partial_{\pm+}^{n\pm}\partial_{-+}\lambda_{1+}$ and $\partial_{\pm+}^{n\pm}\partial_{++}\lambda_{1-}$ coincides and the overlap must be subtracted. The combination of the minus sign comes from this subtraction and their contribution are $-pq$ gives pq in the Table 3.1.

We can compute each contribution called single letter from each BPS multiplet [161]. In particular, let us compute the vector multiplet case and the half-hypermultiplet case with respect to the weights of η . Using the Table. 3.1,

$$f^{\frac{1}{2}H}(p, q, t) = \frac{\frac{pq}{t} + 2pq - p - q - t}{(1-p)(1-q)} \quad (3.4.35)$$

$$f^V(p, q, t) = \frac{t^{1/2}(1 - \frac{pq}{t})}{(1-p)(1-q)}. \quad (3.4.36)$$

The flavor symmetry part is simple. If a multiplet follows the representation R for the flavor symmetry F , by definition of characters, the contribution is given by $\chi_R^F(a)$ where a is the corresponding fugacities.

3.4.1 Evaluations of Indices based on free Lagrangians

Now, let us remark the computation procedure when we have some Lagrangian. See the definitions and formulae in Appendix. C.1.

Fundamental SCIs from single letter functions

Using the single letter function (3.4.36), we can evaluate the SCI as

$$\mathcal{I}_{\text{multiplet}}^{\text{full}}(a; p, q, t) = \exp \left[\sum_{n=1}^{\infty} \frac{1}{n} f_{\text{multiplet}}(p^n, q^n, t^n) \chi_R^F(a^n) \right] =: \text{P.E.}[f_{\text{multiplet}}(p, q, t) \chi_R^F(a)] \quad (3.4.37)$$

where P.E. is called the plethystic exponential.

Vector multiplet SCI : $\mathcal{I}_{\text{vector}}^{\text{full}}(a)$

Using the equations (C.1.23) and (C.1.21), we can see

$$\begin{aligned} \mathcal{I}_{\text{vector}}^{\text{full}}(a) &:= \exp \left(\sum_{n=1}^{\infty} \frac{1}{n} f^V(p^n, q^n, t^n) \chi_{\text{Adj}}(a^n) \right) \\ &= \exp \left(\sum_{n=1}^{\infty} \frac{1}{n} \frac{-p^n - q^n - t^n + p^n q^n (2 + 1/t^n)}{(1-p^n)(1-q^n)} \left[\sum_{i,j=1}^N \sum_{i \neq j} \left(\frac{a_i}{a_j} \right)^n + N - 1 \right] \right) \\ &= \left(\frac{(p; p)(q; q)}{\Gamma(t; p, q)} \right)^{N-1} \prod_{i < j} \left(\frac{1}{(1-a_i/a_j)(1-a_j/a_i)} \frac{1}{\Gamma((a_i/a_j)^{\pm}; p, q) \Gamma(t(a_j/a_i)^{\pm}; p, q)} \right) \end{aligned} \quad (3.4.38)$$

$$= \left(\frac{(p; p)(q; q)}{\Gamma(t; p, q)} \right)^{N-1} \frac{1}{\Delta(a) \Delta(a^{-1})} \prod_{i \neq j} \left(\frac{\Gamma(pqt^{-1}(a_i/a_j); p, q)}{\Gamma((a_i/a_j); p, q)} \right). \quad (3.4.39)$$

Half-hypermultiplet SCI : $\mathcal{I}_{\text{hyper}}^{\text{full}}(a)$

Let us see the $SU(N) \times SU(N)$ bi-fundamental half-hypermultiplet case and $SU(2)$ tri-fundamental half-hypermultiplet case.

In the bi-fundamental case, the global symmetry is given by $SU(N)_A \times SU(N)_B \times U(1)_B$ whose class S realization is $T^S[C([1^N], [1^N], [N-1, 1])]$ as we have seen in Sec. 2.4. Let a, b and m be the fugacities of $SU(N)_A, SU(N)_B$ and $U(1)_B$ respectively. Now, the full SCI for the half-hypermultiplet is given as

$$\mathcal{I}_{\text{b.f. h.h.}}^{\text{full}}(a, b, m) := \exp \left(\sum_{n=1}^{\infty} \frac{1}{n} f^{\frac{1}{2}H}(p^n, q^n, t^n) m^n \chi_{\square}^{SU(N)}(a^n) \chi_{\square}^{SU(N)}(b^n) \right) \quad (3.4.40)$$

$$\begin{aligned} &= \exp \left(\sum_{n=1}^{\infty} \frac{1}{n} \frac{t^{n/2}(1-p^n q^n/t^n)}{(1-p^n)(1-q^n)} \sum_{i,j=1}^N (ma_i b_j)^n \right) \\ &= \prod_{i,j=1}^N \Gamma(\sqrt{t}(bx_i y_j); p, q). \end{aligned} \quad (3.4.41)$$

The other similar example is the $SU(2)$ tri-fundamental half-hypermultiplet.

$$\mathcal{I}_{\text{t.f. h.h.}}^{\text{full}}(a, b, c) := \exp \left(\sum_{n=1}^{\infty} \frac{1}{n} f^{\frac{1}{2}H}(p^n, q^n, t^n) \left[\chi_{\square}^{SU(2)}(a^n) \chi_{\square}^{SU(2)}(b^n) \chi_{\square}^{SU(2)}(c^n) \right] \right) \quad (3.4.42)$$

$$= \exp \left(\sum_{n=1}^{\infty} \frac{1}{n} \frac{t^{n/2}(1-p^n q^n/t^n)}{(1-p^n)(1-q^n)} (a^{\pm} b^{\pm} c^{\pm})^n \right) \\ = \Gamma(\sqrt{t}(a^{\pm} b^{\pm} c^{\pm}); p, q). \quad (3.4.43)$$

3.4.2 Results in various limit

In this subsection, we summarize the expressions $\mathcal{I}_{\text{multiplet}}^{(m)}$ for the superconformal index with respect to a single flavor charge (weight) in the various limits. The final answer is given as their products over all the weights.

$$\mathcal{I}_{\text{multiplet}}^{\text{full}}(a; p, q, t) = \prod_{w \in \Pi(R)} \mathcal{I}_{\text{multiplet}}^{(m), \text{full}}(a^w) \quad (3.4.44)$$

For the vector multiplet of the simple Lie group G , R is always the adjoint representation Adj .

$$\mathcal{I}_{\text{vector}}^{(m), \text{full}}(x) := \frac{1}{(1-x)\Gamma(x; p, q)\Gamma(tx^{-1}; p, q)} = \frac{\Gamma(\frac{pq}{t}x; p, q)}{(1-x)\Gamma(x; p, q)} \quad (3.4.45)$$

$$\mathcal{I}_{\text{hyper}}^{(m), \text{full}}(x) := \Gamma(t^{\frac{1}{2}}x; p, q) \quad (3.4.46)$$

where $\mathcal{I}_{\text{vector}}^{(m), \text{full}}(x)$ does not coincide with P.E. $[f^V(p, q, t)\chi_{\text{Ad}}^G(x)]$ and see the derivation around (C.1.23). In the Macdonald limit,

$$\mathcal{I}_{\text{vector}}^{(m), \text{Macdonald}}(x) := \lim_{p \rightarrow 0} \mathcal{I}_{\text{vector}}^{(m), \text{full}}(x) = (qx; q)_{\infty} \left(\frac{t}{x}; q\right)_{\infty} \quad (3.4.47)$$

$$\mathcal{I}_{\text{hyper}}^{(m), \text{Macdonald}}(x) := \lim_{p \rightarrow 0} \mathcal{I}_{\text{hyper}}^{(m), \text{full}}(x) = \frac{1}{(t^{\frac{1}{2}}x; q)_{\infty}} \quad (3.4.48)$$

where we have used (C.1.20).

In the Schur limit,

$$\mathcal{I}_{\text{vector}}^{(m), \text{Schur}}(x) := \lim_{q \rightarrow t} \mathcal{I}_{\text{vector}}^{(m), \text{Macdonald}}(x) = \frac{\theta(x; q)}{1-x} = (qx^{\pm})_{\infty} \quad (3.4.49)$$

$$\mathcal{I}_{\text{hyper}}^{(m), \text{Schur}}(x) := \lim_{q \rightarrow t} \mathcal{I}_{\text{hyper}}^{(m), \text{Macdonald}}(x) = \frac{1}{(q^{\frac{1}{2}}x; q)_{\infty}} \quad (3.4.50)$$

and, for the pair of the opposite charges,

$$\mathcal{I}_{\text{hyper}}^{(m), \text{Schur}}(x^{\pm}) = \frac{1}{\theta(q^{\frac{1}{2}}x)}. \quad (3.4.51)$$

In the Hall-Littlewood limit,

$$\mathcal{I}_{\text{vector}}^{(m),\text{HL}}(x) := \lim_{q \rightarrow 0} \mathcal{I}_{\text{vector}}^{(m),\text{Macdonald}}(x) = 1 - \frac{t}{x} \quad (3.4.52)$$

$$\mathcal{I}_{\text{hyper}}^{(m),\text{HL}}(x) := \lim_{q \rightarrow 0} \mathcal{I}_{\text{hyper}}^{(m),\text{Macdonald}}(x) = \frac{1}{1 - t^{\frac{1}{2}}x}. \quad (3.4.53)$$

In the Coulomb limit,

$$\mathcal{I}_{\text{vector}}^{(m),q\text{-Coulmob}}(x) := \lim_{p \rightarrow 0} \mathcal{I}_{\text{vector}}^{(m),\text{full}}(x) = \frac{(qx; q)_{\infty}}{(Tx; q)_{\infty}} \xrightarrow{q \rightarrow 0} \frac{1}{1 - Tx} =: \mathcal{I}_{\text{vector}}^{(m),\text{Coulmob}}(x) \quad (3.4.54)$$

$$\mathcal{I}_{\text{hyper}}^{(m),q\text{-Coulomb}}(x) := \lim_{p \rightarrow 0} \mathcal{I}_{\text{hyper}}^{(m),\text{full}}(x) = 1 := \mathcal{I}_{\text{hyper}}^{(m),\text{Coulmob}}(x) \quad (3.4.55)$$

where $T := \frac{pq}{t}$ and q are fixed in $p \rightarrow 0$. We have also used the equality

$$\lim_{p \rightarrow 0} \Gamma(p^{\frac{1}{2}}y; p, q) = 1. \quad (3.4.56)$$

In particular, using (C.1.18),

$$\mathcal{I}_{\text{vector}}^{(m),\text{full}}(1) = \frac{(p; p)_{\infty}(q; q)_{\infty}}{\Gamma(t; p, q)} \quad (3.4.57)$$

$$\mathcal{I}_{\text{vector}}^{(m),\text{Macdonald}}(1) = (q; q)_{\infty}(t; q)_{\infty} \quad (3.4.58)$$

$$\mathcal{I}_{\text{vector}}^{(m),\text{Schur}}(1) = (q; q)_{\infty}^2 \quad (3.4.59)$$

$$\mathcal{I}_{\text{vector}}^{(m),\text{HL}}(1) = 1 - t \quad (3.4.60)$$

$$\mathcal{I}_{\text{vector}}^{(m),q\text{-Coulmob}}(1) = \frac{1}{1 - T} = \mathcal{I}_{\text{vector}}^{(m),\text{Coulmob}}(1) \quad (3.4.61)$$

which corresponds to the neutrally charged vector multiplet, to say, including the photon.

Gauging process

We revisit the gauging process.

$$\mathcal{P}_a \mathcal{Q}^a := \int_G [dU] \mathcal{I}_{\text{vector}}(U) \mathcal{P}(U) \mathcal{Q}(U^{-1}) \quad (3.4.62)$$

$$= \frac{(\Gamma(pq/t; p, q)(p; p)(q; q))^{\text{rk}_{\mathfrak{g}}}}{|\mathcal{W}_{\mathfrak{g}}|} \oint [d\mathbf{a}] \prod_{\alpha \in \Delta_{\mathfrak{g}}} \frac{\Gamma(pqt^{-1}a^{\alpha}; p, q)}{\Gamma(a^{\alpha}; p, q)} \mathcal{P}(a) \mathcal{Q}(a^{-1}) \quad (3.4.63)$$

$$= \oint [d\mathbf{a}] \oint [d\mathbf{b}] \eta(a, b) \mathcal{P}(a) \mathcal{Q}(b^{-1}) \quad (3.4.64)$$

and

$$\gamma_{p,q,t} := \Gamma(pq/t; p, q)(p; p)(q; q) = \frac{(p; p)(q; q)}{\Gamma(t; p, q)} \quad (3.4.65)$$

$$\eta(a, b) := \mathcal{I}_v(a) \tilde{\Delta}(a) \delta(ab) = \frac{\gamma_{p,q,t}^{\text{rk g}}}{|\mathcal{W}_{\mathfrak{g}}|} \prod_{\alpha \in \Delta_{\mathfrak{g}}} \frac{\Gamma(pqt^{-1}a^\alpha; p, q)}{\Gamma(a^\alpha; p, q)} \delta(ab) \quad (3.4.66)$$

where $\oint [d\mathbf{a}] \delta(a) = 1$.

Pole

We also roughly look at the pole structure. The contribution of some descendant of the chiral operator \mathcal{O} may have the form, at the leading order,

$$\frac{1}{1 - p^r q^s a^{f_{\mathcal{O}}}} \quad (3.4.67)$$

where $a^{f_{\mathcal{O}}} = \prod_i a_i^{f_{\mathcal{O},i}}$ and a can include p, q and t other than the flavor fugacities.

In this case, the operator is given by $(\partial_z)^r (\bar{\partial}_w)^s \mathcal{O}$ and, at the classical level, they can acquire the constant VEV like

$$\langle (\partial_z)^m (\bar{\partial}_w)^n \mathcal{O} \rangle_{\text{infinitynspace}} \sim v \delta_{m,r} \delta_{n,s} \quad (3.4.68)$$

and \mathcal{O} has a variant VEV

$$\mathcal{O} \sim v z^r \bar{w}^s \quad (3.4.69)$$

for large $|z|, |w|$.

3.5 4D/2D duality : class S Schur indices and 2D q -deformed Yang-Mills correlators

In this section, we further focus on the Schur limit. The important result throughout this thesis is the 4D/2D duality relations. In a special case, this claims that the class S 4D Schur indices are equivalent to the 2D q -deformed topological Yang-Mills partition functions [39].

As we have seen in Sec. 2.4, all the class S theories are constructed from several T_N theories by conformally gauging some flavor groups G and by partially closing some full punctures into required ones. Hereafter, we focus on $\mathfrak{g} = \mathfrak{su}(N)$. The discussion in the $\mathfrak{g} = \mathfrak{so}(2N)$ case is discussed in [162].

In [39], they proposed the conjecture that, for every (good) class S theory, up to the common overall factors depending only N and q , its Schur index equals to the partition function of 2D topological q -deformed Yang-Mills theory on C with appropriate prescriptions for punctures.

First of all, let us directly define the three points correlator as

$$\mathcal{Z}^{qYM}[C([1^N], [1^N], [1^N])](a, b, c) = \sum_{\lambda \in \mathcal{P}(\mathfrak{su}(N))} \frac{\chi_R(a)\chi_R(b)\chi_R(c)}{\dim_q R(\lambda)}. \quad (3.5.1)$$

Gluing them together as discussed in Sec. 3.8, we can construct the ℓ -points correlators as

$$\mathcal{Z}^{qYM}[C(\ell \cdot [1^N])](a = \{a_i\}_{i=1, \dots, N}) = \sum_{\lambda \in \mathcal{P}(\mathfrak{su}(N))} (\dim_q R(\lambda))^{\widetilde{\chi}_C} \prod_{i=1}^{\ell} \chi_R(a_i). \quad (3.5.2)$$

where $\widetilde{\chi}_C$ is the Euler character of the punctured Riemann surface C . Notice that $\widetilde{\chi}_C = \chi_C - \ell$ where χ_C is the ordinary Euler character on ignoring the punctures.

The difference between $\mathcal{Z}^{qYM}(a; q)$ and $\mathcal{I}^{\text{Schur}}(a; q)$ consists of two factors : each factor associated to each puncture and overall factor. The factor associated to each puncture is given by

$$\mathcal{K}(a; q) = \mathcal{K}_{[1^N]}(a; q) = \frac{1}{\mathcal{I}_{\text{vector}}^{\text{Schur}}(a; q)^{1/2}} \stackrel{3.4.50}{=} \prod_{\alpha \in \text{Adj}} \frac{1}{(qa^\alpha)} \quad (3.5.3)$$

and the overall factor is given by

$$\mathcal{N}(q) := \mathcal{K}_{[N]}(; q) = \prod_{i=2}^N (q^i; q). \quad (3.5.4)$$

Now, we have the relation

$$\mathcal{I}^{\text{Schur}}[C(\ell \cdot [1^N])](a; q) = \mathcal{N}(q) \prod_{i=1}^{\ell} \mathcal{K}(a_i) \mathcal{Z}^{qYM}[C(\ell \cdot [1^N])](a) \quad (3.5.5)$$

In the $N = 2$ case, the T_2 theory is just 8 free half-hypermultiplets and we already know both expressions. However, either side (the Schur index) is the infinite product and the other side (q -deformed Yang-Mills) is the infinite summation. To prove the equality, we must analyze the poles and the residues. In the $N = 3$ case, the direct computation of the Schur index of the T_3 theory is difficult but was derived in [163] by using some inversion formula for cycle integrals.

Next, let us consider the effect of the partial closure in Sec. 2.4.1. Recall the equation (2.4.7). This relation and the RG invariance implies

$$q^{-I_{IR}^3} a_{IR} = q^{-I_{UV}^3} a_Y \quad (3.5.6)$$

where a_{IR} is the fugacities in the Cartan subgroup of G_Y and a_Y belong to \mathbb{T}^{N-1} . Therefore, the partially closing operation on each maximal puncture is equivalent to the following replacement [39, 77, 142] :

$$a_Y \longrightarrow q^{\frac{\rho_Y^3}{2}} a_{IR}. \quad (3.5.7)$$

As for the notation used here, see the beginning of Sec. 4.3.

However, in this limit, the factor $\mathcal{K}(a; q)$ diverge. Recalling the discussion in Sec. 3.3, there appears some zero modes from the symmetry breaking of the $SU(N)$ symmetry into the subgroup G_Y .

As seen before, the embedding $\rho : \mathfrak{su}(2) \rightarrow \mathfrak{su}(N)$ for Nahm boundary describe the mixture of $SU(2)_R$ symmetry and the flavor symmetry $SU(N)$ because μ^+ is the highest weight of the $SU(2)_R$ -triplet. In other words, the $SU(2)_R^{UV}$ singlet matter in \mathbf{N} for the $SU(N)$ symmetry are charged under $SU(2)_R^{IR}$ following the decomposition

$$\mathbf{N} \longrightarrow \bigoplus_i \mathbf{n}_i. \quad (3.5.8)$$

Under the $SU(2)_R^{IR} \times G_Y$ symmetry, the \mathbf{N} matter belongs to

$$\bigoplus_i \mathbf{n}_i = \bigoplus_a \mathbf{m}_a \otimes \mathbf{d}_a \quad (3.5.9)$$

for $Y = [n]$, $G_Y = S(\prod_a U(d_a))$. This is true for the gauge multiplet. Under the $G \rightarrow SU(2)_R \times G_Y$,

$$\text{Adj} \longrightarrow \bigoplus_m \mathbf{m} \otimes R_m \quad (3.5.10)$$

where R_m is the representation under G_Y and m runs over a subset of the irreducible representations of $SU(2)$, namely, positive integer (dimension).

Therefore, recalling that the expression for $\mathcal{K}_{[1^N]}(a; q)$ is the product over all the weights of the gauge multiplet, the reduced expression should be given by the product of the factor $(q^{1+I} a^w; q)_\infty$ ($j_2 - j_1 = 1$) over all the weights w of R_d and over possible d . Therefore, the reduced expression is given by

$$\mathcal{K}_Y(a_{IR}; q) = \prod_d \prod_{w \in \Pi(R_d)} \frac{1}{(q^{\frac{d+1}{2}} a_{IR}^w)} \quad (3.5.11)$$

where a_{IR} is the fugacity of G_Y . Notice that the highest of \mathbf{d} for $SU(2)_R^{IR}$ has the additional $\frac{d-1}{2}$ charge compared to the UV where the gaugino (not all) contribute to SCIs as qa^w . This reproduces the rule given in [39].

By introducing the new function for each Y defined as

$$\psi_R^{(Y)}(a; q) := \mathcal{K}_Y(a; q) \chi_R(a_Y), \quad (3.5.12)$$

we write down the complete expression of general class S Schur indices as

$$\mathcal{I}_{T^S[C(Y_1, Y_2, \dots, Y_\ell)]}^{\text{Schur}}(a; q) = \mathcal{N}(q) \sum_{\lambda \in \mathcal{P}(\mathfrak{su}(N))} (\dim_q R(\lambda))^{\tilde{\chi}_C} \prod_{i=1}^{\ell} \psi_R(a_i^{G_Y}; q). \quad (3.5.13)$$

3.6 Concrete computations from 2D q -deformed Yang-Mills theory

In this section, we compare the two expressions of free hypermultiplets between the direct computation and the q -deformed Yang-Mills theory. To this end, we expand them in the parameter q around 0 ($|q| < 1$).

For any free hypermultiplet, by using (3.4.50), the expression has the form like

$$\mathcal{I}_{\text{freehyper}}^{\text{Schur}}(a; q) = 1 + q^{1/2} \sum_w a^w + q \left(\sum_{w_1 \neq w_2} a^{w_1+w_2} + \sum_w a^{2w} \right) + \mathcal{O}(q^{3/2}) \quad (3.6.1)$$

$$= 1 + q^{1/2} \sum_w a^w + q \left[\frac{1}{2} \left(\sum_w a^w \right)^2 + \frac{1}{2} \sum_w a^{2w} \right] + \mathcal{O}(q^{3/2}) \quad (3.6.2)$$

where w runs over all the weights for the whole flavor symmetry F .

Prefactors

For example, the prefactor associated with the full puncture is given as

$$\begin{aligned} \mathcal{K}_{[1^N]}(a; q) &= \frac{1}{\prod_{\alpha \in \text{Adj}} (qa^\alpha)_\infty} \\ &= 1 + q\chi_{\text{Adj}}(a) + q^2 \left[\sum_{\alpha \in \text{Adj}} (a^{2\alpha} + a^\alpha) + \frac{1}{2} \sum_{\alpha \neq \beta \in \text{Adj}} a^{\alpha+\beta} \right] \end{aligned} \quad (3.6.3)$$

$$\begin{aligned} &+ q^3 \left[\sum_{\alpha \in \text{Adj}} (a^{3\alpha} + a^\alpha) + \sum_{\alpha, \beta \in \text{Adj}} a^\alpha a^\beta + \sum_{\alpha \neq \beta \in \text{Adj}} a^{2\alpha+\beta} + \frac{1}{3!} \sum_{\alpha, \beta, \gamma \in \text{Adj}^{\text{distinct}}} a^{\alpha+\beta+\gamma} \right] + \mathcal{O}(q^4) \\ &= 1 + q\chi_{\text{Adj}}(a) + q^2 \left[\frac{1}{2} \chi_{\text{Adj}}(a)^2 + \frac{1}{2} \chi_{\text{Adj}}(a^2) + \chi_{\text{Adj}}(a) \right] \end{aligned}$$

$$+ q^3 \left[\frac{1}{6} \chi_{\text{Adj}}(a)^3 + \frac{1}{2} \chi_{\text{Adj}}(a) \chi_{\text{Adj}}(a^2) + \frac{1}{3} \chi_{\text{Adj}}(a^3) + \chi_{\text{Adj}}(a)^2 + \chi_{\text{Adj}}(a) \right] + \mathcal{O}(q^4) \quad (3.6.4)$$

$$\begin{aligned} &= 1 + q\chi_{\text{Adj}}(a) + q^2 \left[\chi_{2(\omega_1+\omega_{N-1})} + \chi_{\omega_2+\omega_{N-2}} + 2\chi_{\omega_1+\omega_{N-1}} + 1 \right] \\ &+ q^3 \left[\chi_{3(\omega_1+\omega_{N-1})}(a) + 2\chi_{2(\omega_1+\omega_{N-1})}(a) + 5\chi_{\omega_1+\omega_{N-1}}(a) + 2 \right. \\ &+ \chi_{\omega_1+\omega_2+\omega_{N-2}+\omega_{N-1}}(a) + 2\chi_{\omega_2+\omega_{N-2}}(a) + 2\chi_{\omega_2+2\omega_{N-1}}(a) + 2\chi_{2\omega_1+\omega_{N-2}}(a) \\ &\left. + \chi_{\omega_3+\omega_{N-3}}(a) \right] + \mathcal{O}(q^4) \end{aligned} \quad (3.6.5)$$

where $N \geq 7$.

When $N = 2$,

$$\frac{1}{(q)_\infty (qa^{\pm 2})_\infty} = 1 + q\chi_{\mathbf{3}}^{SU(2)}(a) + q^2 \left[\chi_{\mathbf{5}}^{SU(2)}(a) + \chi_{\mathbf{3}}^{SU(2)}(a) + 1 \right]$$

$$+ q^3 \left[\chi_{\mathbf{7}}^{SU(2)}(a) + \chi_{\mathbf{5}}^{SU(2)}(a) + 3\chi_{\mathbf{3}}^{SU(2)}(a) + 1 \right] + \mathcal{O}(q^4). \quad (3.6.6)$$

Wehn $N = 3$,

$$\begin{aligned} \frac{1}{\prod_{\alpha \in \text{Adj}(\mathfrak{su}(3))} (qa^\alpha)_\infty} &= 1 + q\chi_{[11]}^{SU(3)}(a) + q^2 \left[\chi_{[22]}^{SU(3)}(a) + 2\chi_{[11]}^{SU(3)}(a) + 1 \right] \\ &+ q^3 \left[\chi_{[33]}^{SU(3)}(a) + 2\chi_{[22]}^{SU(3)}(a) + 4\chi_{[11]}^{SU(3)}(a) + 2 + 2\chi_{[30]}^{SU(3)}(a) + 2\chi_{[03]}^{SU(3)}(a) \right] + \mathcal{O}(q^4). \end{aligned} \quad (3.6.7)$$

For instance, for the simple puncture,

$$\begin{aligned} \mathcal{K}_{[N-1,1]}(a; q) &= \frac{1}{\prod_{d=1}^{N-1} (q^d)_\infty (q^{N/2} a^\pm)_\infty} \\ &= (1 + q + 3q^2 + \mathcal{O}(q^3)) (1 + q^{N/2}(a + a^{-1}) + q^{N/2+1}(a + a^{-1}) + \mathcal{O}(q^N, q^{N/2+2})) \\ &= \begin{cases} 1 + q + q^{3/2}(a + a^{-1}) + 3q^2 + 2q^{5/2}(a + a^{-1}) + \mathcal{O}(q^3) & \text{for } N = 3 \\ 1 + q + q^2(a + a^{-1} + 3) + \mathcal{O}(q^3) & \text{for } N = 4 \\ 1 + q + 3q^2 + q^{5/2}(a + a^{-1}) + \mathcal{O}(q^3) & \text{for } N = 5 \\ 1 + q + 3q^2 + \mathcal{O}(q^3) & \text{for } N > 6. \end{cases} \end{aligned} \quad (3.6.8)$$

q -deformed Yang-Mills part

First of all, we can expand the inverse of q -dimension as

$$\frac{1}{\dim_q R(\lambda)} = q^{\rho^\alpha \lambda_\alpha} (1 - \#\{\alpha \mid \lambda_\alpha \neq 0\} + \mathcal{O}(q^2)) \quad (3.6.9)$$

where

$$\rho^\alpha = \frac{1}{2}\alpha(N - \alpha). \quad (3.6.10)$$

Therefore, the leading exponent is given by

$$g_R := \frac{1}{2} \sum_{\alpha=1}^{N-1} \alpha(N - \alpha) \lambda_\alpha. \quad (3.6.11)$$

For characters,

$$\chi_{R(\lambda)}(a_Y) =: q^{\rho_{L;Y}^\alpha \lambda_\alpha} (f_{R,Y}(a^{G_Y}) + \mathcal{O}(q^{1/2})) \quad (3.6.12)$$

where $\rho_{L;Y}^\alpha \leq 0$ for $\alpha = 1, 2, \dots, N - 1$. For $Y = [1^N]$, $\rho_{L;Y}^\alpha = 0$. For $Y = [1^N]$, $\rho_{L;Y}^\alpha = -\frac{1}{2}\alpha(N - \alpha)$. See Table. 3.2 for the A_5 example.

In the total expressions,

$$\sum_{\lambda \in \mathcal{P}(\mathfrak{su}(N))} \frac{\prod_{i=1}^n \chi_{R(\lambda)}(a_{i,Y_i})}{(\dim_q R(\lambda))^{-\tilde{\chi}}} = \sum_{\lambda \in \mathcal{P}(\mathfrak{su}(N))} q^{(-\chi^{\rho^\alpha} + \sum \rho_{L;Y_i}^\alpha \lambda_a)} (f_R(\{a\}) + \mathcal{O}(q^{1/2})) \quad (3.6.13)$$

and we can see that the leading exponent is linear in the dominant weight. To have a well-defined q -series, we must require that $L^\alpha := (-\chi\rho^\alpha + \sum \rho_{L_i}^\alpha) > 0$ for all α . We conjecture that this is always true for any good class S theories whose formal number of the Coulomb branch operators at each scaling dimension is non-negative [91]. In particular, for bad theories with vanishing $\rho_{L,Y}^\alpha$, we can compute the Schur indices but δ functions appear to reproduce the symmetry breaking. ²⁰⁾

$[1^6]$	$[21^4]$	$[2^2 1^2]$	$[2^3]$
$[0, 0, 0, 0, 0]$	$[-1, -1, -1, -1, -1]$	$[-1, -2, -2, -2, -1]$	$[-1, -2, -3, -2, -1]$
$[1, 2, 3, 4, 5]$	$[1, 2, 3, 4, 4]$	$[1, 2, 3, 3, 4]$	$[1, 2, 2, 3, 4]$
$[31^3]$	$[321]$	$[3^2]$	$[41^2]$
$[-2, -2, -2, -2, -2]$	$[-2, -3, -3, -3, -2]$	$[-2, -4, -4, -4, -2]$	$[-3, -4, -4, -4, -3]$
$[1, 2, 3, 3, 3]$	$[1, 2, 2, 3, 3]$	$[1, 1, 2, 2, 3]$	$[1, 2, 2, 2, 2]$
$[42]$	$[51]$	$[6]$	
$[-3, -4, -5, -4, -3]$	$[-4, -6, -6, -6, -4]$	$[-5, -8, -9, -8, -5]$	
$[1, 1, 2, 2, 2]$	$[1, 1, 1, 1, 1]$	$[0, 0, 0, 0, 0]$	

Table 3.2: The list for $\mathfrak{g} = \mathfrak{su}(6)$ (A_5): the puncture type $Y = [n]$, $2\rho_{L,Y}^\alpha$ and the numbers of Coulomb branch operators with scaling dimensions 2, 3, 4, 5, 6 in this order.

Bi-fundamental type : $T^S[C([1^N], [1^N], [N-1, 1])]$

$$\psi_R^{([N-1, 1])}(a; q) = \mathcal{K}_{[N-1, 1]}(a; q) \chi_R(q^{\rho_{[N-1, 1]}} a^{\nu_{[N-1, 1]}}) = 1 + q^{1/2} + \mathcal{O}(q) \quad (3.6.14)$$

and

$$f_R(a) = \begin{cases} a^{-N\lambda_{\frac{N}{2}}} + a^{-N\lambda_{\frac{N}{2}+1}} & \text{for } N : \text{even and } \lambda_{\frac{N}{2}} \neq 0 \\ a^{-N\lambda_{[\frac{N+1}{2}]}} & \text{for } N : \text{otherwise} \end{cases} \quad (3.6.15)$$

See (A.1.6) for λ_i .

$$\rho_{\text{simple,L}}^\alpha = \begin{cases} \frac{1}{2}\alpha^2 - \frac{1}{2}(N-1)\alpha & \text{for } 1 \leq \alpha \leq [\frac{N}{2}] \\ \frac{1}{2}\alpha^2 - \frac{1}{2}(N+1)\alpha + \frac{1}{2}N & \text{for } [\frac{N}{2}] + 1 \leq \alpha \leq N-1 \end{cases} \quad (3.6.16)$$

$$g_R + \rho_{\text{simple,L}}^\alpha(\lambda_R)_\alpha = \frac{1}{2} \sum_{1 \leq \alpha \leq [\frac{N}{2}]} \alpha \lambda_\alpha + \frac{1}{2} \sum_{[\frac{N}{2}] + 1 \leq \alpha \leq N-1} (N-\alpha) \lambda_\alpha \quad (3.6.17)$$

²⁰⁾The author thanks Y.Tachikawa for the discussion on these things.

where $\lambda_{\frac{N+1}{2}} = 0$ when N is even. Since this is strictly increasing as any λ_α increases, this assures that the SCI is well-defined as the q -expansion around $q = 0$.

Up to $\mathcal{O}(q)$, the following contributes to the computation.

$$q^0 : R = \cdot \quad (3.6.18)$$

$$q^{1/2} : R = \square, \bar{\square} \quad (3.6.19)$$

$$q^1 : R = \mathbf{Adj}, \text{Sym}^2 \square, \text{Sym}^2 \bar{\square}, \wedge^2 \square, \wedge^2 \bar{\square} \quad (3.6.20)$$

When $N \geq 3$

$$\begin{aligned} \mathcal{I}(a; q) &= 1 + q^{1/2} [z\chi_{\square}(a)\chi_{\square}(b) + z^{-1}\chi_{\bar{\square}}(a)\chi_{\bar{\square}}(b)] \\ &\quad + q [z^2(\chi_{\wedge^2 \square}(a)\chi_{\wedge^2 \square}(b) + \chi_{\square\square}(a)\chi_{\square\square}(b)) + z^{-2}(\chi_{\wedge^2 \bar{\square}}(a)\chi_{\wedge^2 \bar{\square}}(b) + \chi_{\bar{\square}\bar{\square}}(a)\chi_{\bar{\square}\bar{\square}}(b)) \\ &\quad + (\chi_{\text{Adj}}(a) + 1)(\chi_{\text{Adj}}(b) + 1)] + \mathcal{O}(q^{3/2}) \end{aligned} \quad (3.6.21)$$

By using the equality

$$\chi_{\square}(a^2)\chi_{\square}(b^2) = 2\chi_{\wedge^2 \square}(a)\chi_{\wedge^2 \square}(b) + 2\chi_{\square\square}(a)\chi_{\square\square}(b) - \chi_{\square}(a)^2\chi_{\square}(b)^2, \quad (3.6.22)$$

the above expression matches with the original expression (3.6.2) up to q^1 -order.

Second rank anti-symmetric type

In this case,

$$L^a = \begin{cases} \left\lfloor \frac{a+1}{2} \right\rfloor & \text{for } 1 \leq a \leq \lfloor \frac{N}{2} \rfloor \\ \left\lfloor \frac{N-a+1}{2} \right\rfloor & \text{for } \lfloor \frac{N+1}{2} \rfloor \leq a \leq N-1 \end{cases} \quad (3.6.23)$$

and, up to $\mathcal{O}(q^{1/2})$,

$$q^0 : R = \cdot \quad (3.6.24)$$

$$q^{1/2} : R = \square, \bar{\square}, \wedge^2 \square, \wedge^2 \bar{\square}. \quad (3.6.25)$$

In case that $N = 2n$ is even, $b_{[n,n]} = (q^{\rho_n} b_1, q^{\rho_n} b_2)$ ($b_1 b_2 = 1$) and $c_{[n,n-1,1]} = (q^{\rho_n} c_1, q^{\rho_n-1} c_2, c_3)$ ($c_1^n c_2^{n-1} c_3 = 1$). On the other hand, in the case that N is odd, $\tilde{b}_{[n,n,1]} = (q^{\rho_n} \tilde{b}_1, q^{\rho_n} \tilde{b}_2, \tilde{b}_3)$ ($\tilde{b}_1 \tilde{b}_2 \tilde{b}_3 = 1$) and $\tilde{c}_{[n+1,n]} = (q^{\rho_{n+1}} \tilde{c}_1, q^{\rho_n} \tilde{c}_2)$ ($\tilde{c}_1^{n+1} \tilde{c}_2^n = 1$). From the concrete computations, we will find the relation between two as

$$b = (\tilde{b}_1/\tilde{b}_2)^{1/2} \quad c_i = (\tilde{b}_1 \tilde{b}_2)^{1/2} \tilde{c}_i \quad \text{for } i = 1, 2. \quad (3.6.26)$$

When $N = 4$, $SU(2)$ and $U(1)$ fugacity is given by $c = c_1 c_2$ ($c^{-1} = c_1 c_3$) and c_1 respectively.

At $q^{1/2}$ order, the Schur index is given by

$$q^{1/2} : \chi_{\square}^{SU(N)}(a)\chi_{\square}^{SU(2)}(b)c_1 + \chi_{\wedge^2 \square}^{SU(N)}(a)c_1c_2 + (c.c.) \quad (3.6.27)$$

where (c.c.) is obtained by replacement of each fugacity x by x^{-1} .

Using the above computations, we can determine the undetermined $U(1)$ -charges as

$$N = 4$$

$$(\mathbf{4}, \mathbf{2}, \mathbf{1}, 1) \oplus (\overline{\mathbf{4}}, \mathbf{2}, \mathbf{1}, -1) \oplus (\mathbf{6}, \mathbf{1}, \mathbf{2}, 0) \quad (3.6.28)$$

$$N : \text{even}$$

$$(\mathbf{N}, \mathbf{2}, (1, 0)) \oplus (\overline{\mathbf{N}}, \mathbf{2}, (-1, 0)) \oplus (\wedge^2 \mathbf{N}, \mathbf{1}, (1, 1)) \oplus (\wedge^2 \overline{\mathbf{N}}, \mathbf{1}, (-1, -1)) \quad (3.6.29)$$

$$N : \text{odd}$$

$$(\mathbf{N}, (\mathbf{2}, 1), 1) \oplus (\overline{\mathbf{N}}, (\mathbf{2}, -1), -1) \oplus (\wedge^2 \mathbf{N}, (\mathbf{1}, 2), -\frac{2}{N-1}) \oplus (\wedge^2 \overline{\mathbf{N}}, (\mathbf{1} - 2), \frac{2}{N-1}) \quad (3.6.30)$$

where we adopt the normalizations of $U(1)$ -charges as c_1 ($N = 4$), c_1, c_2 ($N : \text{even}$) and \tilde{b}_1, \tilde{c}_1 ($N : \text{odd}$).

Exceptional case 1 : $\mathbf{T}^S[\mathbf{C}([1^6], [2^3], [4, 2])]$

In this case,

$$L^a = (1, 2, 1, 2, 1) \quad (3.6.31)$$

and

$$q^0 : R = \cdot \quad (3.6.32)$$

$$q^{1/2} : R = \square, \overline{\square}, \wedge^3 \square \simeq \wedge^3 \overline{\square} \quad (3.6.33)$$

Up to $q^{1/2}$,

$$\mathcal{I}_{\text{ex1.freehyper}}^{\text{Schur}}(a_{SU(6)}, b_{SU(3)}, c_{U(1)}; q) = 1 + q^{1/2} [\chi_{\mathbf{6}}(a)\chi_{\mathbf{3}}(b)c + \chi_{\overline{\mathbf{6}}}(a)\chi_{\overline{\mathbf{3}}}(b)c^{-1} + \chi_{\mathbf{20}}(a)] + \mathcal{O}(q) \quad (3.6.34)$$

and then we can find

$$(\mathbf{20}, \mathbf{1}, 0) \oplus (\mathbf{6}, \mathbf{3}, 1) \oplus (\overline{\mathbf{6}}, \overline{\mathbf{3}}, -1) \quad (3.6.35)$$

is the answer.

Exceptional case 2 : $\mathbf{T}^S[\mathbf{C}([2, 1^4], [2^3], [3^2])]$

$$L^a = (1, 1, 1, 1, 1) \quad (3.6.36)$$

and

$$q^0 : R = \cdot \tag{3.6.37}$$

$$q^{1/2} : R = \wedge^\alpha \square \quad \text{for } \alpha = 1, 2, 3, 4, 5 \tag{3.6.38}$$

$$\tag{3.6.39}$$

The computation supports

$$(\mathbf{6}, \mathbf{1}, \mathbf{2}, 0) \oplus (\mathbf{4}, \bar{\mathbf{3}}, \mathbf{1}, \frac{1}{2}) \oplus (\bar{\mathbf{4}}, \mathbf{3}, \mathbf{1}, -\frac{1}{2}) \oplus (\mathbf{1}, \mathbf{3}, \mathbf{2}, 1) \oplus (\mathbf{1}, \bar{\mathbf{3}}, \mathbf{2}, -1) \tag{3.6.40}$$

which exactly coincides with the analysis before up to $U(1)$ charge.

3.7 Defect indices

Now, let us turn to the system with defects. If we have (BPS) defects, they break the original superconformal symmetry into the less one. The strategy to define the SCI is totally same if we use the unbroken superconformal algebra. However, in general, the number of fugacities is reduced and several unitarity bounds are no more true.

In our case, the full superconformal algebra is $\mathfrak{su}(2, 2|2)$ and its bosonic part is $SO(4, 2) \times SU(2)_R \times U(1)_r$ in the Minkowski signature. The Cartan subalgebra is $\mathfrak{h} = \mathfrak{u}(1)_1 \oplus \mathfrak{u}(1)_2 \oplus \mathfrak{so}(1, 1)_D \oplus \mathfrak{u}(1)_I \oplus \mathfrak{u}(1)_r$.

3.7.1 SCIs with surface defects

There exist two special types of surface defects which preserve the bosonic subalgebra $\mathfrak{g}_{\text{surf}, i}^b = \mathfrak{so}(2, 2)_{i,D} \times \mathfrak{so}(2)_{\bar{i}}$. For both cases, whole the Cartan subalgebra remain unbroken $\mathfrak{h}_{\text{surf}} = \mathfrak{h}$ and we can define the full SCI.

However, as discussed in Appendix. B.1.1, some unitarity bound do not hold. This breakdown of the unitarity bound do not ensure the well-definedness of SCIs.

3.7.2 SCIs with loop defects

In this case, $\mathfrak{g}_{\text{loop}, i}^b = \mathfrak{sl}(2, \mathbb{R}) \oplus \mathfrak{so}(2)_{\bar{i}} \oplus \mathfrak{su}(2)_R$. The rank of Cartan subalgebra is reduced by 2. Indeed, the SCI is defined only in the Schur limit. See Appendix. B.1.1 for the detail. ²¹⁾

3.8 2D topological q -deformed Yang-Mills theory

In this section, we briefly explain the basis facts about 2D q -deformed Yang-Mills theory. Instead of giving the statistical mechanical rigorous definition based on quantum groups [164] [73], we see that they give a 2D TQFT correlators.

See [74, 165] on the q -deformed Yang-Mills, and see also a review [72] when $q = 1$.

²¹⁾In the appendix convention, the loop operators defined at another Schur limit $p = t$ which exchange the two \mathbb{C} planes.

3.8.1 Brief reviews on the partition functions and loops expectation values

In this section, we review the following three points :

1. Formula for no network defect cases
2. Gluing (= gauging process on the 4D side)
3. Formula in the presence of loops

Let us introduce the q -number as

$$[n]_q := \frac{q^{n/2} - q^{-n/2}}{q^{1/2} - q^{-1/2}}. \quad (3.8.1)$$

$\dim_q R$ denotes the q -dimension of an irreducible representation R . See (E.1.7) for its definition.

1. Formula for no network defect cases

When \tilde{C} is a genus \tilde{g} Riemann surface with \tilde{n} punctures with $SU(N)$ holonomies,²²⁾ its partition function $I_{\tilde{C}}(\{z\})$ is given by [74]

$$I_{\tilde{C}}(\{z\}) = \sum_R (\dim_q R)^{\chi_{\tilde{C}}} \prod_{i=1}^n \chi_R(z_i) \quad (3.8.2)$$

where R runs over all unitary irreducible representations of $SU(N)$, $\{z\}$ represents the set of holonomies and i is the index of punctures.

For each summand labelled by R , we can represent the Riemann surface with which R is assigned. This interpretation will be important later.

2. Gluing

There is a natural operation, gluing, which identifies two holonomies on different punctures and connect them geometrically. On the 4D SCFT side, there are two $SU(N)$ flavor symmetries which are identified by adding the vector multiplet [149].

If we have two pairs of a Riemann surface with punctures and generic networks on it allowing the case of empty, which are denoted by (C_A, Γ_A) and (C_B, Γ_B) , we can construct new one $(C_{AB}, \Gamma_A \sqcup \Gamma_B)$ by gluing each pair of several punctures. See Fig. 3.1. Let $I_{C,\Gamma}(\{z\})$ be the expectation values of the 2D topological q -deformed Yang-Mills theory on C with a Wilson network defect Γ . The corresponding expectation values can be constructed as

$$I_{C_{AB}, \Gamma_A \sqcup \Gamma_B}(\{a\}, \{b\}) = \prod_i \left(\oint [dz_i]_{\text{Haar}} \right) I_{C_A, \Gamma_A}(\{z^{-1}\}, \{a\}) I_{C_B, \Gamma_B}(\{z\}, \{b\}) \quad (3.8.3)$$

²²⁾In the language of class S theory, they are called maximal (or full) punctures.

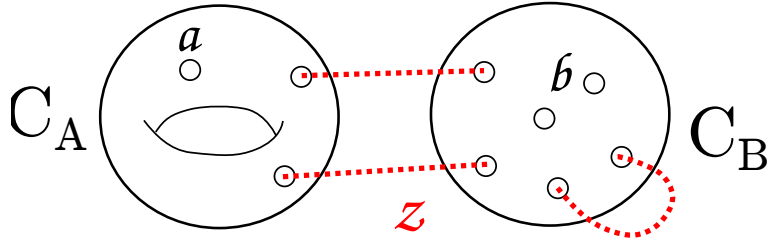


Figure 3.1: Any Riemann surface can be constructed from more fundamental ones by gluing pairs of punctures as dashed lines.

where $[dz]_{\text{Haar}}$ is the Haar measure of $SU(N)$ introduced in (3.2.22), $\{z\}$ are gauged fugacities and $\{a\}$ and $\{b\}$ are ungauged ones on C_A and C_B , respectively. The independence of the order in the glues is obvious.

3. Formula in the presence of loops

According to the result in [47, 48], the SCI in the presence of 4D loop operators turns out to coincide with the VEV of Wilson loops in the 2D q -deformed Yang-Mills as discussed in [75]. This can be obtained by simply adding the corresponding $SU(N)$ character on gluing as seen soon later.

In this case, Γ is a pure loop γ along a one cycle in C as depicted in Fig. 3.2. Let us

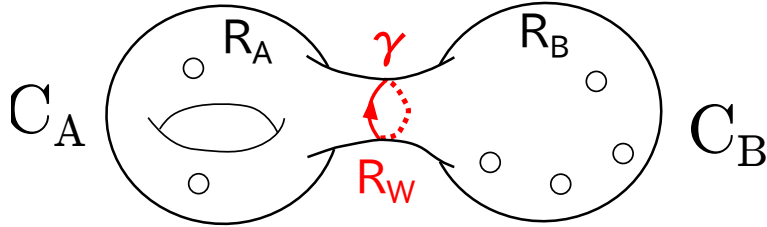


Figure 3.2: A 2D Wilson loop in R_W around the cylindrical part in C .

cut along the Wilson loop labelled by an irreducible representation R_W , which is exactly the reversed operation to the previous gluing process, and assume that they are separated after the cut for simplicity.²³⁾ Let z denote the new holonomy or fugacity along the new boundary cycle. Using the new Riemann surfaces C_A and C_B which have two additional punctures in total compared to C , we can express the Wilson loop expectation value of the 2D q -deformed Yang-Mills as

$$I_{C,\gamma}(\{a\}) = \oint [dz]_{\text{Haar}} \chi_{R_W}(z) I_{C_A}(z^{-1}, \{a\}) I_{C_B}(z, \{b\}) \quad (3.8.4)$$

$$= \sum_{R_A, R_B} N_{R_B R_W}^{R_A} (\dim_q R_A)^{\chi_{C_A}} (\dim_q R_B)^{\chi_{C_B}} \prod_i \chi_{R_A}(a_i) \prod_i \chi_{R_B}(b_i) \quad (3.8.5)$$

²³⁾If not, it is enough to replace two expectation values I_{C_A} and I_{C_B} by a single one in (3.8.4).

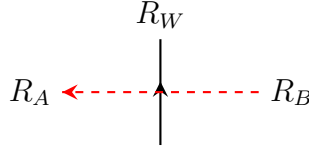


Figure 3.3: Two adjacent regions across an edge labelled by R_W .

where $N_{R_B R_W}^{R_A}$ is the Littlewood-Richardson coefficient which counts the multiplicity of the representation R_A appearing in the tensor product of R_B and R_W . The recursive applications can give the computations in all the general cases that Γ consists of multiple loops and networks.

If we have two isolated regions across an edge labelled by R_W , to each summand in (3.8.5), we can assign irreducible representations R_A and R_B to C_A and C_B , respectively. See Fig.3.3. The summand vanishes unless $N_{R_B R_W}^{R_A} \neq 0$ and then we have the constraint $R_B \in R_A \otimes R_W$ meaning that the irreducible decomposition of $R_A \otimes R_B$ includes R_W . In particular, in our convention, the charge on each edge is a fundamental representation $\wedge^a \square$ and the above constraint on R_A and R_B becomes powerful, which will turn out to be useful in the analysis in Sec. 4.5.2.

Let us make a few remarks. When \mathcal{Z}_R denotes the center charge of R , this constraint leads to $\mathcal{Z}_{R_B} + a = \mathcal{Z}_{R_A} \pmod N$ when $R_W = \wedge^a \square$. This implies that the expectation values vanish unless all the intersection numbers of any one cycles ²⁴⁾ with the Wilson networks vanish. For example, in the case that C is an once-punctured torus, the expectation value of the fundamental Wilson loop along α -cycle vanishes. In particular, when the puncture is special called simple or minimum, this introduces a Wilson loop in \square in some duality frames on the 4D $SU(N)$ gauge theory side but it is localized at a point in S^3 which is a compact space. Its center charge is not screened by the dynamical matter because all belongs to the adjoint representations and this theory is anomalous because there is a single source with a non-trivial Abelian charge on the compact space [12, 166].

²⁴⁾We define it by summing up all the intersecting edge's charges flowing from the left to the right along the one cycle following its orientation.

Chapter 4

Geometrical Eyes on Class S Defects

Now that we have reviewed several subjects necessary to discuss the geometrical descriptions of 4D BPS-defects originating from the codimension four defects in 6D.

The first discussion in this approach was done in [25]. In that paper, they constructed a bijective map from the non-intersecting (unoriented) loops on C to the charge lattice of Wilson-'t Hooft loops of the associated 4D theory when $\mathfrak{g} = \mathfrak{su}(2)$. In particular, the natural ‘‘coordinate’’ on the collection of loops called lamination corresponds to the choice of duality frames via the pants decomposition. See Appendix. G for the details.

There arise several questions :

- Why non-intersecting ?
- How can we extend the results to higher rank cases ($\mathfrak{g} = \mathfrak{su}(N)$) ?
- What the intersections mean physically ?

The answer to the first question is simple [26]. The reason we only have to consider non-intersecting loops on the Riemann surface for the A_1 case is the existence of a skein relation resolving each crossing into a sum of two non-crossing ones :

$$\left(\begin{array}{c} \diagup \diagdown \\ \diagdown \diagup \end{array} \right) = \mathfrak{q}^{-1/2} \left(\begin{array}{c} \diagup \diagdown \\ \diagup \diagdown \end{array} \right) + \mathfrak{q}^{1/2} \left(\begin{array}{c} \text{---} \\ \text{---} \end{array} \right), \quad (4.0.1)$$

where $\mathfrak{q} = e^{\pi i b^2}$ in the Liouville theory and $\mathfrak{q} = q^{1/2}$ in the q -deformed Yang-Mills.

Next, let us move to the answer to the second question. However, in the higher rank cases, namely for $SU(N)$ with $N > 2$ or equivalently for A_k with $k = N - 1 > 1$, there is no such simple skein relation, since junctions of lines inevitably appear. This results in the networks¹⁾ of lines on the Riemann surface, as already mentioned in [28, 67]. Such networks were treated and discussed in [62, 68], putting special emphasis on the $SU(3)$ case. In [62] the analysis was mainly carried out using the approach of the higher Teichmüller

¹⁾The same objects are also called as *webs* or *spiders*. In this paper, we only use the terminology *networks*.

theory classically ($\mathfrak{q} = 1$), and in [68] the study was done mainly in the framework of Toda CFTs for general \mathfrak{q} . These analyses gave rise to the skein relations that had been discovered in the context of mathematics before [167].

One of our aims in this chapter is to describe the skein relations of the networks in the general $SU(N)$ case. We have, for example, the relation

$$\begin{array}{c} \diagup \\ \square \end{array} \begin{array}{c} \diagdown \\ \square \end{array} = \mathfrak{q}^{\frac{1}{N}-1} \begin{array}{c} \uparrow \\ \square \end{array} \begin{array}{c} \uparrow \\ \square \end{array} + \mathfrak{q}^{\frac{1}{N}} \begin{array}{c} \square \\ \diagdown \quad \diagup \\ \square \end{array} \begin{array}{c} \square \\ \diagup \quad \diagdown \\ \square \end{array} \quad (4.0.2)$$

that reduces to the equation (4.0.1) when $N = 2$. These skein relations were first found in [168] in the context of knot invariants.

The guiding principle for us is that the representation theory of the quantum group $SU_q(N)$ underlies these networks and their skein relations. The relation of the loop operators of 2d CFTs and the quantum group has been known for quite some time, mainly in the context when \mathfrak{q} is a root of unity, see e.g. [169]. In the case of 2d q -deformed Yang-Mills, the relation of their loops and the quantum group is very direct, because the q -deformed Yang-Mills is a gauge theory whose gauge group is the quantum group [73, 164]. This is one of the main subjects in Sec. 4.2.

Finally, the answer to the third question is given in Sec. 4.1.

At this stage, let us define the class S skein relations.

Class S skein relations

Once we have introduced the 3D geometry discussed in Sec. 4.3.2, the meaning of skein relations are exactly same as those in the knot theory. Instead, throughout this paper, we use the skein relations in the following sense.

Let $W_q[\Gamma](\{a\})$ be the expectation value of the 2D Wilson network operator associated with Γ in the 2D q -deformed Yang-Mills theory. $\{a\}$ are all holonomies around punctures of C . And let us consider two sub graphs γ_A and γ_B . For any pair of two graphs Γ_A and Γ_B which include γ_A and γ_B respectively but are same on removing these sub graphs, when the equality shown just below always holds true, we identify γ_A and γ_B and write this as $\gamma_A \sim \gamma_B$. The equality is

$$W_q[\Gamma_A](\{a\}) = C_q(\gamma_A \rightarrow \gamma_B)W_q[\Gamma_B](\{a\}) \quad (4.0.3)$$

where $C_q(\gamma_A \rightarrow \gamma_B)$ is a function of only q and independent of all holonomies around punctures and is also determined by γ_A and γ_B only.²⁾ Notice that, in many cases, this

²⁾In all examples we know, C_q is a product of a polynomial of $q^{\frac{1}{2}}$ and a monomial with a negative rational power of q . In addition, $C_q = C_{q^{-1}}$ always holds true. This comes from the symmetry (an assumption, however) of the 2D q -deformed Yang-Mills theory. Actually, we can compute the skein relations in the 2D topological q -deformed Yang-Mills theory not in the Schur indices because they differ by just the overall factors.

relation is enough local and independent of the choice of C . Now we have the equivalence relations \sim and refer to them as the "skein relations" hereafter.

Finally, we make a few comments. Under the parameter identification $q = e^{2\pi i b^2}$ [75, 170] where b is a physical parameter in the Liouville/Toda CFT, the skein relations are common both in the CFTs and in the 2D q -deformed Yang-Mills theory. This is because the skein relations are expected to be the local relations about codimension four defects in the 6D $\mathcal{N}=(2,0)$ SCFTs and to be independent of the four dimensional global background geometries, namely, the choice of S_b^4 or $S^1 \times_q S^3$.

Notice also that the crossing skein relation may suggest the new direction of the 2D q -deformed Yang-Mills theory but the appearance is not so obvious in this 2D theory itself. However, this class S picture from the 6D $\mathcal{N}=(2,0)$ SCFTs strongly suggest that. See also Sec 4.3.2.

Finally, we dare to say that the above definition is a bit incomplete. Indeed, we will discuss new kinds of skein relations in Sec. 5.2.

4.1 Loop operators in 4d and skein relations in 2d

In the Liouville theory, a Verlinde loop operator is defined in terms of monodromy actions on the conformal block \mathcal{F} along a loop γ . It is possible to insert more than one Verlinde operator and $\mathcal{L}_{\gamma_A} \mathcal{L}_{\gamma_B} \mathcal{F} \neq \mathcal{L}_{\gamma_B} \mathcal{L}_{\gamma_A} \mathcal{F}$ in general when γ_A and γ_B intersect each other, as we see from the concrete calculations. See Fig. 4.1 for an illustration.

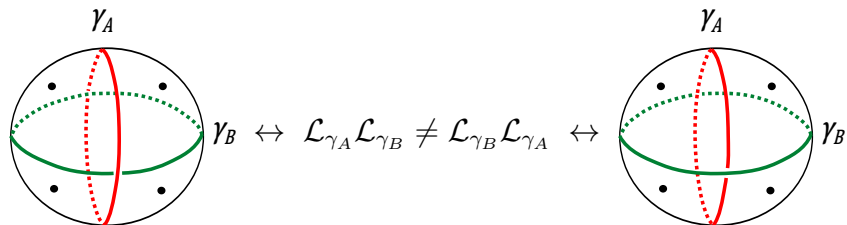


Figure 4.1: Non-commutativity of actions of loop operators.

Under the 2d-4d correspondence, the Verlinde operators map to loop operators of the 4d theory. Therefore, there should be a concept of ordering of loops on the 4d side, such that the product becomes non-commutative. In this section we review how this ordering arises, following [47, 49, 50, 83]. See also the recent reviews [171, 172].

4.1.1 Sums and products of loops

We consider the 4d set-ups where some kind of localization computations is possible. Typically there is a supercharge preserved in the background, whose square involves a linear combination of two isometries $k_{1,2}$. Supersymmetric loops wrap along the direction of k_1 and sit at the fixed point of k_2 .

In the neighborhood of the loop, we can approximate the geometry as $S^1 \times \mathbb{C} \times \mathbb{R}$, where k_1 shifts the coordinate along S^1 and k_2 is the phase rotation of \mathbb{C} . The loop now wraps S^1 and sits at the origin of \mathbb{C} , and the position $x \in \mathbb{R}$ is arbitrary. Therefore, we can place multiple loops $L_{1,2,\dots}$ on $x_{1,2,\dots}$ preserving the same supercharge.

This gives an intrinsic ordering of loops on the 4d side, and furthermore, the expectation values are unchanged under infinitesimal changes of the positions x_i . The choice of the local supersymmetric background at a loop can be characterized by a single parameter which we denote by \mathfrak{q} . These statements can be explicitly checked in the case of the localizations on $S^1 \times S^3$ [28], $S^1 \times \mathbb{R}^3$ [49] and S_b^4 [30].

Given two types of loop defects L_1 and L_2 , we denote loops placed at $x \in \mathbb{R}$ by $L_i(x)$. We define a formal sum $L_1 + L_2$ of two loops by

$$\langle \cdots (L_1 + L_2)(x) \rangle := \langle \cdots L_1(x) \rangle + \langle \cdots L_2(x) \rangle \quad (4.1.1)$$

where the ellipses stand for other operator insertions. The product $L_1 \cdot L_2$ of two loops are now defined by

$$\langle \cdots (L_1 \cdot L_2)(x) \rangle := \langle \cdots L_1(x_1) L_2(x_2) \rangle \quad (4.1.2)$$

where we demand $x_1 > x > x_2$ so that L_1 and L_2 are the loops closest to x from the left and from the right. Since the expectation values depend only on the order but independent of the relative distance, this gives a consistent definition.

At this stage, we can make sense of the operator product expansion for defects. Suppose that there is a set $L_{1,2,\dots}$ of loops which cannot be decomposed into any sum of other simpler ones. We then have the following expansion of correlation functions

$$\langle \cdots L_i \cdot L_j(x) \rangle = \sum_k c_{ij}^k(\mathfrak{q}) \langle \cdots L_k(x) \rangle \quad (4.1.3)$$

that can be written succinctly as

$$L_i \cdot L_j = \sum_k c_{ij}^k(\mathfrak{q}) L_k. \quad (4.1.4)$$

The OPE coefficients $c_{ij}^k(\mathfrak{q})$ are asymmetric under the exchange $i \leftrightarrow j$ due to the intrinsic ordering along \mathbb{R} . However, we can simultaneously flip the \mathbb{R} direction and S^1 direction in the local $S^1 \times \mathbb{C} \times \mathbb{R}$ geometry to obtain another supersymmetric background. The background is parameterized by \mathfrak{q} as remarked before, and we use the parameterization such that this flip is represented by $\mathfrak{q} \mapsto \mathfrak{q}^{-1}$. Then we should have the relation

$$c_{ij}^k(\mathfrak{q}) = c_{ji}^k(\mathfrak{q}^{-1}). \quad (4.1.5)$$

There is also an order for the defect networks on the two dimensional geometry side. In order to make the relation between two orders, let us consider the case when the 4d side is S_b^4 and the 2d side is the Liouville/Toda theory [17, 38]. In this case the Verlinde operators associated to the networks on the 2d side act on the space $\mathcal{H}_{\text{conf}}$ of conformal blocks, and the loop operators on the 4d side act on the space $\mathcal{H}_{\text{hemi}}$ of holomorphic

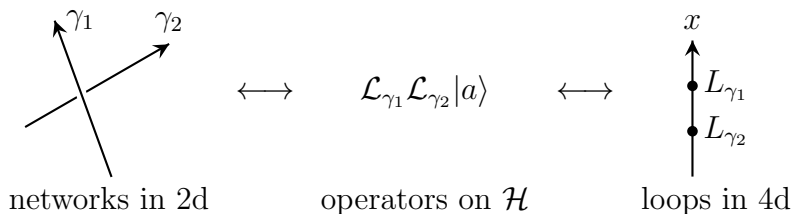


Figure 4.2: Left: the part of networks γ_1 and γ_2 . For any other crossing of $\gamma_{1,2}$, γ_1 is always above γ_2 . Middle: the expressions acting on $\mathcal{H} = \mathcal{H}_{\text{conf}} = \mathcal{H}_{\text{hemi}}$. Right: the ordering on the 4d side, along \mathbb{R} .

Nekrasov partition functions defined on a hemisphere [26, 27, 46, 68]. Since $\mathcal{H}_{\text{conf}}$ and $\mathcal{H}_{\text{hemi}}$ are naturally isomorphic, we can see the relations among three orderings as shown in Fig. 4.2.

Corresponding to (4.1.4), there should be the operator product expansions of defect networks which are indeed skein relations as resolutions of the crossings. In Sec. 5.3, we will see that we can calculate many OPE coefficients in terms of defect networks.

4.1.2 Non-commutativity and the angular momentum

Let us recall the origin of the non-commutativity when the geometry is globally $S^1 \times \mathbb{C} \times \mathbb{R}$, following the discussions in [49, 83]. Considering the S^1 as the time direction, the partition function of $S^1 \times \mathbb{C} \times \mathbb{R}$ is given by

$$\Omega = \text{Tr}_{\mathcal{H}} [(-1)^F e^{2\pi i \lambda \mathcal{J}_3}] \quad (4.1.6)$$

where \mathcal{H} is the Hilbert space of the system, $\mathcal{J}_3 = J_3 + I_3$ is the sum of the spin along \mathbb{R} and the Cartan of the $SU(2)$ R-symmetry. Our parameter \mathfrak{q} is then given by $\mathfrak{q} = e^{\pi i \lambda}$.

Suppose now that we have a $U(1)$ gauge theory, that the first loop L_1 is purely electrically charged with electric charge e and that the second loop L_2 is purely magnetically charged with magnetic charge m . Then there appears the Poynting vector carrying the angular momentum $J_P = (\hbar/2)em$ along the \mathbb{R} direction. The magnitude of J_P is independent of the distance between two particles but the sign depends on the ordering, and therefore we have

$$L_1 \cdot L_2 = \mathfrak{q}^{-2em} L_2 \cdot L_1. \quad (4.1.7)$$

In the classical limit ($\mathfrak{q} \rightarrow 1$), this product becomes commutative.

4.2 Networks and skein relations in 2d

In this section we discuss possible types of networks in class S theories of type $SU(N)$ and their skein relations. Our guiding principle is that they are described by the struc-

ture of the quantum groups underlying both the q -deformed Yang-Mills and the Liouville/Toda CFT, and that the skein relations are universal under an appropriate parameter identification. The skein relations exhibited below already appear in the mathematical works [168, 173, 174], up to the overall factors and the changes in conventions.

Skein relations introduce equivalence relations among all possible networks, and it would be extremely useful if we can pick a natural representative element out of a given equivalence class of networks allowing linear combinations of networks. In this thesis we at least give a general method to simplify a given network:

- In principle, edges in a network can carry arbitrary representations of $SU(N)$. We will first rewrite them in terms of representations $\wedge^k \square$ for $k = 1, \dots, N - 1$. These are the fundamental representations in the mathematical terminology,³⁾ and within the diagrams we just denote them by $1, 2, \dots, N - 1$.
- Then we rewrite all crossings in terms of linear combinations of junctions that are at most rectangular. The concrete formulas are given in (4.2.36). We call this process *crossing resolutions*.

In the A_1 case, these procedures eliminate all the crossings and no junctions remain, thus reproducing the classification in [25]. In the A_2 case, we will see that all digons and rectangles can be eliminated, and we will find a natural representative for a given equivalence class of networks. We will detail this process in Sec. 5.3.4.

Hereafter we use a version of the standard quantum number defined as

$$\langle n \rangle := (-1)^{n-1} [n] := (-1)^{n-1} \frac{q^n - q^{-n}}{q - q^{-1}} \quad (4.2.1)$$

and the factorial defined as

$$\langle 0 \rangle! = 1, \quad \langle n \rangle! = \langle n \rangle \langle n - 1 \rangle! \quad (4.2.2)$$

As this section is rather long, let us pause here to explain the organization: in Sec. 4.2.1, we start by recalling that codimension-4 operators of the 6d $\mathcal{N}=(2, 0)$ theory are labeled by representations and they can have junctions corresponding to the invariant tensors. In Sec. 4.2.2, we describe how an arbitrary representation can be rewritten in terms of just the fundamental representations of the form $\wedge^k \square$. In Sec. 4.2.3, we then describe the trivalent junctions where three edges labeled by fundamental representations meet. In Sec. 4.2.4, we show how a crossing of two edges can be rewritten in terms of junctions. We start from the crossing of two edges labeled by \square and then describe the general case. In Sec. 4.2.5 we summarize the Reidemeister moves that are fundamental equivalence relations guaranteeing the isotopy invariance. In Sec. 4.2.6 we note other useful skein relations that can be used to simplify networks. Finally in Sec. 4.2.7, we explicitly display the skein relations for A_2 and A_3 .

³⁾Contrary to the standard physics usage, we do not restrict the fundamental representation to be the defining N -dimensional representation in this thesis.

In general, it would also be important in the class S theory to study skein relations with full and other punctures in [14] or networks ending on other punctures. We do not, however, consider such objects in this thesis.

4.2.1 Generalities

Before proceeding, let us first recall the fact that a codimension-4 operator of the 6d $\mathcal{N}=(2,0)$ theory of type $SU(N)$ has a label given by a representation of $SU(N)$, and how a multiple number of such operators can be joined.

A cylinder of the $\mathcal{N}=(2,0)$ theory gives rise to a 4d $\mathcal{N}=2$ vector multiplet with gauge group $SU(N)$. On the 4d side, then, we can consider the Wilson loop operator in a representation R of $SU(N)$. This should come from some codimension-4 operator of the $\mathcal{N}=(2,0)$ theory wrapped around the cylinder. Then this codimension-4 operator also needs to be labeled by a representation R .

When we multiply two parallel Wilson loops with representations R_1 and R_2 , we get a Wilson loop with representation $R_1 \otimes R_2$, and the product is commutative. The same should be then true among codimension-4 operators of the $\mathcal{N}=(2,0)$ theory.

On the 4d side, three Wilson loops in representations $R_{1,2,3}$ can be joined at a point consistently if $R_1 \otimes R_2 \otimes R_3$ contains an $SU(N)$ invariant subspace, or equivalently when there is an invariant tensor in this triple tensor product. The number of independent ways to join them is given by the number of linearly independent invariant tensors. Then, three codimension-4 operators of the $\mathcal{N}=(2,0)$ theory labeled by $R_{1,2,3}$ can be joined along a one-dimensional subspace when there are invariant tensors in $R_1 \otimes R_2 \otimes R_3$. The number of distinct ways to connect is given by the number of linearly independent invariant tensors.

Since this should be an intrinsic property of codimension-4 operators of the 6d theory, we can join three codimension-4 operators along a one-dimensional loop on the 4d side. This gives a junction of three edges labeled by R_1, R_2, R_3 on the 2d side. Using many such junctions, we end up having networks on the 2d side.

4.2.2 Restriction of labels

First, note that Wilson loop on the 4d side in a representation R in a direction can be thought of as a Wilson loop in the representation \bar{R} in the opposite direction. This feature should also be carried over to the codimension-4 defects of the $\mathcal{N}=(2,0)$ theory, and to the networks on the 2d side. This can be represented diagrammatically as

$$\longrightarrow R = R^* \longleftarrow . \quad (4.2.3)$$

As it is cumbersome to use arbitrary representations R as labels, we next rewrite them in terms of fundamental representations $\wedge^k \square$, $k = 1, \dots, N - 1$. An irreducible representation R can be specified by a Young diagram (ℓ_i) where ℓ_i is the number of boxes in the i -th row, so that $\sum \ell_i = N$. For example, $\wedge^k \square$ is represented by $(\underbrace{1 \ 1 \ 1 \ \dots \ 1}_k) = (1^k)$.

Note that any symmetric polynomial of N variables x_1, x_2, \dots, x_N , under a constraint $x_1 x_2 \dots x_N = 1$, can be written as a polynomial of the elementary symmetric polynomials. As a character $\chi_R(\text{diag}(x_1, \dots, x_N))$ of $\text{SU}(N)$ in a representation R is such a symmetric polynomial, and $\chi_{(1^k)}(\text{diag}(x_1, \dots, x_N))$ for $k = 0, 1, 2, \dots, N - 1$ are exactly elementary symmetric polynomials, this means that any representation R can be decomposed as the direct sum (allowing negative integral coefficients) of the tensor products of $\wedge^k \square$.

For example, we have the equalities

$$\chi_{(2)} = \chi_{(1)}^2 - \chi_{(1^2)}, \quad \chi_{(21)} = \chi_{(1^2)}\chi_{(1)} - \chi_{(1^3)}, \quad (4.2.4)$$

$$\chi_{(3)} = \chi_{(1)}^3 - 2\chi_{(1^2)}\chi_{(1)} + \chi_{(1^3)}, \quad \chi_{(2^2)} = \chi_{(1^2)}\chi_{(1^2)} - \chi_{(1)}\chi_{(1^3)} \quad (4.2.5)$$

which we can diagrammatically depict, in the case of closed loops, as

$$\begin{array}{c} \begin{array}{c} \square \\ \square \end{array} \\ \circlearrowleft \end{array} = \begin{array}{c} 1 \\ \circlearrowleft \\ 1 \end{array} - \begin{array}{c} 2 \\ \circlearrowleft \end{array}, \quad \begin{array}{c} \square \\ \square \\ \square \end{array} \\ \circlearrowleft \end{array} = \begin{array}{c} 2 \\ \circlearrowleft \\ 1 \end{array} - \begin{array}{c} 3 \\ \circlearrowleft \end{array}, \quad (4.2.6)$$

$$\begin{array}{c} \square \\ \square \\ \square \\ \square \end{array} \\ \circlearrowleft \end{array} = \begin{array}{c} 2 \\ \circlearrowleft \\ 2 \end{array} - \begin{array}{c} 3 \\ \circlearrowleft \\ 1 \end{array}, \quad \begin{array}{c} \square \\ \square \\ \square \\ \square \end{array} \\ \circlearrowleft \end{array} = \begin{array}{c} 1 \\ \circlearrowleft \\ 1 \end{array} - 2 \begin{array}{c} 2 \\ \circlearrowleft \\ 1 \end{array} + \begin{array}{c} 3 \\ \circlearrowleft \end{array}. \quad (4.2.7)$$

These relations are locally applicable on parallel edges. Therefore, we can insert some punctures or networks inside the circle, for example.

4.2.3 Canonical junctions and removal of digons

Canonical junctions

Now our edges are labelled by the fundamental representations $\wedge^k \square$, $k = 0, 1, \dots, N - 1$. We can just use the integer k to label the edge, and an edge labelled by 0 can be removed. Reversing the orientation now corresponds to replacing the label k by $N - k$. An edge labeled by k has charge k under the center of $\text{SU}(N)$, and therefore we call these integer labels as the *charge*.⁴⁾

For each trivalent junction, the sum of three inflowing charges must equal to zero modulo N . Say we have three edges labelled by a , b and $c = a + b$. There is only a single invariant tensor in $\wedge^a \square \otimes \wedge^b \square \otimes \wedge^{N-c} \square$, and this corresponds to the projection from $\wedge^a \square \otimes \wedge^b \square$ to $\wedge^{c=a+b} \square$. Therefore, there is no need to place a label on a junction to distinguish the possible invariant tensors.

Sometimes these labels k are then taken to be defined modulo N as in [62, 68], but it is useful to consider them just as integers between 0 and $N - 1$. This is because we can

⁴⁾Note that it is a special property of A_k that there is the one-to-one correspondence between the set of the fundamental representations $\wedge^k \square$ including the trivial one and the charge under the center.

write down the invariant tensor rather explicitly using the quantum group representation theory when the net inflowing charge to a junction vanishes in \mathbb{Z} . We call such a junction *canonical*. We call a junction non-canonical if the net inflowing charge vanishes only in \mathbb{Z}_N . See Fig. 4.3 for examples.

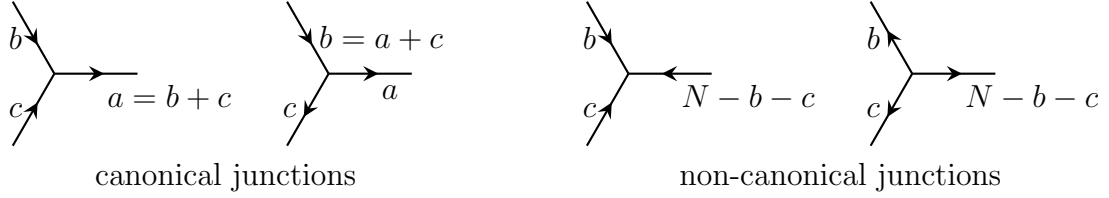


Figure 4.3: Canonical and non-canonical junctions

Let us now describe the invariant tensors associated to the canonical junctions. Let \square be spanned by the vectors e_1, \dots, e_N . We define the \mathfrak{q} -deformed wedge product by the rule

$$e_i \wedge e_j = -\mathfrak{q} e_j \wedge e_i, \quad (i \leq j) \quad (4.2.8)$$

where in particular $e_i \wedge e_i = 0$ where we do not sum over i . This defines the projection π from $\square \otimes \square$ to $\wedge^2 \square$ by

$$\pi_{1,1 \rightarrow 2} : e_i \otimes e_j \mapsto e_i \wedge e_j. \quad (4.2.9)$$

Furthermore, $\wedge^2 \square$ can be naturally embedded within $\square \otimes \square$ by the rule

$$\iota_{2 \rightarrow 1,1} : e_i \wedge e_j \mapsto -\mathfrak{q} e_i \otimes e_j + e_j \otimes e_i, \quad (i < j). \quad (4.2.10)$$

More generally, we associate to any canonical junction that combines labels a, b to $a + b$ the projection

$$\pi_{a,b \rightarrow a+b} : e_{i_1} \wedge \dots \wedge e_{i_a} \otimes e_{j_1} \wedge \dots \wedge e_{j_b} \mapsto e_{i_1} \wedge \dots \wedge e_{i_a} \wedge e_{j_1} \wedge \dots \wedge e_{j_b} \quad (4.2.11)$$

and to any canonical junction that splits the label $a + b$ to two labels a, b the map $\iota_{a+b \rightarrow a,b}$ where

$$\begin{aligned} \iota_{a+b \rightarrow a,b} : e_{k_1} \wedge \dots \wedge e_{k_{a+b}} \\ \mapsto (-\mathfrak{q})^{ab} \sum_{i_1 < \dots < i_a, j_1 < \dots < j_b} (-\mathfrak{q}^{-1})^{n(i,j;k)} e_{i_1} \wedge \dots \wedge e_{i_a} \otimes e_{j_1} \wedge \dots \wedge e_{j_b} \end{aligned} \quad (4.2.12)$$

where we assume $k_1 < \dots < k_{a+b}$, the sum is over the disjoint split of indices

$$\{k_1, \dots, k_{a+b}\} = \{i_1, \dots, i_a\} \sqcup \{j_1, \dots, j_b\}, \quad (4.2.13)$$

and $n(i, j; k)$ is the minimal number of adjacent transpositions to bring the sequence $i_1, \dots, i_a, j_1, \dots, j_b$ to k_1, \dots, k_{a+b} . These maps are described in more detail mathematically in [175].

Then these maps $\pi_{a,b \rightarrow a+b}$ and $\iota_{a+b \rightarrow a,b}$ naturally combine according to the following diagrams together with the ones with reversed arrows:

$$\begin{array}{c} d \\ \uparrow \\ x \\ \swarrow \quad \searrow \\ a \quad b \quad c \end{array} = \begin{array}{c} d \\ \uparrow \\ y \\ \swarrow \quad \searrow \\ a \quad b \quad c \end{array} \quad (4.2.14)$$

or equivalently

$$\begin{array}{c} a \quad d \\ \swarrow \quad \searrow \\ x \\ \swarrow \quad \searrow \\ b \quad c \end{array} = \begin{array}{c} a \quad d \\ \swarrow \quad \searrow \\ y \\ \swarrow \quad \searrow \\ b \quad c \end{array} . \quad (4.2.15)$$

Here $x = a + b = d - c$, $y = b + c = d - a$ and $d = a + b + c$.

Removal of digons

Now, we can check that any digons can be removed as

$$\begin{array}{c} \bullet \\ \uparrow k \\ \bullet \quad \bullet \quad \bullet \quad \bullet \\ \downarrow k \\ \bullet \end{array} \begin{array}{c} i_1 \\ \curvearrowright \\ i_2 \\ \curvearrowright \\ i_3 \\ \curvearrowright \\ \dots \\ i_\ell \end{array} = \frac{\langle k \rangle!}{\langle i_1 \rangle! \langle i_2 \rangle! \dots \langle i_\ell \rangle!} \left| \begin{array}{c} \bullet \\ \uparrow k \\ \bullet \\ \downarrow k \\ \bullet \end{array} \right. \quad (4.2.16)$$

where $\sum_{a=1}^{\ell} i_a = k$.

Note that in the classical limit $q \rightarrow 1$ the prefactor becomes

$$(-1)^{\sum_{a < b} i_a i_b} \frac{k!}{i_1! i_2! \dots i_\ell!} \quad (4.2.17)$$

due to the fact that the classical limit of $\iota_{a+b \rightarrow a,b}$ is $(-1)^{ab}$ times the standard map that follows from the classical epsilon symbol.

This somewhat unusual sign is however necessary to match with the known skein relations in the Liouville/Toda theory, and it also simplifies the signs appearing in the general crossing resolutions (4.2.36). In the q -deformed Yang-Mills theory it would be more conventional to drop this sign and the canonical junctions would be defined to be $\pi_{a,b \rightarrow a+b}$ and $(-1)^{ab} \iota_{a+b \rightarrow a,b}$. Notice that this convention change exactly corresponds to that of the Fermion number convention of SCI on the 4D side discussed in Sec. . Concretely

speaking, the choice (3.4.17) corresponds to the Liouville/Toda convention at the skein relation level. We will stick to the Liouville/Toda convention in this chapter.

When the sum of i_l is N , we can use the rule to evaluate a network with two trivalent junctions, since edges labelled by N can be removed. For example, when $i + j + k = N$, we have

$$\begin{array}{c} \bullet \\ \swarrow \quad \downarrow \quad \searrow \\ i \quad j \quad k \\ \swarrow \quad \downarrow \quad \searrow \\ \bullet \end{array} = \frac{\langle N \rangle!}{\langle i \rangle! \langle j \rangle! \langle k \rangle!}. \quad (4.2.18)$$

More simply, we can evaluate a closed loop with label k by considering it as a digon with edges labelled by k and $N - k$:

$$\begin{aligned} \begin{array}{c} k \\ \circlearrowleft \end{array} &= \frac{\langle N \rangle!}{\langle k \rangle! \langle N - k \rangle!} \\ &= (-1)^{k(N-k)} \chi_{\wedge^k \square}(\text{diag}(\mathfrak{q}^{N-1}, \mathfrak{q}^{N-3}, \dots, \mathfrak{q}^{1-N})) = (-1)^{k(N-k)} \dim_{\mathfrak{q}} \wedge^k \square. \end{aligned} \quad (4.2.19)$$

Again, this shows that our convention is different by a factor of $(-1)^{k(N-k)}$ from the convention in the q -deformed Yang-Mills. We also see at this point that, to compare with the skein relation of the Toda theory or the q -deformed Yang-Mills theory, we need to use the relation

$$\mathfrak{q} = e^{\pi i b^2} = q_{\text{SCI}}^{1/2}. \quad (4.2.20)$$

4.2.4 Crossing resolutions

The \mathcal{R} matrix

Let us first discuss the best-known case: the \mathcal{R} -matrix for $\square \otimes \square$ of $\text{SU}(N)$, which is given by

$$\mathcal{R} = A(Q + \mathfrak{q}^{-1} I_{\square \otimes \square}). \quad (4.2.21)$$

Here, I_V is the identity operator on a vector space V , Q is an operator

$$Q = \sum_{i \neq j} e_{ij} \otimes e_{ji} - \mathfrak{q} \sum_{i < j} e_{ii} \otimes e_{jj} - \mathfrak{q}^{-1} \sum_{i > j} e_{ii} \otimes e_{jj} \quad (4.2.22)$$

where e_{ij} is a matrix whose only non-zero entry is 1 at the i -th row and j -th column and A is the overall normalization which we will be fixed later.

The action of Q on the base $e_a \otimes e_b$ of $\square \otimes \square$ is

$$Q(e_a \otimes e_b) = \begin{cases} e_b \otimes e_a - \mathfrak{q} e_a \otimes e_b, & (a < b) \\ 0, & (a = b) \\ e_b \otimes e_a - \mathfrak{q}^{-1} e_a \otimes e_b, & (a > b) \end{cases}. \quad (4.2.23)$$

The resulting entries are the basis vectors of the second rank antisymmetric representation of $SU_q(N)$. Indeed, the operator Q is the composition of the projection $\pi_{1,1 \rightarrow 2} : \square \otimes \square \rightarrow \Lambda_q^2 \square$ and the natural embedding $\iota_{2 \rightarrow 1,1} : \Lambda_q^2 \square \rightarrow \square \otimes \square$:

$$Q = \iota_{2 \rightarrow 1,1} \pi_{1,1 \rightarrow 2}. \quad (4.2.24)$$

Note also that Q satisfies

$$Q^2 = -(\mathfrak{q} + \mathfrak{q}^{-1})Q = \langle 2 \rangle Q. \quad (4.2.25)$$

This is a special case of the digon elimination.

We can now represent the R-matrix \mathcal{R} diagrammatically as

$$\begin{array}{c} \diagup \diagdown \\ \square \quad \square \end{array} = A \left(\begin{array}{c} \square \quad \square \\ \diagdown \quad \diagup \\ \Lambda^2 \square \\ \diagup \quad \diagdown \\ \square \quad \square \end{array} + \mathfrak{q}^{-1} \begin{array}{c} \uparrow \\ \square \end{array} \quad \begin{array}{c} \uparrow \\ \square \end{array} \right). \quad (4.2.26)$$

The inverse of the R-matrix \mathcal{R} is

$$\mathcal{R}^{-1} = A^{-1}(Q + \mathfrak{q}I_{\square \otimes \square}) \quad (4.2.27)$$

that we represent as

$$\begin{array}{c} \diagdown \diagup \\ \square \quad \square \end{array} = A^{-1} \left(\begin{array}{c} \square \quad \square \\ \diagup \quad \diagdown \\ \Lambda^2 \square \\ \diagdown \quad \diagup \\ \square \quad \square \end{array} + \mathfrak{q} \begin{array}{c} \uparrow \\ \square \end{array} \quad \begin{array}{c} \uparrow \\ \square \end{array} \right) \quad (4.2.28)$$

Below, we call the crossing (4.2.26) as positive and the crossing (4.2.28) as negative.

The A_1 -case: In this case, $\Lambda^2 \square$ is the trivial one-dimensional representation and there is the pseudo-reality condition $\overline{\square} \simeq \square$ which we can diagrammatically write as

$$\longrightarrow \square = \square \longleftarrow =: \text{---}. \quad (4.2.29)$$

Then the general equation (4.2.26) reduces to

$$\begin{array}{c} \diagdown \diagup \\ \square \quad \square \end{array} = \mathfrak{q}^{-1/2} \left(\begin{array}{c} \diagdown \diagup \\ \square \quad \square \end{array} + \mathfrak{q}^{1/2} \begin{array}{c} \text{---} \\ \text{---} \end{array} \right). \quad (4.2.30)$$

where we have set $A = \mathfrak{q}^{1/2}$. We then have

$$\mathfrak{q}^{-1/2} \begin{array}{c} \diagdown \diagup \\ \square \quad \square \end{array} - \mathfrak{q}^{1/2} \begin{array}{c} \diagup \diagdown \\ \square \quad \square \end{array} = (\mathfrak{q}^{-1} - \mathfrak{q}) \left(\begin{array}{c} \text{---} \\ \text{---} \end{array} \right) \quad (4.2.31)$$

These reproduce the standard skein relations of the Liouville theory found in [26,27] under the identification $\mathfrak{q} = e^{i\pi b^2}$.

The relation $Q^2 = \langle 2 \rangle Q$ shows

$$\bigcirc = \langle 2 \rangle = -\chi_{\square}(\text{diag}(\mathfrak{q}, \mathfrak{q}^{-1})). \quad (4.2.32)$$

From this we see that $\mathfrak{q} = q_{\text{SCI}}^{1/2}$ where q_{SCI} is the parameter used commonly in the literature on the superconformal index. The minus sign here is a convention common in the Liouville/Toda literature, i.e. the definition of a loop in the representation \square differs by an overall minus sign between the Liouville theory and the q -deformed Yang-Mills.

The A_2 -case: Here we have $\bar{\square} = \bigwedge^2 \square$, and therefore we have

$$\longrightarrow \square = \bigwedge^2 \square \longleftarrow. \quad (4.2.33)$$

As we now only have one type of the label \square , we can drop it altogether. The general R-matrix (4.2.26) then becomes

$$\begin{array}{c} \nearrow \\ \searrow \\ \swarrow \\ \searrow \end{array} = \mathfrak{q}^{1/3} \begin{array}{c} \nearrow \\ \searrow \\ \swarrow \\ \searrow \end{array} + \mathfrak{q}^{-2/3} \begin{array}{c} | \\ | \\ | \\ | \end{array} \begin{array}{c} | \\ | \\ | \\ | \end{array} \quad (4.2.34)$$

where we have set $A = \mathfrak{q}^{1/3}$. This reproduces the fundamental skein relations of the SU(3) Toda theory found in [68], again under the identification $\mathfrak{q} = e^{i\pi b^2}$.

General case: The analysis so far suggests that we should take

$$A = \mathfrak{q}^{\frac{1}{N}} \quad (4.2.35)$$

in general. As we will see soon, this is consistent with the general crossing resolutions (4.2.36).

General crossing resolutions

Now let us move on to the crossing resolutions in the general case. The expression was found in [168] up to an overall factor, which we quote here:

$$\begin{array}{c} a \\ \nearrow \\ \searrow \\ b \end{array} = \mathfrak{q}^{\frac{ab}{N}} \sum_{i=0}^s \mathfrak{q}^{-i} \begin{array}{c} a \qquad b \\ \nearrow \quad \nearrow \\ a-i \quad a-i \\ \searrow \quad \searrow \\ i \qquad a+b-i \\ \swarrow \quad \swarrow \\ b \quad b-i \\ \searrow \quad \searrow \\ a \end{array} \quad (4.2.36)$$

where $s = \min(a, b, N - a, N - b)$ and $a, b = 0, 1, 2, \dots, N - 1$. With this choice of the overall factor, this equality is invariant with a reversal of an arrow and the rotation of the diagrams by 90° . Note also that when $a = b = 1$, this equality reduces to (4.2.26) we already discussed.

Let us introduce the names to the fundamental objects on the right hand side of (4.2.36):

$$Q_{(i)}^{ab} := \begin{array}{c} a \qquad b \\ \swarrow \quad \searrow \\ \text{---} a-i \text{---} \\ \uparrow \qquad \uparrow \\ i \qquad a+b-i \\ \text{---} b-i \text{---} \\ \swarrow \quad \searrow \\ b \qquad a \end{array} = a+b-i \begin{array}{c} a \qquad b \\ \swarrow \quad \searrow \\ \text{---} b-i \text{---} \\ \uparrow \qquad \uparrow \\ a+b-i \qquad i \\ \text{---} a-i \text{---} \\ \swarrow \quad \searrow \\ b \qquad a \end{array} . \quad (4.2.37)$$

Note that the number of possible choices of i matches with the number of irreducible summands of the decomposition of the tensor product $\wedge^a \square \otimes \wedge^b \square$. We expect that all these $Q_{(i)}^{ab}$ cannot be further decomposed as parts of networks.

The intersection number and the powers of \mathfrak{q}

Let us briefly discuss the significance of the prefactor $\mathfrak{q}^{\frac{ab}{N}}$ in (4.2.36). In general, two loop operators in a class S theory of type $SU(N)$ can be mutually nonlocal, and the nonlocality can be measured in terms of the Dirac pairing that takes values in \mathbb{Z}_N [176]. In terms of the 2d networks realizing the 4d loop operators, the Dirac pairing is given by their intersection number. We can define it by assigning a local intersection number to a crossing as follows:

$$\begin{array}{c} a \qquad b \\ \swarrow \quad \searrow \\ \text{---} \\ \swarrow \quad \searrow \\ \text{---} \end{array} : + ab, \quad \begin{array}{c} a \qquad b \\ \swarrow \quad \searrow \\ \text{---} \\ \swarrow \quad \searrow \\ \text{---} \end{array} : - ab. \quad (4.2.38)$$

This is consistent with the reversal of arrows, since it sends the label a to $N - a$.

The intersection number $I(\Gamma_1, \Gamma_2)$ of two networks Γ_1 and Γ_2 is then defined by summing the contributions from all the crossings:

$$\sum_{c : \text{crossing}} \text{sign}(c) a_c^{(1)} a_c^{(2)} \in \mathbb{Z}_N \quad (4.2.39)$$

where $\text{sign}(c)$ is the sign of the crossing c and $a_c^{(i)}$ is the charge of Γ_i at c .

In the Liouville/Toda setup, we expect the expectation value of any network without crossings is a single-valued function of $\mathfrak{q} = e^{\pi i b^2}$ invariant under $\mathfrak{q} \rightarrow e^{2\pi i} \mathfrak{q}$. Similarly, in the superconformal index, the expectation value of a loop operator on the 4d side is

a single valued function of $\mathfrak{q} = q_{\text{SCI}}^{1/2}$, since the index is a trace $\text{Tr} [(-1)^F q^{\Delta-I_3}]$ and the scaling dimensions Δ of a class S theory are integral or half-integral.

Non-invariance of the expectation value under $\mathfrak{q} \rightarrow e^{2\pi i} \mathfrak{q}$ then captures the mutual non-locality, and we can think of the prefactor $\mathfrak{q}^{\frac{ab}{N}}$ in (4.2.36) as encoding the difference in the local intersection number between the left hand side and the right hand side, to keep track of this non-locality. The difference in the powers of \mathfrak{q} among different summands in the resolutions of the crossings should be integral, and the relation (4.2.36) indeed satisfies this requirement.

$SL(2, \mathbb{Z})$ action on the torus

We can define the operation I which we call the *inversion* by reversing all the arrows simultaneously. This is an involution that we can identify with the charge conjugation on the 4d side.

When the network is on a torus, we can also consider the action of $SL(2, \mathbb{Z})$ on the networks. Two basic actions are the T -action and the S -action. T corresponds to sending $\alpha \mapsto \alpha$, $\beta \mapsto \beta + \alpha$ and S corresponds to $\alpha \mapsto \beta$, $\beta \mapsto -\alpha$, where α, β are two bases of the 1-cycles on the torus.

The operation $C = S^2$ generates the center of $SL(2, \mathbb{Z})$ and is the charge conjugation action in the 4d $\mathcal{N}=4$ SYM theory. Then we need to have two operations, C and I , to be consistent on the torus. The relation (4.2.37) relating two forms of the networks representing the same object $Q_{(i)}^{ab}$ is exactly the one required to have $C = I$, when these networks are put on the torus and open edges are connected to the opposite ones.

4.2.5 Reidemeister moves

In knot theory, a projective representation in two dimension of knots and links in a three dimensional space is not unique, and any different representations can be mapped to each other by a combination of three so-called *Reidemeister moves*, see e.g. [177]. The move I straightens a twist in an edge, the move II slides one edge over another edge to two parallel edges, and the move III changes the order of three crossings. In the presence of junctions, we need to add another move, where we move an edge over a junction. We call this as the move IV.

Since we expect that the charge of a loop in the 4d theory is determined by the isotropy class of networks, we would like to require that a network is invariant under these moves. This is indeed possible for the moves II, III and IV, but the move I results in a \mathfrak{q} -dependent factor. In the context of 3d Chern-Simons theory, this can be understood from the change in the framing of the link [70]. Let us describe these moves explicitly below.

R-Move II: This relation says that the the negative crossing is given by the inverse \mathcal{R}^{-1} of the R-matrix \mathcal{R} corresponding to the positive crossing.

$$\begin{array}{c} \curvearrowright \\ V_1 \quad V_2 \end{array} = \begin{array}{c} \uparrow \quad \uparrow \\ V_1 \quad V_2 \end{array} = \begin{array}{c} \curvearrowleft \\ V_1 \quad V_2 \end{array} . \quad (4.2.40)$$

R-Move III This is the Yang-Baxter equation which the R-matrix \mathcal{R} should satisfy.

$$\begin{array}{c} \curvearrowright \\ V_1 \quad V_2 \quad V_3 \end{array} = \begin{array}{c} \curvearrowleft \\ V_1 \quad V_2 \quad V_3 \end{array} . \quad (4.2.41)$$

R-Move IV This is the additional move for the networks with junctions.

$$\begin{array}{c} \curvearrowright \\ V_1 \quad V_2 \quad V_3 \quad W \end{array} = \begin{array}{c} \curvearrowleft \\ V_1 \quad V_2 \quad V_3 \quad W \end{array} . \quad (4.2.42)$$

R-Move I Finally, this move involves a non-trivial factor. The other one is Reidemeister move I :

$$\begin{array}{c} \curvearrowright \\ R \end{array} = \sigma_R \mathfrak{q}^{-C_2(R)} \begin{array}{c} \uparrow \\ R \end{array} , \quad \begin{array}{c} \curvearrowleft \\ R \end{array} = \sigma_R \mathfrak{q}^{C_2(R)} \begin{array}{c} \uparrow \\ R \end{array} . \quad (4.2.43)$$

where R can be any irreducible representation other than fundamental representations $\wedge^a \square$.

Indeed, when the representation R is $\wedge^k \square$, the coefficient $C_k(\mathfrak{q})$ can be calculated by using the general crossing resolution (4.2.36) and the relation (4.2.16) removing digons. The i -th network on the right hand side of (4.2.36) gives a coefficient $\frac{\langle N-k+i \rangle!}{\langle i \rangle! \langle k-i \rangle! \langle N+i-2k \rangle!}$ thanks to (4.2.16). We then find that the overall factor gives $C_k(\mathfrak{q}) = (-1)^{k(N+1)} \mathfrak{q}^{-(1+\frac{1}{N})k(N-k)}$ and expect the above relation holds true for any R . A direct understanding of this coefficient in 4d and 6d would be an interesting problem.

4.2.6 More simplifying relations

Let us list various other skein relations that can be used to simplify networks. All relations except (4.2.47) are known in [174] [173] and references therein.

$$\begin{array}{c} 1 \\ \swarrow \\ \times \\ \searrow \\ 2 \end{array} = q^{1/2} \begin{array}{c} 1 \quad 2 \\ \swarrow \quad \nearrow \\ \quad 3 \\ \nearrow \quad \swarrow \\ 2 \quad 1 \end{array} + q^{-1/2} \begin{array}{c} 1 \quad 2 \\ \swarrow \quad \nearrow \\ \quad 1 \\ \nearrow \quad \swarrow \\ 2 \quad 1 \end{array}, \quad (4.2.53)$$

$$\begin{array}{c} 2 \quad 2 \\ \swarrow \quad \nearrow \\ \times \\ \searrow \quad \swarrow \end{array} = q \begin{array}{c} 2 \quad 2 \\ \text{---} \\ 2 \quad 2 \end{array} + \begin{array}{c} 2 \quad 1 \quad 2 \\ \swarrow \quad \nearrow \\ \quad 1 \\ \nearrow \quad \swarrow \\ 2 \quad 1 \quad 2 \end{array} + q^{-1} \begin{array}{c} 2 \quad 2 \\ \text{---} \\ 2 \quad 2 \end{array}. \quad (4.2.54)$$

There are three decaying relations for one rectangle:

$$\begin{array}{c} 2 \quad 1 \quad 1 \\ \swarrow \quad \nearrow \\ \quad 1 \\ \nearrow \quad \swarrow \\ 1 \quad 2 \quad 1 \end{array} = \begin{array}{c} 2 \\ \text{---} \\ 1 \end{array} + \begin{array}{c} 2 \quad 1 \\ \swarrow \quad \nearrow \\ \quad 1 \\ \nearrow \quad \swarrow \\ 2 \quad 1 \end{array}, \quad (4.2.55)$$

$$\begin{array}{c} 1 \quad 1 \quad 1 \\ \swarrow \quad \nearrow \\ \quad 1 \\ \nearrow \quad \swarrow \\ 2 \quad 1 \quad 2 \end{array} = \langle 2 \rangle \begin{array}{c} 1 \\ \text{---} \\ 1 \end{array} + \begin{array}{c} \longrightarrow 1 \\ 1 \longleftarrow \end{array}, \quad (4.2.56)$$

$$\begin{array}{c} 1 \quad 1 \quad 1 \\ \swarrow \quad \nearrow \\ \quad 1 \\ \nearrow \quad \swarrow \\ 2 \quad 1 \quad 2 \end{array} = \langle 2 \rangle \begin{array}{c} 1 \quad 1 \\ \swarrow \quad \nearrow \\ \quad 2 \\ \nearrow \quad \swarrow \\ 1 \quad 1 \end{array}. \quad (4.2.57)$$

4.3 Wilson punctured network defects in 2D and composite surface-line systems in 4D

As explained in the introduction, in the 2D system, the geometric counterparts of 4D line operators and 4D surface operators are networks and punctures, respectively. As long as we treat either only surface operators or only line operators, the projection onto C is natural to discuss the 4D physics. However, if we have line defects bounded on 2D surface defects in 4D, it is not unique picture and there appears the new direction which line defects are localized in but surface defects extend along.

In this section, we introduce the 2D counterpart of the 4D composite surface-line defects in the 4D/2D duality relation. We call such objects Wilson punctured network defects. Such defects in the topological 2D q -deformed Yang-Mills theory are defined by

the isotopy class of the networks in some 3D space as explained hereafter.⁵⁾

To explain the physical idea, let us go back to the brane picture [26, 53, 55]. First of all, on the surface defects which we focus on, some 2D $\mathcal{N}=(2, 2)$ gauge theory with a $U(1)$ factor lives. Indeed, we consider the surface operators coming from the codimension four defects in the 6D $\mathcal{N}=(2, 0)$ SCFT and the surface defects can be realized as a type IIA brane set-up constructed from the combination of NS5-D4-D6 systems by Witten [20] and NS5'-D2-NS5-D4 systems by Hanany-Hori [109]. In particular, as discussed in [109], the complexified FI parameter corresponds to the position on the punctured Riemann surface locally, at least, around a simple puncture. Therefore, we set a natural assumption that the end point position of M2-branes (or the position of another M5-brane far from the bulk M5-branes) on the punctured Riemann surface determines the some parameter of surface operators which can be a complexified FI parameter in an appropriate duality frame. Now, recalling the defects characterization by varying parameters explained in Sec. 1.1.2, the composite surface-line defects are realized as the M2-branes varying in C as they go in the direction transverse to line defects but along the surface defects. See Fig. 4.4.

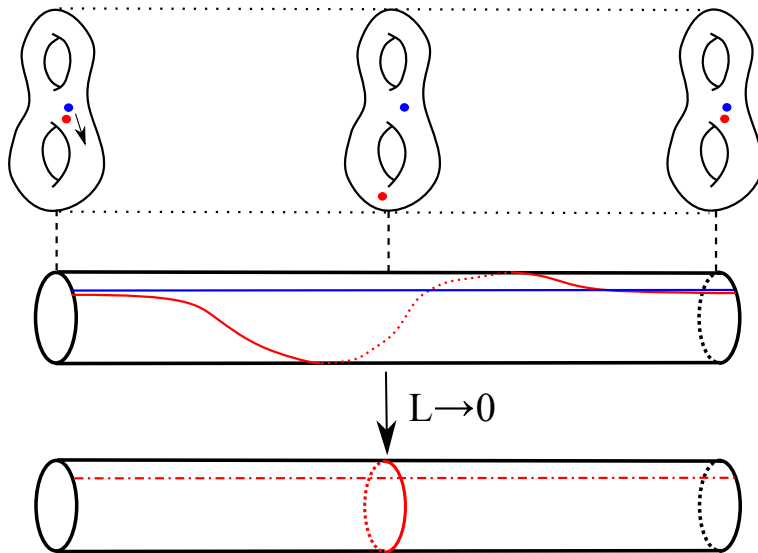


Figure 4.4: The 4D loop/line defect (interface for the surface defects) is generated from a position-dependent variation of the (UV) parameter space of surface operators which is identified with the punctured Riemann surface C . The horizontal direction and the cycle direction correspond to one of the directions in the surface operator and to a non-trivial 1-cycle in C respectively. L is the varying scale relative to the system scale and $\Lambda L \rightarrow 0$ means flowing to the IR. If only a surface operator exists, we get a line operator bound to the surface operator. (red cycle and red dash-dotted line) If there are a pair of surface operators with opposite charges each other, they vanish to leave only a line operator after the parameter for one of the two is varied. (red line and blue line)

⁵⁾We can also define them for the finite area q -deformed Yang-Mills theory.

In Sec. 4.3.1, we review several basic facts needed later. Next, we take a look at the geometrical configurations of two types of defects in Sec. 4.3.2. In Sec. 4.3.3, we discuss the skein relations including fully degenerate punctures. First, by introducing new topological moves, we derive such skein relations in some simple cases. Then, in the last Sec. 4.3.4, we rederive more general skein relations assuming the projection invariance.

4.3.1 Brief review on surface defects in the Schur indices

Notation

Although we summarize the Lie algebra notation in Appendix. A.1, we take a brief look at necessary ones. For a maximal torus element $a \in \mathbb{T}^{N-1}$ of $SU(N)$ and a weight vector $\lambda \in \Lambda_{wt} \simeq \mathbb{Z}^{N-1}$, we introduce a symbol $a^\lambda := (a_1^{\lambda_1}, a_2^{\lambda_2}, \dots, a_N^{\lambda_N})$ where $\lambda_i := (\lambda, h_i)$ $i = 1, 2, \dots, N$.⁶⁾ ρ denotes the Weyl vector, which is defined as $\sum_{a=1}^{N-1} \omega_a$. $C_2(R)$ is the quadratic Casimir defined as $(\lambda, \lambda + 2\rho)$ which is normalized as $C_2(\square) = N - \frac{1}{N}$. We also introduce a symbol $\sigma_R = (-1)^{|R|(N-1)}$ where $|R|$ is the number of the boxes in the Young diagram corresponding to the irreducible representation R .

The first of all, let us recall the discussions of Sec. 3.3. It was discussed in [77] that the SCIs in the presence of surface defects can be physically obtained by coupling a free hypermultiplet carrying $U(1)$ baryon symmetry to the original theory at UV and by taking the IR limit of that theory after giving variant VEVs to Higgs branch operators. At the mathematical level, this corresponds to taking the residues at a pole in the fugacity complex planes, associated with the surface operator's charges and finally results in a difference operator acting on the flavor fugacities of the original theory.

The above procedure is expected to reproduce in the IR the same defects as those from codimension four defects in 6D $\mathcal{N}=(2,0)$ SCFTs and, in fact, this was checked in [55] by comparing these results with 4D SCIs coupled to the elliptic genera of the 2D $\mathcal{N}=(2,2)$ theories living on the surface defects. The difference operators in the Schur limit actually form the representation ring of $\mathfrak{su}(N)$ because the codimension four defects are labelled by representations of $\mathfrak{su}(N)$ [78, 79].

According to [77–79], we rewrite the difference operator for the surface defect labelled by an irreducible representation S as

$$\widehat{\mathcal{G}}_S = (\sqrt{I_{\text{vector}}(a)}) \cdot \left[\sum_{\lambda \in \Pi(S)} \mathfrak{q}^{-N(\lambda, \lambda)} a^{N\lambda} \widehat{\Delta}_{-\lambda} \right] \cdot (\sqrt{I_{\text{vector}}(a)})^{-1} \quad (4.3.1)$$

$$= (\sqrt{\Delta_{\text{Haar}}(a)})^{-1} \left[\sum_{\lambda \in \Pi(S)} \widehat{\Delta}_{-\lambda} \right] \cdot (\sqrt{\Delta_{\text{Haar}}(a)}) \quad (4.3.2)$$

⁶⁾Note that we keep the symbol λ_α as the Dynkin labels which are coefficients of ω_α of the highest weight. See also Appendix. E as for Lie algebra notations. The inner product $(,)$ is also defined there.

where we have renormalized so that they form the representation ring of $\mathfrak{su}(N)$ exactly, $I_{\text{vector}}(a)$ is the SCI contribution from the vector multiplet whose concrete expression does not matter in this paper, $\Delta_{\text{Haar}}(a)$ is the Haar measure of $SU(N)$ and $\widehat{\Delta}_{-\lambda}$ acts on a holonomy a by $\mathfrak{q}^{-2\lambda}a$. The characters $\chi_R(a)$ are common eigenfunctions of these operators for any S and their eigenvalues are given by

$$\bar{\mathcal{E}}_R^{(S)} = \chi_S(\mathfrak{q}^{-2(\rho+\lambda_R)}) = \frac{\dim_{\mathfrak{q}} S}{\dim_{\mathfrak{q}} R} \chi_R(\mathfrak{q}^{-2(\rho+\lambda_S)}). \quad (4.3.3)$$

Finally, we remark on the mathematical relation between the codimension four defects and the codimension two defects [28]. In the Liouville-Toda CFT set-up, the general vertex operator is given by $V_{\alpha}(z) =: e^{\langle \alpha, \phi(z) \rangle} :$ where α is a vector in \mathfrak{h}^{\vee} which is the dual to Cartan subalgebra, $z \in C$ and $\phi(z)$ is the Liouville-Toda scalar field. This corresponds to the general codimension two defect ($[1^N]$ type or full/maximal puncture) when $\alpha - (b + 1/b)\rho \in i\mathbb{R}^{N-1} \simeq \mathfrak{h}^{\vee}$. On the other hand, the codimension four defect labelled by a $\mathfrak{su}(N)$ irreducible representation S is obtained by taking the limit $\alpha \rightarrow -b\lambda_S$ or $-\frac{1}{b}\lambda_S$.⁷⁾ The vertex operator in this limit is called fully degenerate and we also refer to the corresponding punctures as fully degenerate punctures which exactly represent the 4D surface defects.

In the 2D q -deformed Yang-Mills theory, the procedure similar to the above one is given as

$$\lim_{a \rightarrow \mathfrak{q}^{-\rho-\lambda}} \frac{\chi_R(a)}{\dim_{\mathfrak{q}} R} = \frac{\bar{\mathcal{E}}_R^{(S)}}{\dim_{\mathfrak{q}} S} \quad (4.3.4)$$

where the denominator on the right hand side is just simply the normalization factor of the surface defect. In our normalization, the surface defects exactly reproduce the $\mathfrak{su}(N)$ representation ring :

$$\widehat{\mathcal{G}}_{S_1} \circ \widehat{\mathcal{G}}_{S_2} = \sum_{S_3} N_{S_1 S_2}^{S_3} \widehat{\mathcal{G}}_{S_3} \quad \text{or} \quad \bar{\mathcal{E}}_R^{(S_1)} \bar{\mathcal{E}}_R^{(S_2)} = \sum_{S_3} N_{S_1 S_2}^{S_3} \bar{\mathcal{E}}_R^{(S_3)}. \quad (4.3.5)$$

4.3.2 Geometrical configurations

Originally, the bulk geometry of 6D $\mathcal{N}=(2,0)$ SCFT is $S^3 \times S_E^1 \times C$. Both surface defects and line defects in 4D wrap S_E^1 . After the S_E^1 reduction, the geometry is the product of C and a S_H^1 -fibration over S^2 in our viewpoint. S_H^1 is a Hopf fiber which is the support of surface defects in 4D.⁸⁾ On the other hand, line defects in 4D are networks on C . Therefore, both types of defects are knots with junction in the fiber geometry $S_H^1 \times C =: M$ and localized at the same point in base geometry S^2 . In the following

⁷⁾The two limits correspond to two types of configurations of surface defects in S_b^4 . See the next subsection 4.3.2.

⁸⁾There are at least two kinds of surface defects when line defects are absent. The other one is obtained by exchanging two SCI fugacities p and q as seen in [77].

discussion, we regard S_H^1 as an interval I_H whose two end points are identified. Then let C_{in} and C_{out} denote two boundaries of $I_H \times C$. We interpret the surface defects as a defect running from a point in C_{in} to the same point in C_{out} along the I_H -direction.

Note that if we consider a 6D $\mathcal{N}=(2,0)$ SCFT on $S^4 \times C$, a similar argument holds true. This is because OPEs of two BPS defects are expected to be determined locally and independent from the global background geometry. Concretely, a surface defect extends along a $S^2 = \{(z, w = 0, x) \in \mathbb{C} \times \mathbb{C} \times \mathbb{R} \mid b^2|z|^2 + x^5 = 1\}$ in $S^4 = \{(z, w, x) \in \mathbb{C} \times \mathbb{C} \times \mathbb{R} \mid b^2|z|^2 + b^{-2}|w|^2 + x^5 = 1\}$ [76] and some line defects live on $S^1 = \{(z, w = 0, x_5 = x_*) \in \mathbb{C} \times \mathbb{C} \times \mathbb{R}\}$ where x_* is an arbitrary constant satisfying $|x_*| < 1$ [30]. Since only the local geometry around the defect locus is relevant, instead of S_H^1 , we take the new direction as the x^5 direction (open interval) in this case. Therefore, it is expected that the skein relations discussed in Sec. 4.3.3 are also applied to the Liouville-Toda CFTs and we can check, in several examples, the claim that they are common in both systems. The relation between \mathfrak{q} and b is given in [47] or [75] as $\mathfrak{q} = e^{i\pi b^2}$.

The phenomenon inherent in the S_b^4 case is that there simultaneously exist two types of line operators and, in a such case, it seems to be necessary to treat them in the full five dimensional geometry rather than three dimensional one. Notice also that there are two distinct origins of the non-commutativity of line operators correspondingly. One comes from the Poynting vector in the bulk generated by line's charges as discussed in [49,83] and this classical picture also may be valid in the Schur index case. The other interpretation is similar but different. There, both line operators cannot be genuine line operators and either should be the boundary of an open surface operator. Then, two operators have some contact interactions under the exchange of their ordering in the 4D bulk [97,98,115].

4.3.3 Skein relations with fully degenerate punctures

At first, we use the same projection of M onto the 2D plane as before. This is the projection onto C which we call “ C -projection”.

If the 4D surface defects are topological in M , by deforming its orbit in M , we expect the following relation :

$$S \odot = S \circlearrowleft \odot = \sigma_S \mathfrak{q}^{C_2(S)} S \circlearrowright \odot = \sigma_S \mathfrak{q}^{-C_2(S)} S \circlearrowright \odot . \quad (4.3.6)$$

Here we must take the framing factor appearing in R-move I (4.2.43) into consideration.

Let a white dot (a circle) and a black one (a filled circle) in the C -projection plane represent each intersection point of a surface defect with C_{in} and C_{out} , respectively. Then new moves appear :

$$\begin{array}{c} S \\ \uparrow \\ \circ \\ \longrightarrow R \end{array} = \begin{array}{c} S \\ \uparrow \\ \circ \\ \longrightarrow R \end{array} \quad \begin{array}{c} S \\ \downarrow \\ \bullet \\ \longrightarrow R \end{array} = \begin{array}{c} S \\ \downarrow \\ \bullet \\ \longrightarrow R \end{array} . \quad (4.3.7)$$

On the left hand side, a line labelled by S stems from the white dot in M and, on the right hand side, a line by S goes into the black dot in M . We call this relation Reidemeister move V (R-move V). In particular, because two types of dots are identified in S_H^1 , they coincide in C -projection and we have

$$\begin{array}{c} \uparrow \\ \text{---} \rightarrow R \\ \bullet \\ \uparrow \end{array} = \begin{array}{c} \uparrow \\ \bullet \\ \text{---} \rightarrow R \\ \uparrow \end{array} . \tag{4.3.8}$$

We refer to the edges with dots on it as ‘‘punctured edges’’. Be aware that the punctured edges are just open lines in the three dimensional space M . A view from the right hand towards the left hand is shown in Fig. 4.5. See also Sec. 4.3.4 for the detail.

$$\begin{array}{c} S \\ \uparrow \\ S \\ \bullet \\ S \\ \uparrow \end{array} \leftrightarrow \begin{array}{c} S \\ \nearrow \\ S \\ \searrow \\ S \end{array} \begin{array}{l} \text{---} C_{out} \\ \\ \text{---} C_{in} \end{array} \tag{4.3.9}$$

Figure 4.5: A punctured edge labelled by S in the left can be depicted as the right in the projection from M onto other 2D plane extending along the Hopf fiber direction.

What we are interested in is the situation where a line in C passes near a fully degenerate puncture. The above relation (4.3.8) leads to

$$\begin{array}{c} \uparrow \\ \circlearrowleft \\ \bullet \\ \uparrow \end{array} = \begin{array}{c} \uparrow \\ \bullet \\ \circlearrowleft \\ \uparrow \end{array} \tag{4.3.10}$$

and now we can apply the crossing resolutions (4.2.36) to the network representation on the right hand.⁹⁾

⁹⁾Another more useful way to derive the same result is to separate the locations of ingoing and outgoing punctures (white and black dots) in C firstly, to apply the skein relations secondly and to merge them again finally.

Special case

Let us take S and R as \square (or 1) and $\wedge^k \square$ (or k), respectively. There are two ways to do the calculations :

$$\begin{array}{c} k \\ \uparrow \\ 1 \odot \end{array} = \sigma_{\square} \mathfrak{q}^{C_2(\square)} \begin{array}{c} k \\ \uparrow \\ 1 \odot \end{array} = \mathfrak{q}^{\frac{2k}{N}} \begin{array}{c} k \\ \uparrow \\ \odot 1 \end{array} + (-1)^k \mathfrak{q}^{\frac{2k-1}{N}+k-1} (\mathfrak{q} - \mathfrak{q}^{-1}) \begin{array}{c} k \\ \uparrow \\ \odot 1 \end{array} \cdot \quad (4.3.11)$$

On the other hand,

$$\begin{array}{c} k \\ \uparrow \\ 1 \odot \end{array} = \sigma_{\square} \mathfrak{q}^{-C_2(\square)} \begin{array}{c} k \\ \uparrow \\ 1 \odot \end{array} = \mathfrak{q}^{\frac{2k}{N}-2} \begin{array}{c} k \\ \uparrow \\ \odot 1 \end{array} + (-1)^{k-N-1} \mathfrak{q}^{\frac{2k+1}{N}+k-1-N} (\mathfrak{q} - \mathfrak{q}^{-1}) \begin{array}{c} k \\ \uparrow \\ \odot 1 \end{array} \cdot \quad (4.3.12)$$

Comparing both expressions, we have

$$\begin{array}{c} k \\ \uparrow \\ \odot 1 \end{array} = (-1)^{k-N-1} \mathfrak{q}^{\frac{1}{N}+k-N} \begin{array}{c} k \\ \uparrow \\ \odot 1 \end{array} + (-1)^{k+1} \mathfrak{q}^{k-\frac{1}{N}} \begin{array}{c} k \\ \uparrow \\ \odot 1 \end{array} \quad (4.3.13)$$

$$= \mathfrak{q}^{-\frac{k}{N}} \left[\begin{array}{c} k \\ \uparrow \\ \odot 1 \end{array} + \mathfrak{q} \begin{array}{c} k \\ \uparrow \\ \odot 1 \end{array} \right] \cdot \quad (4.3.14)$$

In the same way, we also have

$$\begin{array}{c} k \\ \uparrow \\ 1 \odot \end{array} = \mathfrak{q}^{\frac{k}{N}} \left[\begin{array}{c} k \\ \uparrow \\ 1 \odot \end{array} + \mathfrak{q}^{-1} \begin{array}{c} k \\ \uparrow \\ 1 \odot \end{array} \right] \cdot \quad (4.3.15)$$

In the simplest case $N = 2$ and $k = 1$ which do not need any junctions and arrows on edges, this becomes simpler as follows :

$$\begin{array}{c} 1 \\ | \\ \odot 1 \end{array} = \mathfrak{q}^{-\frac{1}{2}} \begin{array}{c} 1 \\ | \\ \bullet \\ | \\ 1 \end{array} + \mathfrak{q}^{\frac{1}{2}} \begin{array}{c} 1 \\ | \\ \bullet \\ | \\ 1 \end{array} \quad (4.3.16)$$

and the other relation can be obtained by mapping \mathfrak{q} to \mathfrak{q}^{-1} .

If we apply either relation to the loop wrapping a cylinder and one fully degenerate puncture near it, there appear two kinds of knots. One winds around the cylinder by one time as it goes from C_{in} to C_{out} and the other does in the opposite way. Recalling the fact that there lives a 2D $\mathcal{N}=(2,2)$ $U(1)$ gauged linear σ model on the surface defect labelled by \square [55, 76], it is expected that these loops in M represent the $U(1)$ Wilson loops charged ± 1 according to the winding orientation, in the 2D system on the surface defect.

General case

How do the similar relations look like for any pair $S = \wedge^\ell \square$ and $R = \wedge^k \square$? From the above examples, we can expect that the general skein relations are

$$\begin{array}{c} k \\ | \\ \odot \ell \end{array} = \mathfrak{q}^{\frac{k\ell}{N}} \sum_{s=0}^{\min(k,\ell)} \mathfrak{q}^{-s} \begin{array}{c} k \\ | \\ \bullet \\ \diagup \quad \diagdown \\ \ell \quad \ell \\ \diagdown \quad \diagup \\ s \\ | \\ k \end{array} \quad (4.3.17)$$

where the coefficients are the same as those of the crossing resolution (4.2.36). The other relations are

$$\begin{array}{c} k \\ | \\ \bullet \\ | \\ \odot \ell \end{array} = \mathfrak{q}^{-\frac{k\ell}{N}} \sum_{s=0}^{\min(k,\ell)} \mathfrak{q}^s \begin{array}{c} k \\ | \\ \bullet \\ \diagup \quad \diagdown \\ \ell \quad \ell \\ \diagdown \quad \diagup \\ s \\ | \\ k \end{array} . \quad (4.3.18)$$

In the case of $\ell = 1$, each reduces into (4.3.14) or (4.3.15). We see in the next subsection 4.3.4 that these relations are indeed reproduced in another approach.

4.3.4 Other projections

The requirement of the topological property of networks in M means that their projection onto a 2D plane can be taken arbitrarily. So far we have used C -projection, but actually, we can consider other projections onto a plane extending along I_H -direction. We call those projections “ H -projections”.

Now it is possible to directly obtain the same result as before by applying the skein relation in a H -projection. Let us view the crossing network on the left hand side in (4.3.18) from the right hand and apply the crossing resolution on the new projection. This can be expressed as

$$\begin{array}{c} \dots\dots\dots C_{out} \\ \bullet \\ \vdots \\ \xrightarrow{k} \\ \vdots \\ \circ \\ \dots\dots\dots C_{in} \end{array} = q^{\frac{k\ell}{N}} \sum_{s=0}^{\min(k,\ell)} q^{-s} \begin{array}{c} \dots\dots\dots C_{out} \\ \bullet \\ \vdots \\ \xrightarrow{s} \\ \vdots \\ \circ \\ \dots\dots\dots C_{in} \end{array} \cdot \quad (4.3.19)$$

This relation exactly matches with the previous expressions (4.3.18) and we have a relation between distinct projections like

$$\begin{array}{c} k \\ \uparrow \\ \diagdown \quad \diagup \\ \quad \bullet \\ \diagup \quad \diagdown \\ \downarrow \\ k \end{array} = \begin{array}{c} \dots\dots\dots C_{out} \\ \bullet \\ \vdots \\ \xrightarrow{s} \\ \vdots \\ \circ \\ \dots\dots\dots C_{in} \end{array} \quad (4.3.20)$$

where the left hand side is the usual C -projection but the right one is a H -projection including I_H direction.

Finally, we make a brief comment on the reproduction of the relation (4.3.4). This can be geometrically expressed as

$$R \left(S \odot \right) = \sigma_{R\chi_R}(q^{-\rho-\lambda_S}) S \odot \quad (4.3.21)$$

or locally

$$\begin{array}{c} \uparrow \\ \circ \\ \downarrow \\ S \end{array} = \sigma_{R\chi_R}(q^{-\rho-\lambda_S}) \begin{array}{c} \uparrow \\ \vdots \\ \uparrow \\ S \end{array} \cdot \quad (4.3.22)$$

We can derive this relation in some simple cases.

4.4 Coexistence of closed networks and isolated punctures

In this section, we compare the previous new skein relations with the computation of q -deformed Yang-Mills expectation values or the Schur indices. From the comparison, we can extract the operator action of some punctured networks. Based on this discussion, in Sec. 4.5.3, we propose the modified formula for general punctured networks and interpret the modification as the addition of the local Boltzmann factors assigned with dual arrowed edges.

Let C be a two-sphere with several punctures and γ be a 2D Wilson loop wrapping a tube in C . This is the same situation as discussed in part 3 in Sec. 3.8.1. The general set-up can be discussed in the similar way. Recalling the discussion around (3.8.5), let us cut along γ and decompose the Riemann surface C into the two parts which we call C_A and C_B here. In the following, we see the operator structure in two distinct basis.

Fugacity/Holonomy basis

The formula (3.8.5) says that the whole partition function is given by

$$\oint [da]_{\text{Haar}} I_{C_A}(a, \dots) \chi_M(a) I_{C_B}(a^{-1}, \dots). \quad (4.4.1)$$

Now let us add a surface defect labelled by S . There are two choices of its addition, namely, the fully degenerate puncture on C_A or on C_B as shown in Fig. 4.6.

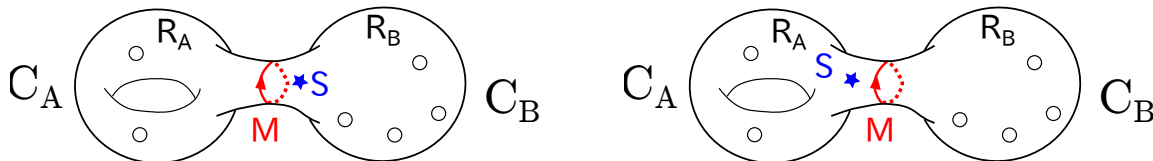


Figure 4.6: Coexistence of a 2D Wilson loop and a fully degenerate puncture in C . Left corresponds to (4.4.2) (4.4.19) and right does to (4.4.4) (4.4.19).

They are evaluated as

$$I_{C_A \sqcup_{W_M(\gamma)} (C_B, S)} := \oint [da]_{\text{Haar}} I_{C_A}(a, \dots) \chi_M(a) (\widehat{\mathcal{F}}_S I_{C_B})(a^{-1}, \dots) \quad (4.4.2)$$

and

$$I_{(C_A, S) \sqcup_{W_M(\gamma)} C_B} := \oint [da]_{\text{Haar}} (\widehat{\mathcal{F}}_S I_{C_A})(a, \dots) \chi_M(a) I_{C_B}(a^{-1}, \dots) \quad (4.4.3)$$

$$= \oint [da]_{\text{Haar}} I_{C_A}(a, \dots) \widehat{\mathcal{F}}_S (\chi_M(a) I_{C_B})(a^{-1}, \dots) \quad (4.4.4)$$

where we use the self-adjoint property of the difference operator $\widehat{\mathcal{S}}_s$. And two expressions give different answers.

In particular, the special case $M = \wedge^\ell \square$ and $S = \wedge^k \square$ is important. Let $\Pi(R)$ be the set of weights for an irreducible representation R and we also introduce a subset defined as

$$\Pi(\wedge^k \square, \wedge^\ell \square)_s := \{(\lambda, \mu) \in \Pi(\wedge^k \square) \times \Pi(\wedge^\ell \square) \mid (\lambda, \mu) = s - \frac{k\ell}{N}\}. \quad (4.4.5)$$

In the following network representations in this subsection, we identify two end points of any open edge in networks such that they once wrap a tube in C .

On one side, we have a relation like

$$\begin{array}{c} k \\ \uparrow \\ \bullet \otimes \ell \end{array} \longleftrightarrow \widehat{W}_{\wedge^k \square} \widehat{\mathcal{S}}_{\wedge^\ell \square} = \sum_{\substack{\lambda \in \Pi(\wedge^k \square) \\ \mu \in \Pi(\wedge^\ell \square)}} a^\lambda \widehat{\Delta}_{-\mu}^\chi = \sum_{s=0}^{\min(k,\ell)} \mathfrak{q}^{s - \frac{k\ell}{N}} \widehat{\mathcal{O}}_s^{(k,\ell)} \quad (4.4.6)$$

where we have defined new difference operators conjugate to $\widehat{\Delta}_{-\lambda}$

$$\widehat{\Delta}_{-\lambda}^\chi := (\sqrt{\Delta_{\text{Haar}}(a)})^{-1} \cdot \widehat{\Delta}_{-\lambda} \cdot (\sqrt{\Delta_{\text{Haar}}(a)}) \quad (4.4.7)$$

and another difference operator

$$\widehat{\mathcal{O}}_s^{(k,\ell)} := \sum_{(\lambda,\mu) \in \Pi(\wedge^k \square, \wedge^\ell \square)_s} a^{\lambda/2} \Delta_{-\mu}^\chi a^{\lambda/2} = \sum_{(\lambda,\mu) \in \Pi(\wedge^k \square, \wedge^\ell \square)_s} \mathfrak{q}^{\frac{k\ell}{N} - s} a^\lambda \Delta_{-\mu}^\chi. \quad (4.4.8)$$

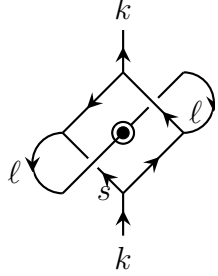
We also use the formula

$$a^\lambda \widehat{\Delta}_{-\mu}^\chi = \mathfrak{q}^{2(\lambda,\mu)} \widehat{\Delta}_{-\mu}^\chi a^\lambda \quad a^\lambda \widehat{\Delta}_{-\mu}^\chi = \mathfrak{q}^{2(\lambda,\mu)} \widehat{\Delta}_{-\mu}^\chi a^\lambda. \quad (4.4.9)$$

On the other hand, we have


$$\begin{array}{c} k \\ \uparrow \\ \ell \otimes \bullet \end{array} \longleftrightarrow \widehat{\mathcal{S}}_{\wedge^\ell \square} \widehat{W}_{\wedge^k \square} = \sum_{\substack{\lambda \in \Pi(\wedge^k \square) \\ \mu \in \Pi(\wedge^\ell \square)}} \widehat{\Delta}_{-\mu}^\chi a^\lambda = \sum_{s=0}^{\min(k,\ell)} \mathfrak{q}^{\frac{k\ell}{N} - s} \widehat{\mathcal{O}}_s^{(k,\ell)}. \quad (4.4.10)$$

Comparing (4.3.17) and (4.3.18) with these results, we naturally get the correspondence



$$\hat{\mathcal{O}}_s^{(k,\ell)}. \quad (4.4.11)$$

In the special case $s = k = \ell$, we have



$$\hat{\mathcal{O}}_k^{(k,k)} = \mathfrak{q}^{-\frac{1}{N}k(N-k)} \sum_{\lambda \in \Pi(\wedge^k \square)} a^\lambda \widehat{\Delta}_{-\lambda}^\chi. \quad (4.4.12)$$

Representation basis

We repeat the same analysis in another new basis. For that purpose, let us expand the partition functions on C_A and C_B by the $SU(N)$ characters as

$$\mathcal{F}_{R_A}(\{b\}) := \oint [da'] \chi_{R_A}(a'^{-1}) I_{C_A}(a', \{b\}) \quad (4.4.13)$$

$$\mathcal{G}_{R_B}(\{c\}) := \oint [da'] \chi_{R_B}(a'^{-1}) I_{C_B}(a', \{b\}) \quad (4.4.14)$$

and then we can express the expectation value of the Wilson loop in the representation M as

$$\langle \mathcal{F} | \hat{W}_M | \mathcal{G} \rangle := \sum_{R_A, R_B} \oint [da]_{\text{Haar}} \chi_{R_A}(a^{-1}) \mathcal{F}_{R_A}(\{b\}) \chi_M(a) \chi_{R_B}(a) \mathcal{G}_{R_B}(\{c\}). \quad (4.4.15)$$

where we introduced a matrix representation like

$$|\mathcal{F}\rangle = \sum_R \mathcal{F}_R(\{b\}) |R\rangle \quad (4.4.16)$$

$$|\mathcal{G}\rangle = \sum_R \mathcal{G}_R(\{c\}) |R\rangle \quad (4.4.17)$$

$$\langle R_1 | R_2 \rangle = \delta_{R_1, R_2} \quad \text{orthonormal basis.} \quad (4.4.18)$$

Using the eigenvalues of difference operators (4.3.3), the addition of surface operators in this basis corresponding to (4.4.2) and (4.4.4) are expressed as

$$\langle \mathcal{F} | \hat{W}_M \hat{\mathcal{S}}_S | \mathcal{G} \rangle = \sum_{R_A, R_B} N_{R_B S}^{R_A} \mathcal{F}_{R_A}(\{b\}) \bar{\mathcal{E}}_{R_B}^{(S)} \mathcal{G}_{R_B}(\{c\}) \quad (4.4.19)$$

and

$$\langle \mathcal{F} | \hat{\mathcal{S}}_S \hat{W}_M | \mathcal{G} \rangle = \sum_{R_A, R_B} N_{R_B S}^{R_A} \bar{\mathcal{E}}_{R_A}^{(S)} \mathcal{F}_{R_A}(\{b\}) \mathcal{G}_{R_B}(\{c\}), \quad (4.4.20)$$

respectively. Note that 4D Wilson loops act as “difference operators” and 4D surface defects do as diagonal multiplications in this basis.

When $M = \wedge^\ell \square$ and $S = \wedge^k \square$, we can also repeat the similar computation to the previous one. First of all, let us rewrite the eigenvalue $\bar{\mathcal{E}}_R^{(S)}$ by using (4.3.3) into

$$\bar{\mathcal{E}}_R^{(S)} = \sum_L \mathfrak{q}^{-2 \sum_{\underline{j} \in L} (\rho + \lambda_R)_{\underline{j}}} = \sum_L \mathfrak{q}^{-2(\rho + \lambda_R, h_L)} \quad (4.4.21)$$

where L runs over all the ℓ -element subsets of $\{1, 2, \dots, N\}$. Next, the sum including the Littlewood-Richardson coefficient can be written as follows.

$$\sum_{R_A, R_B} N_{R_B \wedge^k \square}^{R_A} = \sum_{\lambda_{R_B}} \sum_K \quad (4.4.22)$$

where $\lambda_{R_A} - \lambda_{R_B} = \sum_{i \in K} h_i =: h_K \in \Pi(\wedge^k \square)$ and K runs over all the k -element subsets of $\{1, 2, \dots, N\}$.

Now (4.4.20) leads to

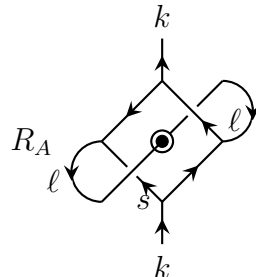
$$\langle \mathcal{F} | \hat{\mathcal{S}}_S \hat{W}_M | \mathcal{G} \rangle = \sum_{\lambda_B} \sum_{K, L} \mathfrak{q}^{-2(\rho + \lambda_B + h_K, h_L)} \mathcal{F}_{R(\lambda_B + h_K)}(\{b\}) \mathcal{G}_{R(\lambda_B)}(\{c\}) \quad (4.4.23)$$

$$= \sum_{s=0}^{\min(k, \ell)} \mathfrak{q}^{-2 \binom{s - k\ell}{s}} \sum_{\substack{\lambda_B \geq 0 \\ \lambda_B \geq -h_K}} \sum_{\substack{K, L \\ |K \cap L| = s}} \mathfrak{q}^{-2(\rho + \lambda_B, h_L)} \mathcal{F}_{R(\lambda_B + h_K)}(\{b\}) \mathcal{G}_{R(\lambda_B)}(\{c\}) \quad (4.4.24)$$

$$(4.4.25)$$

where we use $(h_K, h_L) = \sum_{(i, j) \in K \times L} (h_i, h_j) = |K \cap L| - \frac{k\ell}{N}$ in the second line and $\lambda \geq 0$

means that it is a dominant weight, that is to say, $\lambda_\alpha \geq 0$ for all α . By evaluating (4.4.19) in the same way, we have the similar correspondence



$$\longleftrightarrow \sum_{\substack{K, L \\ |K \cap L| = s}} \delta_{\lambda_A - \lambda_B, h_K} \mathfrak{q}^{-(2\rho + \lambda_B + \lambda_A, h_L)} \quad (4.4.26)$$

which is the dual expression of the operator $\hat{O}_s^{(k,\ell)}$.

Setting $s = k = \ell$, we finally get the following one needed later soon.

$$R_A \begin{array}{c} \uparrow k \\ \bullet \\ \downarrow k \end{array} R_B \longleftrightarrow \sum_K \delta_{\lambda_A - \lambda_B, h_K} \mathfrak{q}^{-(2\rho + \lambda_A + \lambda_B, \lambda_A - \lambda_B)}. \quad (4.4.27)$$

4.5 Proposal of conjectural formula for Wilson punctured network defects in 2D q -deformed Yang-Mills

In this section, we see how the expectation values of any closed Wilson punctured network defects can be evaluated. Here “closed” means that the networks do not touch on general punctures coming from codimension two defects in 6D SCFTs not codimension four ones. We divide the evaluation procedure into two steps : giving the computational procedures for special cases (See Sec. 4.5.2) and then constructing the general cases by using them (See Sec. 4.5.1). However, we will explain these two steps in the reversed order by starting the general cases and then by decomposing them into several special building blocks for which we will give the procedure.

In Sec. 4.5.1, we show the procedure to obtain the special building blocks from the general set-ups. In Sec. 4.5.2, we go back to the evaluation of defect expectation values. There, we map such evaluations for special building blocks into the computations of partition functions of statistical mechanical systems with infinite degrees of freedom. The construction of such a mapping and giving the Boltzmann factor are the main points. Finally, we make a few comments on the above mapping of \mathcal{R} -matrix in a special case in Sec. 4.5.5. The properties necessary in this section are already summarized in Sec. 3.8.1.

We also summarize the conventions remarked before.

There are two different conventions called “Liouville-Toda” convention and “ q -deformed Yang-Mills” one. Although we focus on the 2D q -deformed Yang-Mills theory, we also use the former convention which is mostly used in the context of the 4D/2D duality. There, instead of q , we use another symbol \mathfrak{q} which is related to q by $\mathfrak{q} = q^{1/2}$. Note also that the skein relations in the q -deformed Yang-Mills convention are obtained under the replacement of \mathfrak{q} by $-q^{1/2}$, where the additional minus sign appears compared to the above actual relation. This is because the normalizations of the junctions differ in two conventions.

For a while, we consider the Wilson network operators without any crossings. They are defined as some networks satisfying the following two conditions:

1. Each network consists of trivalent junctions and arrowed edges with a charge $a \in \{0, 1, 2, \dots, N - 1\} \simeq \mathbb{Z}_N$ on each. Each charge corresponds to the fundamental

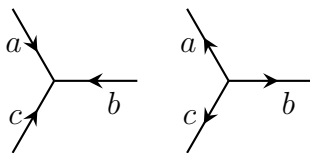


Figure 4.7: Inflowing (Left) and outflowing (right) (a, b, c) -junctions.

representations $\wedge^a \square$ of $SU(N)$ which form the minimal set to generate all the irreducible representations. Notice also that edges with 0 can be removed and we ignore them hereafter.

Flipping arrow is equivalent to the replacement by the charge conjugate representation as we have seen. In particular, as we only consider the fundamental representations $\wedge^a \square$, this operation corresponds to $a \rightarrow N - a$.

If we use an edge labelled by an irreducible representation R , we interpret it as a bunch of edges according to a polynomial expression of R of $SU(N)$ representation ring generators of $\wedge^a \square$.

2. There is the charge conservation on each junction. More precisely, if we have all three inflowing/outgoing edges with charges a, b and c , they must satisfy $a + b + c = 0 \pmod N$. On forgetting to take the N -modulo operation, there are two possibilities : $a + b + c = N$ or $2N$. We call the former one (a, b, c) -junction for both inflowing one and outflowing one, see Fig. 4.7. If $a + b + c = 2N$, the redefinition $a' = N - a$, $b' = N - b$ and $c' = N - c$ makes $a' + b' + c' = N$ and the exchange between inflowing and outflowing, and we have $(N - a, N - b, N - c)$ -junction for the latter case.
3. Any crossing can be resolved into networks without any crossing as discussed in Sec. 4.2.4. Therefore, we can remove all the crossings from the network by applying the above relation to each but have a sum of several networks instead.

4.5.1 Reduction onto special cases

Here we see how the most general pairs of the Riemann surface and defects on it decompose into the several special ones as the building blocks.

Let C be a Riemann surface with genus g and n punctures and Γ be any closed networks on it. To each puncture, we assign a holonomy which corresponds to the fugacity in the SCI language. On the types of punctures and their holonomies, see the review in Sec. 3.8.1 later. Γ may consist of several disconnected components and we write the decomposition as $\Gamma = \bigsqcup_{\alpha} \check{\Gamma}_{\alpha}$. Next, consider a neighborhood of $\check{\Gamma}_{\alpha}$ which is sometimes called a ribbon graph or a fat graph. This fat graph denoted by \check{C}_{α} is a two dimensional open surface and its boundary consists of several copies of S^1 . See Fig. 4.8. Cutting along the boundaries of \check{C}_{α} , we have a decomposition of C . By the above construction, in addition to \check{C}_{α} 's, there are other connected components denoting \check{C}_A which have no network defects. Note that we identify each boundary isomorphic to S^1 with a puncture.

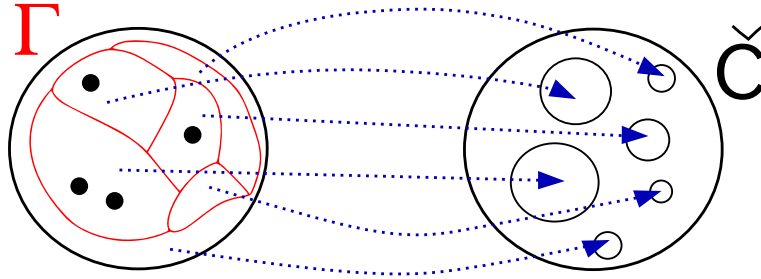


Figure 4.8: A fat graph \check{C} from a network $\check{\Gamma}$. The red graph represents the network and each region is mapped to a hole. In this example, this is isomorphic to the six-punctured sphere.

Let us make one comment on the topological property of \check{C} . If $\check{\Gamma}$ has 2ℓ ($\ell > 0$) junctions and the boundary of its fat graph \check{C} is isomorphic to k copies of S^1 , \check{C} is the k -punctured genus $(\ell - k)/2 + 1$ Riemann surface. Note that its Euler character is $-\ell$.¹⁰ In particular, when $\check{\Gamma}$ is a pure loop without junctions, \check{C} is the twice-punctured sphere.

Now \check{C} consists of two types of connected components: \check{C}_α which is homotopic to $\check{\Gamma}_\alpha$ and \check{C} for which we already know how to compute their partition functions as remarked later. Since we can reconstruct the expectation values of the original system by gluing together as shown around (3.8.3), all we have to do is know the expectation values for each pair $(\check{C}_\alpha, \check{\Gamma}_\alpha)$. Before showing that procedure (Sec. 4.5.2), we review several facts needed for the complete reconstruction and later discussions.

4.5.2 A proposal for closed Wilson networks

At this stage, any expectation value of any network defect is a function of holonomies for $SU(N)$ global symmetries on each maximal puncture. Recall that we can always take each $SU(N)$ holonomy in the maximal torus \mathbb{T}^{N-1} which is a N -tuple of $U(1)$ holonomies a_1, a_2, \dots, a_N with the constraint $a_1 a_2 \cdots a_N = 1$ but there left the ambiguity of its permutations. The invariance under the permutations (or conjugacy actions of $SU(N)$) implies that the expectation values can be expanded with the characters of $SU(N)$ again and written as

$$I_{\check{C}, \check{\Gamma}}(\{a\}) = \sum_{\{R_p\}} B_{\check{\Gamma}; \{R_p\}} \prod_{p=1}^n \chi_{R_p}(a_i). \quad (4.5.1)$$

where $\{R_p\}$ means that each R_p runs over the set of the unitary irreducible representations of $SU(N)$. We also use the same n as before for the number of maximal punctures on \check{C} . As we have seen in (3.8.2), for any 2D q -deformed Yang-Mills partition functions

¹⁰ Let $e, v (= 2\ell)$ and f be the number of edges, junctions of $\check{\Gamma}$ and regions in \check{C} , respectively. By construction, $f = k$ holds true. The closedness of the network $\check{\Gamma}$ and the trivalence property of junctions also say $2e = 3v$. The Euler's theorem applied to \check{C} ignoring all the punctures gives $2 - 2g = f - e + v$. Combined with all, we finally have the claim $\chi_{\check{C}} = 2 - 2g - k = -\frac{1}{2}v = -\ell$.

without defects, the coefficient B in the character expansion is diagonal in $\{R_i\}$ and each component is given by $(\dim_q R)^{\chi_{\check{C}}}$. In other words,

$$B_{\{\check{R}\}} = (\dim_q R)^{\chi_{\check{C}}} \prod_{p=1}^n \delta_{R_p, R} \quad (4.5.2)$$

where $\delta_{R_p, R}$ gives 1 when $R_p = R$ and 0 otherwise.

Now our goal is to give the procedure for computations of $B_{\check{\Gamma}, \{\check{R}\}}$. For that purpose, let us interpret this as a Boltzmann factor of a statistical mechanics on a lattice system defined by following three steps :

1. Make a dual ideal triangulation

The Riemann surface \check{C} decomposes into the several components by removing the locus of network defects $\check{\Gamma}$. The previous construction via fat graphs ensures the natural one-to-one correspondence between the components of regions and the boundaries/punctures. Now consider the dual quiver on \check{C} associated with the network $\check{\Gamma}$. This is obtained when each region or puncture and network's edge are mapped into a vertex and an arrow with the charge, respectively. At this stage, the summation in (4.5.1) says that there lives a discrete but infinite physical degree of freedom labelled by the irreducible representations of $SU(N)$ or the dominant weights on each vertex. Any junction is mapped into a triangle because of the trivalence property of the network. Note that similar operations already appeared many times in various contexts, see [15, 62] for example. So we have (ideal) triangulations with a charge on each edge, of \check{C} . Two or three vertices of a triangle are allowed to be common at this stage but, in Sec. 4.5.2, we will see that we can ignore such triangulations. Notice also that the number of triangles is given by $-2\chi_{\check{C}}$ on recalling footnote. 10).

2. Consider the allowed configurations of dominant weights

The whole configuration space is the set of all maps from each quiver vertex to an irreducible representation or a dominant weight. However, for many configurations, $B_{\check{\Gamma}, \{\check{R}\}}$ in (4.5.1) vanishes as we will discuss in 4.5.2 and we can restrict the range of the summation to the non-vanishing configurations.

3. Give the Boltzmann factor for each configuration

As with the ordinary statistical mechanics such as Ising models, we assume the Boltzmann factor of a given configuration is the product of local Boltzmann factors over all the triangles. In other words, the local Boltzmann factor denoted $B_{\lambda_A, \lambda_B, \lambda_C}^{\Delta}$ is a function on triples of dominant weights living on three vertices of a single triangle Δ and the total Boltzmann factor is given by

$$B_{\check{\Gamma}, \{\check{R}\}} = \prod_{\Delta} B_{\lambda_{\Delta, A}, \lambda_{\Delta, B}, \lambda_{\Delta, C}}^{\Delta} \quad (4.5.3)$$

where Δ runs over all the triangles on the ideal triangulation of \check{C} . The concrete formula of $B_{\lambda_A, \lambda_B, \lambda_C}^{\Delta}$ will be given as (4.5.8) in Sec. 4.5.2.

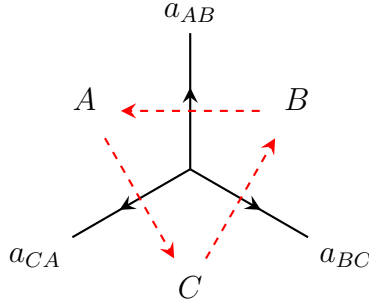


Figure 4.9: There are three regions around each junction. The red dashed arrows represent its dual quiver.

Selection rules on dominant weights

Here we exhaust all the configurations whose Boltzmann factors are non-vanishing. The strategy is same as that used in [75].

Let us consider (a_{AB}, a_{BC}, a_{CA}) -junction and three regions around it as shown in Fig.4.9. There are still two types of junctions, inflowing one and outgoing one but hereafter we focus on outflowing one only because the final expressions for B^Δ are same for both types. Let three dominant weights living on its vertices be λ_A, λ_B and λ_C and define $\lambda_{XY} := \lambda_X - \lambda_Y$ for $X, Y \in \{A, B, C\}$. The gluing procedure stated in Sec. 3.8.1 tells that $R(\lambda_Y) \otimes \wedge^{a_{XY}} \square$ contains $R(\lambda_X)$ for $(X, Y) = (A, B), (B, C)$ and (C, A) . This statement equals to $\lambda_{XY} \in \Pi(\wedge^{a_{XY}} \square)$ where $\Pi(R)$ is a set of all weights of the highest representation R . Then there is a unique subset E_{XY} of $\{1, 2, \dots, N\}$ consisting of a_{XY} elements such that $\lambda_{XY} = \sum_{s \in E_{XY}} h_s$. The cycle condition $\lambda_{AB} + \lambda_{BC} + \lambda_{CA} = 0$ means

that E_{AB}, E_{BC} and E_{CA} has no common element and $E_{AB} \sqcup E_{BC} \sqcup E_{CA} = \{1, 2, \dots, N\}$. In conclusion, allowed configurations have several sectors determined by the choice of E_{AB}, E_{BC} and E_{CA} which is a partition of $\{1, 2, \dots, N\}$ into three sets. Note that there are $\frac{N!}{a_{AB}!a_{BC}!a_{CA}!}$ sectors for single junction. And in each sector, there is a summation over λ_A for example, ¹¹⁾ with a constraint that all λ_A, λ_B and λ_C are dominant weights. ¹²⁾

Notice also that two adjacent vertices must have different center charges as we have seen at part 3 in Sec. 3.8.1 and we can say that there is no edge whose starting vertex and terminating one are common.

¹¹⁾Of course, it is possible to choose λ_B or λ_C instead. In all cases, the other two dominant weights are determined if we specify the sector at first.

¹²⁾In other words, this is just summation over λ_A and pairs of $\lambda_B - \lambda_A$ and $\lambda_C - \lambda_A$. The later two pairs label the sectors.

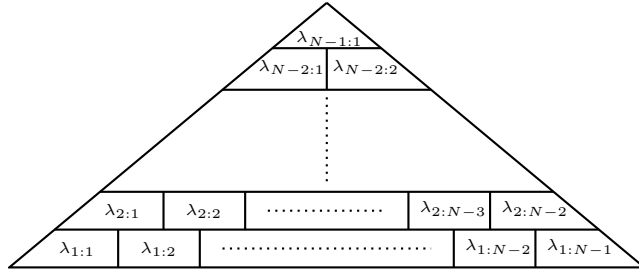


Figure 4.10: Pyramid, an assembly of $\frac{1}{2}N(N-1)$ integers.

Conjectural formula for the local Boltzmann factor

The last task is to show the way to get the local Boltzmann factor for any allowed triple of dominant weights λ_A, λ_B and λ_C .

Before going to the final result, we must prepare some tools to express it simply. First of all, we introduce a mathematical object playing central roles in our computations. This is just an assembly of integers designated by two labels h and $\alpha = \alpha_h$. h runs over $1, 2, \dots, N-1$ and α does over $1, 2, \dots, N-h$ for each h . Therefore, this object consists of $\frac{1}{2}N(N-1)$ integers. We call such object ‘‘pyramid’’ hereafter. See Fig. 4.10.

In particular we have a natural map defined just below which sends a weight $\lambda = [\lambda_1, \lambda_2, \dots, \lambda_{N-1}]$ where $\lambda = \sum_{\beta=1}^{N-1} \lambda_\beta \omega_\beta$ to a pyramid and denote the image by $\hat{\lambda}$ or $\hat{\lambda}_{h:\alpha}$.

The definition of the map is

$$\hat{\lambda}_{h:\alpha} := \sum_{\beta=\alpha}^{\alpha+h-1} \lambda_\beta. \quad (4.5.4)$$

Hereafter, we permit an abuse of notation. We use the same symbol $\hat{\lambda}$ for the pyramids not in the image of this inclusion map too. In such cases, $\hat{\lambda}$ is to be considered as a single symbol as a whole and λ is meaningless.

Next, we define majority function mj for three variables :

$$mj(a, b, c) := \begin{cases} a & b = a \text{ or } c = a \\ b & a = b \text{ or } c = b \\ c & a = c \text{ or } b = c \end{cases}. \quad (4.5.5)$$

Since, hereafter, there appears no case that all variables are distinct, this definition is well-defined in our usage. In particular, we extend this to the case that the variables are pyramids as follows :

$$mj(\hat{\lambda}_A, \hat{\lambda}_B, \hat{\lambda}_C) := \{mj((\hat{\lambda}_A)_{h:\alpha}, (\hat{\lambda}_B)_{h:\alpha}, (\hat{\lambda}_C)_{h:\alpha})\}_{h:\alpha}. \quad (4.5.6)$$

Finally, we define q -dimension function D :

$$D[\hat{\lambda}] := \prod_{h=1}^{N-1} \prod_{\alpha=1}^{N-h} \frac{[(\hat{\lambda})_{h:\alpha} + h]_q}{[h]_q}. \quad (4.5.7)$$

Now that we get all necessary tools, let us write down the local Boltzmann factors for three dominant weights λ_A, λ_B and λ_C living on its vertices. This is expressed as

$$B_{\lambda_A, \lambda_B, \lambda_C}^\Delta = \frac{1}{D[mj(\hat{\lambda}_A, \hat{\lambda}_B, \hat{\lambda}_C)]^{\frac{1}{2}}}. \quad (4.5.8)$$

Based on this proposal, we derive several skein relations in App. E.3, which provides a (mathematical) evidence that this proposal works well. The other physical evidences come from the consistency checks in the next Chapter. 5.

Then, the number of appearances of each q -number is always even.

We do not claim that the local Boltzmann factors are physically significant but only the total Boltzmann factor is physical. In other words, there may exist other expressions for the local Boltzmann factor but giving the same for the total Boltzmann factor and satisfying the skein relations. For the research of 4D/2D duality relations, it is enough to know the total Boltzmann factor.

4.5.3 Formulae for Wilson punctured networks

We have independently discussed the computations of expectation values for closed networks in the previous section and the geometrical structures of the composite surface-line systems (Sec. 4.4) and here we will unify two things.

After performing the crossing resolutions, there appear several networks allowing the punctured edges as shown in Fig. 4.11.

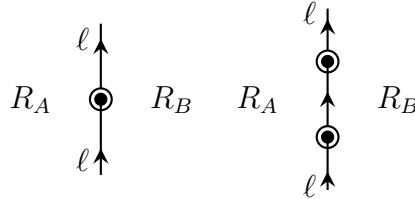


Figure 4.11: Punctured edge.

The modification of the statistical model previously introduced in Sec. 4.5.2 is simple : add another local Boltzmann factor for pairs of two adjacent dominant weights or, equivalently, edges. The last result (4.4.27) in the previous section suggests that this factor is given by

$$B_{\rightarrow\lambda_A, \lambda_B\rightarrow}^{\rightarrow, n} = \mathbf{q}^{-n(2\rho + \lambda_A + \lambda_B, \lambda_A - \lambda_B)} = \mathbf{q}^{-n(\tilde{\lambda}_A + \tilde{\lambda}_B, \tilde{\lambda}_A - \tilde{\lambda}_B)} \quad (4.5.9)$$

where n is the number of “punctured” on the edge and $\tilde{\lambda} := \lambda + \rho$.

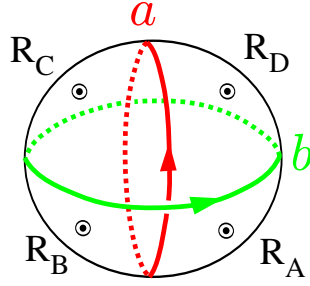


Figure 4.12: Two dual intersecting loops. If the upper punctures are simple / minimum type $[N - 1, 1]$, the red loop corresponds to the fundamental Wilson loop and the green one does to some 't Hooft loop.

As a simple application, we can see a new but naturally expected skein relation like

$$(4.5.10)$$

because of the following equality

$$q^{-(\tilde{\lambda}_A + \tilde{\lambda}_C, \tilde{\lambda}_A - \tilde{\lambda}_C)} = q^{-(\tilde{\lambda}_A + \tilde{\lambda}_B, \tilde{\lambda}_A - \tilde{\lambda}_B)} q^{-(\tilde{\lambda}_B + \tilde{\lambda}_C, \tilde{\lambda}_B - \tilde{\lambda}_C)}. \quad (4.5.11)$$

It is the interesting problem to prove the equalities (4.3.17) or (4.3.18) based on the dual statistical model but we have no proof for them in general cases yet.

4.5.4 Dual intersecting loops in $T_{4\text{fulls}}$

Let us consider the case with $a = b = 1$ in Fig. 4.12. This theory reduces into $SU(N)$ superconformal QCD (SCQCD) on partially closing two of four punctures into the simple ($[N - 1, 1]$ -type) punctures. On that theory, these two loops correspond to the ordinary fundamental Wilson loop and some 't Hooft loop.¹³⁾ Using the crossing resolutions, this decomposes into four components. By evaluating each component and then by summing them up, we have the following results for the whole Boltzmann factor (the definition of E_{XY} is given in Sec. 4.5.2) :

1. case $E_{BA} = E_{DA} = E_{CB} = E_{CD} = \{\ell\}$ for $\ell \in \{1, 2, \dots, N\}$

$$B_{\beta \circ \alpha : \{\lambda\}} = \frac{1}{D[\hat{\lambda}_B]^2} \quad (4.5.12)$$

¹³⁾At least, its 't Hooft's topological charge is neutral. It is an interesting problem to identify what line defect on the 4D SCQCD precisely corresponds to the given loops on the 2D geometry side.

where $\lambda_B = \lambda_D$.

2. case $E_{BA} = E_{DA} = \{\ell\}$ and $E_{CB} = E_{CD} = \{k\}$ for $\ell \neq k \in \{1, 2, \dots, N\}$

$$B_{\beta\alpha:\{\lambda\}} = \frac{1}{D[\hat{\lambda}_B]^2[\kappa + \sigma_0]_q^2} \quad (4.5.13)$$

where $h_0 := |k - \ell|$, $\alpha_0 := \min(k, \ell)$, $\sigma_0 := \text{sgn}(\ell - k)$ and $\kappa := (\hat{\lambda}_B)_{h_0:\alpha_0} + h_0$. Note also $\lambda_B = \lambda_D$.

3. case $E_{CD} = E_{BA} = \{\ell\}$ and $E_{DA} = E_{CB} = \{k\}$ for $\ell \neq k \in \{1, 2, \dots, N\}$

$$B_{\beta\alpha:\{\lambda\}} = \frac{1}{D[\hat{\lambda}_B + \hat{f}_{\{\ell\},\{k\}}]D[\hat{\lambda}_D + \hat{f}_{\{k\},\{\ell\}}]} \quad (4.5.14)$$

where $\lambda_B - h_k = \lambda_D - h_\ell$ and see App. E as to $\hat{f}_{\{k\},\{\ell\}}$.

It is possible to rewrite the above expression into

$$B_{\beta\alpha:\{\lambda\}} = \frac{1}{D[\hat{\lambda}_B]D[\hat{\lambda}_D]} \frac{[\kappa]_q[\kappa + 2\sigma_0]_q}{[\kappa + \sigma_0]_q^2}. \quad (4.5.15)$$

There is a relation $\kappa = (\hat{\lambda}_B)_{h_0:\alpha_0} + h_0 = (\hat{\lambda}_D)_{h_0:\alpha_0} + h_0 - 2\sigma_0$.

Note that the ordering of additions of the two loops is irrelevant in q -deformed Yang-Mills theory (not so in the Liouville-Toda CFT case) and they commutes each other. We can naturally understand this if we put them in three dimensional space $C \times S^1$ as discussed in Sec. 4.3.

4.5.5 A remark on \mathcal{R} -matrix

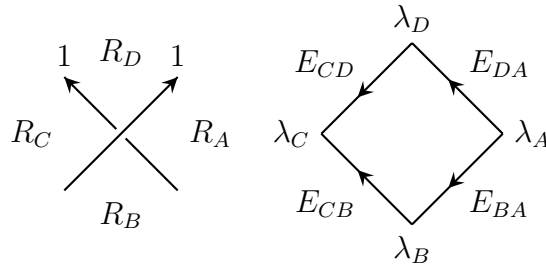


Figure 4.13: There are four regions around any crossing. This means that the \mathcal{R} -matrices (Left) can be mapped into the local Boltzmann factors associated with rectangles (Right).

As we see in the last example in the previous section, it is possible to compute the local Boltzmann factor for a single crossing or on the dual rectangle. See Fig. 4.13. Roughly speaking, the factors are the square root of the previous results, but there appear some additional powers of q . The factors can be given as follows :

1. case $E_{BA} = E_{DA} = E_{CB} = E_{CD} = \{\ell\}$

$$B_{\text{crossing}}^{\square} = (-q^{1/2})^{\frac{1}{N}} \frac{-q^{-1/2}}{D[\hat{\lambda}_B]} \quad (4.5.16)$$

where $\lambda_B = \lambda_D$ again.

2. case $E_{BA} = E_{DA} = \{\ell\}$ and $E_{CB} = E_{CD} = \{k\}$ for $\ell \neq k$

$$B_{\text{crossing}}^{\square} = (-q^{1/2})^{\frac{1}{N}} \frac{-\sigma_0 q^{-\sigma_0 \kappa - 1}}{D[\hat{\lambda}_B][\kappa + \sigma_0]_q} \quad (4.5.17)$$

where we use the same κ and σ_0 as before. Note also $\lambda_B = \lambda_D$ again.

3. case $E_{CD} = E_{BA} = \{\ell\}$ and $E_{DA} = E_{CB} = \{k\}$ for $\ell \neq k$

$$B_{\text{crossing}}^{\square} = (-q^{1/2})^{\frac{1}{N}} \frac{1}{D[\hat{\lambda}_B]^{1/2} D[\hat{\lambda}_D]^{1/2}} \frac{[\kappa]_q^{1/2} [\kappa + 2\sigma_0]_q^{1/2}}{[\kappa + \sigma_0]_q}. \quad (4.5.18)$$

The other crossing is obtained by just replacing q by q^{-1} . All the above results can have similar structures to those for triangles.

It is a very interesting problem to analyze all types of crossings or to relate the above local Boltzmann factors to the known models such as face or (R)SOS models [169, 178–181].

Chapter 5

Return to SCIs and skein relations

5.1 Schur indices with line defects

In this section, we analyse three cases : rank 1 SCFTs, free hypermultiplets and superconformal QCDs in class S theories.

Among the possible networks on the trinion, there are the minimal ones depicted in Fig. 5.1. They were discussed explicitly at first in [62] and shown to be elementary generators of the line operator algebra in [64]. They are called pants networks there and one shown in Fig. 5.1 is called (a_{AB}, a_{BC}, a_{CA}) -type and denoted by $\wp(a_{AB}, a_{BC}, a_{CA})$. The computation of the SCI in the simplest case, the T_3 theory case, was done in our paper [75]. However, the extension to other types of pants networks had been impossible before our work [90] explained in the previous section. Notice that these pants networks are expected to generate all the possible networks not touching on the punctures.

Through this and next sections, there is an important assumption : there is the same number of independent elementary pants networks as the rank of IR charge lattice which equals to the Coulomb branch dimension. The first example we can check readily is the T_N -theory. As seen in Sec. 2.4.1, the Coulomb branch dimension of the T_N -theory equals to $\frac{(N-1)(N-2)}{2}$. On the other hand, the number of possible junctions in the type A_{N-1} case is given by the number of the possible partitions of N into three parts, that is, just $\frac{(N-1)(N-2)}{2}$.

Next, let us see the rank 0 SCFTs, namely, free hypermultiplets. They have no Coulomb branch moduli and there is no dynamical gauge field. Therefore, if all loop operators given by pants networks are types of Wilson loops, they are expected to be flavor Wilson loops which are just the classical holonomies because the gauge fields are just the background fields.

At the computation level, this fact is realized as the factorization of the Schur indices

¹⁾In the other types, this is not true. For example, in the $\mathfrak{g} = \mathfrak{so}(2N)$ case, the Coulomb branch *real* dimension is given as $2N(N-2)$. In particular, when $N = 4$ or $\mathfrak{so}(8)$, sixteen independent pants networks are expected if we follow the above assumption. However, the actual number of possible junctions is 10. The reason why we consider the real dimension is just these networks are invariant under charge conjugation.

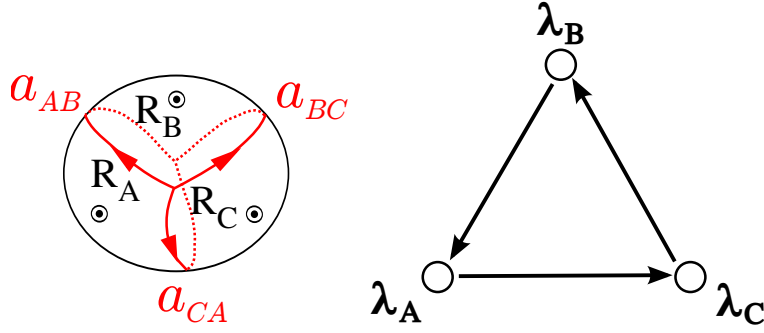


Figure 5.1: The (a_{AB}, a_{BC}, a_{CA}) -type pants network $\wp(a_{AB}, a_{BC}, a_{CA})$ and the associated dual quiver.

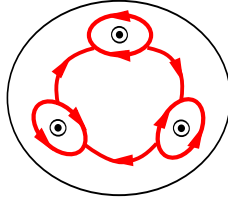


Figure 5.2: An example of complicated networks on the trinion which appears in the product resolution of two elementary pants networks.

with the pants networks into the no defect Schur indices and some simple factors. In particular, by interpreting that new kinds of skein relations happen on C as discussed in Sec. 5.2, we assume that these factors are invariant under $q \rightarrow q^{-1}$ as explained before and check that this is true in the concrete examples.

We find that both the above two assumptions and the conjectural formula are consistent and support each other by the computation in this section and the analysis in the next section.

5.1.1 Free hypermultiplets

Bi-fundamental representation

Let us see the simple case at first. This is the A_2 bi-fundamental hypermultiplet whose flavor symmetry is given by $SU(3) \times SU(3) \times U(1)$. There, we consider the $(a_{AB}, a_{BC}, a_{CA}) = (1, 1, 1)$ -type pants network on $T^{\mathcal{S}}[C([1^3], [1^3], [2, 1])] = \text{Hyper}(\square, \square, 1)$. Let a, b and c be the holonomies of $SU(3) \times SU(3) \times U(1)$. There are six sectors. Up to $q^{1/2}$ -order, we can see that the q -deformed Yang-Mills correlators receive the contributions from all the triple of dominant weights at punctures listed in Table. 5.1.

The result is given by

$$\begin{aligned} \mathcal{I}_{F_{A_2}^{(\text{bf})}}^{\text{Schur}}(a, b, c) &= [\chi_{\mathbf{3}}(a)c^{-1} + \chi_{\bar{\mathbf{3}}}(b)c] + q^{1/2} [2\chi_{\bar{\mathbf{3}}}(a)\chi_{\mathbf{3}}(b) + \chi_{\bar{\mathbf{3}}}(b)c^{-2} + \chi_{\mathbf{3}}(a)c^2 \\ &+ \chi_{\mathbf{8}}(a)\chi_{\bar{\mathbf{3}}}(b)c^{-2} + \chi_{\mathbf{3}}(a)\chi_{\mathbf{8}}(b)c^2 + \chi_{\mathbf{6}}(a)\chi_{\mathbf{3}}(b) + \chi_{\bar{\mathbf{3}}}(a)\chi_{\bar{\mathbf{6}}}(b)] + q [c^3\chi_{\bar{\mathbf{3}}}(a)\chi_{\mathbf{3}}(b) \end{aligned}$$

	$((\lambda_A)_1, (\lambda_A)_2)$	$((\lambda_B)_1, (\lambda_B)_2)$	$((\lambda_C)_1, (\lambda_C)_2)$
$q^0, q^{1/2}$	(0, 0)	(0, 1)	(1, 0)
	(1, 0)	(0, 0)	(0, 1)
$q^{1/2}$	(2, 0)	(1, 0)	(1, 1)
	(1, 1)	(0, 1)	(0, 2)
	(1, 0)	(1, 1)	(0, 2)
	(0, 1)	(0, 2)	(1, 1)
	(0, 1)	(1, 0)	(0, 0)
	(0, 1)	(1, 0)	(1, 1)

Table 5.1: The dominant configurations contributing to q^0 and $q^{1/2}$ terms.

$$\begin{aligned}
& + c^{-1}\chi_{\mathbf{15}'}(a)\chi_{\mathbf{8}}(b) + 2c^{-1}\chi_{\overline{\mathbf{6}}}(a)\chi_{\mathbf{8}}(b) + c^{-3}\chi_{\overline{\mathbf{15}'}}(a)\chi_{\overline{\mathbf{6}}}(b) + c^{-1}\chi_{\overline{\mathbf{6}}}(a)\chi_{\overline{\mathbf{10}}}(b) + c\chi_{\mathbf{10}}(a)\chi_{\mathbf{6}}(b) \\
& + c^{-3}\chi_{\mathbf{6}}(a)\chi_{\mathbf{3}}(b) + c^3\chi_{\mathbf{6}}(a)\chi_{\mathbf{15}'}(b) + 3c\chi_{\overline{\mathbf{3}}}(b) + 3c^{-1}\chi_{\mathbf{3}}(a) + c\chi_{\overline{\mathbf{15}'}}(b) + 3c^{-1}\chi_{\mathbf{3}}(a)\chi_{\mathbf{8}}(b) \\
& + c^{-3}\chi_{\overline{\mathbf{3}}}(a)\chi_{\overline{\mathbf{6}}}(b) + c^3\chi_{\overline{\mathbf{3}}}(a)\chi_{\overline{\mathbf{6}}}(b) + 2c\chi_{\mathbf{8}}(a)\chi_{\mathbf{6}}(b) + c\chi_{\mathbf{8}}(a)\chi_{\overline{\mathbf{15}'}}(b) + 3c\chi_{\mathbf{8}}(a)\chi_{\overline{\mathbf{3}}}(b) \\
& + c^{-1}\chi_{\mathbf{15}'}(a) + c^{-1}\chi_{\overline{\mathbf{6}}}(a) + c^{-3}\chi_{\overline{\mathbf{3}}}(a)\chi_{\mathbf{3}}(b) + c^3\chi_{\mathbf{6}}(a)\chi_{\mathbf{3}}(b) + c\chi_{\mathbf{6}}(b) \Big] + \mathcal{O}(q^{3/2}) \\
& = [\chi_{\mathbf{3}}(a)c^{-1} + \chi_{\overline{\mathbf{3}}}(b)c] \mathcal{I}_{F_{A_2}^{(\text{bf})}}^{\text{Schur}}(a, b, c) \tag{5.1.1}
\end{aligned}$$

where

$$\begin{aligned}
\mathcal{I}_{F_{A_2}^{(\text{bf})}}^{\text{Schur}}(a, b, c) &= 1 + q^{1/2} [c\chi_{\mathbf{3}}(a)\chi_{\mathbf{3}}(b) + c^{-1}\chi_{\overline{\mathbf{3}}}(a)\chi_{\overline{\mathbf{3}}}(b)] + q [1 + \chi_{\mathbf{8}}(a) + \chi_{\mathbf{8}}(b) + \chi_{\mathbf{8}}(a)\chi_{\mathbf{8}}(b) \\
& + c^2\chi_{\overline{\mathbf{3}}}(a)\chi_{\overline{\mathbf{3}}}(b) + c^{-2}\chi_{\overline{\mathbf{6}}}(a)\chi_{\overline{\mathbf{6}}}(b) + c^2\chi_{\mathbf{6}}(a)\chi_{\mathbf{6}}(b) + c^{-2}\chi_{\mathbf{3}}(a)\chi_{\mathbf{3}}(b)] + \mathcal{O}(q^{3/2}) \tag{5.1.2}
\end{aligned}$$

and $\mathbf{15}' = R(2\omega_1 + \omega_2)$.

Then, we find the flavor Wilson loop factor. In terms of the representations of the global symmetry, it is

$$W_{\varphi(1,1,1)}^{\text{bi-fund}} = (\mathbf{3}, \mathbf{1}, -1) \oplus (\mathbf{1}, \overline{\mathbf{3}}, 1). \tag{5.1.3}$$

In the general A_N case ($T^S[C([1^N], [1^N], [N-1, 1])] = \text{Hyper}(\square, \square, 1) = \frac{1}{2}\text{Hyper}(\square, \square, 1) \oplus \frac{1}{2}\text{Hyper}(\overline{\square}, \overline{\square}, -1)$), we conjecture that the (a, b, c) -type ($N = a + b + c$) pants network gives the flavor Wilson loops

$$W_{(a,b,c)}^{\text{bi-fund}} = \binom{b+c-1}{b}_q W^{\text{flavor}}(\wedge^a \square, \mathbf{1}, -b) \oplus \binom{b+c-1}{c}_q W^{\text{flavor}}(\mathbf{1}, \wedge^a \overline{\square}, c). \tag{5.1.4}$$

In the same way, we can check this factorizations for several second rank anti-fundamental type hypermultiplets and both exceptional types [91].

5.1.2 rank 1 SCFTs

In this section, we focus on the rank 1 SCFT with enhancement global symmetry, $E_{6,7,8}$ symmetry.

Rank 1 E_6 SCFT case

The first result is already discussed in [75] in another way. There is only one type elementary pants network specified by $(1, 1, 1)$.

$$\begin{aligned} \mathcal{I}_{\text{rank 1 } E_6 \text{ SCFT w./ } \wp(1,1,1)}^{\text{Schur}}(a, b, c) &= q^{1/2} \chi_{27}^{E_6}(a, b, c) + q^{3/2} \chi_{1728}^{E_6}(a, b, c) \\ &+ q^{5/2} (\chi_{46332}^{E_6}(a, b, c) + \chi_{1728}^{E_6}(a, b, c) + \chi_{351}^{E_6}(a, b, c) + \chi_{27}^{E_6}(a, b, c)) \\ &+ q^{7/2} (\chi_{741312}^{E_6}(a, b, c) + \chi_{51975}^{E_6}(a, b, c) + \chi_{46332}^{E_6}(a, b, c) + \chi_{17550}^{E_6}(a, b, c) \\ &+ 2\chi_{1728}^{E_6}(a, b, c) + \chi_{351}^{E_6}(a, b, c) + 2\chi_{27}^{E_6}(a, b, c)) + \mathcal{O}(q^{9/2}). \end{aligned}$$

Here all the irreducible representations appearing in characters are non-trivially charged under its center group Z_3 .

Notice that the Schur indices in the absence of defects up to q^3 order is given as

$$\begin{aligned} \mathcal{I}_{\text{rank 1 } E_6 \text{ SCFT}}^{\text{Schur}}(a, b, c) &= 1 + q\chi_{78}^{E_6}(a, b, c) + q^2 (\chi_{2430}^{E_6}(a, b, c) + \chi_{78}^{E_6}(a, b, c) + 1) \\ &+ q^3 (\chi_{43758}^{E_6}(a, b, c) + \chi_{2925}^{E_6}(a, b, c) + \chi_{2430}^{E_6}(a, b, c) + 2\chi_{78}^{E_6}(a, b, c) + 1) + \mathcal{O}(q^4). \end{aligned}$$

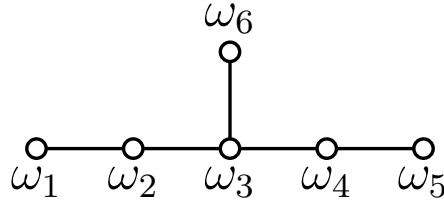


Figure 5.3: E_6 Dynkin diagram. ω_i gives $i \pmod 3$ charge under the center group Z_3 .

dimension	27	351	1728	17550	46332	51975
Dynkin labels	(100000)	(000100)	(100001)	(000101)	(100002)	(101000)
dimension	741312	78	2430	2925	43758	
Dynkin labels	(100003)	(000001)	(000002)	(001000)	(000003)	

Table 5.2: The dimensions of irreducible representations and their Dynkin labels in E_6 .

Rank 1 E_7 SCFT case

In this theory, we find that the $(2, 1, 1)$ -type pants network gives the non-trivial 4D loop operator respecting the E_7 -symmetry. Indeed, the computation up to $q^{7/2}$ gives²⁾

$$\begin{aligned} \mathcal{I}_{\text{rank 1 } E_7 \text{ SCFT w./ } \wp(2,1,1)}^{\text{Schur}}(a, b, c) &= q^{1/2} \chi_{56}^{E_7}(a, b, c) + q^{3/2} \chi_{6480}^{E_7}(a, b, c) \\ &+ q^{5/2} (\chi_{320112}^{E_7}(a, b, c) + \chi_{6480}^{E_7}(a, b, c) + \chi_{912}^{E_7}(a, b, c) + \chi_{56}^{E_7}(a, b, c)) \\ &+ q^{7/2} (\chi_{9405760}^{E_7}(a, b, c) + \chi_{362880}^{E_7}(a, b, c) + \chi_{320112}^{E_7}(a, b, c) + \chi_{86184}^{E_7}(a, b, c) \\ &+ 2\chi_{6480}^{E_7}(a, b, c) + \chi_{912}^{E_7}(a, b, c) + 2\chi_{56}^{E_7}(a, b, c)) + \mathcal{O}(q^{9/2}). \end{aligned} \quad (5.1.5)$$

Notice that all the irreducible representations appearing in characters are non-trivially charged under its center group Z_2 .

The no defect Schur index of this SCFT is given by

$$\begin{aligned} \mathcal{I}_{\text{rank 1 } E_7 \text{ SCFT}}^{\text{Schur}}(a, b, c) &= 1 + q\chi_{133}^{E_7}(a, b, c) + q^2 (\chi_{7371}^{E_7}(a, b, c) + \chi_{133}^{E_7}(a, b, c) + 1) \\ &+ q^3 (\chi_{238602}^{E_7}(a, b, c) + \chi_{8645}^{E_7}(a, b, c) + \chi_{7371}^{E_7}(a, b, c) + 2\chi_{133}^{E_7}(a, b, c) + 1) + \mathcal{O}(q^4). \end{aligned} \quad (5.1.6)$$

The other two pants networks are just flavor Wilson loops, that is to say, factorized into the Schur index without any networks and the following factors.

$$\begin{aligned} (1, 2, 1) &: \chi_{\bar{4}}(b)\chi_2^{SU(2)}(c) + \chi_4(a) \\ (1, 1, 2) &: \chi_4(a)\chi_2^{SU(2)}(c) + \chi_{\bar{4}}(b) \end{aligned}$$

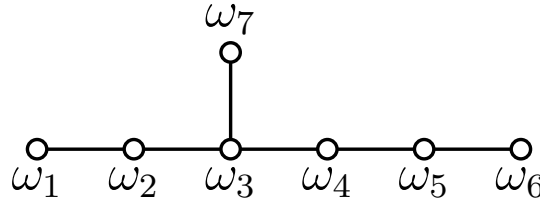


Figure 5.4: E_7 Dynkin diagram. $\omega_{4,6,7}$ gives non-trivial charge under the center group Z_2 .

Rank 1 E_8 SCFT case

In this SCFT, only the $(3, 1, 2)$ -type pants network is the non-trivial network respecting the E_8 -symmetry. The result is following.

$$\mathcal{I}_{\text{rank 1 } E_8 \text{ SCFT w./ } \wp(3,1,2)}^{\text{Schur}}(a, b, c) - [2]_q \mathcal{I}_{\text{rank 1 } E_8 \text{ SCFT}}^{\text{Schur}}(a, b, c) = q^{1/2} (\chi_{248}^{E_8}(a, b, c) + 1)$$

²⁾We do not exactly check the terms at $q^{7/2}$ but only see the match of the values at the trivial fugacities $a = b = c = 1$. Notice also that there is the common structure between the previous E_6 SCFT and this E_7 SCFT on replacing the fundamental weights $\omega_6^{E_6}, \omega_3^{E_6}, \omega_1^{E_6}, \omega_4^{E_6}$ by $\omega_1^{E_7}, \omega_2^{E_7}, \omega_6^{E_7}, \omega_7^{E_7}$ respectively. The similar structure also appears in the $SU(2)$ $N_f = 4$ SQCD, namely, the $SO(8)$ SCFT with or without the fundamental Wilson line, for example. However, it seems to be not true in the E_8 SCFT as we see later.

dimension	56	912	6480	86184	320112	362880
Dynkin labels	(0000010)	(0000001)	(1000010)	(1000001)	(2000010)	(0100010)
dimension	9405760	133	7371	8645	238602	
Dynkin labels	(3000010)	(1000000)	(2000000)	(0100000)	(3000000)	

Table 5.3: The dimensions of irreducible representations and their Dynkin labels in E_7 .

$$\begin{aligned}
& + q^{3/2} (\chi_{30380}^{E_8}(a, b, c) + \chi_{27000}^{E_8}(a, b, c) + \chi_{248}^{E_8}(a, b, c) + 1) \\
& + q^{5/2} (\chi_{4096000}^{E_8}(a, b, c) + \chi_{1763125}^{E_8}(a, b, c) + \chi_{30380}^{E_8}(a, b, c) + 2\chi_{27000}^{E_8}(a, b, c) \\
& \quad + \chi_{3875}^{E_8}(a, b, c) + 3\chi_{248}^{E_8}(a, b, c) + 1) + \mathcal{O}(q^{7/2})
\end{aligned}$$

where we have subtracted the Schur index without the defects expressed as

$$\begin{aligned}
\mathcal{I}_{\text{rank } 1 \ E_8 \ \text{SCFT}}^{\text{Schur}}(a, b, c) & = 1 + q\chi_{248}^{E_8}(a, b, c) + q^2 (\chi_{27000}^{E_8}(a, b, c) + \chi_{248}^{E_8}(a, b, c) + 1) \\
& + q^3 (\chi_{1763125}^{E_8}(a, b, c) + \chi_{30380}^{E_8}(a, b, c) + \chi_{27000}^{E_8}(a, b, c) + 2\chi_{248}^{E_8}(a, b, c)) + \mathcal{O}(q^4).
\end{aligned} \tag{5.1.7}$$

Notice that in the presence of $(3, 1, 2)$ -type pants network, the lowest exponent of q is $-\frac{1}{2}$. The other pants networks are written as the flavor Wilson loops as follows :

$$\begin{aligned}
(1, 1, 4) & : [2]_q \chi_6(a) \chi_2^{SU(2)}(c) + [2]_q \chi_{\bar{3}}^{SU(3)}(b) \\
(1, 2, 3) & : [3]_q \chi_6(a) + \chi_6(a) \chi_3^{SU(2)}(c) + ([2]_q)^2 \chi_{\bar{3}}^{SU(3)}(b) \chi_2^{SU(2)}(c) \\
(1, 3, 2) & : [3]_q [2]_q \chi_{\bar{3}}^{SU(3)}(b) + [2]_q \chi_{\bar{3}}^{SU(3)}(b) \chi_3^{SU(2)}(c) + [2]_q \chi_6(a) \chi_2^{SU(2)}(c) \\
(1, 4, 1) & : ([2]_q)^2 \chi_{\bar{3}}^{SU(3)}(b) \chi_2^{SU(2)}(c) + \chi_6(a) \\
(2, 1, 3) & : \chi_{15}(a) \chi_2^{SU(2)}(c) + \chi_6(a) \chi_{\bar{3}}^{SU(3)}(b) + \chi_{\bar{6}}(a) + \chi_{\bar{3}}^{SU(3)}(b) \chi_2^{SU(2)}(c) \\
(2, 2, 2) & : ([2]_q)^2 \chi_{\bar{3}}^{SU(3)}(b) + \chi_{15}(a) + \chi_6(a) \chi_{\bar{3}}^{SU(3)}(b) \chi_2^{SU(2)}(c) + \chi_{\bar{6}}(a) \chi_2^{SU(2)}(c) \\
& \quad + \chi_{\bar{3}}^{SU(3)}(b) \chi_3^{SU(2)}(c) + \chi_{\bar{6}}^{SU(3)}(b) \\
(2, 3, 1) & : ([2]_q)^2 \chi_{\bar{3}}^{SU(3)}(b) \chi_2^{SU(2)}(c) + \chi_6(a) \chi_{\bar{3}}^{SU(3)}(b) + \chi_{\bar{6}}(a) + \chi_{\bar{6}}^{SU(3)}(b) \chi_2^{SU(2)}(c) \\
(3, 2, 1) & : ([2]_q)^2 \chi_2^{SU(2)}(c) + \chi_6(a) \chi_3^{SU(3)}(b) + \chi_{\bar{6}}(a) \chi_{\bar{3}}^{SU(3)}(b) + \chi_{\bar{8}}^{SU(3)}(b) \chi_2^{SU(2)}(c) \\
(4, 1, 1) & : \chi_6(a) + \chi_{\bar{6}}(a) \chi_{\bar{3}}^{SU(3)}(b) + \chi_{\bar{3}}^{SU(3)}(b) \chi_2^{SU(2)}(c)
\end{aligned}$$

dimension	248	3875	27000	30380	1763125	4096000
Dynkin labels	(00000010)	(10000000)	(00000020)	(00000100)	(00000030)	(000000110)

Table 5.4: The dimensions of irreducible representations and their Dynkin labels in E_8 .

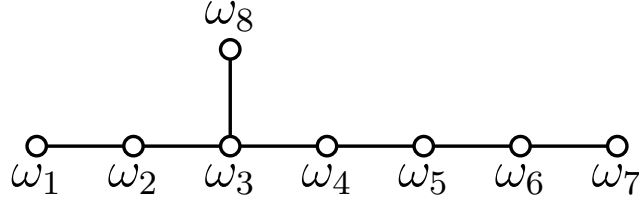


Figure 5.5: E_8 Dynkin diagram. The center group is trivial.

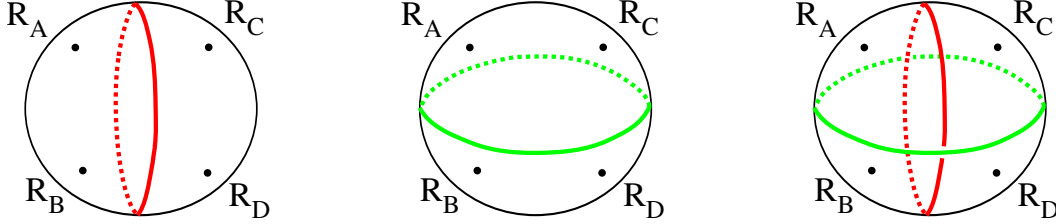


Figure 5.6: For the A_1 or $SU(2)$ SCQCD cases obtained by the four punctured sphere, we show a 4D Wilson loop in $\square = R(\omega_1) = \mathbf{2}$ (Left), a 4D 't Hooft loop labelled by $\square = R(\omega_1) = \mathbf{2}$ (Middle) and both Wilson and 't Hooft loops (Right).

5.1.3 Superconformal QCDs

$SU(2)$ $N_f = 4$ SQCD

Here we introduce the following symbol.

$$\chi(R_A, R_B, R_C, R_D) = \chi_{R_A}^{SU(2)}(a) \chi_{R_B}^{SU(2)}(b) \chi_{R_C}^{SU(2)}(c) \chi_{R_D}^{SU(2)}(d). \quad (5.1.8)$$

See also Appendix. A.2 on the $\mathfrak{so}(8)$ convention.

We also written down the Schur index expression of $SU(2)$ $N_f = 4$ SQCD for comparison.

$$\begin{aligned} \mathcal{I}_\phi(a, b, c, d) &= \mathcal{I}_{SU(2), N_f=4}(a, b, c, d) = \\ &1 + q\chi_{\mathbf{28}}^{SO(8)} + q^2 \left[\chi_{\mathbf{300}}^{SO(8)} + \chi_{\mathbf{28}}^{SO(8)} + 1 \right] \end{aligned} \quad (5.1.9)$$

$$+ q^3 \left[\chi_{\mathbf{1925}}^{SO(8)} + \chi_{\mathbf{350}}^{SO(8)} + \chi_{\mathbf{300}}^{SO(8)} + 2\chi_{\mathbf{28}}^{SO(8)} + 1 \right] + \mathcal{O}(q^4) \quad (5.1.10)$$

where $\chi_{\mathbf{28}}^{SO(8)}$ corresponds to the meson operator $M_{AB} = \epsilon^{ab} Q_{aA} Q_{bB}$ ($a, b : SU(2)$ indices, $A, B : SO(8)$ indices) with $\Delta = 1$ and $I_3 = \frac{1}{2}$.

When we add the Wilson loop W_\square , the Schur index computed from the q -deformed Yang-Mills formula is given by

$$\begin{aligned} \mathcal{I}_{W_\square}(a, b, c, d) &= q^{1/2} [\chi(\mathbf{2}, \mathbf{2}, \mathbf{1}, \mathbf{1}) + \chi(\mathbf{1}, \mathbf{1}, \mathbf{2}, \mathbf{2})] \\ &+ q^{3/2} [\chi(\mathbf{2}, \mathbf{2}, \mathbf{1}, \mathbf{1}) + \chi(\mathbf{1}, \mathbf{1}, \mathbf{2}, \mathbf{2}) + \chi(\mathbf{2}, \mathbf{2}, \mathbf{3}, \mathbf{3}) + \chi(\mathbf{3}, \mathbf{3}, \mathbf{2}, \mathbf{2}) \\ &+ \chi(\mathbf{3}, \mathbf{1}, \mathbf{2}, \mathbf{2}) + \chi(\mathbf{1}, \mathbf{3}, \mathbf{2}, \mathbf{2}) + \chi(\mathbf{2}, \mathbf{2}, \mathbf{3}, \mathbf{1}) + \chi(\mathbf{2}, \mathbf{2}, \mathbf{1}, \mathbf{3})] \end{aligned}$$

$$+ \chi(\mathbf{4}, \mathbf{2}, \mathbf{1}, \mathbf{1}) + \chi(\mathbf{2}, \mathbf{4}, \mathbf{1}, \mathbf{1}) + \chi(\mathbf{1}, \mathbf{1}, \mathbf{4}, \mathbf{2}) + \chi(\mathbf{1}, \mathbf{1}, \mathbf{2}, \mathbf{4})] + \mathcal{O}(q^{5/2}) \quad (5.1.11)$$

$$= q^{1/2} \chi_{[1,0,0,0]}(a, b, c, d) + q^{3/2} \chi_{[1,1,0,0]}(a, b, c, d) + \mathcal{O}(q^{5/2}) \quad (5.1.12)$$

$$= q^{1/2} \chi_{\mathbf{8}_v}(a, b, c, d) + q^{3/2} \chi_{\mathbf{160}_v}(a, b, c, d) + \mathcal{O}(q^{5/2}) \quad (5.1.13)$$

which matches with the known result in [151] for example.³⁾

Next, let us see the dual 't Hooft operators. Although its field theoretical definition is not known yet, from the geometrical point of view, this acts on the above Wilson loop expression simply as the permutation of two simple punctures. In particular, this permutation is equivalent to the triality action of $SO(8)$, that is to say, the exchange of the simple roots α_1 and α_4 . Therefore, its Schur index expression is

$$\begin{aligned} \mathcal{I}_{\square}^{\text{dual}}(a, b, c, d) &= q^{1/2} \chi_{\mathbf{8}_s} + q^{3/2} \chi_{\mathbf{160}_s} \\ &+ q^{5/2} [\chi_{\mathbf{8}_s} + \chi_{\mathbf{56}_s} + \chi_{\mathbf{160}_s} + \chi_{\mathbf{1400}_s}] + \mathcal{O}(q^{7/2}). \end{aligned} \quad (5.1.14)$$

We can interpret the Schur index as the count of local operators playing the role of line changing operators between the fundamental Wilson loop and the minimal 't Hooft loop.

Although we can directly compute this Schur index by using the result in Sec. 4.5.4, let us do the computation in another equivalent way. By representing the four punctured sphere as the disk by removing one point in the sphere, we can geometrically compute the OPE of the Wilson loop and the dual 't Hooft loop with the crossing resolutions as follows:

$$\begin{aligned} &= \text{[Diagram 1]} + \text{[Diagram 2]} \\ &- q^{1/2} \text{[Diagram 3]} - q^{-1/2} \text{[Diagram 4]} \end{aligned} \quad (5.1.15)$$

$$\begin{aligned} &= \text{[Diagram 5]} + \text{[Diagram 6]} \\ &- q^{1/2} \text{[Diagram 7]} - q^{-1/2} \text{[Diagram 8]} \end{aligned} \quad (5.1.16)$$

³⁾Of course, this is obviously true when that of the free bi-fundamental hypermultiplets does. The insertion of the corresponding character and the integration over the gauge group are same operations.

The first two terms give

$$\chi_2(b)\chi_2(d) + \chi_2(a)\chi_2(c) = \chi_{\mathbf{8}_c}^{SO(8)}(a, b, c, d) \quad (5.1.17)$$

and the latter two have the same Schur index (different in the 4D loop operators) up to the prefactors $q^{\pm 1/2}$. The final expression is

$$\begin{aligned} \mathcal{I}_{T_{\square}^{\text{dual}} \circ W_{\square}}(a, b, c, d) &= \mathcal{I}_{W_{\square} \circ T_{\square}^{\text{dual}}}(a, b, c, d) = \chi_{\mathbf{8}_c} \mathcal{I}_{\phi} - [2]_q \mathcal{I}_{WT_{\square}} \\ &= q\chi_{\mathbf{56}_c} + q^2 [\chi_{\mathbf{8}_c} + \chi_{\mathbf{840}_c}] + \mathcal{O}(q^3). \end{aligned} \quad (5.1.18)$$

Since we have no duality frame where both loops are simultaneously magnetically neutral, it is difficult to interpret this result based on the Lagrangian description.

$SU(3)$ $N_f = 6$ SCQCD case

Here we adopt the different notation from the previous one : the labels of punctures different as shown in Fig. 5.7.

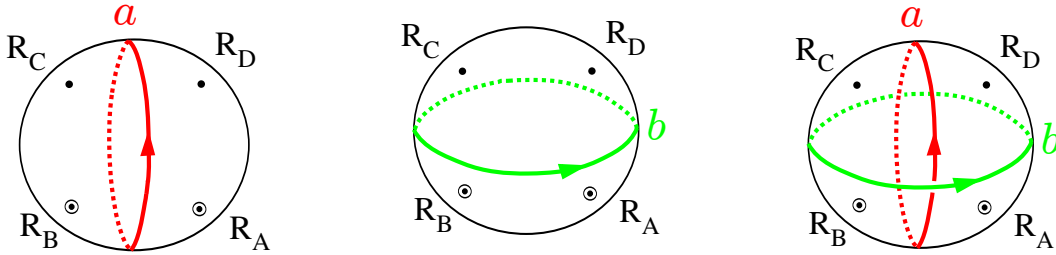


Figure 5.7: For the higher rank cases, Wilson loop in $\wedge^a \square$ (Left), A 't Hooft loop labelled by $\wedge^b \square$ (Middle) and both Wilson and 't Hooft loops (Right). Notice that the ordering of the insertions of two loops is irrelevant in this case.

In the absence of loop defects,

$$\begin{aligned} \mathcal{I}_{SU(3) N_f=6 \text{ SQCD}}^{\text{Schur}}(a, b, c, d) &= 1 + q (2 + c^{-1}d^{-1}\chi_{\mathbf{3}}(a)\chi_{\mathbf{3}}(b) + \chi_{\mathbf{8}}(a) \\ &\quad + cd\chi_{\mathbf{3}}(a)\chi_{\mathbf{3}}(b) + \chi_{\mathbf{8}}(b)) + q^{3/2} (c^{-2}d\chi_{\mathbf{3}}(a)\chi_{\mathbf{3}}(b) + cd^{-2}\chi_{\mathbf{3}}(a)\chi_{\mathbf{3}}(b) \\ &\quad + c^{-1}d^2\chi_{\mathbf{3}}(a)\chi_{\mathbf{3}}(b) + c^2d^{-1}\chi_{\mathbf{3}}(a)\chi_{\mathbf{3}}(b) + c^{-3} + c^3 + d^3 + d^{-3}) + \mathcal{O}(q^2) \end{aligned} \quad (5.1.19)$$

$$= 1 + q(\chi_{\text{Adj}}^{U(6)} + 1) + q^{3/2}(\chi_{\wedge^3 \mathbf{6}}^{U(6)} + \chi_{\wedge^3 \overline{\mathbf{6}}}^{U(6)}) + \mathcal{O}(q^2) \quad (5.1.20)$$

where $\chi_{\mathbf{6}}^{U(6)} = c\chi_{\mathbf{3}}(b) + d^{-1}\chi_{\mathbf{3}}(a)$ and $\chi_{\overline{\mathbf{6}}}^{U(6)} = d\chi_{\mathbf{3}}(a) + c^{-1}\chi_{\mathbf{3}}(b)$.

When we add both fundamental Wilson loop and dual 't Hooft loop as shown in fig:loops in SQCD for higher rank, the answer is

$$\begin{aligned} \mathcal{I}_{SU(3) N_f=6 \text{ SQCD w./ } T_{\square}^{\text{dual}} \circ W_{\square}}^{\text{Schur}}(a, b, c, d) &= q^{1/2} (c\chi_{\mathbf{3}}(a) + c^2d\chi_{\mathbf{3}}(b)) \\ &\quad + q (c^{-2}\chi_{\mathbf{3}}(a) + cd^{-3}\chi_{\mathbf{3}}(a) + c^2d^{-2}\chi_{\mathbf{3}}(b) + 2c^{-1}d\chi_{\mathbf{3}}(b) + cd^3\chi_{\mathbf{3}}(a) + d^2\chi_{\mathbf{3}}(a)\chi_{\mathbf{3}}(b)) \\ &\quad + q^{3/2} (3d^{-1}\chi_{\mathbf{3}}(a)\chi_{\mathbf{3}}(b) + 2c^{-1}d^{-2}\chi_{\mathbf{3}}(b) + c^3d^2\chi_{\mathbf{3}}(a)\chi_{\mathbf{6}}(b) + c^{-3}d^2\chi_{\mathbf{3}}(a)\chi_{\mathbf{3}}(b) + c^{-4}d\chi_{\mathbf{3}}(b)) \end{aligned}$$

$$\begin{aligned}
& + 5c\chi_{\bar{3}}(a) + 3c\chi_{\bar{3}}(a)\chi_{\mathbf{8}}(b) + c^2d\chi_{\bar{6}}(b) + d^{-1}\chi_{\mathbf{3}}(a)\chi_{\mathbf{6}}(b) + c^{-2}d^3\chi_{\bar{3}}(a) + c^3d^2\chi_{\mathbf{3}}(a)\chi_{\bar{3}}(b) \\
& + 2c^2d\chi_{\mathbf{8}}(a)\chi_{\mathbf{3}}(b) + c^{-1}d^{-2}\chi_{\mathbf{8}}(a)\chi_{\mathbf{3}}(b) + c^2d\chi_{\mathbf{15}'}(b) + 2d^{-1}\chi_{\bar{6}}(a)\chi_{\bar{3}}(b) + 4c^2d\chi_{\mathbf{3}}(b) \\
& + c\chi_{\bar{15}'}(a) + c\chi_{\mathbf{6}}(a) + c^{-2}d^{-3}\chi_{\bar{3}}(a) + \mathcal{O}(q^2). \tag{5.1.21}
\end{aligned}$$

$$\begin{aligned}
& = q^{1/2}cd\chi_{\mathbf{6}}^{U(6)} + q \left[cd\chi_{\wedge^2\bar{6}}^{U(6)} + cd(c^{-3} + d^{-3})\chi_{\mathbf{6}}^{U(6)} \right] \\
& + q^{3/2} (c^{-2}d) \left[d^3\chi_{[20001]}^{U(6)} + d^3\chi_{[01001]}^{U(6)} + \chi_{[10100]}^{U(6)} + (1 + c^3d^{-3})\chi_{[00010]}^{U(6)} + c^3\chi_{[10000]}^{U(6)} \right] + \mathcal{O}(q^2) \tag{5.1.22}
\end{aligned}$$

where we use the Boltzmann weight result for each crossing given in [90]. Notice that $\chi_{[0\dots 1\dots]}^{U(6)} := \chi_{\wedge^k\mathbf{6}}^{U(6)}$ and $\chi_{\wedge^6\mathbf{6}}^{U(6)} = c^3d^{-3}$.

5.2 New kinds of skein relations

In this section, we show several new kinds of skein relations based on the formula. Notice that all the skein relations satisfy the mirror operation defined as

$$M : \quad \begin{array}{c} \begin{array}{ccc} & c & \\ & \uparrow & \\ a & \bigcirc & b \\ & \downarrow & \\ & c & \end{array} & \longleftrightarrow & \begin{array}{ccc} & c & \\ & \uparrow & \\ b & \bigcirc & a \\ & \downarrow & \\ & c & \end{array} \end{array} \tag{5.2.1}$$

$$M : \quad x \longleftrightarrow x^* = x^{-1} \tag{5.2.2}$$

$$M : \quad \begin{array}{ccc} & c & \\ & \uparrow & \\ Y \odot & & \\ & \uparrow & \\ & c & \end{array} \longleftrightarrow \begin{array}{ccc} & c & \\ & \uparrow & \\ & & \odot Y \\ & \uparrow & \\ & c & \end{array} \tag{5.2.3}$$

and some skein relations are invariant and others gives the new relations. This operation is clearly involution and no more relations appear.

5.2.1 Simple punctures

This puncture corresponds to $Y = [N - 1, 1]$ -type and the $U(1)^N$ fugacity is expressed as $c_{[N-1,1]} = (q^{\frac{N-2}{2}}c, q^{\frac{N-4}{2}}c, \dots, q^{\frac{-N+4}{2}}c, q^{\frac{-N+2}{2}}c, c^{-(N-1)})$ where c is the $U(1)$ fugacity where this $U(1)$ is the maximal torus of G_Y .

$$\begin{array}{c}
a+b \\
\uparrow \\
\textcircled{Y} \\
\uparrow \\
a+b
\end{array}
= c^{-a} \binom{a+b-1}{a}_q Y \bullet \uparrow
+ c^b \binom{a+b-1}{b}_q \uparrow \bullet Y$$

(5.2.4)

where we have introduced the q -binomial coefficient

$$\binom{x+y}{y}_q := \frac{[x+y]_q!}{[x]_q! [y]_q!} = \frac{\prod_{i=1}^{x+y} [i]_q}{\prod_{i=1}^x [i]_q \prod_{i=1}^y [i]_q}.$$

(5.2.5)

5.2.2 A_3 case

$Y = [2^2]$

$$\begin{array}{c}
3 \\
\uparrow \\
\textcircled{Y} \\
\uparrow \\
3
\end{array}
= Y \bullet \uparrow
+ \chi_2^{SU(2)}(c) \uparrow \bullet Y$$

(5.2.6)

$$\begin{array}{c}
3 \\
\uparrow \\
\textcircled{Y} \\
\uparrow \\
3
\end{array}
= \chi_2^{SU(2)}(c) Y \bullet \uparrow
+ \uparrow \bullet Y$$

(5.2.7)

5.2.3 A_5 case

Let us focus on $T^S[C([1^6], [2^3], [42])]$. Since this theory is a just free hypermultiplet as seen in Sec. 2.4.2, it is expected that all the pants networks are flavor Wilson loops and decompose into the networks without any junctions. In fact, the actual computations

implies that the pants networks specified by $(1, 1, 4), (1, 2, 3), (1, 3, 2)$ and $(1, 4, 1)$ naturally decompose into the flavor Wilson loops. The other pants networks are also not independent and we can expect the following relation

$$(2, 1, 3) \sim (2, 2, 2) \sim (2, 3, 1) \underset{\text{ii}}{\sim} (1, 4, 1) \underset{\text{ii}}{\sim} (4, 1, 1) \sim (3, 2, 1) \sim (3, 1, 2) \quad (5.2.8)$$

where ii corresponds to the relation for $Y = [2^3]$ and others to $Y = [42]$ which give new relations.

This analysis and the previous analysis of rank 1 E_8 SCFT suggest the following skein relations

$$\mathbf{Y} = [42]$$

The flavor symmetry associated with this puncture $Y = [42]$ is $S(U(1) \times U(1)) \simeq U(1)$. The associated fugacity is given by $c_{[42]} = (q^{3/2}c_1, q^{1/2}c_1, q^{-1/2}c_1, q^{-3/2}c_1, q^{1/2}c_2, q^{-1/2}c_2)$. In particular, we introduce $c := c_1$. It is expected that there are 7 independent skein relations.

i-1 & i-2

$$\begin{array}{c} 5 \\ \uparrow \\ \textcircled{Y} \\ \uparrow \\ 5 \end{array} \begin{array}{c} 1 \\ \leftarrow \\ \textcircled{Y} \\ \rightarrow \\ 4 \end{array} = ([3]_q c^{-1} + c^2) \begin{array}{c} 5 \\ \uparrow \\ Y \bullet \\ \uparrow \\ 5 \end{array} + c \begin{array}{c} 5 \\ \uparrow \\ \bullet Y \\ \uparrow \\ 5 \end{array} \quad (5.2.9)$$

$$\begin{array}{c} 5 \\ \uparrow \\ \textcircled{Y} \\ \uparrow \\ 5 \end{array} \begin{array}{c} 2 \\ \leftarrow \\ \textcircled{Y} \\ \rightarrow \\ 3 \end{array} = [3]_q (c + c^{-2}) \begin{array}{c} 5 \\ \uparrow \\ Y \bullet \\ \uparrow \\ 5 \end{array} + ([3]_q + c^3) \begin{array}{c} 5 \\ \uparrow \\ \bullet Y \\ \uparrow \\ 5 \end{array} \quad (5.2.10)$$

ii

$$\begin{array}{c} 4 \\ \uparrow \\ \textcircled{Y} \\ \uparrow \\ 4 \end{array} \begin{array}{c} 2 \\ \leftarrow \\ \textcircled{Y} \\ \rightarrow \\ 2 \end{array} - [2]_q c \begin{array}{c} 4 \\ \uparrow \\ \textcircled{Y} \\ \uparrow \\ 4 \end{array} \begin{array}{c} 3 \\ \leftarrow \\ \textcircled{Y} \\ \rightarrow \\ 1 \end{array} = c^{-2} \begin{array}{c} 4 \\ \uparrow \\ Y \bullet \\ \uparrow \\ 4 \end{array} - [3]_q c^2 \begin{array}{c} 4 \\ \uparrow \\ \bullet Y \\ \uparrow \\ 4 \end{array} \quad (5.2.11)$$

and its mirror operated relation.

iii

$$\begin{array}{c} 3 \\ | \\ \textcircled{Y} \\ | \\ 3 \end{array} \begin{array}{c} 2 \\ \leftarrow \\ \textcircled{Y} \\ \rightarrow \\ 1 \end{array} - \begin{array}{c} 3 \\ | \\ \textcircled{Y} \\ | \\ 3 \end{array} \begin{array}{c} 1 \\ \leftarrow \\ \textcircled{Y} \\ \rightarrow \\ 2 \end{array} = c^2 \left(\begin{array}{c} 3 \\ | \\ \textcircled{Y} \end{array} - c^{-1} \begin{array}{c} 3 \\ | \\ Y \textcircled{\bullet} \end{array} \right) . \quad (5.2.12)$$

$\mathbf{Y} = [3^2]$

The flavor symmetry associated with this puncture $Y = [3^2]$ is $S(U(2)) \simeq SU(2)$. The associated fugacity is given by $c_{[3^2]} = (qc, c, q^{-1}c, qc^{-1}, c^{-1}, qc^{-1})$. It is expected that there are 6 independent skein relations.

i

$$\begin{array}{c} 5 \\ | \\ \textcircled{Y} \\ | \\ 5 \end{array} \begin{array}{c} 4 \\ \leftarrow \\ \textcircled{Y} \\ \rightarrow \\ 1 \end{array} = Y \textcircled{\bullet} \begin{array}{c} 5 \\ | \\ \uparrow \end{array} + [2]_q \chi_2^{SU(2)}(c) \begin{array}{c} 5 \\ | \\ \uparrow \\ \textcircled{Y} \end{array} \quad (5.2.13)$$

and

$$\begin{array}{c} 5 \\ | \\ \textcircled{Y} \\ | \\ 5 \end{array} \begin{array}{c} 2 \\ \leftarrow \\ \textcircled{Y} \\ \rightarrow \\ 3 \end{array} = ([3]_q + \chi_3^{SU(2)}(c)) Y \textcircled{\bullet} \begin{array}{c} 5 \\ | \\ \uparrow \end{array} + [2]_q \chi_2^{SU(2)}(c) \begin{array}{c} 5 \\ | \\ \uparrow \\ \textcircled{Y} \end{array} \quad (5.2.14)$$

and their mirror operated relations.

ii

$$\chi_2^{SU(2)}(c) \begin{array}{c} 4 \\ \uparrow \\ \textcircled{Y} \\ \uparrow \\ 4 \end{array} \begin{array}{c} 1 \\ \rightarrow \\ \textcircled{Y} \\ \leftarrow \\ 2 \end{array} - \begin{array}{c} 4 \\ \uparrow \\ \textcircled{Y} \\ \uparrow \\ 4 \end{array} \begin{array}{c} 2 \\ \rightarrow \\ \textcircled{Y} \\ \leftarrow \\ 2 \end{array} = \chi_3^{SU(2)}(c) \begin{array}{c} 4 \\ \uparrow \\ \textcircled{Y} \end{array} - \begin{array}{c} 4 \\ \uparrow \\ Y \textcircled{\bullet} \end{array} \quad (5.2.15)$$

and its mirror operated relation.

$$\mathbf{Y} = [2^3]$$

The flavor symmetry associated with this puncture $Y = [2^3]$ is $S(U(3)) \simeq SU(3)$. The associated fugacity is given by $c_{[2^3]} = (q^{1/2}c_1, q^{-1/2}c_1, q^{1/2}c_2, q^{-1/2}c_2, q^{1/2}c_3, q^{-1/2}c_3)$ ($c_1c_2c_3 = 1$). It is expected that there are 3 independent skein relations.

i

$$\begin{array}{c} 5 \\ \uparrow \\ \textcircled{Y} \\ \uparrow \\ 5 \end{array} \begin{array}{c} 2 \\ \rightarrow \\ \textcircled{Y} \\ \leftarrow \\ 3 \end{array} - \chi_3^{SU(3)}(c) \begin{array}{c} 5 \\ \uparrow \\ \textcircled{Y} \\ \uparrow \\ 5 \end{array} \begin{array}{c} 1 \\ \rightarrow \\ \textcircled{Y} \\ \leftarrow \\ 4 \end{array} = \begin{array}{c} 5 \\ \uparrow \\ Y \textcircled{\bullet} \end{array} - \chi_6^{SU(3)}(c) \begin{array}{c} 5 \\ \uparrow \\ \textcircled{Y} \end{array} \quad (5.2.16)$$

and its mirror operated relation.

$$\begin{array}{c} 5 \\ \uparrow \\ \textcircled{Y} \\ \uparrow \\ 5 \end{array} \begin{array}{c} 4 \\ \rightarrow \\ \textcircled{Y} \\ \leftarrow \\ 1 \end{array} - \begin{array}{c} 5 \\ \uparrow \\ \textcircled{Y} \\ \uparrow \\ 5 \end{array} \begin{array}{c} 1 \\ \rightarrow \\ \textcircled{Y} \\ \leftarrow \\ 4 \end{array} = \chi_3^{SU(3)}(c) \begin{array}{c} 5 \\ \uparrow \\ Y \textcircled{\bullet} \end{array} - \chi_3^{SU(3)}(c) \begin{array}{c} 5 \\ \uparrow \\ \textcircled{Y} \end{array} \quad (5.2.17)$$

As application, let us consider $T^S[C([1^6], [2^3], [2^3])]$ which is rank 4 SCFT. Using the above relations, there are equivalence relation up to trivial factors between elementary pants networks as follows.

$$(1, 2, 3) \sim (1, 1, 4) \underset{\text{ii}}{\sim} (1, 4, 1) \underset{\text{ii}}{\sim} (4, 1, 1) \sim (3, 2, 1)$$

$$(1, 3, 2) \sim (1, 4, 1) \sim (2, 3, 1) \tag{5.2.18}$$

ii corresponds to the second skein relation. Notice that $(2, 2, 2)$, $(2, 1, 3)$ and $(3, 1, 2)$ are independent

There are (at least) four independent pants networks. We assume that there are no more skein relations and this is consistent with the fact the complex dimension of Coulomb branch is 4.

We can derive the similar relations for any general punctures. All other examples in A_3, A_4 and A_5 -type theories and the general conjectural skein relations are shown in [91].

5.3 Networks for $\mathcal{N}=4$ Yang-Mills

As the fundamental aspects of defect networks in the two dimensional theories have been discussed, we can move on to the discussion of the correspondence between networks on the 2d side and loops on the 4d side. In this section, we restrict ourselves to the most familiar $\mathcal{N}=4$ case. On the gauge theory side, the charges of the loop operators were classified in [44]. It is not easy to construct the corresponding networks for the general A_k case, but we will see that the skein relations allow us to describe and classify the networks for A_2 concretely.

Before proceeding, let us quickly recall the possible charges of the loop operators of $\mathcal{N}=4$ $SU(N)$ Yang-Mills, following [44]. We denote the weight lattice by Λ . We use the notations ω_i for the fundamental weights and h_i for the weight vectors in the defining N -dimensional representation. They are explicitly given by

$$\omega_i = \left(1 - \frac{i}{N}, \dots, 1 - \frac{i}{N}, -\frac{i+1}{N}, \dots, -\frac{i}{N}\right), \tag{5.3.1}$$

$$h_i = \left(-\frac{1}{N}, \dots, -\frac{1}{N}, 1 - \frac{1}{N}, -\frac{1}{N}, \dots, -\frac{1}{N}\right). \tag{5.3.2}$$

Note that $\omega_1 = h_1$ and $\omega_{N-1} = -h_N$.

Let us consider a Wilson loop labeled by an irreducible representation R . We can also use its highest weight λ as the label, and possible highest weights are in one-to-one correspondence with Λ/\mathcal{W} where \mathcal{W} is the Weyl group. Similarly, a 't Hooft loop can be characterized by a charge vector in Λ , considered up to the action of the Weyl group.

For a dyonic loop operator, we need to specify a pair of electric and magnetic charges $(\mu, \lambda) \in \Lambda \times \Lambda$ but the charges need to be identified under a simultaneous action of the Weyl group. Therefore a dyonic charge corresponds to an element in $(\Lambda \times \Lambda)/\mathcal{W}$ and represent the element as $[(\mu, \lambda)]$. We also call it $[(\mu', \lambda')]$ *lower than* $[(\mu, \lambda)]$ if μ' and λ' are lower than μ and λ respectively when mapped to Λ/\mathcal{W} .

5.3.1 The product of Wilson loops and 't Hooft loops

It is well known how pure Wilson loops and pure 't Hooft loops are represented as loops on the torus :

$$W_{\omega_a} \iff \begin{array}{|c|} \hline \xrightarrow{a} \\ \hline \end{array}, \quad T_{\omega_b} \iff \begin{array}{|c|} \hline \nearrow b \\ \hline \end{array} \quad (5.3.3)$$

where we identify each pair of parallel opposite edges to make the parallelogram the torus. Here W_R is the Wilson loop in the representation R , and we identify an irreducible representation and its highest weight vector. We use a similar notation for the 't Hooft loop. We also fix the horizontal one cycle as α -cycle and the vertical one as β -cycle. Note that the S transformation on the torus is naturally identified with S duality transformation of $\mathcal{N}=4$ gauge theory.

We can now decompose the product $W_{\omega_a} \cdot T_{\omega_b}$ using the crossing resolution (4.2.36). Here we express it in a form to make the data of electromagnetic charges manifest:

$$\begin{array}{|c|} \hline \nearrow a \\ \searrow b \\ \hline \end{array} = \sum_{[(\mu_b^{(i)}, \lambda_a^{(i)})] \in \mathcal{D}(\omega_b, \omega_a)} \mathfrak{q}^{-\langle \mu_b^{(i)}, \lambda_a^{(i)} \rangle} \begin{array}{|c|} \hline \begin{array}{c} b \\ \leftarrow b-i \\ \leftarrow i \\ \leftarrow a+b-i \\ \leftarrow a-i \\ \leftarrow b \\ a \end{array} \\ \hline \end{array} \quad (5.3.4)$$

where

$$\mathcal{D}(\mu, \lambda) := (\mathcal{W}(\mu) \times \mathcal{W}(\lambda)) / \mathcal{W} \quad (5.3.5)$$

is the set parameterizing the possible ways to combine a magnetic charge $\mathcal{W}(\mu)$ Weyl-conjugate to μ and an electric charge $\mathcal{W}(\nu)$ Weyl-conjugate to ν .

The number of elements in the set $\mathcal{D}(\omega_b, \omega_a)$ is given by $s = \min(a, b, N-a, N-b)$ and is in a one-to-one correspondence with the label i in the summation (4.2.36). The label i and a representative $[(\mu_b^{(i)}, \nu_a^{(i)})] \in \mathcal{D}(\omega_b, \omega_a)$ can be naturally related by the equation

$$i = \frac{ab}{N} + \langle \mu_b^{(i)}, \lambda_a^{(i)} \rangle. \quad (5.3.6)$$

Recalling the fact reviewed in Sec. 4.1.2 and that $\langle \mu_b^{(i)}, \lambda_a^{(i)} \rangle$ is the x -component of the classical angular momentum associated to the Poynting vector under electric charge $\lambda_a^{(i)}$ and magnetic charge $\mu_b^{(i)}$ in the Coulomb phase with the gauge group $U(1)^{N-1}$, we naturally expect the following correspondence : ⁴⁾

$$\begin{array}{|c|} \hline \begin{array}{c} b \\ \nearrow i \\ \leftarrow a \\ \searrow i \\ \leftarrow a \\ \nearrow i \\ b \end{array} \\ \hline \end{array} \iff D_{[(\mu_b^{(i)}, \lambda_a^{(i)})]} \iff \begin{array}{|c|} \hline \left. \begin{array}{c} \blacksquare \\ \blacksquare \\ \blacksquare \\ \blacksquare \\ \square \\ \square \\ \square \end{array} \right\} b \\ \left. \begin{array}{c} \square \\ \square \\ \square \\ \square \\ \square \\ \square \\ \square \end{array} \right\} a \\ \hline \end{array} \quad (5.3.7)$$

⁴⁾There are other three equivalent networks connected to each other under (4.2.14) or (4.2.15).

where we use the symbol $D_{[(\mu,\nu)]}$ to denote the dyonic loop operator with the charge $[(\mu,\nu)] \in (\Lambda \times \Lambda)/\mathcal{W}$. We also use a simple symbol $D_{(i)}^{b,a}$ for $D_{[(\mu_b^{(i)}, \lambda_a^{(i)})]}$. See also Fig. 5.8 for the brane realization. Below, we call these dyonic loops $D_{(i)}^{b,a}$ and the corresponding networks *elementary*.

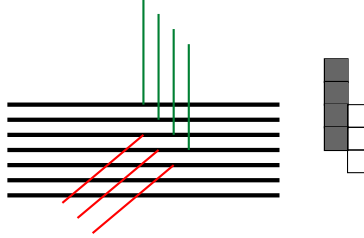


Figure 5.8: The corresponding brane picture for $Q_{(i)}^{ba}$ on the 2-torus. On the stack of N D3-branes, a F1-strings (Red) and b D1-strings (Green) end on. The number of D3-branes on which both F1- and D1-strings end is given by i . In this case, $a = 3$, $b = 4$ and $i = 2$.

5.3.2 Analysis in the Liouville/Toda theory

Let us now connect our analysis so far with a computation on the Liouville/Toda theory side, using the localization in the gauge theory [29, 46].

Hereafter we use symbols $a = (a_1, a_2, \dots, a_N)$ under the constraint $\sum_{i=1}^N a_i = 0$, $A_i(a) := \exp[2\pi i b \langle a, h_i \rangle]$ and $A(a) = \text{diag}(A_1(a), A_2(a), \dots, A_N(a))$. We also denote the $\mathcal{N}=4$ holomorphic partition function by $\mathcal{Z}(a)$.

As seen in [29] and [46], Wilson loop W_R and 't Hooft loop T_R are written in the form of matrix model :

$$\langle W_R \rangle = \int_{i\mathbb{R}^{N-1}} da \mathcal{Z}(a)^* \chi_R(A(a)) \mathcal{Z}(a), \quad (5.3.8)$$

$$\langle T_R \rangle = \int_{i\mathbb{R}^{N-1}} da \mathcal{Z}(a)^* \sum_{\lambda \in \Pi(R)} T_\lambda^{(R)}(a) \mathcal{Z}(a - b\lambda) \quad (5.3.9)$$

where χ_R is the character of R and $\Pi(R)$ is the set of weights corresponding to the irreducible representation R . $T_\lambda^{(R)}(a)$ are some functions of a related to the character χ_R via a Fourier transformation in a [28, 46] but the concrete expressions are unnecessary hereafter.

In general, any loop operator is expected to be represented as

$$\langle X \rangle = \int_{i\mathbb{R}^{N-1}} da \mathcal{Z}(a)^* \sum_{\nu} X_\nu(a) \mathcal{Z}(a - b\nu) \quad (5.3.10)$$

where ν runs over some finite set in the weight lattice Λ and $X_\nu(a)$ are some functions the detail of which we do not need either. The additions of W_R and T_R in the ordering of

loops seen in Sec. 4.1.1 are written as follows :

$$\begin{aligned}\langle W_R X \rangle &= \int_{i\mathbb{R}^{N-1}} da \mathcal{Z}(a)^* W_R \sum_{\nu} X_{\nu}(a) \mathcal{Z}(a - b\nu) \\ &= \int_{i\mathbb{R}^{N-1}} da \mathcal{Z}(a)^* \sum_{\nu} X_{\nu}(a) \chi_R(A(a - b\nu)) \mathcal{Z}(a - b\nu),\end{aligned}\quad (5.3.11)$$

$$\begin{aligned}\langle T_R X \rangle &= \int_{i\mathbb{R}^{N-1}} da \mathcal{Z}(a)^* T_R \sum_{\nu} X_{\nu}(a) \mathcal{Z}(a - b\nu) \\ &= \int_{i\mathbb{R}^{N-1}} da \mathcal{Z}(a)^* \sum_{\mu \in \Pi(R)} \sum_{\nu} T_{\mu}^{(R)}(a - b\nu) X_{\nu}(a) \mathcal{Z}(a - b\nu - b\mu).\end{aligned}\quad (5.3.12)$$

In particular, let us choose R as one of the fundamental representations $\wedge^n \square$ and introduce $W^{(k)} := W_{\wedge^k \square}$ and $T^{(\ell)} := T_{\wedge^{\ell} \square}$. Then consider insertions both of $W^{(k)}$ and of $T^{(\ell)}$. One way to insert is

$$\begin{aligned}\langle \dots T^{(\ell)} W^{(k)} X \rangle &= \int_{i\mathbb{R}^{N-1}} da \mathcal{Z}(a)^* \dots \\ &\quad \sum_{\mu \in \Pi(\wedge^{\ell} \square)} \sum_{\nu} T_{\mu}^{(\ell)}(a - b\nu) X_{\nu}(a) \chi_{\wedge^k \square}(A(a - b\nu)) \mathcal{Z}(a - b\nu - b\mu)\end{aligned}\quad (5.3.13)$$

where the ellipsis represents further insertions of other loops.

Recalling $\chi_R(A(a)) = \sum_{\lambda \in \Pi(R)} \exp[2\pi i b \langle a, \lambda \rangle]$, then define the following operators labelled by $m = 1, 2, \dots, \min(k, \ell)$:

$$\begin{aligned}\langle \dots [TW]_m^{(\ell, k)} X \rangle &:= \int_{i\mathbb{R}^{N-1}} da \mathcal{Z}(a)^* \dots \\ &\quad \sum_{(\lambda, \mu) \in \Pi(\wedge^{\ell} \square, \wedge^k \square)_m} \sum_{\nu} T_{\mu}^{(\ell)}(a - b\nu) X_{\nu}(a) \exp[2\pi i b \langle a - b\nu, \lambda \rangle] \mathcal{Z}(a - b\nu - b\mu).\end{aligned}\quad (5.3.14)$$

where we decompose the set $\Pi(\wedge^{\ell} \square) \times \Pi(\wedge^k \square) = \mathcal{W}(\omega_{\ell}) \times \mathcal{W}(\omega_k)$ into several sectors defined by

$$\Pi(\wedge^{\ell} \square, \wedge^k \square)_m := \{(\mu, \lambda) \in \Pi(\wedge^{\ell} \square) \times \Pi(\wedge^k \square) \mid \langle \mu, \lambda \rangle = m - \frac{k\ell}{N}\} = \mathcal{D}(\omega_{\ell}, \omega_k).\quad (5.3.15)$$

We then have

$$\langle \dots T^{(\ell)} W^{(k)} X \rangle = \sum_m \langle \dots [TW]_m^{(\ell, k)} X \rangle.\quad (5.3.16)$$

Note that the decomposition of $T^{(\ell)} W^{(k)}$ is independent of the ellipsis \dots and X assuring that this expansion is local and represent the product as $T^{(\ell)} \cdot W^{(k)}$ or $T^{(\ell)} \times W^{(k)}$.

On the other hand, the insertion in the opposite order is

$$\begin{aligned} \langle \dots W^{(k)} T^{(\ell)} X \rangle &= \int_{i\mathbb{R}^{N-1}} da \mathcal{Z}(a)^* \dots \\ &\sum_{\mu \in \Pi(\wedge^\ell \square)} \sum_{\nu} T_{\mu}^{(\ell)}(a - b\nu) X_{\nu}(a) \chi_{\wedge^k \square}(A(a - b\mu - b\nu)) \mathcal{Z}(a - b\nu - b\mu) \end{aligned} \quad (5.3.17)$$

and we also have

$$\langle \dots T^{(\ell)} W^{(k)} X \rangle = \sum_m \langle \dots \mathfrak{q}^{2\left(\frac{k\ell}{N} - m\right)} [TW]_m^{(\ell, k)} X \rangle \quad (5.3.18)$$

where we use

$$\exp[2\pi i b \langle a - b\mu - b\nu, \lambda \rangle] = \mathfrak{q}^{2\left(\frac{k\ell}{N} - m\right)} \exp[2\pi i b \langle a - b\nu, \lambda \rangle]. \quad (5.3.19)$$

In summary, we have found the relations

$$T^{(\ell)} \times W^{(k)} = \sum_{m=0}^{\min(k, \ell)} [TW]_m^{(\ell, k)}, \quad W^{(k)} \times T^{(\ell)} = \sum_{m=0}^{\min(k, \ell)} \mathfrak{q}^{2\left(\frac{k\ell}{N} - m\right)} [TW]_m^{(\ell, k)}. \quad (5.3.20)$$

Comparing the product expansion (5.3.20) and the graphical expansion (5.3.4) we find the following identification :

$$\begin{array}{ccccccc} (Q^{\ell k}_{(m)} \text{ on } T^2) & \leftrightarrow & D_{(m)}^{\ell, k} & \leftrightarrow & [(\mu_{\ell}^{(m)}, \lambda_k^{(m)})] & \leftrightarrow & \mathfrak{q}^{-\langle \mu_{\ell}^{(m)}, \lambda_k^{(m)} \rangle} [TW]_m^{(\ell, k)} \\ \text{network} & & \text{4d loop} & & \text{charge} & & \text{operator} \end{array} \quad (5.3.21)$$

Here the pair of weights $[(\mu_{\ell}^{(m)}, \lambda_k^{(m)})]$ was chosen as in (5.3.4), and therefore we have $\langle \mu_{\ell}^{(m)}, \lambda_k^{(m)} \rangle = m - \frac{k\ell}{N}$.

Let us see how T transformation of the $SL(2, \mathbb{Z})$ duality action acts on these loop operators. The θ dependence originally comes from the classical part of $\mathcal{N}=4$ partition function $\mathcal{Z}(a) = \exp[-\pi i \tau \langle a, a \rangle]$ where holomorphic gauge coupling $\tau = \frac{\theta}{2\pi} + \frac{4\pi i}{g_{YM}^2}$ and the monodromy action under the change $\theta \rightarrow \theta + 2\pi$ is following :

$$\begin{aligned} \mathcal{Z}(a)^* \mathcal{Z}(a - b\lambda) &\xrightarrow{\tau \rightarrow \tau + 1} \exp[-\pi i (\langle a - b\lambda, a - b\lambda \rangle - \langle a, a \rangle)] \mathcal{Z}(a)^* \mathcal{Z}(a - b\lambda) \\ &= \mathfrak{q}^{-\langle \lambda, \lambda \rangle} e^{2\pi i b \langle \lambda, a \rangle} \mathcal{Z}(a)^* \cdot \mathcal{Z}(a - b\lambda) \end{aligned} \quad (5.3.22)$$

The Witten effect on the partition function can be re-expressed in the loop operators which acts on the partition functions. In particular, when λ is in $\Pi(\wedge^\ell \square) = \mathcal{W}(\omega_{\ell})$, $\mathcal{Z}(a)^* \mathcal{Z}(a - b\lambda)$ is accompanied by

$$\mathfrak{q}^{-\ell + \frac{\ell^2}{N}} e^{2\pi i b \langle \lambda, a \rangle} \quad (5.3.23)$$

as θ shifts by 2π . Summing it up over $\Pi(\wedge^\ell \square)$,

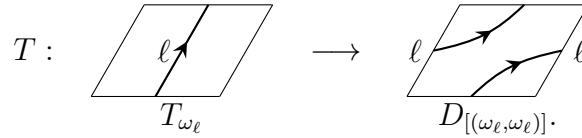
$$T^{(\ell)} \longrightarrow \mathfrak{q}^{-\ell + \frac{\ell^2}{N}} [TW]_\ell^{(\ell, \ell)} = D_{[(\omega_\ell, \omega_\ell)]} = D_{(\ell)}^{\ell, \ell} \quad (5.3.24)$$

under $\theta \rightarrow \theta + 2\pi$. Since $D_{[(\omega_\ell, \omega_\ell)]} = D_{(\ell)}^{\ell, \ell}$ is given by



$$\ell \begin{array}{c} \nearrow \\ \searrow \end{array} \ell \quad . \quad (5.3.25)$$

This $\theta \rightarrow \theta + 2\pi$ action is graphically represented as



$$T : \begin{array}{c} \text{parallelogram with vertical arrow } \ell \\ T_{\omega_\ell} \end{array} \longrightarrow \begin{array}{c} \text{parallelogram with two diagonal arrows } \ell \\ D_{[(\omega_\ell, \omega_\ell)]} \end{array} \quad (5.3.26)$$

and matches with the T transformation on the torus.

5.3.3 Examples of products of loops in A_2

Let us focus on the A_2 case and perform some explicit computations. The examples in the general A_k case will be given in Appendix 5.4. We will see the geometric $SL(2, \mathbb{Z})$ action on the torus is nicely mapped to the $SL(2, \mathbb{Z})$ action on the electric and magnetic weight systems.

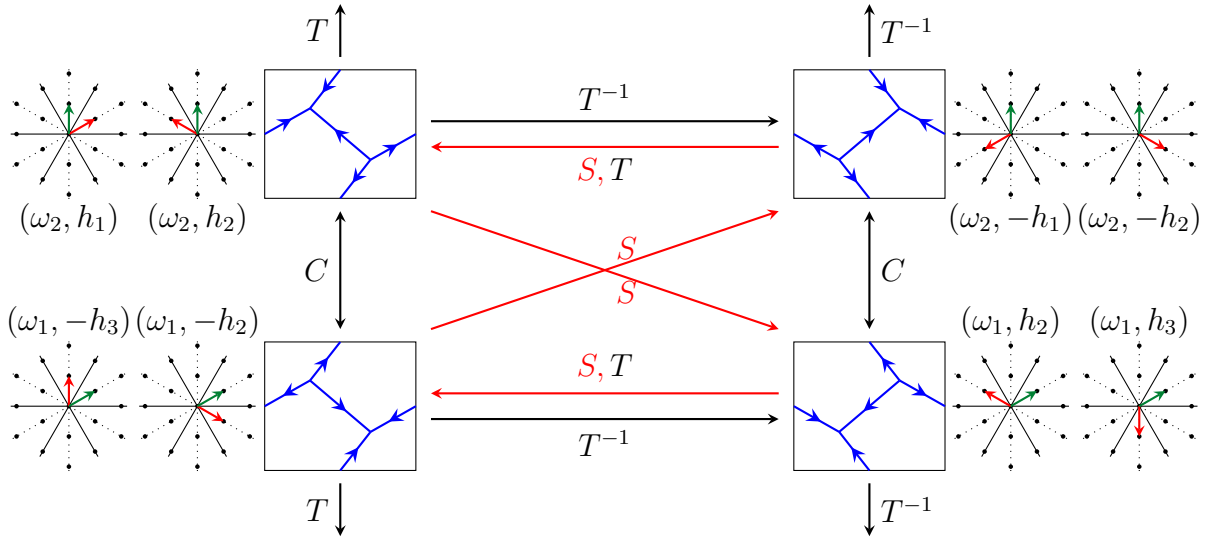


Figure 5.9: The $SL(2, \mathbb{Z})$ duality orbit of $D_{(0)}^{1,1}$ (below right) and their dyonic charges. Two adjacent expressions of a pair of weights are equivalent via some Weyl reflections. Red weights correspond to electric weights and green's to magnetic ones.

Example 1. The simplest case is $W_{\square} \times T_{\square}$, which corresponds to the equation (5.3.4) with $a = 1$ and $b = 1$:

$$W_{\square} \times T_{\square} = \mathfrak{q}^{1/3} D_{(0)}^{1,1} + \mathfrak{q}^{-2/3} D_{(1)}^{1,1} \quad (5.3.27)$$

where $D_{(0)}^{1,1} = D_{[(\omega_1, h_2)]} = D_{[(\omega_1, h_3)]}$ and $D_{(1)}^{1,1} = D_{[(\omega_1, \omega_1)]}$. This was originally found in [62, 68] in the context of class S theory.

The dyonic loop $D_{(1)}^{1,1}$ is obtained from the 't Hooft loop T_{\square} by an application of the T operation. In particular this loop can be mapped to a Wilson loop in some duality frame. The object $D_{(0)}^{1,1}$ cannot be mapped into a network localized on any one cycle by the torus modular transformations. In the language of charges, this means that the electric weight and the magnetic weight are not parallel. We can now work out how the $SL(2, \mathbb{Z})$ transformations act on this particular network and the pair of weights, see Fig.5.9.

Example 2. The next example is $W_{\square} \times T_{\square}$:

$$= \mathfrak{q}^{2/3} \left[\begin{array}{c} \text{Square with vertical and 3 horizontal lines} \\ \text{Square with diagonal and 2 lines} \\ \text{Square with 2 parallel diagonal lines} \\ \text{Square with 2 curved lines} \end{array} \right] \quad (5.3.28)$$

In this example, the first term on the right hand side is a network that cannot be mapped by $SL(2, \mathbb{Z})$ to any of the networks we already studied explicitly. It is natural to posit the following expansion

$$W_{\square} \times T_{\square} = \mathfrak{q}^{2/3} D_{[(\omega_1, 2h_2)]} + \mathfrak{q}^{-1/3} D_{[(\omega_1, h_1+h_2)]} + \mathfrak{q}^{-4/3} D_{[(\omega_1, 2\omega_1)]} + (\text{loops with lower weights}) \quad (5.3.29)$$

since we expect that the exponent of \mathfrak{q} multiplying $D_{[(\lambda_m, \lambda_e)]}$ equals $-\langle \lambda_m, \lambda_e \rangle$ to capture the angular momentum. Then we can identify

$$D_{[(\omega_1, 2h_2)]} \sim \begin{array}{c} \text{Square with vertical and 3 horizontal lines} \end{array} \quad (5.3.30)$$

up to the lower contribution $D_{[(\omega_1, h_i+h_{j(>i)})]}$ from lower weights. Hereafter, we try to map networks and charges of the dyonic loops up to the contributions from lower weights.⁵⁾

⁵⁾The complication comes from two sources. One is common with what we encountered in Sec. 4.2.2: irreducible representations are linear combinations of networks even in the Wilson loop case. Another is related to the bubbling effect of the monopole moduli space. See the related works to this subject [45, 46, 182, 183].

Example 3. The third example is $W_{\text{Adj}} \times T_{\square}$: The skein relation gives us

$$\begin{array}{c} \square \\ \hline \text{Adj} \end{array} = \mathfrak{q} \left(\begin{array}{c} \diagup \diagdown \\ \diagdown \diagup \end{array} \right) + \begin{array}{c} \leftarrow \rightarrow \\ \leftarrow \rightarrow \\ \leftarrow \rightarrow \end{array} + \mathfrak{q}^{-1} \left(\begin{array}{c} \diagdown \diagup \\ \diagup \diagdown \end{array} \right) \quad (5.3.31)$$

while from gauge theory we expect

$$\begin{aligned}
 W_{\text{Adj}} \times T_{\square} &= \mathfrak{q} D_{[(\omega_1, h_2 - h_1)]} + D_{[(\omega_1, h_1 + 2h_2)]} + \mathfrak{q}^{-1} D_{[(\omega_1, 2h_1 + h_2)]} \\
 &+ (\text{loops with lower weights}). \quad (5.3.32)
 \end{aligned}$$

For a graphical representation of weights involved, see Fig. 5.10.

The first term and the third term can be obtained by $SL(2, \mathbb{Z})$ transformations on $D_{(0)}^{1,1}$. The second term is a new type:

$$D_{[(\omega_1, h_1 + 2h_2)]} \sim \begin{array}{c} \leftarrow \rightarrow \\ \leftarrow \rightarrow \\ \leftarrow \rightarrow \end{array} . \quad (5.3.33)$$

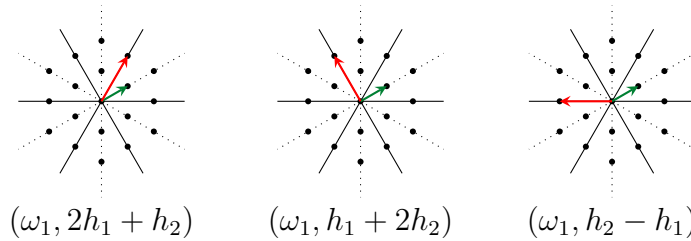


Figure 5.10: Representative weights in $\mathcal{D}(\omega_1, \omega_1 + \omega_2)$

Example 4. Our final example is $W_{\text{Adj}} \times T_{\text{Adj}}$. The skein relation gives

$$\begin{array}{c} \text{Adj} \\ \hline \text{Adj} \end{array} = 4(2 + \mathfrak{q}^2 + \mathfrak{q}^{-2}) \square + 2 \begin{array}{c} \text{Adj} \\ \hline \square \end{array} + 2 \begin{array}{c} \square \\ \hline \text{Adj} \end{array} + \mathfrak{q}^{-2} \begin{array}{c} \text{Adj} \\ \text{Adj} \end{array} + \mathfrak{q}^2 \begin{array}{c} \text{Adj} \\ \text{Adj} \end{array}$$

$$+ \mathfrak{q}^{-1} \left(\begin{array}{c} \text{Diagram 1} \\ \text{Diagram 2} \end{array} \right) + \mathfrak{q} \left(\begin{array}{c} \text{Diagram 3} \\ \text{Diagram 4} \end{array} \right) \quad (5.3.34)$$

while the gauge theory computation yields

$$\begin{aligned} W_{\text{Adj}} \times T_{\text{Adj}} &= \mathfrak{q}^{-2} D_{[(\lambda_{\text{Adj}}, \lambda_{\text{Adj}})]} + \mathfrak{q}^2 D_{[(\lambda_{\text{Adj}}, -\lambda_{\text{Adj}})]} \\ &+ \mathfrak{q}^{-1} D_{[(\lambda_{\text{Adj}}, \lambda_{1+})]} + \mathfrak{q}^{-1} D_{[(\lambda_{\text{Adj}}, \lambda_{2+})]} + \mathfrak{q} D_{[(\lambda_{\text{Adj}}, \lambda_{2-})]} + \mathfrak{q} D_{[(\lambda_{\text{Adj}}, \lambda_{1-})]} \\ &+ (\text{loops with the lower weights}) \end{aligned} \quad (5.3.35)$$

where $\lambda_{\text{Adj}} = \omega_1 + \omega_2$ is the highest weight of the adjoint representation and see Fig. 5.11 for $\lambda_{1,2\pm}$. It would be interesting to reproduce the terms with lower weights from a purely 4d gauge theoretic computations.

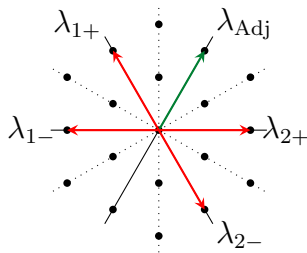


Figure 5.11: Representative weights in $\mathcal{D}(\omega_1 + \omega_2, \omega_1 + \omega_2)$

5.3.4 Classification of networks on T^2 for A_2

We have seen some basic examples of products of loops and the identification of the charge and the network. Here we establish the general mapping between the networks and the charges in the case of the A_2 theory on the torus, or equivalently the $\mathcal{N}=4$ $SU(3)$ Yang-Mills. This is a minimal extension of the dictionary of Drukker, Morrison and Okuda [25].

Let us first classify the possible A_2 networks on the torus purely in terms of the skein relation. First, recall that all networks with crossings are resolved into those with junctions only. In particular, for the A_2 case, there are only two types of junctions, namely the one where the heads of three arrows meet and another one where the tails of three arrows meet. Therefore the networks are bipartite [62] and there appear only polygons with degree-even vertices.

We now use the skein relations we discussed so far. Recall the basic conventions we discussed in Sec. 4.2.7. All digons can be contracted, and all rectangles are resolved to two pairs of curves, as we discussed in (4.2.51).

At this point, the network might contain several disconnected components. If there are no vertices at all, the network consists of parallel loops wrapping the same one-cycle

on T^2 . Assume now there is at least one vertex. Pick a connected component. It has the topology of either a disk, an annulus or a torus.

Now, let us denote the number of edges, or equivalently the number of vertices, of the i -th polygon in this connected component by $p_i (= 2, 4, 6, \dots)$. Denote the number of polygons by f . The total number of vertices, edges and faces of the network is then given by

$$V = \frac{1}{3} \sum_i p_i, \quad E = \frac{1}{2} \sum_i p_i, \quad F = f. \quad (5.3.36)$$

Furthermore, denote the number of boundary edges by B which vanish if the connected component has the topology of torus. From Euler's theorem we should have

$$\chi + \frac{1}{6}B = V - E + F = F - \frac{1}{6} \sum_i p_i \geq 0 \quad (5.3.37)$$

since the connected component is either a disk ($\chi = 1, B > 0$), an annulus ($\chi = 0, B > 0$), or a torus ($\chi = 0, B = 0$). Since we removed all digons and rectangles, $p_i \geq 6$, and therefore we have

$$F - \frac{1}{6} \sum_i p_i \leq 0. \quad (5.3.38)$$

From this we see that the connected component has the topology of the torus, and every polygon is a hexagon. Therefore, the possible A_2 networks on T^2 are mapped into the bipartite hexagon tilings with three corner condition at every vertex.

It is interesting to note at this point that bipartite hexagon tilings of the torus appeared in the string theory literature in the context of brane tilings [184–186]. In this case the bipartite hexagon tilings corresponded to Abelian orbifolds of \mathbb{C}^3 .

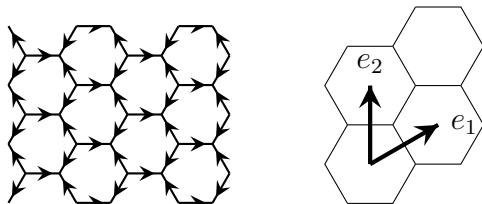


Figure 5.12: The infinite bipartite hexagonal tiling and its basis vectors

Now let us make the dictionary between the bipartite hexagon tilings and the dyonic charges. Instead of thinking of filling a torus by hexagons, we can take the quotient of the bipartite hexagon tiling filling the entire plane, and then we define the vectors e_1 and e_2 there, see Fig.5.12. To specify a bipartite hexagon tiling, we choose the α and the β cycles of the torus from $\mathbb{Z}e_1 \oplus \mathbb{Z}e_2$ so that they are linearly independent. In Fig. 5.13 we show the hexagonal tilings and the dyonic charges that already appeared in our analysis so far.

From these examples, we can find the general map. We first naturally identify the A_2 weight lattice Λ and the dual lattice of the hexagonal tiling. Then, the rule is

$$(\lambda_e, \lambda_m) \mapsto (\alpha, \beta) = (\lambda_m, -\lambda_e). \quad (5.3.39)$$

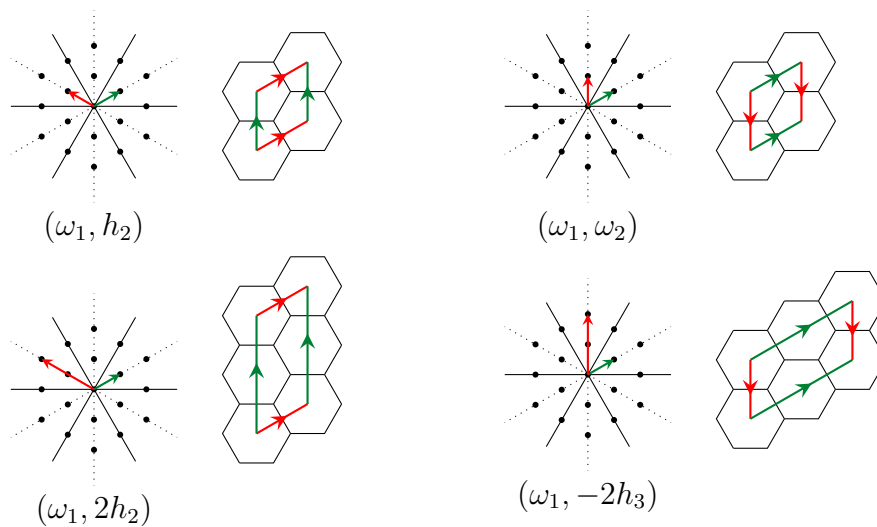


Figure 5.13: Some examples of the hexagonal tilings and the dyonic charges that we have already identified

under the condition $q_1 p_2 - q_2 p_1 > 0$ where $\lambda_e = q_1 \omega_1 + q_2 \omega_2$ and $\lambda_m = p_1 \omega_1 + p_2 \omega_2$.

It is clear that the action of the Weyl group is consistent. Because the cycles α, β define the basis of charges, the action of $SL(2, \mathbb{Z})$ on the dyonic charges (λ_e, λ_m) and that on the cycles (α, β) should be transpose of each other, and indeed the mapping (5.3.39) satisfies this condition. Let us end this section by exhibiting some more examples of the mapping between the dyonic charges and the hexagonal tilings, see Fig. 5.14.

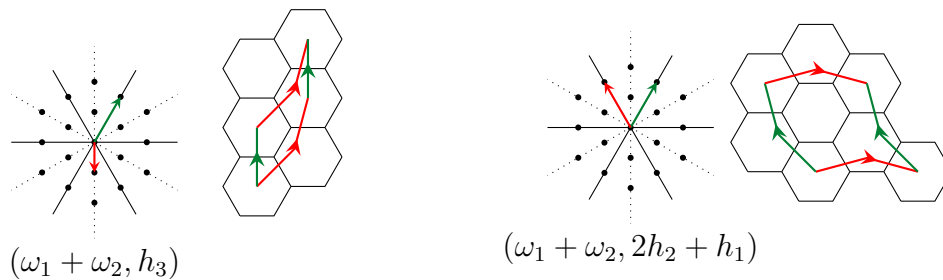


Figure 5.14: Some more examples of the hexagonal tilings and the dyonic charges

In this section we only discussed the A_2 case. In Sec. 5.5, we briefly discuss the general map from the charge of the dyonic loops to the networks for or general $A_{k>2}$ cases.

5.4 Examples of OPE and charge/network dictionary

Here we present some more examples of the OPE and the correspondence of the dyonic charge and the networks for the $\mathcal{N}=4$ theory, or equivalently for the torus. The results of the OPE are for $A_{N-1>2}$ unless otherwise stated. For the A_2 case, the edges with 3

should be removed and those with 2 can be replaced by the reversed ones with 1. We use the convention that the magnetic weight lies in the fundamental Weyl chamber Λ/\mathcal{W} but the electric one is unrestricted.

5.4.1 Pure dyonic loops

Dyonic loops can be roughly classified into two, which we call pure and complex. The pure ones are those that can be mapped to a Wilson loop in a duality frame, and the complex ones are those without any such duality frame. Let us first discuss the representation of the pure ones as loops on the torus.

We abbreviate a bundle of arrows with charges s_1, s_2, \dots, s_{r-1} and s_r as an single arrow without any label:

$$\begin{array}{c} \uparrow \end{array} := \begin{array}{c} s_1 \ s_2 \ s_3 \ \dots \ s_{r-1} \ s_r \\ \uparrow \uparrow \uparrow \dots \uparrow \uparrow \end{array} . \tag{5.4.1}$$

Let $\omega_I = \sum_{i=1}^r \omega_{s_i}$. Then there are four types as follows:

$$\begin{array}{cc}
 (\mu_m, \lambda_e) = (p\omega_I, q\omega_I), & (\mu_m, \lambda_e) = (p\omega_I, -q\omega_I) \\
 \begin{array}{c} p \\ \left. \begin{array}{c} \text{Diagram 1} \end{array} \right\} q, \end{array} & \begin{array}{c} p \\ \left. \begin{array}{c} \text{Diagram 2} \end{array} \right\} q, \end{array} \\
 q \geq p : & \tag{5.4.2}
 \end{array}$$

$$\begin{array}{cc}
 \begin{array}{c} p \\ \left. \begin{array}{c} \text{Diagram 3} \end{array} \right\} q, \end{array} & \begin{array}{c} p \\ \left. \begin{array}{c} \text{Diagram 4} \end{array} \right\} q. \end{array} \\
 p \geq q : & \tag{5.4.3}
 \end{array}$$

This is essentially the same as the discussion in [25].

5.4.2 $W_{\square} \times T_{\square}$

Let us compute the skein relation of W_{\square} and T_{\square} . Comparing with what we expect from the gauge theory, we can then identify various networks with complex dyonic loops. From

the skein relation, we have

$$\begin{array}{c} \square \\ \square \end{array} = q^{2/N} \left[\begin{array}{c} \text{Diagram 1} \\ \text{Diagram 2} \end{array} - \begin{array}{c} \text{Diagram 3} \\ \text{Diagram 4} \end{array} \right] + q^{-1} \begin{array}{c} \text{Diagram 5} \\ \text{Diagram 6} \end{array} + q^{-2} \begin{array}{c} \text{Diagram 7} \\ \text{Diagram 8} \end{array} \quad (5.4.4)$$

The first term is a new one, the second and third ones are elementary and the final one is pure. Then we identify:

$$D_{[(\omega_1, 2h_{i(\neq 1)})]} \sim \begin{array}{c} \text{Diagram 1} \\ \text{Diagram 2} \end{array}, \quad D_{[(\omega_1, h_{i(\neq 1)} + h_{j(>i)})]} \sim \begin{array}{c} \text{Diagram 3} \\ \text{Diagram 4} \end{array}, \quad (5.4.5)$$

$$D_{[(\omega_1, h_1 + h_{i(\neq 1)})]} \sim \begin{array}{c} \text{Diagram 5} \\ \text{Diagram 6} \end{array}, \quad D_{[(\omega_1, 2\omega_1)]} \sim \begin{array}{c} \text{Diagram 7} \\ \text{Diagram 8} \end{array}. \quad (5.4.6)$$

5.4.3 $W_{(2,1)} \times T_{\square}$

Let us next consider $W_{(2,1)} \times T_{\square}$:

$$\begin{array}{c} \square \\ \square \end{array} = q^{3/N} \left[\begin{array}{c} \text{Diagram 1} \\ \text{Diagram 2} \end{array} - \begin{array}{c} \text{Diagram 3} \\ \text{Diagram 4} \end{array} \right] + q^{-1} \begin{array}{c} \text{Diagram 5} \\ \text{Diagram 6} \end{array} + q^{-2} \begin{array}{c} \text{Diagram 7} \\ \text{Diagram 8} \end{array} \quad (5.4.7)$$

The first and the third terms are new, the second one is elementary and the fourth one is obtained by a T action of some elementary one. When $N = 3$, the second one does not appear and indeed this case is the same as Example 5.4.5.

We can therefore identify:

$$D_{[(\omega_1, 2h_{i(\neq 1)} + h_{j(>i)})]} \sim \text{Diagram 1}, \quad D_{[(\omega_1, h_{i(\neq 1)} + h_{j(>i)} + h_{k(>j)})]} \sim \text{Diagram 2}, \quad (5.4.8)$$

$$D_{[(\omega_1, h_1 + 2h_{i(\neq 1)})]} \sim \text{Diagram 3}, \quad D_{[(\omega_1, 2h_1 + h_{i(\neq 1)})]} \sim \text{Diagram 4}. \quad (5.4.9)$$

5.4.4 $W_{\square\square\square} \times T_{\square}$

Our next example is $W_{\square\square\square} \times T_{\square}$:

$$\begin{aligned} & \begin{array}{c} \square \\ \square \\ \square \end{array} = q^{3/N} \left[\begin{array}{c} \text{Diagram 5} \\ \text{Diagram 6} \\ \text{Diagram 7} \\ \text{Diagram 8} \\ \text{Diagram 9} \\ \text{Diagram 10} \end{array} \right] \\ & - 2 \left[\begin{array}{c} \text{Diagram 11} \\ \text{Diagram 12} \end{array} \right] \\ & + q^{-1} \left(\begin{array}{c} \text{Diagram 13} \\ \text{Diagram 14} \end{array} \right) \\ & + q^{-2} \left[\begin{array}{c} \text{Diagram 15} \\ \text{Diagram 16} \end{array} \right] \quad (5.4.10) \end{aligned}$$

The first term is new, the fifth one is elementary, the seventh one is pure and others have appeared in the previous case. When $N = 3$, the third one does not appear. We therefore

identify:

$$D_{[(\omega_1, 3h_{i(\neq 1)})]} \sim \begin{array}{c} \begin{array}{|c|} \hline \begin{array}{c} \text{Diagram 1} \\ \text{Three parallel black lines with arrows pointing right. A blue line with arrows pointing right crosses them, labeled '2' in blue.} \end{array} \\ \hline \end{array} , \quad D_{[(\omega_1, h_1+h_{i(\neq 1)}+h_{j(>i)})]} \sim \begin{array}{|c|} \hline \begin{array}{c} \text{Diagram 2} \\ \text{A black line with an arrow pointing up-right crosses two black lines with arrows pointing right. A blue line with arrows pointing right crosses the black lines, labeled '2' in blue. Two red lines with arrows pointing right cross the black lines, labeled '3' in red.} \end{array} \\ \hline \end{array} , \quad (5.4.11)$$

$$D_{[(\omega_1, 3\omega_1)]} \sim \begin{array}{|c|} \hline \begin{array}{c} \text{Diagram 3} \\ \text{Three parallel black lines with arrows pointing right.} \end{array} \\ \hline \end{array} . \quad (5.4.12)$$

5.4.5 $W_{\text{Adj}} \times T_{\square}$

As a further example, let us consider $W_{\text{Adj}} \times T_{\square}$:

$$\begin{array}{|c|} \hline \square \\ \hline \begin{array}{c} \text{Diagram 4} \\ \text{A square with a red horizontal line with an arrow pointing right and a green vertical line with an arrow pointing up.} \end{array} \\ \hline \end{array} \text{Adj} = \begin{array}{|c|} \hline \begin{array}{c} \text{Diagram 5} \\ \text{Diagram 1} \\ \text{Three parallel black lines with arrows pointing right. A blue line with arrows pointing right crosses them, labeled '2' in blue.} \end{array} \\ \hline \end{array} + \begin{array}{|c|} \hline \begin{array}{c} \text{Diagram 6} \\ \text{A black line with an arrow pointing up-right crosses two black lines with arrows pointing right. A blue line with arrows pointing right crosses the black lines, labeled '2' in blue.} \end{array} \\ \hline \end{array} + q^{-1} \begin{array}{|c|} \hline \begin{array}{c} \text{Diagram 7} \\ \text{Diagram 3} \\ \text{Three parallel black lines with arrows pointing right.} \end{array} \\ \hline \end{array} \quad (5.4.13)$$

The second term is new, and the first and the third ones are obtained by some duality actions of some elementary one. Our identifications are:

$$D_{[(\omega_1, h_{i(\neq 1)}-h_1)]} \sim \begin{array}{|c|} \hline \begin{array}{c} \text{Diagram 8} \\ \text{Diagram 1} \\ \text{Three parallel black lines with arrows pointing right. A blue line with arrows pointing right crosses them, labeled '2' in blue.} \end{array} \\ \hline \end{array} , \quad D_{[(\omega_1, h_{i(\neq 1)}-h_{j(\neq i)}+h_{j(>i)})]} \sim \begin{array}{|c|} \hline \begin{array}{c} \text{Diagram 6} \\ \text{Diagram 6} \\ \text{A black line with an arrow pointing up-right crosses two black lines with arrows pointing right. A blue line with arrows pointing right crosses the black lines, labeled '2' in blue.} \end{array} \\ \hline \end{array} , \quad (5.4.14)$$

$$D_{[(\omega_1, h_1-h_{i(\neq 1)})]} \sim \begin{array}{|c|} \hline \begin{array}{c} \text{Diagram 9} \\ \text{Diagram 3} \\ \text{Three parallel black lines with arrows pointing right.} \end{array} \\ \hline \end{array} . \quad (5.4.15)$$

5.4.6 $W_{\text{Adj}} \times T_{\text{Adj}}$

We now move on to the example $W_{\text{Adj}} \times T_{\text{Adj}}$:

$$D_{[(\lambda_{\text{Adj}}, -h_1 + h_{i(\neq 1, N)})]} \sim \left[\text{Diagram 1} \right], \quad D_{[(\lambda_{\text{Adj}}, h_N - h_{i(\neq 1, N)})]} \sim \left[\text{Diagram 2} \right] \quad (5.4.19)$$

where $\lambda_{\text{Adj}} = h_1 - h_N$ is the highest weight of the adjoint representation.

5.4.7 An OPE of complex dyonic loops

Finally we give an example of the OPE of two elementary dyonic loops $D_{(0)}^{1,1}$ and $D_{(0)}^{\ell,k}$ for $\ell, k \leq N/2$ in $\mathcal{N}=4$ SYM:

$$\left[\text{Diagram 3} \right] = \mathfrak{q}^{k-\ell/N} \left[\text{Diagram 4} \right] + \mathfrak{q}^{-1} \left[\text{Diagram 5} \right] + \mathfrak{q} \left[\text{Diagram 6} \right] \quad (5.4.20)$$

where

- the first term corresponds to $D_{[(\omega_\ell + \omega_1, 2h_{j_{s=1}} + \sum_{s=2}^k h_{j_s})]}$ where $j_s > \ell$,
- the second one to $D_{[(\omega_{\ell+1}, h_{i(\leq \ell+1)} + 2h_{j_{s=1}} + \sum_{s=2}^{k-1} h_{j_s})]}$ where $j_s > \ell + 1$,
- the third one to $D_{[(\omega_\ell + \omega_1, h_{(1 < i) (\leq \ell)} + \sum_{s=1}^k h_{j_s})]}$ where $j_s > \ell$.

Here we require j_s differ for each s . It would be interesting to apply the diagrammatic approach to more complicated OPEs and read off the charge information from networks in general.

5.5 General charge/network correspondence

We have seen the one-to-one mapping between the charge lattice for $\mathcal{N}=4$ $\mathfrak{su}(3)$ theory proposed by Kapustin [44] and A_2 networks on the 2-torus. Here we state the mapping

for general A_N . This is a minimal extension of a work for general A_1 class S theories [25].

⁶⁾ The generalization and refinement to general class S theories are interesting future problems. Note that the following relations can hold true in the Liouville-Toda CFTs and also that the expectation values vanish in the 2D q -deformed Yang-Mills when their electric/magnetic weights are not in the root lattices as explained in part 3 in Sec. 3.8.1.

5.5.1 Useful symbol

Here we introduce a useful symbol expressing an element of $\mathfrak{su}(N)$ Wilson-'t Hooft loop charge lattice $(\Lambda_{mw} \times \Lambda_{wt})/\mathcal{W}_{\mathfrak{su}(N)}$ where Λ_{mw} , Λ_{wt} and $\mathcal{W}_{\mathfrak{su}(N)}$ are the magnetic weight lattice, the weight lattice and the Weyl reflection group, respectively. Be aware that $\Lambda_{mw} \simeq \Lambda_{wt}$ for $\mathfrak{su}(N)$ and then we use the same basis. For a given pair of (μ, λ) , it is always possible to take μ into a dominant weight μ' using a Weyl reflection. According to this operation, λ is also mapped into an element λ' which is not always uniquely determined. There, we have a Young diagram Y_M associated with μ' . In the same way as (E.2.1), λ' can be expanded with h_s and we have unique elements λ'^s ($s = 1, 2, \dots, N$) which are non-negative integers. By putting λ'^s boxes in the s -th row in the similar way as the ordinary Young diagrams, we have a diagram referred to as Y_E . Now, we make a new diagram which is a pair of the horizontally flipped and filled Y_M and the diagram Y_E . See Fig. 5.15 below for examples.

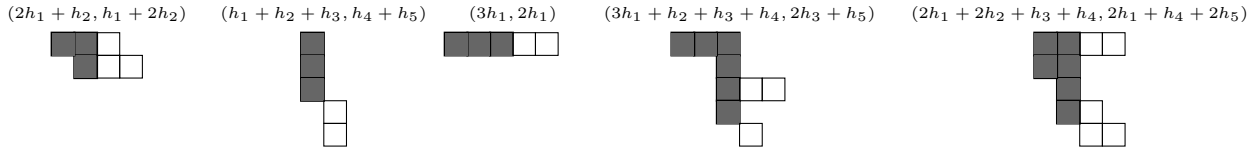


Figure 5.15: Several examples for the relation between an element of the $\mathfrak{su}(N)$ charge lattice (above) and its diagrammatic symbol (below).

5.5.2 Charge to network

For a given charge pair (μ, λ) , let M_i be subsets of $1, 2, \dots, N$ so that there is a box in Y_M specified by i -th column and a -th row only if $a \in M_i$. By replacing Y_M by Y_E , we also define E_i in the same way. Then, define s^{pq} as the number of elements of $M_p \cap E_q$

⁶⁾Here we consider $\mathcal{N}=4$ SYM as the very special case of class S theories. The similar relations are expected to hold true in the $\mathcal{N}=2^*$ gauge theory but precise dictionaries are not established completely because there appears a flavor symmetry related to the hypermultiplet mass term.

and $Q_{(s)}^{pq}$ as an open network like

$$Q_{(s)}^{pq} \longleftrightarrow \text{network} \quad (5.5.1)$$

By using these, the BPS Wilson-'t Hooft line operator in $\mathcal{N}=4$ $SU(N)$ SYM is geometrically represented by

$$\text{parallelogram} \quad (5.5.2)$$

where edges are connected on any adjacent parallelograms and each pair of opposite edges is identified. Note also that this relation holds up to lower charges (see the beginning of Sec.4 in [75]). We show two examples.

$$\text{Young diagrams} \longleftrightarrow \text{networks} \quad (5.5.3)$$

The reversed operation can be done by computing the trace functions associated with the network because the trace function is a polynomial (allowing negative powers) of two $U(1)^N/U(1)$ fugacities along α -cycle and β -cycle of the 2-torus.

Chapter 6

Conclusion : summary and discussions

In this dissertation, we focus on the defects and class S theories.

Since defects naturally appear in the brane systems in string theories, the study of defects expected to offer some clues to understand the properties in the presence of several different type defects and then their dynamics hopefully. The defects are also important in the sense that they provide the refinement checks of dualities in field theories and some information on the spectrum, for example. For these two motivations, we focus on a certain class of 4D supersymmetric gauge theories. In the recent developments, many $\mathcal{N}=2$ SCFTs are constructed from the 6D $\mathcal{N}=2$ SCFTs with several codimension two defects. They are called class S theories and closely related to M5-brane systems. We do not directly answer the first motivation but we believe that our works such as discoveries of the new kinds of the skein relations are useful to understand this, in particular, the composite systems of M5-branes and M2-branes. On the other hand, in this set-up, we give some answers to the questions arising from the second motivation because the Schur indices with line defects give such checks and information. Before remarking this point, let us see the methods we have adopted.

The class S theories are originally obtained from a special but interesting 6D theory closely related to the string theory. Although their field theoretical treatments are far from clear yet because of the lack of Lagrangians, we can describe BPS sectors of them geometrically once we admit the 4D/2D duality relations. Additions of several defects are interesting problems and, in fact, their developments have revealed the properties of (BPS) defects themselves and supported the 4D/2D duality relations. However, as for the correspondence between 4D BPS loop/line operators and 2D some topological network defects, there are only a few works before our developments. Therefore, we have two natural questions arise here as explained in the introduction.

- In general, QFTs allow the existence of defects but how can we characterize them ?
In particular, how can we study the defects in the Lagrangian unknown theories ?
- If they are defined once, how can we compute the spectrum ?

We believe that our works [75, 90] shed new light on these subjects, at least, the geometrical descriptions and the computation of class S Schur indices with any closed 6D codimension four defects. This approach gives a partial answer that we characterize the line defects in the class S theories as the networks on C with the (class S) skein relations identifications. We identify the class S skein relations with the skein relations already known in the mathematics context as we do several consistency checks in the Lagrangian theories. Since the skein relations are local relations on C , they are independent of the existence of Lagrangians in 4D and we can apply them to the general class S theories, almost all of which are Lagrangian unknown theories. The only problem left is to determine all the skein relations but this partial analysis is still enough to see non-trivial results as shown through this dissertation. We also answer the second questions by proposing the computation formula via the above 4D/2D duality relations. Finally, this helps us to find new kinds of the skein relations in the sense that they include the codimension two defects.

Now, go back to the motivations. Since the codimension two defects come from the M5-branes and the networks from the M2-branes, the new skein relations are expected to be the relations between M5-branes and M2-branes. Although we cannot translate these relations to the string theory language at this stage actually, we may give some hints for the dynamics of the M5-M2 brane systems. As for the roles as dualities checks and spectrum information, we have good answers. Indeed, our works support the 4D-2D duality relations and some dualities between 4D SCFTs and allow us to see the BPS local operators coupled to some non-trivial line operators defined by the 2D networks. The new questions to answer in the future are whether these spectra have some universal properties beyond class S theories, to what extent we can reproduce in the 4D theory framework and how we can relate them to the first motivation, namely, the string language.

Achievements Now, the main achievements in this thesis are summarized as follows.

- Developments of class S skein relations and the charge/network correspondence in the 4D/2D duality relations (4.2,5.3,5.4,5.5)
- Discussions of composite surface-line defects in the context of the Schur indices and their geometrical counterparts, what we call, Wilson punctured network defects in the 2D q -deformed Yang-Mills theory (4.3,4.4)
- Proposal of conjectural formula for the Wilson punctured network defects and its non-trivial consistency checks (4.5,5.1,App.E)
- Discovery of new kinds of skein relations (5.2)

The first work discusses the relation between the “charge” of 4D BPS loop operators and their network realizations on the punctured Riemann surfaces with skein relations. For 4D $\mathcal{N}=4$ super Yang-Mills where some Lagrangian exists, we establish the correspondence dictionary for leading charges of 4D Wilson-’t Hooft loop operators. The second work is new in the context of the 4D/2D duality relations and unify both loop and surface

defects in term of the 6D SCFTs Such networks are geometrically knots with junctions in the three dimensional space which includes C and one of 4D directions and expected to be the counterparts of composite surface-line systems in 4D. The third work is the proposal of totally new formula although there is no derivation and many evidences are given in the final work. This allows us to compute the Schur indices in the presence of 4D BPS loop operators specified by networks on C . It seems to be strange because there is no definition of charges for loop operators but instead they are defined by the geometry on 2D side. However, even in the absence of defects, we cannot define the 4D theory in their own framework and we believe that these developments will sometimes help us to understand the 4D SCFTs themselves.

Future perspective Now, we list several problems to be solved in future. Related to the first work, the comparison with some localization computations including the precise study of “dyon” bubbling are very important. This will helps us establish more general dictionary of the charge/network correspondence. Another interesting problems are relations with 4D loop operators defined in the IR [64, 151, 187]. In our framework, we see the loop operators at UV superconformal point before the relevant perturbations. Of course, they are related via RG flows and it is believed there is a correspondence between two [188]. For a given network (a UV loop operator), the construction of this RG flow map to the IR loops is needed because we know the effective Lagrangian there.

As for the second work, they also need other approaches. In the gauge theory perspectives, it is necessary to discuss the 4D descriptions of the composite surface-line systems and compare the SCIs with the expectation values. The 4D line operators are bounded to the surface operators and expected to be some interfaces including 2D Wilson lines of the two dimensional $\mathcal{N}=(2, 2)$ gauged linear sigma models [189–191]. Although we do not discuss the detail in this thesis, the extension to another 4D/2D relation called AGT correspondence [17, 38] is possible and we can formally check the above conjecture in special case. However, the general discussion is still far from clear. On the other hand, since the three geometry is encoded in 5D space, it is possible to describe them based on 5D SYM language like [129]. It is also interesting to relate them to the well-known 3D-3D correspondence story [47, 170] where the 3D $\mathcal{N}=2$ gauge theories on S^3 and complex Chern-Simons theories on hyperbolic spaces are related. More additions of defects in this correspondence were also discussed in [192], for example.

The last two works have many unsolved problems. The derivation of the conjectural formula in the framework of 2D q -deformed Yang-Mills theory (there is no derivation even at $q = 1$) and their relations to other integrable systems [193], the extensions to general open networks [87] which are composite systems of codimension two and four defects, the reproductions in the higher dimensional gauge theory like [74, 129] for example, the analysis of large N limit [194] and relations to higher Teichmüller space structure [62], spectral networks [195] or Liouville-Toda analysis [196, 197].

All the above works should be generalized to other simple Lie algebras (simply-laced in the context of class S), in particular D -series [198, 199] or in the presence of twisted lines in A_{2N-1} -series [121]. Finally, we hope that these works would help us understand

the string dynamics, in particular, some new brane dynamics.

Acknowledgements The author would like to gratefully thank the collaborator of the first work, Yuji Tachikawa (Kavli iPMU) for many discussions on the class S subjects and defects. He would like to thank his supervisor Kentaro Hori for two and four dimensional supersymmetric theories and brane constructions, Masahito Yamazaki, Kazuya Yonekura, Dongmin Gang and Takuya Okuda for various discussions related to these subjects. He also wishes to thank all the colleague at IPMU including the former people. He is also motivated by the members at Perimeter Institute. The author is supported by the Advanced Leading Graduate Course for Photon Science, one of the Program for Leading Graduate Schools lead by Japan Society for the Promotion of Science, MEXT and also the World Premier International Research Center Initiative (WPI), Kavli IPMU, the University of Tokyo.

Appendix A

Lie algebra convention

- $\Pi(R)$: weights of the representation R
- $\Delta_{\mathfrak{g}}$: the set of roots other than 0
- $\Delta_{\mathfrak{g}}^+$: the set of positive roots
- $\mathcal{P}(\mathfrak{g})$: the set of dominant weights
- ρ : Weyl vector = $\sum_{a=1}^{\text{rk}\mathfrak{g}} \omega_a = \frac{1}{2} \sum_{\alpha \in \Delta_{\mathfrak{g}}^+} \alpha$

$R(\lambda)$ denotes the irreducible representation associated with a dominant weight λ , λ_R does the dominant weight to R conversely.

A.1 A-type Lie algebra convention

In this thesis, for many reasons, we use several conventions on representations. To express the $\mathfrak{su}(N)$ irreducible representation, for example, we use the Young diagram $\wedge^k \square$ or (1^k) , the Dynkin weights (labels) $[0, \dots, \underset{k}{1}, \dots, 0]$ or $(0 \cdots 0 \underset{k}{1} 0 \cdots 0)$, weight vector ω_k and the dimension $\wedge^k \mathbf{N}$. If necessary, we refer to the convention in the beginnings of several (sub)sections again.

Basis of weights systems

Let $\{\alpha_a\}_{a=1,2,\dots,\text{rk}\mathfrak{g}=N-1}$ be a set of chosen positive simple roots. Notice all choices are equivalent under the Weyl reflection actions.

ω_α for $\alpha = 1, 2, \dots, N-1$ are fundamental weights, h_i for $i = 1, 2, \dots, N$ are weights in $\Pi(R(\omega_1) = \square)$ ¹⁾ and there are relations among them as $h_a = \omega_a - \omega_{a-1}$ where $\omega_N = \omega_0 = 0$

¹⁾The perfect order of the indices of h_i is determined by the partial order in the weight lattice.

and $\alpha_a = e_a - e_{a+1}$. We also use the standard metric in weight vectors determined by $h_i = e_i - \frac{1}{N} \sum_{i=1}^N e_i$ and $(e_i, e_j) = \delta_{i,j}$.

The coefficients for some basis are

$$\lambda_a := (\lambda, \alpha_a) \quad \lambda^a := (\lambda, \omega_a) \quad \tilde{\lambda} := \lambda + \rho \quad (\text{A.1.1})$$

and, in addition to them, we define

$$\lambda_{\underline{i}} := (\lambda, h_i) \quad \lambda_{\widehat{i}} := \lambda_{\underline{i}} - \lambda_{\underline{N}} \quad (\text{A.1.2})$$

which satisfy

$$\sum_{i=1}^N \lambda_{\underline{i}} = 0. \quad (\text{A.1.3})$$

Notice that $\lambda_{\widehat{i}}$ represents the number of the boxes in the i -th row of the corresponding Young tableau.

Of course, among the above coefficients, there are relations. Since $\alpha_a = h_a - h_{a+1}$,

$$\lambda_a = \lambda_{\widehat{a}} - \lambda_{\widehat{a+1}}. \quad (\text{A.1.4})$$

Conversely,

$$\lambda_{\underline{i}} = \sum_{a=i}^{N-1} \lambda_a - \frac{1}{N} \sum_{a=1}^{N-1} a \lambda_a \quad \lambda_{\widehat{i}} = \sum_{a=i}^{N-1} \lambda_a \quad (\text{A.1.5})$$

$$\lambda_{\underline{i}} = \lambda_{\widehat{i}} - \frac{1}{N} \sum_{k=1}^{N-1} \lambda_{\widehat{k}} \quad (\text{A.1.6})$$

$$\lambda = \sum_{i=1}^{N-1} \lambda_{\widehat{i}} h_i = \sum_{i=1}^N \lambda_{\underline{i}} h_i = \sum_{a=1}^{N-1} \lambda_a \omega_a \quad (\text{A.1.7})$$

We have the vector representation of weights, for example,

$$\lambda = (\lambda_{\underline{1}}, \lambda_{\underline{2}}, \dots, \lambda_{\underline{N}}) \quad (\text{A.1.8})$$

Notice other useful relations:

$$(h_i)_{\underline{k}} = (h_i, h_k) = \delta_{ik} - \frac{1}{N} \quad (\text{A.1.9})$$

$$(\lambda, \mu) = \sum_{i=1}^N \lambda_{\underline{i}} \mu_{\underline{i}} = \sum_{i=1}^N (\lambda, h_i) (h_i, \mu) \quad (\text{A.1.10})$$

$$(\lambda, \mu) = \sum_{a=1}^{N-1} (\lambda, \omega_a) \mu_a = \sum_{a=1}^{N-1} \lambda^a \mu_a \quad (\text{A.1.11})$$

$$\lambda^a = \sum_{i=1}^a \lambda_{\underline{i}}. \quad (\text{A.1.12})$$

Formulae

$$\mathrm{Tr}_R [T^a T^b] = T(R) \delta^{ab} \quad (\text{A.1.13})$$

$$\sum_{a=1}^{\dim \mathfrak{g}} (\rho_R(T^a))^2 = C_2(R) \mathbf{I}_R \quad (\text{A.1.14})$$

where this is the relation on the representation space of R .

There is a relation between two like

$$T(R) = \frac{\dim R}{\dim \mathfrak{g}} C_2(R) \quad (\text{A.1.15})$$

$$C_2(R) = (\lambda_R, \lambda_R + 2\rho) \quad (\text{A.1.16})$$

where λ_R is the dominant weight of R .

The dimension of $R(\lambda)$ is given by

$$\dim R = \prod_{\alpha \in \Delta_{\mathfrak{g}}^+} \frac{(\lambda_R + \rho, \alpha)}{(\rho, \alpha)}. \quad (\text{A.1.17})$$

See Appendix. E as for quantum dimension.

$$C_2(\wedge^k \square) = \left(1 + \frac{1}{N}\right) k(N - k) \quad (\text{A.1.18})$$

$$T(\wedge^k \square) = \binom{N - 2}{k - 1} \quad (\text{A.1.19})$$

A.2 $\mathfrak{so}(8)$ convention

fundamental weights

$$\omega_1 = e_1 \quad \omega_2 = e_1 + e_2 \quad \omega_3 = \frac{1}{2}(e_1 + e_2 + e_3 - e_4) \quad \omega_4 = \frac{1}{2}(e_1 + e_2 + e_3 + e_4) \quad (\text{A.2.1})$$

positive simple roots

$$\alpha_1 = e_1 - e_2 \quad \alpha_2 = e_2 - e_3 \quad \alpha_3 = e_3 - e_4 \quad \alpha_4 = e_3 + e_4 \quad (\text{A.2.2})$$

The $\mathfrak{so}(8)$ fugacity is assigned by $e_i \rightarrow X_i$.

We have another fugacities (a, b, c, d) :

$$X_1 = ab \quad X_2 = a/b \quad X_3 = cd \quad X_4 = c/d \quad (\text{A.2.3})$$

and their relations to fundamental weights are

$$a \longleftrightarrow \frac{1}{2}(e_1 + e_2) = \frac{1}{2}\omega_2 \quad b \longleftrightarrow \frac{1}{2}(e_1 - e_2) = \omega_1 - \frac{1}{2}\omega_2 \quad (\text{A.2.4})$$

$$c \longleftrightarrow \frac{1}{2}(e_3 + e_4) = \omega_4 - \frac{1}{2}\omega_2 \quad d \longleftrightarrow \frac{1}{2}(e_3 - e_4) = \omega_3 - \frac{1}{2}\omega_2. \quad (\text{A.2.5})$$

The triality which is the outermorphism of $\mathfrak{so}(8)$ is realized as

$$\begin{aligned} a \longleftrightarrow b : \omega_2 &\longrightarrow 2\omega_1 - \omega_2 & (\text{A.2.6}) \\ b \longleftrightarrow c : \omega_1 &\longleftrightarrow \omega_4 \\ c \longleftrightarrow d : \omega_3 &\longleftrightarrow \omega_4 \\ b \longleftrightarrow d : \omega_1 &\longleftrightarrow \omega_3 \end{aligned}$$

fundamental representations

$$\mathbf{8}_v \longleftrightarrow [1000] = \omega_1 \quad \mathbf{8}_c \longleftrightarrow [0010] = \omega_3 \quad \mathbf{8}_s \longleftrightarrow [0001] = \omega_4 \quad (\text{A.2.7})$$

and

$$\text{Adj} = \mathbf{28} = \wedge^2 \mathbf{8}_v \longleftrightarrow [0100] = \omega_2 \quad (\text{A.2.8})$$

branching rules For the decomposition $\mathfrak{so}(8) \rightarrow \mathfrak{su}(2)_A \oplus \mathfrak{su}(2)_B \oplus \mathfrak{su}(2)_C \oplus \mathfrak{su}(2)_D$,

$$\mathbf{8}_v = (\mathbf{2}_A \otimes \mathbf{2}_B) \oplus (\mathbf{2}_C \otimes \mathbf{2}_D) \quad (\text{A.2.9})$$

$$\mathbf{8}_s = (\mathbf{2}_A \otimes \mathbf{2}_C) \oplus (\mathbf{2}_B \otimes \mathbf{2}_D) \quad (\text{A.2.10})$$

$$\mathbf{8}_c = (\mathbf{2}_A \otimes \mathbf{2}_D) \oplus (\mathbf{2}_B \otimes \mathbf{2}_C) \quad (\text{A.2.11})$$

$$(\text{A.2.12})$$

and

$$\text{Adj} = \mathbf{28} = (\mathbf{2}_A \otimes \mathbf{2}_B \otimes \mathbf{2}_C \otimes \mathbf{2}_D) \oplus \mathbf{3}_A \oplus \mathbf{3}_B \oplus \mathbf{3}_C \oplus \mathbf{3}_D \quad (\text{A.2.13})$$

in the character sense.

For higher irreducible representations,

$$\begin{aligned} [0, 1, 0, 0] : \mathbf{28} &= (\mathbf{2}, \mathbf{2}, \mathbf{2}, \mathbf{2}) \oplus (\mathbf{3}, \mathbf{1}, \mathbf{1}, \mathbf{1}) \oplus (\mathbf{1}, \mathbf{3}, \mathbf{1}, \mathbf{1}) \oplus (\mathbf{1}, \mathbf{1}, \mathbf{3}, \mathbf{1}) \oplus (\mathbf{1}, \mathbf{1}, \mathbf{1}, \mathbf{3}) \\ [2, 0, 0, 0] : \mathbf{35}_v &= \mathbf{1} \oplus (\mathbf{2}, \mathbf{2}, \mathbf{2}, \mathbf{2}) \oplus (\mathbf{3}, \mathbf{3}, \mathbf{1}, \mathbf{1}) \oplus (\mathbf{1}, \mathbf{1}, \mathbf{3}, \mathbf{3}) \\ [0, 0, 1, 1] : \mathbf{56}_v &= (\mathbf{3}, \mathbf{1}, \mathbf{2}, \mathbf{2}) \oplus (\mathbf{1}, \mathbf{3}, \mathbf{2}, \mathbf{2}) \oplus (\mathbf{2}, \mathbf{2}, \mathbf{3}, \mathbf{1}) \oplus (\mathbf{2}, \mathbf{2}, \mathbf{1}, \mathbf{3}) \oplus \mathbf{8}_v \\ [1, 1, 0, 0] : \mathbf{160}_v &= \mathbf{56}_v \oplus (\mathbf{2}, \mathbf{4}, \mathbf{1}, \mathbf{1}) \oplus (\mathbf{4}, \mathbf{2}, \mathbf{1}, \mathbf{1}) \oplus (\mathbf{1}, \mathbf{1}, \mathbf{2}, \mathbf{4}) \oplus (\mathbf{1}, \mathbf{1}, \mathbf{4}, \mathbf{2}) \oplus \\ &\quad (\mathbf{3}, \mathbf{3}, \mathbf{2}, \mathbf{2}) \oplus (\mathbf{2}, \mathbf{2}, \mathbf{3}, \mathbf{3}). \end{aligned} \quad (\text{A.2.14})$$

We introduce a symbol like $\chi(R_A, R_B, R_C, R_D) := \chi_{R_A}^{SU(2)}(a)\chi_{R_B}^{SU(2)}(b)\chi_{R_C}^{SU(2)}(c)\chi_{R_D}^{SU(2)}(d)$.

A.3 $\mathfrak{so}(4)$ convention : the four vector and spinors

Pauli matrices

$$\sigma_x = \begin{pmatrix} 0 & 1 \\ 1 & 0 \end{pmatrix} \quad \sigma_y = \begin{pmatrix} 0 & -i \\ i & 0 \end{pmatrix} \quad \sigma_z = \begin{pmatrix} 1 & 0 \\ 0 & -1 \end{pmatrix} \quad (\text{A.3.1})$$

$$\sigma_+ = \begin{pmatrix} 0 & 1 \\ 0 & 0 \end{pmatrix} \quad \sigma_- = \begin{pmatrix} 0 & 1 \\ 0 & 0 \end{pmatrix} \quad (\text{A.3.2})$$

and

$$(\sigma_E^\mu)^{\alpha\dot{\beta}} = (i\sigma^{x,y,z}, 1) \quad (\text{A.3.3})$$

where μ runs over 1, 2, 3, 4.

Using this, we can identify the four vector and bi-spinor as

$$P^{\alpha\dot{\beta}} = \frac{1}{2} P_\mu (\sigma_E^\mu)^{\alpha\dot{\beta}} = \frac{1}{2} \times \begin{array}{c} \alpha \setminus \dot{\beta} \\ + \quad \dot{+} \quad \dot{-} \\ - \quad \left(\begin{array}{cc} P_4 + iP_3 & iP_1 + P_2 \\ iP_1 - P_2 & P_4 - iP_3 \end{array} \right) \end{array}. \quad (\text{A.3.4})$$

Appendix B

Superconformal algebra

The relevant superconformal algebras in this thesis $\mathfrak{su}(2, 2|2)$. However, if we have defects, they are replaced by its subalgebras. The relation to the convention used in superalgebra literatures are following : $\mathfrak{su}(m+1|n+1) = A(m, n)$ for $m \neq n$ and $\mathfrak{psu}(n+1|n+1) = A(n, n)$. See [200] on Lie superalgebra.

Super Lie algebra

The super Lie algebras \mathfrak{g} are \mathbb{Z}_2 -graded algebra with the supercommutator denoted by $[\]$ defined just later. First of all, the \mathbb{Z}_2 -grading means that each algebra is the direct sum of two algebras as the vector spaces like $\mathfrak{g} = \mathfrak{g}^B \oplus \mathfrak{g}^F$. In particular, we introduce the grading operator $(-1)^F$ called the Fermion number such that $(-1)^F \cdot \mathfrak{g}^B = \mathfrak{g}^B$ and $(-1)^F \cdot \mathfrak{g}^F = -\mathfrak{g}^F$. Here, we can define the supercommutator as follows:

$$[X, Y] := XY - (-1)^F YX(-1)^F = \begin{cases} \{X, Y\} = XY + YX & \text{for } X, Y \in \mathfrak{g}^F \\ [X, Y] = XY - YX & \text{otherwise.} \end{cases} \quad (\text{B.0.1})$$

This supercommutator must satisfy the super Jacobi identity

$$\text{Ad}_{[X, Y]}(Z) = [\text{Ad}_X, \text{Ad}_Y](Z) \quad (\text{B.0.2})$$

where $\text{Ad}_X(Y) := [X, Y]$ which defines \mathfrak{g} action itself.

B.1 4D SCA

First of all, let us consider 4D $\mathcal{N} = m$ superconformal algebra $A(3, m-1)$. Their fermion part consists of eight superPoincaré charges denoted by \mathcal{Q} and eight superconformal charges denoted by \mathcal{S} which are conjugate each other in the radial time sense. Here we follow the convention in [31] mainly. ¹⁾

¹⁾There is a bit difference between the literature and this thesis (or recent literatures in class S theories) on the r -charge normalization. It is $r = r_{\text{here}} = \frac{1}{m} r_{\text{there}}$. This corresponds to the fact $U(m) \simeq (SU(m) \times U(1))/\mathbb{Z}_m \neq SU(m) \times U(1)$.

4D $\mathcal{N}=m$ supercharges \mathcal{Q} and \mathcal{S} belong to the representation $(\mathbf{4}, \overline{\mathcal{N}}) \oplus (\overline{\mathbf{4}}, \mathcal{N})$ of $\mathfrak{su}(4) \oplus \mathfrak{u}(\mathcal{N})$ ²⁾ where we used analytic continuation of the conformal algebra $\mathfrak{su}(4) \sim \mathfrak{so}(5, 1)$. However, instead of the full conformal group, we use the subalgebra $\mathfrak{su}(2)_1 \oplus \mathfrak{su}(2)_2 \oplus \mathfrak{so}(1, 1)$.

Hereafter, we take a basis of the representation vector space and give their indices as follows. α, β, \dots run over $+, -$ which are indices for $\mathfrak{su}(2)_1$, $\dot{\alpha}, \dot{\beta}, \dots$ over $\dot{+}, \dot{-}$ for $\mathfrak{su}(2)_2$ and A, B, \dots over $1, 2, \dots, m$ for $\mathfrak{su}(m)_R$. For the Abelian symmetry group $\mathfrak{so}(1, 1)$ and $\mathfrak{su}(1)_r$, we abbreviate them because their irreducible representations are always one-dimensional. Now, let us see the supercommutation relations below.

$$\mathfrak{sc}^B = \{\mathfrak{sc}^F, \mathfrak{sc}^F\}$$

The non-trivial anti-commutators are given as follows:

$$\{\mathcal{Q}^{\alpha A}, \tilde{\mathcal{Q}}_B^{\dot{\beta}}\} = P^{\alpha\dot{\beta}} \otimes \delta_B^A \quad (\text{B.1.1})$$

$$\{\mathcal{S}_{\alpha A}, \tilde{\mathcal{S}}_B^{\dot{\beta}}\} = K_{\alpha\dot{\beta}} \otimes \delta_A^B \quad (\text{B.1.2})$$

$$\{\mathcal{Q}^{\alpha A}, \mathcal{S}_{\beta B}\} = (J_1)_{\beta}^{\alpha} \otimes \delta_B^A - \delta_{\beta}^{\alpha} \otimes R_B^A + \left(\frac{D}{2} - \frac{4-m}{4}r\right) \delta_{\beta}^{\alpha} \otimes \delta_B^A \quad (\text{B.1.3})$$

$$\{\tilde{\mathcal{Q}}_A^{\dot{\alpha}}, \tilde{\mathcal{S}}_B^{\dot{\beta}}\} = (J_2)_{\dot{\beta}}^{\dot{\alpha}} \otimes \delta_A^B + \delta_{\dot{\beta}}^{\dot{\alpha}} \otimes R_A^B + \left(\frac{D}{2} + \frac{4-m}{4}r\right) \delta_{\dot{\beta}}^{\dot{\alpha}} \otimes \delta_A^B \quad (\text{B.1.4})$$

where other relations are anti-commuting.³⁾

$$\mathfrak{sc}^F = [\mathfrak{sc}^B, \mathfrak{sc}^F]$$

These commutation relations are encoded in the supercharges representations (or indices) of bosonic symmetry. See the Table. B.1.

	$\mathfrak{su}(2)_1$	$\mathfrak{su}(2)_2$	$\mathfrak{so}(1, 1)_D$	$\mathfrak{su}(m)_R$	$\mathfrak{u}(1)_r$
\mathcal{Q}	$\mathbf{2}$	$\mathbf{1}$	$\frac{1}{2}$	\mathbf{m}	$\frac{1}{m}$
\mathcal{S}	$\overline{\mathbf{2}} \simeq \mathbf{2}$	$\mathbf{1}$	$-\frac{1}{2}$	$\overline{\mathbf{m}}$	$-\frac{1}{m}$
$\tilde{\mathcal{Q}}$	$\mathbf{1}$	$\mathbf{2}$	$\frac{1}{2}$	$\overline{\mathbf{m}}$	$-\frac{1}{m}$
$\tilde{\mathcal{S}}$	$\mathbf{1}$	$\overline{\mathbf{2}} \simeq \mathbf{2}$	$-\frac{1}{2}$	\mathbf{m}	$\frac{1}{m}$

Table B.1: The representations of supercharges.

²⁾Hereafter, we sometimes identify the algebra and its universal covering Lie group. In addition, for the bosonic symmetry algebra $\mathfrak{g}_1 \oplus \mathfrak{g}_2$, we also use the abbreviate notation (R_1, R_2) for $R_1 \otimes_{\mathbb{C}} R_2$. The corresponding Lie group denotes $G_1 \times G_2$. The same notation is used for the case that more simple algebras are directly summed.

³⁾There is possibility that the "central charge" usually denoted by Z can appear in the anti-commutators $\{\mathcal{Q}, \mathcal{Q}\}$ and so on when $m = 2$. However, this does not commute with D and if a state has a non-zero eigenvalue, it breaks the scale symmetry.

If we introduce $\hat{R}_B^A := R_B^A + r$, they are the natural generators of $\mathfrak{u}(m)_R$ and satisfy

$$[\hat{R}_B^A, \mathcal{Q}^C / \mathcal{S}^C] = \delta_B^C \mathcal{Q}^A / \mathcal{S}^A \quad [\hat{R}_B^A, \tilde{\mathcal{Q}}_C / \tilde{\mathcal{S}}_C] = -\delta_B^C \tilde{\mathcal{Q}}_A / \tilde{\mathcal{S}}_A \quad (\text{B.1.5})$$

There are other generators in $\mathfrak{so}(5, 1)$ not in the $\mathfrak{so}(4) \oplus \mathfrak{so}(1, 1)$: $P_{\alpha\dot{\beta}}$ and $K_{\alpha\dot{\beta}}$.

Roughly speaking, by ignoring the $\mathfrak{so}(4)$ spinor indices, P and K acts on $\begin{pmatrix} \mathcal{Q} \\ \tilde{\mathcal{S}} \end{pmatrix}$ and $\begin{pmatrix} \tilde{\mathcal{Q}} \\ \mathcal{S} \end{pmatrix}$ as raising and lowering operators respectively. Precisely, we fix the numerical factors as follows. ⁴⁾

$$[P^{\alpha\dot{\alpha}}, \tilde{\mathcal{S}}_{\dot{\beta}}^A] = -\delta_{\dot{\beta}}^{\dot{\alpha}} \mathcal{Q}^{\alpha A} \quad [K_{\alpha\dot{\alpha}}, \mathcal{Q}^{\beta A}] = \delta_{\dot{\alpha}}^{\beta} \tilde{\mathcal{S}}_{\dot{\alpha}}^A \quad (\text{B.1.6})$$

$$[P^{\alpha\dot{\alpha}}, \mathcal{S}_{\beta A}] = -\delta_{\beta}^{\alpha} \tilde{\mathcal{Q}}_{\dot{\alpha}}^A \quad [K_{\alpha\dot{\alpha}}, \tilde{\mathcal{Q}}_{\dot{\alpha}}^{\beta}] = \delta_{\dot{\alpha}}^{\beta} \mathcal{S}_{\alpha A} \quad (\text{B.1.7})$$

$$\mathfrak{sc}^B = [\mathfrak{sc}^B, \mathfrak{sc}^B]$$

$$[(J_1)_{\beta}^{\alpha}, P^{\gamma\dot{\delta}}] = \delta_{\beta}^{\gamma} P^{\alpha\dot{\delta}} - \frac{1}{2} \delta_{\beta}^{\alpha} P^{\gamma\dot{\delta}} \quad (\text{B.1.8})$$

$$[(J_1)_{\beta}^{\alpha}, K_{\gamma\dot{\delta}}] = -\delta_{\gamma}^{\alpha} K_{\beta\dot{\delta}} + \frac{1}{2} \delta_{\beta}^{\alpha} K_{\gamma\dot{\delta}} \quad (\text{B.1.9})$$

$$[(J_2)_{\dot{\beta}}^{\dot{\alpha}}, P^{\gamma\dot{\delta}}] = \delta_{\dot{\beta}}^{\dot{\alpha}} P^{\gamma\dot{\delta}} - \frac{1}{2} \delta_{\dot{\beta}}^{\dot{\alpha}} P^{\gamma\dot{\delta}} \quad (\text{B.1.10})$$

$$[(J_2)_{\dot{\beta}}^{\dot{\alpha}}, K_{\gamma\dot{\delta}}] = -\delta_{\dot{\delta}}^{\dot{\alpha}} K_{\gamma\dot{\beta}} + \frac{1}{2} \delta_{\dot{\beta}}^{\dot{\alpha}} K_{\gamma\dot{\delta}} \quad (\text{B.1.11})$$

where $(J_i)_{\beta}^{\alpha} \in \mathfrak{su}(2)_i$ ($i = 1, 2$). In particular, we use

$$(J_i)_{\beta}^{\alpha} = \begin{pmatrix} (J_i)^z & (J_i)^+ \\ (J_i)^- & -(J_i)^z \end{pmatrix} = \begin{pmatrix} \frac{1}{2}\sigma^z & \sigma^+ \\ \sigma^- & -\frac{1}{2}\sigma^z \end{pmatrix} \quad (\text{B.1.12})$$

where the last expression means the matrix representation acting on $\begin{pmatrix} \mathcal{Q}^{+A} \\ \mathcal{Q}^{-A} \end{pmatrix}$ for $i = 1$

or $\begin{pmatrix} \tilde{\mathcal{Q}}_A^+ \\ \tilde{\mathcal{Q}}_A^- \end{pmatrix}$ for $i = 2$.

The other non-trivial relations are

$$[D, P^{\alpha\dot{\beta}}] = P^{\alpha\dot{\beta}} \quad [D, K_{\alpha\dot{\beta}}] = -K_{\alpha\dot{\beta}} \quad (\text{B.1.13})$$

$$[K_{\alpha\dot{\alpha}}, P^{\beta\dot{\beta}}] = \delta_{\dot{\alpha}}^{\dot{\beta}} (J_1)_{\alpha}^{\beta} + \delta_{\alpha}^{\beta} (J_2)_{\dot{\alpha}}^{\dot{\beta}} + \delta_{\alpha}^{\beta} \delta_{\dot{\alpha}}^{\dot{\beta}} D. \quad (\text{B.1.14})$$

These form the algebra $\mathfrak{so}(1, 5)$.

⁴⁾There may be some mistakes in Appendix A.1 in [31]. We use the oscillator construction in Appendix A.2 there.

BPZ conjugation

When an operator quantization is given after fixing the time direction and the associated Killing vector identified with a Hamiltonian, there is a conjugation operation defined as

$$|\text{out}\rangle \otimes X|\text{in}\rangle \simeq X^\dagger|\text{out}\rangle \otimes |\text{in}\rangle \longrightarrow \langle \text{out}|X|\text{in}\rangle. \quad (\text{B.1.15})$$

Unless we mention otherwise, we use the symbol \dagger for the radian quantization sense, sometimes called "BPZ" conjugation [201]. This corresponds to the inversion operation and \dagger^2 is just the identity operation, that is to say, the involution. We require that this \dagger operation is closed in the symmetry algebra.

In particular, \dagger acts on P, K as K, P respectively and on the other bosonic generators D, J_i, r trivially. For the fermionic generator,

$$(\mathcal{Q}^{\alpha A})^\dagger = \mathcal{S}_{\alpha A} \quad (\tilde{\mathcal{Q}}_{\dot{\alpha} A})^\dagger = \tilde{\mathcal{S}}_{\dot{\alpha} A}. \quad (\text{B.1.16})$$

B.1.1 4D $\mathcal{N}=2$ superconformal algebra

Hereafter, we focus on the 4D $\mathcal{N}=2$ superconformal algebra, namely, $m = 2$.

We fix the $SU(2)_i$ invariant tensors for the fundamental representation as

$$\epsilon^{+-} = -\epsilon^{-+} = \epsilon_{-+} = -\epsilon_{+-} = +1 \quad (\text{B.1.17})$$

for $i = 1$. The $i = 2$ case is obtained by $+, - \implies \dot{+}, \dot{-}$. Notice that $SU(4)$ invariant tensor are given by δ_B^A .

Now, we use the supercharge basis as $\mathcal{Q}_{\alpha A} := \epsilon_{\alpha\beta}\epsilon_{AB}\mathcal{Q}^{\beta B}$ and $\tilde{\mathcal{Q}}_{\dot{\alpha} A} := \epsilon_{\dot{\alpha}\dot{\beta}}\tilde{\mathcal{Q}}_{\dot{A}}^{\dot{\beta}}$ and they satisfy

$$(\mathcal{Q}_{\alpha A})^\dagger = \mathcal{S}^{\alpha A} \quad (\tilde{\mathcal{Q}}_{\dot{\alpha} A})^\dagger = -\tilde{\mathcal{S}}^{\dot{\alpha} A}. \quad (\text{B.1.18})$$

Here notice that $(\epsilon_{\alpha\beta})^\dagger = \epsilon^{\beta\alpha} = \epsilon_{\alpha\beta}$ and that we use the same invariant tensor for $SU(2)_R$ symmetry as $SU(2)_i$ symmetry.

Δ and r are same and the others are defined as ⁵⁾

$$j_i := -(J_i)^z \quad \text{for } i = 1, 2 \quad I := -R^z = -R_1^1 = R_2^2 \quad (\text{B.1.19})$$

Now let us list the charges, namely, the weight of the Cartan subalgebra $\mathfrak{so}(1, 1)_D \oplus \mathfrak{u}(1)_1 \oplus \mathfrak{u}(1)_2 \oplus \mathfrak{u}(1)_R \oplus \mathfrak{u}(1)_r$.

Using the anticommutator (B.1.3) and (B.1.4), we can compute

$$\{\mathcal{Q}_{\alpha A}, (\mathcal{Q}_{\beta B})^\dagger\} = [-\epsilon_{\alpha\gamma}\epsilon^{\beta\delta}(J_1)_{\delta}^{\gamma}] \delta_A^B + [\epsilon_{AC}\epsilon^{BD}(R)_D^C] \delta_{\alpha}^{\beta} + \frac{1}{2}(D - r)\delta_{\alpha}^{\beta}\delta_A^B \quad (\text{B.1.20})$$

$$\{\tilde{\mathcal{Q}}_{\dot{\alpha} A}, (\tilde{\mathcal{Q}}_{\dot{\beta} B})^\dagger\} = [-\epsilon_{\dot{\alpha}\dot{\gamma}}\epsilon^{\dot{\beta}\dot{\delta}}(J_2)_{\dot{\delta}}^{\dot{\gamma}}] \delta_A^B + (R)_A^B \delta_{\dot{\alpha}}^{\dot{\beta}} + \frac{1}{2}(D + r)\delta_{\dot{\alpha}}^{\dot{\beta}}\delta_A^B \quad (\text{B.1.21})$$

⁵⁾The minus sign before $(J_i)^z$ or R^z is convenient because the lowering $SU(2)$ indices by the ϵ tensor exchanges $+, \dot{+}$ and $-, \dot{-}$.

and the special case $\alpha = \beta$ and $A = B$ give

$$2\{\mathcal{Q}_{\alpha A}, (\mathcal{Q}_{\alpha A})^\dagger\} = 2\eta_\alpha j_1 - 2\eta_A I + D - r \quad (\text{B.1.22})$$

$$2\{\tilde{\mathcal{Q}}_{\dot{\alpha} A}, (\tilde{\mathcal{Q}}_{\dot{\beta} B})^\dagger\} = 2\eta_{\dot{\alpha}} j_2 - 2\eta_A I + D + r \quad (\text{B.1.23})$$

where $\eta_\pm = \pm, \eta_{\dot{\pm}} = \pm$. $\eta_1 = +1$ and $\eta_2 = -1$. See Table. B.2.

	Δ	j_1	j_2	I	r	$2\{\mathcal{Q}, \mathcal{Q}^\dagger\}$
$\mathcal{Q}_{\pm 1}$	$\frac{1}{2}$	$\pm\frac{1}{2}$	0	$\frac{1}{2}$	$\frac{1}{2}$	$\Delta \pm 2j_1 - 2I - r$
$\mathcal{Q}_{\pm 2}$	$\frac{1}{2}$	$\pm\frac{1}{2}$	0	$-\frac{1}{2}$	$\frac{1}{2}$	$\Delta \pm 2j_1 + 2I - r$
$\tilde{\mathcal{Q}}_{\pm 1}$	$\frac{1}{2}$	0	$\pm\frac{1}{2}$	$\frac{1}{2}$	$-\frac{1}{2}$	$\Delta \pm 2j_2 - 2I + r$
$\tilde{\mathcal{Q}}_{\pm 2}$	$\frac{1}{2}$	0	$\pm\frac{1}{2}$	$-\frac{1}{2}$	$-\frac{1}{2}$	$\Delta \pm 2j_2 + 2I + r$

Table B.2: Each charge associated to superPoincaré charges and their anticommutators.

The other relations are almost same to the original ones. For example, we have

$$\{\mathcal{Q}_{\alpha A}, \tilde{\mathcal{Q}}_{\dot{\beta} B}\} = P_{\alpha\dot{\beta}} \epsilon_{AB}. \quad (\text{B.1.24})$$

Now, following the discussion in Sec. 3.2, let us consider supercharges anticommuting with $\mathcal{Q} := \tilde{\mathcal{Q}}_{-1} = \tilde{\mathcal{Q}}_1^+$. The answer is

$$\mathcal{Q}^{\pm 2}, \tilde{\mathcal{Q}}_{\dot{A}}^{\dot{\pm}}, \mathcal{S}_{\alpha A}, \tilde{\mathcal{S}}_{-}^2. \quad (\text{B.1.25})$$

On the other hand, the supercharges anticommuting with $\mathcal{S} := \tilde{\mathcal{S}}_+^1 = -\tilde{\mathcal{S}}^{-1} (= \mathcal{Q}^\dagger)$ are

$$\mathcal{Q}^{\alpha A}, \tilde{\mathcal{Q}}_2^{\dot{-}}, \mathcal{S}_{\pm 2}, \tilde{\mathcal{S}}_{\dot{\alpha}}^A. \quad (\text{B.1.26})$$

Therefore, the supercharges anticommuting with both \mathcal{Q} and \mathcal{S} are following six supercharges (3 superPoincaré and 3 superconformal) :

$$\mathcal{Q}^{\pm 2} = \mp \mathcal{Q}_{\mp 1}, \quad \tilde{\mathcal{Q}}_2^{\dot{-}} = -\tilde{\mathcal{Q}}_{+2}, \quad \mathcal{S}_{\pm 2}, \quad \tilde{\mathcal{S}}_{-}^2 \quad (\text{B.1.27})$$

B.1.2 Differential operator representation of bosonic generators

In our convention, (x^1, x^2, x^3, x^4) is the natural global coordinate on the flat Euclidean space \mathbb{R}^4 . It has a complex structure induced by $z := x^1 + ix^2$ and $w := x^3 + ix^4$, that is to say, $\partial_{x^1} = \partial_1 = \partial_z + \bar{\partial}_z$ and $\partial_{x^2} = \partial_2 = i(\partial_z - \bar{\partial}_z)$ (same for $\partial_{3,4}$).

By recalling the relation

$$[j_1, P^{\pm\dot{\delta}}] = \mp \frac{1}{2} P^{\pm\dot{\delta}} \quad [j_2, P^{\gamma\pm}] = \mp \frac{1}{2} P^{\gamma\pm} \quad (\text{B.1.28})$$

$$[j_1, K_{\pm\dot{\delta}}] = \pm \frac{1}{2} K_{\pm\dot{\delta}} \quad [j_2, K_{\gamma\pm}] = \pm \frac{1}{2} K_{\gamma\pm}, \quad (\text{B.1.29})$$

we can express j_i , P , K and D as

$$j_1 + j_2 = L_{34} = w\partial_w - \bar{w}\bar{\partial}_w \quad j_1 - j_2 = L_{12} = z\partial_z - \bar{z}\bar{\partial}_z, \quad (\text{B.1.30})$$

$$P^{+\dot{+}} = \frac{1}{2}(P_4 + iP_3) = \partial_w \quad P^{-\dot{-}} = \frac{1}{2}(P_4 - iP_3) = -\bar{\partial}_w \quad (\text{B.1.31})$$

$$P^{+\dot{-}} = \frac{1}{2}(iP_1 + P_2) = \partial_z \quad P^{-\dot{+}} = \frac{1}{2}(iP_1 - P_2) = \bar{\partial}_z, \quad (\text{B.1.32})$$

$$K_{+\dot{+}} = K^{-\dot{-}} = \frac{1}{2}(K_4 - iK_3) = w^2\partial_w + w(z\partial_z + \bar{z}\bar{\partial}_z) - |z|^2\bar{\partial}_w \quad (\text{B.1.33})$$

$$K_{-\dot{-}} = K^{+\dot{+}} = \frac{1}{2}(K_4 + iK_3) = -[\bar{w}^2\bar{\partial}_w + \bar{w}(z\partial_z + \bar{z}\bar{\partial}_z) - |z|^2\partial_w] \quad (\text{B.1.34})$$

$$K_{+\dot{-}} = -K^{-\dot{+}} = \frac{1}{2}(K_2 - iK_1) = z^2\partial_z + z(w\partial_w + \bar{w}\bar{\partial}_w) - |w|^2\bar{\partial}_z \quad (\text{B.1.35})$$

$$K_{-\dot{+}} = -K^{+\dot{-}} = \frac{1}{2}(-K_2 - iK_1) = \bar{z}^2\bar{\partial}_z + \bar{z}(w\partial_w + \bar{w}\bar{\partial}_w) - |w|^2\partial_z \quad (\text{B.1.36})$$

and

$$D = -x^\mu\partial_\mu = -z\partial_z - \bar{z}\bar{\partial}_z - w\partial_w - \bar{w}\bar{\partial}_w. \quad (\text{B.1.37})$$

Notice that $j_1 + j_2$ rotates the w -plane and $j_1 - j_2$ does the z -plane.

$$\partial_{-\dot{+}} = -\partial^{+\dot{-}} = -i\partial_z \quad \partial_{+\dot{+}} = \partial^{-\dot{-}} = -i\bar{\partial}_w \quad (\text{B.1.38})$$

$$\partial_{-\dot{-}} = \partial^{+\dot{+}} = i\partial_w \quad \partial_{+\dot{-}} = -\partial^{-\dot{+}} = -i\bar{\partial}_z \quad (\text{B.1.39})$$

	∂_z	$\bar{\partial}_z$	∂_w	$\bar{\partial}_w$
j_1	$-\frac{1}{2}$	$\frac{1}{2}$	$-\frac{1}{2}$	$\frac{1}{2}$
j_2	$\frac{1}{2}$	$-\frac{1}{2}$	$-\frac{1}{2}$	$\frac{1}{2}$
Δ	1	1	1	1
$D - 2j_2$	0	2	2	0
$j_2 - j_1$	1	-1	0	0
$j_2 + j_1$	0	0	-1	1

Table B.3: The charges for the derivatives.

Since the index contributions come from the derivatives satisfying $D = 2j_2 + 2I - r = 2j_2$, only ∂_z and $\bar{\partial}_w$ contribute to the single letters as p and q respectively.

B.1.3 line defects insertion

Let us consider a line operator located on a straight line defined by

$$\arg(z) = \varphi = \text{const.} \quad \text{mod } \pi \quad \text{and } w = 0 \quad (\text{B.1.40})$$

in the z -plane. There, $j_1 + j_2$ is the symmetry but $j_1 - j_2$ is not because it rotates the line operators.⁶⁾

The translations P and the special conformal transformations K are also broken except the two generators

$$P_\varphi := \frac{1}{i} [e^{i\varphi} \partial_z + e^{-i\varphi} \bar{\partial}_z] = \frac{1}{i} [e^{i\varphi} P^{+\dot{+}} + e^{-i\varphi} P^{-\dot{+}}] \quad (\text{B.1.41})$$

$$K_\varphi := i [e^{-i\varphi} K_{+\dot{+}} + e^{i\varphi} K_{-\dot{+}}] \quad (\text{B.1.42})$$

and they generates $\mathfrak{sl}(2, \mathbb{R})$ algebra :

$$[K_\varphi, P_\varphi] = 2D \quad [D, P_\varphi] = P_\varphi \quad [D, K_\varphi] = -K_\varphi \quad (\text{B.1.43})$$

where we have used the relations

$$[K_{\pm\dot{\mp}}, P^{\mp\dot{\pm}}] = 0 \quad (\text{B.1.44})$$

$$[K_{\pm\dot{\mp}}, P^{\pm\dot{\mp}}] = D \mp (j_1 - j_2). \quad (\text{B.1.45})$$

Since these generators, $j_1 + j_2, R$ and r commutes with each other, the bosonic symmetry is at most

$$\mathfrak{sl}(2, \mathbb{R}) \oplus \mathfrak{so}(2)_w \oplus \mathfrak{su}(m)_R \oplus \mathfrak{u}(1)_r. \quad (\text{B.1.46})$$

Now let us focus on the odd part of algebras. If we assume that there exists some degrees of freedom living on the line defect, they might be supersymmetric. In other words, there are some supercharges generates P_φ and K_φ .⁷⁾ For example,

$$iP_\varphi = e^{i\varphi} P^{+\dot{+}} + e^{-i\varphi} P^{-\dot{+}} = e^{i\varphi} \{Q^{+A}, \tilde{Q}_A^-\} + e^{-i\varphi} \{Q^{-B}, \tilde{Q}_B^+\} \quad (\text{B.1.47})$$

where both A and B are free, that is to say, not summed up over $1, 2, \dots, m$. The anti-commuting properties

$$\{Q^{+A}, Q^{-B}\} = \{\tilde{Q}_A^+, \tilde{Q}_B^-\} = 0 \quad (\text{B.1.48})$$

⁶⁾This is called a “full line defect” in [151]. There are also a “half-line defect” case ($\arg(z) = \varphi \text{ mod } 2\pi$) and “multiple half-line defects” case. In the later two case, the unbroken symmetries are subgroups of the first one which we do not discuss in detail. The Schur indices can be defined for any case without any differences.

⁷⁾We also implicitly assume that the $\dot{}$ operation exists, namely, the radial time reversal operation $\tau \rightarrow -\tau$ acts on the symmetry in the closed form.

implies a natural decomposition of P_φ like

$$iP_\varphi = \{Q^{+A} + e^{-i\varphi}\tilde{Q}_B^+, Q^{-B} + e^{i\varphi}\tilde{Q}_A^-\}. \quad (\text{B.1.49})$$

By introducing the new supercharges

$$\mathcal{W}_\varphi^{\pm\langle AB \rangle} := Q^{\pm A} + e^{\mp i\varphi}\tilde{Q}_B^\pm \quad (\text{B.1.50})$$

and

$$(\mathcal{W}_\varphi^{\pm\langle AB \rangle})^\dagger = \mathcal{S}_{\pm A} + e^{\pm i\varphi}\tilde{\mathcal{S}}_\pm^B, \quad (\text{B.1.51})$$

we have the following relations :

$$\{\mathcal{W}_\varphi^{\pm\langle AB \rangle}, \mathcal{W}_\varphi^{\pm\langle CD \rangle}\} = e^{\mp i\varphi}P^{\pm\pm}\delta_B^C + e^{\mp i\varphi}P^{\pm\pm}\delta_D^A \quad (\text{B.1.52})$$

$$\{(\mathcal{W}_\varphi^{\pm\langle AB \rangle})^\dagger, (\mathcal{W}_\varphi^{\pm\langle CD \rangle})^\dagger\} = e^{\pm i\varphi}K_{\pm\pm}\delta_C^B + e^{\pm i\varphi}K_{\pm\pm}\delta_A^D \quad (\text{B.1.53})$$

$$\begin{aligned} \{\mathcal{W}_\varphi^{\pm\langle AB \rangle}, (\mathcal{W}_\varphi^{\pm\langle CD \rangle})^\dagger\} &= (J_1)_\pm^\pm\delta_C^A + e^{\mp i\varphi}(J_2)_\pm^\pm\delta_B^D \\ &+ \delta_\pm^\pm[-R_C^A + e^{\mp i\varphi}R_B^D] + \left(\frac{D}{2} - \frac{4-m}{4}r\right)\delta_\pm^\pm\delta_C^A + e^{\mp i\varphi}\left(\frac{D}{2} + \frac{4-m}{4}r\right)\delta_\pm^\pm\delta_B^D \end{aligned} \quad (\text{B.1.54})$$

Now let us construct a super subalgebra including the subalgebra generated by P_φ, K_φ, D and $j_1 + j_2$. For that purpose, it is natural to choose the following four supercharges

$$\mathcal{W} := \mathcal{W}_\varphi^{+\langle AB \rangle} \quad \tilde{\mathcal{W}} := \mathcal{W}_\varphi^{-\langle BA \rangle} \quad (\text{B.1.55})$$

$$\mathcal{V} := (\mathcal{W}_\varphi^{+\langle AB \rangle})^\dagger \quad \tilde{\mathcal{V}} := (\mathcal{W}_\varphi^{-\langle BA \rangle})^\dagger \quad (\text{B.1.56})$$

and their anti-commutators are given as

$$\{\mathcal{W}, \mathcal{W}\} = 2e^{-i\varphi}\delta_B^A P^{+\dot{+}} \quad \{\tilde{\mathcal{W}}, \tilde{\mathcal{W}}\} = 2e^{i\varphi}\delta_A^B P^{-\dot{-}} \quad (\text{B.1.57})$$

$$\{\mathcal{V}, \mathcal{V}\} = 2e^{i\varphi}\delta_A^B K_{+\dot{+}} \quad \{\tilde{\mathcal{V}}, \tilde{\mathcal{V}}\} = 2e^{-i\varphi}\delta_B^A K_{-\dot{-}} \quad (\text{B.1.58})$$

$$\{\mathcal{W}, \tilde{\mathcal{W}}\} = iP_\varphi \quad \{\mathcal{V}, \tilde{\mathcal{W}}\} = -iK_\varphi \quad (\text{B.1.59})$$

$$\{\mathcal{W}, \mathcal{V}\} = D - R^{\langle AB \rangle} - (j_1 + j_2) \quad \{\tilde{\mathcal{W}}, \tilde{\mathcal{V}}\} = D + R^{\langle AB \rangle} + (j_1 + j_2) \quad (\text{B.1.60})$$

$$\{\mathcal{W}, \tilde{\mathcal{V}}\} = \delta_B^A \left[(J_1)_-^+ + e^{-2i\varphi}(J_2)_-^+ \right] \quad \{\mathcal{V}, \tilde{\mathcal{W}}\} = \delta_B^A \left[(J_1)_+^- + e^{2i\varphi}(J_2)_+^- \right]. \quad (\text{B.1.61})$$

where $R^{\langle AB \rangle} := R_A^A - R_B^B$.

Since $P^{\pm\pm}, P_{\pm\pm}, (J_1)^\pm$ or $(J_2)^\pm$ themselves are not symmetry of the line defect inserted systems, we must require $A \neq B$. This is only possible $m > 1$ at least and we consider only the cases $m = 2, 3, 4$ hereafter.

Finally, let us analysis the R -symmetry actions. First of all, the definition of the above supercharges implies that $\mathfrak{u}(1)_r$ symmetry is completely broken for $m = 2, 3$. For the non-Abelian R -symmetry, since \mathcal{Q} and $\tilde{\mathcal{Q}}$ belong to the different R -symmetry representations

\mathbf{m} and $\overline{\mathbf{m}}$ respectively and $\mathcal{W}, \widetilde{\mathcal{W}}, \mathcal{V}$ and $\widetilde{\mathcal{V}}$ depends on A and B , it seems to be completely broken too. However, in the case of $m = 2$, the full R -symmetry $SU(2)_R$ is unbroken because of $\mathbf{2} \simeq \overline{\mathbf{2}}$, in other words, the existence of the invariant tensor ϵ_{AB} . In the similar way, in the $m = 3$ cases, R -symmetry is not completely broken but broken into the $SU(2)$ -symmetry acting on the index A and B . Furthermore, in the case of $m = 4$, the $SU(2)$ -symmetry is left and, indeed, there remains $SO(5) \sim Sp(2)$ -symmetry.

Notice also that all the supercharges commute with $j_1 + j_2$ but do not commute with $j_1 - j_2$. This means that the $\mathfrak{u}(1)$ -symmetry generated by $j_1 + j_2$ is the global symmetry for the degrees of freedom living on the line defects.

For example, we have

$$[R_B^A - R_D^C, \mathcal{Q}^{\alpha E}] = \delta_B^E \mathcal{Q}^{\alpha A} - \delta_D^E \mathcal{Q}^{\alpha C} - \frac{1}{m} \delta_B^A \mathcal{Q}^{\alpha E} + \frac{1}{m} \delta_D^C \mathcal{Q}^{\alpha E} \quad (\text{B.1.62})$$

and, in the special case,

$$[R^{(AB)}, \mathcal{Q}^{\alpha C}] = (\delta_A^C - \delta_B^C) \mathcal{Q}^{\alpha C}. \quad (\text{B.1.63})$$

By using the similar relation for $\widetilde{\mathcal{Q}}, \mathcal{S}, \widetilde{\mathcal{S}}$, the R -symmetry generators act on the supercharges as

$$[R^{(AB)}, \mathcal{W}] = \mathcal{W} \quad [R^{(AB)}, \widetilde{\mathcal{W}}] = -\widetilde{\mathcal{W}} \quad (\text{B.1.64})$$

$$[R^{(AB)}, \mathcal{V}] = -\mathcal{V} \quad [R^{(AB)}, \widetilde{\mathcal{V}}] = \widetilde{\mathcal{V}}. \quad (\text{B.1.65})$$

In summary, we have $\mathfrak{su}(1, 1|1)$ symmetry:

$$\{\mathcal{W}, \widetilde{\mathcal{W}}\} = iP \quad \{\mathcal{V}, \widetilde{\mathcal{W}}\} = -iK \quad \{\mathcal{W}, \mathcal{V}\} = D - Y \quad \{\widetilde{\mathcal{W}}, \widetilde{\mathcal{V}}\} = D + Y \quad (\text{B.1.66})$$

$$\{\mathcal{W}, \widetilde{\mathcal{V}}\} = 0 \quad \{\mathcal{V}, \widetilde{\mathcal{W}}\} = 0 \quad (\text{B.1.67})$$

$$[P, K] = 2D \quad [D, P] = P \quad [D, K] = -K \quad (\text{B.1.68})$$

$$[K, Y] = [P, Y] = [D, Y] = 0 \quad (\text{B.1.69})$$

$$[D, \mathcal{W}] = \frac{1}{2} \mathcal{W} \quad [D, \mathcal{V}] = -\frac{1}{2} \mathcal{V} \quad [D, \widetilde{\mathcal{W}}] = \frac{1}{2} \widetilde{\mathcal{W}} \quad [D, \widetilde{\mathcal{V}}] = -\frac{1}{2} \widetilde{\mathcal{V}} \quad (\text{B.1.70})$$

$$[Y, \mathcal{W}] = \frac{1}{2} \mathcal{W} \quad [Y, \mathcal{V}] = -\frac{1}{2} \mathcal{V} \quad [Y, \widetilde{\mathcal{W}}] = \frac{1}{2} \widetilde{\mathcal{W}} \quad [Y, \widetilde{\mathcal{V}}] = -\frac{1}{2} \widetilde{\mathcal{V}} \quad (\text{B.1.71})$$

where we redefine the generator $Y := R^{(AB)} + (j_1 + j_2)$.

Notice that Y is quantized, that is to say, the R -symmetry group is $U(1)_{\frac{1}{Y}}^{(\frac{1}{2})}$.

In the $m = 2$ case (4D $\mathcal{N}=2$ SCA), we can choose $A = 2$ and $B = 1$ without the loss of generality. In this case, $Y = R^{(12)} + j_1 + j_2 = j_1 + j_2 + 2I$.

Surface defects insertion

Next, we discuss the surface defects. There are two kinds of maximal BPS flat surface defects

$$\Sigma_q = \{z \in \mathbb{C}, w = 0\} \quad \Sigma_p = \{w \in \mathbb{C}, z = 0\}. \quad (\text{B.1.72})$$

Notice that Σ_q and Σ_p are flipped by $j_1 \rightarrow -j_1$ or the exchange $+ \longleftrightarrow -$.

Without loss of generality, we can focus on Σ_q . The locus of this surface defect break the full conformal symmetry into $SO(3, 1) \times SO(2)_{j_1+j_2}$. $P^{\pm\pm}, K_{\pm\pm}$ and $(J_{1,2})_{\mp}$ are broken generators.

Let us assume that $\tilde{Q}_A^{\dot{\alpha}}$ is the unbroken supersymmetry charge. Since the above generators should not appear in the unbroken symmetry algebra, the following four supercharges are forbidden.

$$Q^{\alpha A}, \quad \tilde{S}_{\dot{\beta}}^A, \quad \mathcal{S}_{\alpha A}, \quad \tilde{Q}_A^{\dot{\beta}} \quad (\text{B.1.73})$$

where $\alpha \neq \beta$. The other fermionic generators $Q^{\beta A}$ and $\mathcal{S}_{\beta A}$ generates $P^{\beta\dot{\alpha}}$ and $K_{\beta\dot{\alpha}}$ which can be the symmetry of the surface defects.

Then, the minimal subalgebra is

$$\mathfrak{su}(1|1)_{2;\dot{\alpha}A} := \tilde{Q}_A^{\dot{\alpha}} \oplus \tilde{S}_{\dot{\alpha}}^A \oplus \tilde{\delta}_A^{\dot{\alpha}} (= D_+ + 2R_A^A + 2(J_2)_{\dot{\alpha}}^{\dot{\alpha}}) \quad (\text{B.1.74})$$

or

$$\mathfrak{su}(1|1)_{1;\beta A} := Q^{\beta A} \oplus \mathcal{S}_{\beta A} \oplus \delta_A^{A\dot{\alpha}} (= D_- - 2R_A^A + 2(J_1)_{\beta}^{\beta}). \quad (\text{B.1.75})$$

The next minimal superalgebra including the above two superalgebras is given as

$$\mathfrak{su}(1|1)_{1;\beta A} \oplus \mathfrak{su}(1|1)_{2;\dot{\alpha}A} \oplus P^{\beta\dot{\alpha}} \oplus K_{\beta\dot{\alpha}} \quad (\text{B.1.76})$$

where $\alpha \neq \beta$ is still assumed. However, this is not physically natural because P^{-+} or K_{-+} itself are not the Hermite operator in the ordinary quantization where P^0 is the Hamiltonian. Requiring the condition that the algebra is invariant both under the Hermite conjugate and under BPZ conjugate, the above algebra is modified as

$$\mathfrak{s}(2D \mathcal{N}=1; \alpha A) := \mathfrak{su}(1|1)_{1;\beta A} \oplus \mathfrak{su}(1|1)_{2;\dot{\alpha}A} \oplus P^{\beta\dot{\alpha}} \oplus K_{\beta\dot{\alpha}} \oplus P^{\alpha\dot{\beta}} \oplus K_{\alpha\dot{\beta}} \oplus (j_1 - j_2). \quad (\text{B.1.77})$$

This algebra is indeed closed because $P^{\alpha\dot{\beta}}$ and $K_{\alpha\dot{\beta}}$ commute with all the supercharges and $[K_{\alpha\dot{\beta}}, P^{\alpha\dot{\beta}}] = D - \eta_{\alpha}(j_1 - j_2)$. Notice that $M = j_1 - j_2$ and $Y_A := \frac{1}{2}r - \eta_A I$ acts on $\mathfrak{s}(2D \mathcal{N}=1; \alpha A)^F$ as constants $-\eta_{\alpha}$ and η_A , respectively. By this construction, this algebra is not simple because there is non-trivial ideal B.1.76 in it.

There are two possibility for further extension to have 4+4 supercharges in total. One is made of $\mathfrak{s}(2D \mathcal{N}=1; \alpha A)$ and $\mathfrak{s}(2D \mathcal{N}=1; \beta B)$ and the other of $\mathfrak{s}(2D \mathcal{N}=1; \alpha A)$ and $\mathfrak{s}(2D \mathcal{N}=1; \alpha B)$.

Here we can set $A = 1$ and $\alpha = -$ without loss of generality.

$\mathcal{N}=(2, 2)$ SCA

The superPoincaré charges are given by

$$Q_{+,1} := Q^{-1}, Q_{-,1} := Q^{+2}, Q_{+,2} := \tilde{Q}_1^+, Q_{-,2} = \tilde{Q}_2^- \quad (\text{B.1.78})$$

and the bosonic part is given by

$$\mathfrak{so}(1, 3) \oplus r_L \oplus r_R \quad (\text{B.1.79})$$

where $\mathfrak{so}(1, 3)$ is the 2D conformal algebra and there are also the $U(1) \times U(1)$ R-symmetry $r_L := r + (j_1 + j_2 + 2I)$ and $r_R := r - (j_1 + j_2 + 2I)$. The bosonic charges for supercharges are given by

$$[M, Q_{\alpha,A}] = \frac{1}{2}\eta_\alpha Q_{\alpha,A} \quad (\text{B.1.80})$$

$$[r_{L/R}, Q_{\alpha,A}] = (+; L/-; R)Q_{\alpha,A}. \quad (\text{B.1.81})$$

Therefore, the bosonic algebra includes the Cartan subalgebra \mathfrak{h} of \mathfrak{g} for 4D $\mathcal{N}=2$ SCA and we can define the full SCIs, which has three non-flavor fugacities.

If we take the SCI supercharge as $\mathcal{Q} = Q_{+,2}$, $Q_{-,1}$ and $Q_{-,2}$ commute with this supercharge. The non-negativity condition of physical norms leads to $\tilde{Y}_1 \geq 0$ and $\tilde{Y}_3 \geq 0$. However, we have missed the constraint $j_1 + j_2 \geq r$. Intuitively speaking, this is because the surface defects, sometimes constructed as the IR defects of vortex strings, generate the angular momentum around $w = 0$ which can arbitrarily decrease $j_1 + j_2$.

$\mathcal{N}=(0, 4)$ SCA

The superPoincaré charges are given by

$$Q_{+,+} := \mathcal{Q}^{-2}, Q_{+,-} := \tilde{\mathcal{Q}}_1^+, Q_{-,+} := \mathcal{Q}^{-1}, Q_{-,-} = \tilde{\mathcal{Q}}_2^+ \quad (\text{B.1.82})$$

and the bosonic part is given by

$$\mathfrak{so}(1, 3) \oplus \mathfrak{su}(2)_R \oplus \mathfrak{u}(1)_{r'} \quad (\text{B.1.83})$$

where $r' = r - j_1 - j_2$. Here we only see the subalgebra of full $SO(4)$ R-symmetry. The bosonic charges for supercharges are given by

$$[M, Q_{A,B}] = \frac{1}{2}Q_{A,B} \quad (\text{B.1.84})$$

$$[I, Q_{A,B}] = \frac{1}{2}\eta_A Q_{A,B} \quad (\text{B.1.85})$$

$$[r - j_1 - j_2, Q_{A,B}] = \frac{1}{2}\eta_B Q_{A,B}. \quad (\text{B.1.86})$$

In this case, we also have three bosonic generators commuting with \mathcal{Q} and can define the full SCIs too.

However, the unitarity bound changes. There is only $Q_{+,+}$ anti-commuting with \mathcal{Q} . $\delta(Q_{+,+})_{\delta(\mathcal{Q})=0} = j_1 + j_2 - r \geq 0$ which is opposite condition to the previous $\mathcal{N}=(2, 2)$ case.

Appendix C

Formulae for SCI

In this Appendix, we list several definitions and formulae necessary to compute the SCIs.

C.1 Symbols used in SCI

$$f(x^\pm) := f(x)f(x^{-1}) \quad (\text{C.1.1})$$

$$f(x^\lambda) := \prod_{w \in \Pi(R(\lambda))} f(x^w) \quad (\text{C.1.2})$$

where λ is the highest weight. When $\mathfrak{g} = \mathfrak{su}(N)$,

$$x^w := \prod_{i=1}^N x_i^{w_i} = \prod_{i=1}^N x_i^{w_i} \quad (\text{C.1.3})$$

where we used the fact that $w_i - w_i$ is independent of i .

Definition

$$(a; q)_n := \prod_{k=0}^{n-1} (1 - aq^k) \quad \text{q-Pochhammer symbol} \quad (\text{C.1.4})$$

$$(a; q) := (a; q)_\infty \quad (\text{C.1.5})$$

$$\theta(z; q) := (z; q)(q/z; q) = \prod_{n=0}^{\infty} (1 - q^n z)(1 - q^{n+1}/z) \quad \text{for } |q| < 1 \quad \text{q-theta function} \quad (\text{C.1.6})$$

$$\Gamma(z; p, q) := \prod_{j, k \geq 0} \frac{1 - z^{-1} p^{j+1} q^{k+1}}{1 - z p^j q^k} \quad \text{for } |p|, |q| < 1 \quad \text{elliptic } \Gamma \text{ function} \quad (\text{C.1.7})$$

Useful formulae

$$(qz; q) = (1 - z)^{-1}(z; q) \quad (C.1.8)$$

$$\theta(qz; q) = \frac{-1}{z}\theta(z; q) \quad \theta(q/z; q) = \theta(z; q) = (-z)\theta(1/z; q) \quad \theta(\sqrt{q}z^{-1}; q) = \theta(\sqrt{q}z; q) \quad (C.1.9)$$

$$\Gamma(z; p, q) = \Gamma(z; q, p) \quad \Gamma(z; p, q)\Gamma(pq/z; p, q) = 1 \quad (C.1.10)$$

$$\Gamma(p; p, q) = \frac{(q; q)}{(p; p)} = \Gamma(q; p, q)^{-1} \quad (C.1.11)$$

$$\Gamma(pz; p, q) = (z; q)(z^{-1}q; q)\Gamma(z; p, q) = \theta(z; q)\Gamma(z; p, q) \quad (C.1.12)$$

$$\Gamma(qz; p, q) = (z; p)(z^{-1}p; p)\Gamma(z; p, q) = \theta(z; p)\Gamma(z; p, q) \quad (C.1.13)$$

$$\theta(z; q)\Gamma(z; p, q)\Gamma(q/z; p, q) = \theta(z; q)\theta(z^{-1}; p)\Gamma(z^\pm; p, q) = 1 \quad (C.1.14)$$

$$\Gamma(\sqrt{q}z^\pm; p, q) = \frac{1}{\theta(\sqrt{q}z; q)} = \frac{1}{(\sqrt{q}z^\pm; q)} \quad (C.1.15)$$

$$\theta(z^\pm; q) = (1 - z)^{-1}(1 - z^{-1})^{-1}(z^\pm; q)^2 = (1 - z)(1 - z^{-1})(qz^\pm; q) \quad (C.1.16)$$

In particular,

$$\frac{1}{\Gamma(x^\pm)} = \frac{(x^\pm; p)_\infty (x^\pm; q)_\infty}{(1 - x)(1 - x^{-1})} \quad (C.1.17)$$

In the limitation,

$$\lim_{z \rightarrow 1} (1 - z)\Gamma(z; p, q) = \frac{1}{(p; p)(q; q)} \quad (C.1.18)$$

$$\theta(z; 0) = 1 - z \quad (C.1.19)$$

$$\Gamma(z; q, 0) = \Gamma(z; 0, q) = \frac{1}{(z; q)} \quad (C.1.20)$$

$\Gamma(x; p, q)$ has a P.E. expression like

$$\begin{aligned} \log(\Gamma(x; p, q)) &= \sum_{j, k \geq 0} \log(1 - z^{-1}p^{j+1}q^{k+1}) - \log(1 - zp^j q^k) \\ &= - \sum_{j, k \geq 0, m \geq 1} \frac{1}{m} [(z^{-1}p^{j+1}q^{k+1})^m - (zp^j q^k)^m] \\ &= - \sum_{m \geq 1} \frac{1}{m(1-p)(1-q)} \left[\left(\frac{pq}{z} \right)^m - z^m \right]. \end{aligned} \quad (C.1.21)$$

Derivation of vector multiplet full SCI

First of all, notice that

$$\text{P.E.} \left[\frac{2pq + \frac{pq}{t} - p - q}{(1-p)(1-q)} x \right] = \text{P.E.} \left[\frac{2(pq - 1) + (\frac{pq}{t} - t)}{(1-p)(1-q)} x + \frac{x}{1-p} + \frac{x}{1-q} \right]$$

$$= \frac{1}{\Gamma(x; p, q)^2 \Gamma(tx; p, q) (x; p) (x; q)}. \quad (\text{C.1.22})$$

By pairing the opposite charge, we have

$$\begin{aligned} \text{P.E.} \left[\frac{2pq + \frac{pq}{t} - p - q}{(1-p)(1-q)} (x + x^{-1}) \right] &= \frac{1}{\Gamma(x^\pm; p, q)^2 \Gamma(tx^\pm; p, q) (x^\pm; p) (x^\pm; q)} \\ &\stackrel{\text{(C.1.17)}}{=} \frac{1}{\overline{\Gamma(x^\pm; p, q) \Gamma(tx^\pm; p, q) (1 - x^\pm)}} \end{aligned} \quad (\text{C.1.23})$$

and we can define the $\mathcal{Z}_{\text{vector}}^{(\text{m}), \text{full}}(x)$ as

$$\frac{1}{\overline{\Gamma(x; p, q) \Gamma(tx; p, q) (1 - x)}} \quad (\text{C.1.24})$$

because there always exists the opposite charged supermultiplet.

Appendix D

Orbit of simple Lie algebra

The references of this appendix are [50, 51, 55, 94, 125, 131, 135, 202].

Lie algebra and group In this appendix, \mathfrak{g} can be any simple Lie algebra both complex or real. However, when we emphasize the field, we use the following symbols: $\mathfrak{g}_{\mathbb{C}}$ and $G_{\mathbb{C}}$ are complexified Lie group and complexified Lie algebra respectively. On the other hand, $G_{\mathbb{R}}$ and $\mathfrak{g}_{\mathbb{R}}$ are their compact real form. In particular, it is enough to consider the case

$$G_{\mathbb{C}} = SL(N, \mathbb{C}) \quad \mathfrak{g}_{\mathbb{C}} = \mathfrak{sl}(N, \mathbb{C}) \quad (\text{D.0.1})$$

$$G_{\mathbb{R}} = SU(N) \quad \mathfrak{g}_{\mathbb{R}} = \mathfrak{su}(N). \quad (\text{D.0.2})$$

Recall that any Lie algebra can be viewed as a vector space, that is to say, $\mathfrak{g} \simeq \mathbb{C}^{\dim \mathfrak{g}}$. Then, for $X, Y \in \mathfrak{g}$, we have an operator acting on \mathfrak{g} defined as $\text{Ad}_X(Y) := [X, Y]_{\mathfrak{g}}$.

The Jordan decomposition theorem says

$$\text{Ad}_X = (\text{Ad}_X)_s + (\text{Ad}_X)_n = \text{Ad}_{X_s} + \text{Ad}_{X_n} \quad (\text{D.0.3})$$

such that

$$\text{diagonalizable} \quad (\text{Ad})_s X_i = \exists \lambda_i X_i \text{ with } \mathfrak{g} \simeq \bigoplus_i \mathbb{C} X_i \quad (\text{D.0.4})$$

$$\text{(local) nilpotency} \quad \exists k \in \mathbb{N} \quad ((\text{Ad}_X)_n)^k \equiv 0 \quad (\text{D.0.5})$$

$$[(\text{Ad}_X)_s, (\text{Ad}_X)_n] \equiv 0 \quad (\text{D.0.6})$$

Correspondingly, we have the decomposition $X = X_s + X_n$ satisfying $[X_s, X_n] = 0$.

partition of N Let Y be a Young diagram with N boxes. Each is specified by a partition of N but we have two representations $[n] = [n_1, n_2, n_3, \dots, n_k]$ (counting the height of each row) and $\{s\} = \{s_1, s_2, s_3, \dots, s_r\}$ (counting the width of each line). We write this as $[n] = \{s\}$ or $\{s\} = \{n\}^t$ where t is the transpose operation for the Young diagrams. By definition,

$$N = \sum_{i=1}^k n_i = \sum_{a=1}^r s_a. \quad (\text{D.0.7})$$

We label each box in Y as $\square_{(i,a)} \in Y$ where i and a runs over the row and the line respectively. Now, there are two ways to express $\sum_{\square_{(i,a)} \in Y} i$ as follows.

$$\text{one way} := \sum_{a=1}^r \sum_{i=1}^{s_a} i = \sum_{a=1}^r \frac{1}{2} s_a (s_a + 1) = \frac{1}{2} \left(\sum_{a=1}^r s_a^2 + N \right) \quad (\text{D.0.8})$$

$$\text{the other way} := \sum_{i=1}^k \sum_{a=1}^{n_i} i = \sum_{i=1}^k i n_i \quad (\text{D.0.9})$$

and therefore we have the relation

$$\sum_{a=1}^r s_a^2 = 2 \sum_{i=1}^k i n_i - N = \sum_{i=1}^k (2i - 1) n_i. \quad (\text{D.0.10})$$

D.1 Semi-simple orbit

Every semi-simple element can be mapped into the diagonal by definition.

$$M = \text{diag}(m_1, m_2, \dots, m_N) \quad (\text{D.1.1})$$

In particular, we can introduce subsets of the elements specified by the partition of N as

$$M(\{n\}) = m_1 I_{n_1} \oplus m_2 I_{n_2} \oplus \dots \oplus m_k I_{n_k} \in \mathfrak{sl}(N, \mathbb{C}). \quad (\text{D.1.2})$$

For this element, the Levi subgroup is defined as

$$L := L(M) := \{g \in G \mid \text{Ad}_g(M) = M\} \quad (\text{D.1.3})$$

and its Lie algebra is given by

$$\mathfrak{l} = \mathfrak{l}(M) := \{X \in \mathfrak{g} \mid [X, M] = 0\} \quad (\text{D.1.4})$$

Therefore, the orbit through M is roughly given by $\mathcal{O}_M \sim G/L$. In the $\mathfrak{g} = \mathfrak{g}_{\mathbb{C}}$ case, notice that

$$\mathcal{O}_M \sim G_{\mathbb{C}}/L_{\mathbb{C}} \sim T^*(G_{\mathbb{R}}/L_{\mathbb{R}}). \quad (\text{D.1.5})$$

Since $G_{\mathbb{R}}/L_{\mathbb{R}}$ is the homogeneous Kähler manifold, $T^*(G_{\mathbb{R}}/L_{\mathbb{R}})$ is the hyper Kähler manifold.

According to [203], any compact and simply connected homogeneous Kähler manifolds are of this form. Let us compute the dimension. It is enough to analyze locally, that is to say, the tangent space (= the Lie algebra) at generic point.

$$\dim_{\mathbb{C}} \mathcal{O}_M = \dim_{\mathbb{C}} G_{\mathbb{C}} - \dim_{\mathbb{C}} L_{\mathbb{C}} \quad (\text{D.1.6})$$

and, in the special case $G = SL(N, \mathbb{C})$,

$$\dim_{\mathbb{C}} \mathcal{O}_m = N^2 - \sum_{i=1}^k n_i^2 \quad (\text{D.1.7})$$

because $\mathbb{L}_{\mathbb{C}} = S(\prod_{i=1}^k U(n_i))$.

Notice

$$G_{\mathbb{R}}/L_{\mathbb{R}} \sim G_{\mathbb{C}}/\mathcal{P} \quad \mathbb{L}_{\mathbb{R}} = G \cap \mathcal{P} \quad (\text{D.1.8})$$

where \mathcal{P} is a parabolic subgroup for $SL(N, \mathbb{C})$ whose complex dimension is given by

$$\frac{N^2 + \sum_i n_i^2}{2} - 1. \quad (\text{D.1.9})$$

D.2 Nilpotent orbit

Next, we consider the nilpotent elements. The nilpotent cone is defined by

$$\mathcal{N}_{\mathfrak{g}} = \{X \in \mathfrak{g}_{\mathbb{C}} \mid \exists k \ (\text{Ad}_X)^k = 0\} \quad (\text{D.2.1})$$

We can decompose the nilpotent cones into sum of $G_{\mathbb{C}}$ -orbits. It is known that this equivalence class $\mathcal{N}_{\mathfrak{g}}/G_{\mathbb{C}}$ is specified by the principal embedding $\rho : \mathfrak{su}(2) \mapsto \mathfrak{g}$ [135]. In particular, in the case $\mathfrak{g} = \mathfrak{su}(N)$, this is equivalent to the decomposition of the defining representation \mathbf{N} into the direct sum of the representations of $\mathfrak{su}(2)$. In other words, this set corresponds to the partition of N . Furthermore, we can take the representative element of $\mathfrak{sl}(N, \mathbb{C})$ for each nilpotent orbit as the form of the Jordan blocks :

$$J_{[n]} = \oplus_i J_{n_i} \quad (\text{D.2.2})$$

for each partition of N .

Without loss of generality, we can take $n_1 \geq n_2 \geq \dots \geq n_k$ by using some adjoint action.

For a matrix A , let us define new $n_i \times n_j$ matrix \check{A}_{ij} for each $i, j = 1, 2, \dots, k$ whose elements are given as

$$(\check{A}_{ij})_{uv} = A_{p_i+u, p_j+v} \quad \text{for } u = 1, 2, \dots, n_i \text{ and } v = 1, 2, \dots, n_j. \quad (\text{D.2.3})$$

In the same way as the semi-simple orbit, the commutant (or the stabilizer for the group action) defined as

$$\mathcal{Z}_{[n]} := \mathcal{Z}_{\mathfrak{g}}(J_{[n]}) := \{X \in \mathfrak{sl}(N, \mathbb{C}) \mid [X, J_{[n]}] = 0\} \quad (\text{D.2.4})$$

Let us analyze this Lie algebra. Introduce

$$(E_{a,b})_{uv} := \delta_{ua} \delta_{vb} \quad (\text{D.2.5})$$

where δ is the ordinary Kronecker's δ . Then,

$$\check{X}_{ij} = \sum_{a=1}^{\min(n_i, n_j)} x_a^{(ij)} \sum_{k=1}^a E_{k, k+n_j-a} \quad (\text{D.2.6})$$

where $x_a \in \mathbb{C}$. This has the constraint coming from the traceless condition, that is to say,

$$\sum_{i=1}^k n_i x_1^{(ii)} = 0. \quad (\text{D.2.7})$$

The number of $x_a^{(ij)}$ is given by

$$\sum_{i,j=1}^k \min(n_i, n_j) = \sum_i (2i-1)n_i = \sum_{a=1}^r s_a^2 \quad (\text{D.2.8})$$

where we used (D.0.10) and $\{s\} = [n]$.

Since the complex dimension of $\mathcal{Z}_{\{n\}}$ equals to the number of ‘‘independent’’ $x_a^{(ij)}$,

$$\dim_{\mathbb{C}} \mathcal{Z}_{[n]} = \sum_{a=1}^r s_a^2 - 1. \quad (\text{D.2.9})$$

Let us exhibit an example : $N = 6$ and its partition $\{3, 2, 1\}$

$$J_{\{321\}} = \left(\begin{array}{ccc|cc} 0 & 1 & 0 & & \\ 0 & 0 & 1 & O & O \\ 0 & 0 & 0 & & \\ \hline & & & 0 & 1 \\ & O & & 0 & 0 \\ \hline & & & O & 0 \end{array} \right) \quad \mathcal{Z}_{\{n\}} = \left\{ \left(\begin{array}{ccc|cc|c} x_1^{(11)} & x_2^{(11)} & x_3^{(11)} & x_1^{(12)} & x_2^{(12)} & x_1^{(13)} \\ 0 & x_1^{(11)} & x_2^{(11)} & 0 & x_1^{(12)} & 0 \\ 0 & 0 & x_1^{(11)} & 0 & 0 & 0 \\ \hline 0 & x_1^{(21)} & x_2^{(21)} & x_1^{(22)} & x_2^{(22)} & x_1^{(23)} \\ 0 & 0 & x_1^{(21)} & 0 & x_1^{(22)} & 0 \\ \hline 0 & 0 & x_1^{(31)} & 0 & x_1^{(32)} & x_1^{(33)} \end{array} \right) \right\} \quad (\text{D.2.10})$$

where $3x_1^{(11)} + 2x_1^{(22)} + x_1^{(33)} = 0$ and $\dim_{\mathbb{C}} \mathcal{Z}_{\{n\}} = 13$.

Therefore, the dimension of the nilpotent orbit is given by

$$\dim_{\mathbb{C}} \mathcal{O}_{J_{\{n\}}} = \dim_{\mathbb{C}} \mathfrak{sl}(N, \mathbb{C}) - \dim_{\mathbb{C}} \mathcal{Z}_{\{n\}} = N^2 - \sum_{a=1}^r s_a^2. \quad (\text{D.2.11})$$

D.3 Induced orbit

Comparing the above two results for the dimension, we expect

$$\mathcal{O}_{[n]}^{ss} \sim \mathcal{O}_{\{s\}}^{nil} \quad (\text{D.3.1})$$

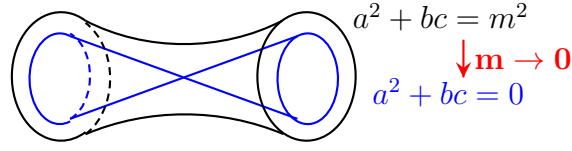


Figure D.1: The image of the principal nilpotent orbit and the semi-simple orbit approaching to it in the case $\mathfrak{sl}(2, \mathbb{C})$. The origin is smaller nilpotent orbit and some special region in the semi-simple orbit approaches to this trivial orbit as the eigenvalues vanish. The limitation and the orbiting do not commute each other.

where $[s] = [n]^t$. Naively speaking, we can expect that $\mathcal{O}_{[n]}^{ss}$ approaches to $\mathcal{O}_{\{s\}}^{nil}$ as we take the eigenvalues which specify the semi-simple orbit to zero. This is the idea of induced orbit (Richardson orbit).¹⁾

Let us consider a general element X of $\mathfrak{sl}(N, \mathbb{C})$. Then, the G -orbit through X is $\mathcal{O}_X = SL(N, \mathbb{C}) \cdot X = \text{Ad}_{SL(N, \mathbb{C})}(X)$. Now recall that the Jordan decomposition $X = X_s + X_n$. By the definition of the semi-simplicity, we can map X_s into an element $M(\{n\})$, that is to say, $X_s \in \mathcal{O}_{\{n\}}^{ss}$.

Then we have a question : When we specify the type of Levi group, namely, $\{n\}$, what is the possible choice of X_n ? For example, when X_s is a generic element of \mathfrak{g} , its commutant a maximal torus of \mathfrak{g} and its intersection with $\mathcal{N}_{\mathfrak{g}}$ is only a zero element 0. Therefore, X_n must be 0. In other words, the Levi type restrict the possible choice of the nilpotent orbit.

In fact, we can take the limit $M(\{n\}) \rightarrow 0$ and then

$$\lim_{M(\{n\}) \rightarrow 0} \mathcal{O}_{X_s + X_n} = \overline{\mathcal{O}_{J_{\{e\}}}} \quad (\text{D.3.2})$$

where the closure of a nilpotent orbit appears.²⁾

parabolic subalgebra The maximal solvable subalgebra of \mathfrak{g} is called a Borel subalgebra denoted \mathfrak{b} . There is a decomposition $\mathfrak{b} = \mathfrak{h} \oplus \mathfrak{n}$ and \mathfrak{n} is the nilradical of \mathfrak{b} and equals to $[\mathfrak{b}, \mathfrak{b}]$. \mathfrak{h} is the Cartan subalgebra of \mathfrak{g} . \mathfrak{p} is called a parabolic subalgebra of \mathfrak{g} if it contain a Borel subalgebra.

Let us construct the, For that purpose, let Θ be a subset of the set of simple roots \mathcal{S} . Then,

$$\mathfrak{p}_{\Theta} := \mathfrak{h} \oplus \sum_{\alpha \in \mathbb{Z}(\mathcal{S}, -\Theta) \cap \Delta^+} \quad \mathfrak{l}_{\Theta} := \mathfrak{h} \oplus \sum_{\alpha \in \mathbb{Z}(\Theta) \cap \Delta^+} \quad \mathfrak{n}_{\Theta} := \mathfrak{p}_{\Theta} \setminus \mathfrak{l}_{\Theta} \quad (\text{D.3.3})$$

¹⁾Originally, induced orbits are introduced to construct the nilpotent orbits not associated to semisimple orbits.

²⁾Naïvely, after taking the limit $M \rightarrow 0$, its G -orbit always remains \mathcal{O}_{X_n} . Since the order of two operations, namely, the limitation ($X_s \rightarrow 0$) and the consideration of its G -orbit do not commute, we must consider the orbit \mathcal{O}_x at first, and then taking the limit $M \rightarrow 0$.

The parabolic subalgebras are one-to-one corresponding to the power set of \mathcal{S} .

Given a parabolic subalgebra $\mathfrak{p} = \mathfrak{l} \oplus \mathfrak{n}$ and a nilpotent orbit $\mathcal{O}^{\mathfrak{l}} \in \mathcal{N}_{\mathfrak{l}}/L$ in \mathfrak{l} , there exists a nilpotent orbit \mathcal{O} such that $(\mathcal{O}_{\mathfrak{l}} + \mathfrak{n}) \cap \mathcal{O}$ is a dense set in \mathfrak{n} and \mathcal{O} is denoted as $\text{Ind}_{\mathfrak{p}}^{\mathfrak{g}}(\mathcal{O}_{\mathfrak{l}})$. This induced orbit is independent of the choice of \mathfrak{p} for fixed \mathfrak{l} . In the special case $\mathcal{O}_{\mathfrak{l}} = O$, the nilpotent orbit \mathcal{O} is called Richardson. For $\mathfrak{g} = \mathfrak{sl}(N, \mathbb{C})$, all the nilpotent orbits are known as Richardson, that is to say, there is a corresponding Levi subalgebra \mathfrak{l} . Any nilpotent orbit not induced from any proper parabolic subalgebra is called rigid.

Nilpotent orbit construction

Let us see the above story concretely [55, 135].

When a partition of N is given as $[n]$, we introduce a new symbol as

$$p_j := \sum_{i=1}^j n_i. \quad (\text{D.3.4})$$

Next, choose Θ as

$$\Theta = (\text{set of all the positive simple roots}) \setminus \langle e_{p_i} - e_{p_{j+1}}, j = 1, 2, \dots, k \rangle \quad (\text{D.3.5})$$

and we can define the parabolic subalgebra. After the identification between the vector e_i and the corresponding Lie algebra element in $\mathfrak{gl}(N, \mathbb{C})$, we can introduce the vector space

$$V_j = \bigoplus_{i=1}^{p_j} \mathbb{C}e_i \quad (\text{D.3.6})$$

and

$$\mathfrak{p}_{[n]} = \{X \in \mathfrak{sl}(n, \mathbb{C}) \mid X(V_j) \subset V_j\} \quad (\text{D.3.7})$$

$$\mathfrak{n}_{[n]} = \{X \in \mathfrak{sl}(n, \mathbb{C}) \mid X(V_j) \subset V_{j-1}\}. \quad (\text{D.3.8})$$

The fact that X^i acts on V_i as 0 for $X \in \mathfrak{n}_{[n]}$ means

$$\text{rk}(X^j) \leq n - \dim_{\mathbb{C}} V_j = n - p_j \quad (\text{D.3.9})$$

where rk is the rank as $N \times N$ matrices. However, the important point is that there exists such X satisfying the equality in the above inequality. By analyzing the kernel of X^i , we can find that the $SL(N, \mathbb{C})$ -orbit through this X is a nilpotent element specified by $[n]^t$.

Appendix E

More mathematics on the dual model

Here we develop some useful tools to compute the local Boltzmann factor B^Δ using (4.5.8) and to prove some skein relations in App.E.3. First of all, recall the notations of Lie algebras and their representations. Consider the case that the Lie algebra is $\mathfrak{su}(N)$. $R(\lambda)$ denotes the irreducible representation associated with a dominant weight λ , λ_R does the dominant weight to R conversely and $\Pi(R)$ does the set of weights in R . ω_α for $\alpha = 1, 2, \dots, N-1$ are fundamental weights, h_i for $i = 1, 2, \dots, N$ are weights in $\Pi(R(\omega_1) = \square)$ ¹⁾ and there are relations between two as $h_a = \omega_a - \omega_{a-1}$ where $\omega_N = \omega_0 = 0$. We also use the standard metric in weight vectors determined by $h_i = e_i - \frac{1}{N} \sum_{i=1}^N e_i$ and $(e_i, e_j) = \delta_{i,j}$.

E.1 Definitions

Let us start by repeating some definitions which appeared in Sec. 4.5.2.

We introduced a mathematical object which we call “pyramid”. This is just an assembly of integers designated by two labels h and $\alpha = \alpha_h$. h runs over $1, 2, \dots, N-1$ and α does over $1, 2, \dots, N-h$ for each h . Therefore, this object consists of $\frac{1}{2}N(N-1)$ integers. There is an inclusion of weights into the pyramid as follows :

$$\hat{\lambda}_{h;\alpha} := \sum_{\beta=\alpha}^{\alpha+h-1} \lambda_\beta \quad (\text{E.1.1})$$

where $\lambda = \sum_{\beta=1}^{N-1} \lambda_\beta \omega_\beta$. We also use the same symbol $\hat{\lambda}$ for the pyramids not in the image of this inclusion map. In such cases, $\hat{\lambda}$ is considered as a single symbol as a whole and λ

¹⁾The perfect order of the indices of h_i is determined by the partial order in the weight lattice.

is meaningless. Note that the addition can be defined as

$$(c_1\hat{s}_1 + c_2\hat{s}_2)_{h:\alpha} := c_1(\hat{s}_1)_{h:\alpha} + c_2(\hat{s}_2)_{h:\alpha} \quad (\text{E.1.2})$$

which is consistent with the above inclusion map in the sense that it preserves the original additional structure in the weight vector space. $\hat{0}$ is the identity element of this operation. There can be also a product defined as

$$(\hat{s}_1 * \hat{s}_2)_{h:\alpha} := (\hat{s}_1)_{h:\alpha}(\hat{s}_2)_{h:\alpha}. \quad (\text{E.1.3})$$

The distributive property is obvious.

We also defined two functions :

1. (4.5.5) majority function mj for three variables :

$$mj(a, b, c) := \begin{cases} a & b = a \text{ or } c = a \\ b & a = b \text{ or } c = b \\ c & a = c \text{ or } b = c \end{cases} \quad (\text{E.1.4})$$

and

$$mj(\hat{\lambda}_1, \hat{\lambda}_2, \hat{\lambda}_3) := \{mj((\hat{\lambda}_1)_{h:\alpha}, (\hat{\lambda}_2)_{h:\alpha}, (\hat{\lambda}_3)_{h:\alpha})\}_{h:\alpha} \quad (\text{E.1.5})$$

As there appears no case that all variables are distinct, this definition is well-defined in our usage

2. (4.5.7) q -dimension function D :

$$D[\hat{\lambda}] := \prod_{h=1}^{N-1} \prod_{\alpha=1}^{N-h} \frac{[(\hat{\lambda})_{h:\alpha} + h]_q}{[h]_q} \quad (\text{E.1.6})$$

and there is a simple relation to the ordinary q -dimension as

$$\dim_q R(\lambda) = D[\hat{\lambda}] \quad (\text{E.1.7})$$

where $\hat{\lambda}$ is the natural inclusion into the pyramid of the dominant weight λ .

Finally, let us introduce following pyramids defined for any two subsets I, J of $\{1, 2, \dots, N\}$ satisfying $I \cap J = \phi$:

$$\hat{f}_{I,J} := mj(\hat{0}, -\hat{h}_I, \hat{h}_J) \quad (\text{E.1.8})$$

where $h_I := \sum_{i \in I} h_i$. They have equivalent definitions

$$(\hat{f}_{I,J})_{h:\alpha} := \begin{cases} +1 & \text{if } \alpha \in J \text{ and } \alpha + h \in I \\ -1 & \text{if } \alpha \in I \text{ and } \alpha + h \in J \\ 0 & \text{otherwise} \end{cases} \quad (\text{E.1.9})$$

or

$$(\hat{f}_{I,J})_{h:\alpha} := \sum_{i \in I, j \in J} \text{sgn}(i-j) \delta_{h,|i-j|} \delta_{\alpha, \min(i,j)} \quad (\text{E.1.10})$$

where δ is the ordinary Kronecker's δ symbol.

These pyramids satisfy the following properties :

$$\hat{f}_{I,J} = -\hat{f}_{J,I} \quad \text{skewsymmetric} \quad (\text{E.1.11})$$

$$\hat{f}_{I,J \sqcup K} = \hat{f}_{I,J} + \hat{f}_{I,K} \quad \text{linearity} \quad (\text{E.1.12})$$

$$\hat{h}_J = \hat{f}_{\bar{J},J}. \quad (\text{E.1.13})$$

E.2 Convenient formulae

Now let us start the argument recalling the discussion in Sec.4.5.2. Consider three regions called A, B and C clockwise around a trivalent junction and denote their dominant weights λ_A, λ_B and λ_C . See Fig.4.9 in Sec.4.5.2. We also denote the outgoing charge associated with the edge between the regions X and Y by a_{XY} for $(X, Y) = (A, B), (B, C)$ and (C, A) .

We define the following objects in order.

$$\lambda_{XY} := \lambda_X - \lambda_Y =: \sum_{\alpha=1}^{N-1} \Lambda_{XY}^\alpha \omega_\alpha =: \sum_{s=1}^N \lambda_{XY}^s h_s. \quad (\text{E.2.1})$$

λ_{XY}^s is not uniquely determined due to the condition $\sum_s h_s = 0$ in the root vector space.

But it is uniquely determined if we impose the conditions $\lambda_{XY}^s \geq 0$ and $\exists s \lambda_{XY}^s = 0$.

We can find that λ_{XY}^s is either 1 or 0 and define $E_{XY} := \{s \in \{1, 2, \dots, N\} | \lambda_{XY}^s = 1\}$ where $|E_{XY}| = a_{XY}$ follows and $\overline{E_{XY}} := \{1, 2, \dots, N\} \setminus E_{XY} = E_{YX}$. The cycle condition $\lambda_{AB} + \lambda_{BC} + \lambda_{CA} = 0$ tells us $E_{AB} \sqcup E_{BC} \sqcup E_{CA} = \{1, 2, \dots, N\}$ (disjoint union). Now we have

$$mj(\lambda_A, \lambda_B, \lambda_C) = \hat{\lambda}_A + \hat{f}_{E_{AB}, E_{CA}} \quad (\text{E.2.2})$$

and we obtain two other similar expressions by permuting the above cyclically as $A \rightarrow B \rightarrow C \rightarrow A$. This formula will turn out to be useful in the next section.

Finally, we list a few propositions also used later.

1.

$$D[\hat{x} + \hat{z}]D[\hat{y}] = D[\hat{x}]D[\hat{y} + \hat{z}] \quad \text{when } (\hat{x} - \hat{y}) * \hat{z} = \hat{0}. \quad (\text{E.2.3})$$

Each element in pyramid satisfies $x = (\hat{x})_{h:\alpha} = (\hat{y})_{h:\alpha} = y$ or $z = (\hat{z})_{h:\alpha} = 0$ and then we can say $[x + z]_q[y]_q = [x]_q[y + z]_q$ for any $(h : \alpha)$.

which is the flip of the triangulations. We have introduced here $P := E_{CB}$, $Q := E_{BA}$ and $R := E_{AD}$. (E.2.2) tells that the local Boltzmann factors' expression associated with this equality is equivalent to

$$D[\hat{\lambda}_B + \hat{f}_{Q,P}]^{-1/2} D[\hat{\lambda}_A + \hat{f}_{R,P \sqcup Q}]^{-1/2} = D[\hat{\lambda}_B + \hat{f}_{Q \sqcup R, P}]^{-1/2} D[\hat{\lambda}_A + \hat{f}_{R,Q}]^{-1/2} \quad (\text{E.3.3})$$

for any $\lambda_A, \lambda_B, \lambda_C$ and λ_D . In the following, we prove this equality.

Introduce $\hat{x} := \hat{\lambda}_B + \hat{f}_{Q,P}$ and $\hat{y} := \hat{\lambda}_A + \hat{f}_{R,Q}$. Now we get

$$(l.h.s)^{-2} = D[\hat{x}]D[\hat{y} + \hat{f}_{R,P}] \quad (\text{E.3.4})$$

$$(r.h.s)^{-2} = D[\hat{x} + \hat{f}_{R,P}]D[\hat{y}]. \quad (\text{E.3.5})$$

To apply the proposition (E.2.3) to the above, it is enough to check $(\hat{x} - \hat{y}) * \hat{f}_{R,P} = \hat{0}$. Since $\hat{\lambda}_B - \hat{\lambda}_A = \hat{h}_Q = \hat{f}_{\bar{Q},Q}$,

$$(\hat{x} - \hat{y}) * \hat{f}_{R,P} = (\hat{f}_{\bar{Q},Q} + \hat{f}_{Q,P} + \hat{f}_{R,Q}) * \hat{f}_{R,P} \quad (\text{E.3.6})$$

$$= (2\hat{f}_{R,Q} + \hat{f}_{P \sqcup \bar{Q} \sqcup R, Q}) * \hat{f}_{R,P} = \hat{0} \quad (\text{E.3.7})$$

where we have used the two propositions (E.2.4) and (E.2.5) in the last line. Now we have proved the expected equality.

E.3.2 Digon contractions

There is more non-trivial skein relations what we call digon contractions as shown below.

$$\begin{array}{c} \begin{array}{ccc} & R_A & \\ a+b & \begin{array}{c} \xrightarrow{a} \\ \xrightarrow{b} \end{array} & a+b \\ & R_B & \end{array} & = & \frac{[a+b]_q!}{[a]_q! [b]_q!} \xrightarrow[\begin{array}{c} R_B \\ a+b \end{array}]{R_A} \end{array} \quad (\text{E.3.8})$$

where $[n]_q! := \prod_{i=1}^n [i]_q$ for a positive integer n .

First of all, let us introduce several definitions. For fixed E_{AB} , we define a natural embedding

$$\ell^{-1} : \{1, 2, \dots, a+b\} \xrightarrow{\text{biject.}} E_{AB} \quad (\text{E.3.9})$$

$$\ell_\gamma^{-1} := \ell^{-1}(\gamma) \quad \text{for } \gamma \in \{1, 2, \dots, a+b\} \quad \ell_i := \ell(i) \quad \text{for } i \in E_{AB} \quad (\text{E.3.10})$$

satisfying that $1 \leq \ell_\gamma^{-1} < \ell_{\gamma'}^{-1} \leq N$ for $1 \leq \gamma < \gamma' \leq a+b$.

$$M := \{(\ell_{\gamma'}^{-1} - \ell_\gamma^{-1}, \ell_\gamma^{-1}) \quad \text{for any } \gamma' > \gamma\}. \quad (\text{E.3.11})$$

By definition, for any two subsets I, J ($I \cap J = \emptyset$) of E_{AB} , it is true that $(\hat{f}_{I,J})_{h;\alpha} \neq 0 \iff (h, \alpha) \in M$.

Next, let \check{M} be the index set of the pyramid for $SU(a+b)$ weights. In other words, for $(\check{h} : \check{\alpha}) \in \check{M}$, \check{h} runs over 1 to $a+b-1$ and $\check{\alpha}$ does over 1 to $a+b-\check{h}$. The map ℓ induces a new bijection map $\check{\ell}$ from M to \check{M} as follows.

$$(\check{h} : \check{\alpha}) := \check{\ell}(h, \alpha) := (\ell_{\alpha+h} - \ell_{\alpha} : \ell_{\alpha}) \quad (\text{E.3.12})$$

If we label the representation assigned to the inside region of the digon as S , the left hand side gives

$$\sum_S \frac{\dim_q S}{D[mj(\hat{\lambda}_A, \hat{\lambda}_B, \hat{\lambda}_S)]} = \sum_{I:=E_{SB} \subset E_{AB}} \frac{D[\hat{\lambda}_B + \hat{h}_I]}{D[\hat{\lambda}_B + \hat{f}_{E_{BA}, I}]} \quad (\text{E.3.13})$$

$$= \sum_{\substack{I \subset E_{AB} \\ |I|=b}} \frac{D[\hat{\lambda}_B + \hat{f}_{E_{BA}, I} + \hat{f}_{E_{AS}, I}]}{D[\hat{\lambda}_B + \hat{f}_{E_{BA}, I}]} = \sum_{\substack{I \subset E_{AB} \\ |I|=b}} \frac{D[\hat{\lambda}_B + \hat{f}_{E_{AS}, I}]}{D[\hat{\lambda}_B]} \quad (\text{E.3.14})$$

$$= \sum_{\substack{I \subset E_{AB} \\ |I|=b}} \prod_{(h, \alpha) \in M} \frac{[(\hat{\lambda}_B + \hat{f}_{E_{AS}, I})_{h, \alpha} + h]_q}{[\hat{\lambda}_B + h]_q} = \sum_{\substack{I \subset E_{AB} \\ |I|=b}} \prod_{(\check{h}, \check{\alpha}) \in \check{M}} \frac{[(\hat{\mu})_{\check{h}, \check{\alpha}} + (\hat{f}_{E_{AS}, I})_{\check{\ell}^{-1}(\check{h}, \check{\alpha})} + \check{h}]_q}{[(\hat{\mu})_{\check{h}, \check{\alpha}} + \check{h}]_q} \quad (\text{E.3.15})$$

where we have used $h_I = \hat{f}_{\bar{I}, I}$, $\bar{I} = E_{BA} \sqcup E_{AS}$ and the proposition (E.2.3) using also (E.2.5) $\hat{f}_{E_{BA}, I} * \hat{f}_{E_{AS}, I} = \hat{0}$. In the 3rd line, we have used $(\hat{f}_{E_{AS}, I})_{h, \alpha} = 0$ for $(h, \alpha) \notin M$ and $M \xrightarrow{\check{\ell}} \check{M}$ and redefined $(\hat{\mu})_{\check{h}, \check{\alpha}} := (\hat{\lambda}_B)_{\check{\ell}^{-1}(\check{h}, \check{\alpha})} + h - \check{h}$ where $h = h(\check{h}, \check{\alpha}) = \ell_{\check{h}+\check{\alpha}}^{-1} - \ell_{\check{\alpha}}^{-1}$.

Now what we should prove are two following equations.

$$\sum_{\beta=\check{\alpha}}^{\check{\alpha}+\check{h}-1} \hat{\mu}_{1:\beta} = \hat{\mu}_{\check{h}, \check{\alpha}} \quad (\text{E.3.16})$$

$$(h_{\ell(I)}^{\widehat{SU(a+b)}})_{\check{h}, \check{\alpha}} = (\hat{f}_{E_{AS}, I})_{\check{\ell}^{-1}(\check{h}, \check{\alpha})} \quad (\text{E.3.17})$$

The former equality says that $\hat{\mu}$ is the image of a weight μ in the pyramid and follows from the direct computation based on the above definitions. The latter one means that $\hat{f}_{E_{AS}, I}$ gives an image of a weight in $\Pi(\wedge^b \square)$ of $SU(a+b)$, and it also readily follows from the equality

$$(h_{\ell(I)}^{\widehat{SU(a+b)}})_{\check{h}, \check{\alpha}} = (\hat{f}_{E_{AB} \setminus I, I})_{\ell_{\check{\alpha}+\check{h}}^{-1} - \ell_{\check{\alpha}}^{-1} : \ell_{\check{\alpha}}^{-1}} \quad (\text{E.3.18})$$

In conclusion, the numerator in (E.3.15) equals to the q -dimension of the $SU(a+b)$ irreducible representation $R(\mu + h_{\ell(I)})$ up to the common factor $\prod_{(\check{h}, \check{\alpha})} [\check{h}]_q$ and, the sum over all the b element subsets of E_{AB} equals to all irreducible representations appearing in the tensor product of $R(\mu)$ and $\wedge^b \square$. Therefore, this gives $\dim_q^{SU(a+b)} \wedge^b \square$ which exactly reproduces the prefactor in the right hand of (E.3.8).

Appendix F

Seiberg-Witten curve and Gaiotto duality

This appendix is based on the review part of my master thesis (unpublished).

F.1 Gaiotto duality

The 4d $\mathcal{N}=2$ SCFT has an UV marginal complexified gauge coupling for each (simple) gauge group *i.e.* forms an UV deformation parameter space. Gaiotto claims that this space is an Teichmüller space for a punctured Riemann surface and that many properties including UV dualities can be naturally interpreted or derived based on this fact.

Let denote $C_{g,n}$, $T_{g,n}$, $\hat{\mathcal{M}}_{g,n}$ and $\hat{\Gamma}_{g,n}$ be the punctured Riemann surface with genus g and n distinguishable punctures¹⁾, its Teichmüller space, its marked moduli space and its mapping class group (MCG) respectively. Note that $\hat{\mathcal{M}}_{g,n} = T_{g,n}/\hat{\Gamma}_{g,n}$ and the moduli space has some cusps in general corresponding to the full degenerations of the Riemann surface $C_{g,n}$. The author in [14] speculated that there exists a weakly-coupled gauge theory (but permitting some strongly-coupled matters with unknown Lagrangian descriptions) for each cusp giving a degenerate Riemann surface. It also reminds that many perturbation descriptions exist for the undefined M-theory or non-perturbative string theory.

Then, what a gauge theory corresponds to each degenerate Riemann surface? The partial answer is as follow: These degenerate Riemann surfaces are graphs constructed out of internal edges I , external edges E and trivalent vertices V . Each internal edge gives a gauge group or a vector multiplet and external edge does a flavor symmetry specified by the data on each puncture. Each trivalent vertex gives a intricate tri-fundamental “matter multiplet”²⁾ in general specified by three legs or punctures. Therefore from the graphs we

¹⁾It is orientable and have no boundaries except punctures. According to the contexts, they include or not a hyperbolic metric or a complex structure. We use “marked” if we distinguish the punctures and “unmarked” if not.

²⁾Since there may be no Langrangian descriptions, we do use this word instead of “hypermultiplet”

can read off roughly how the gauge fields and the charged matters are coupled although the details of the matters are still unknown. Some examples are shown in Fig. F.1 and F.2. As the fully general constructions are unknown and the more detail one must be discussed individually, we will exhibit some examples soon later and discuss some special cases in F.4.

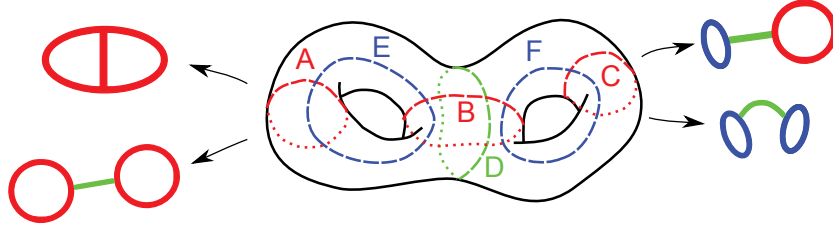


Figure F.1: There exist various pants decompositions for a punctured Riemann surface. Four examples are shown for the genus two and no puncture case : A, B, C (above left), A, C, D (below left), C, D, E (above right) and D, E, F (below right). Here the circles represent the boundaries of the pants to cut along and a gauge group is assigned to each one. The graphs are the degenerate Riemann surfaces or the quiver forms of gauge theories. In general, there exist the infinite pants' choices and each gives a duality frame.

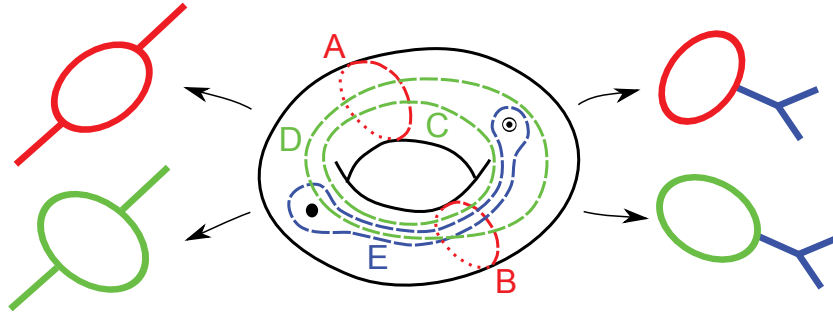


Figure F.2: The external edges can be seen as the zero length limit of thin tubes. They are also open edges in the degenerate graphs. Four examples are shown for the genus one and one puncture case : A, B (above left), C, D (below left), A, E (above right) and C, E (below right).

In this stage, it is expected to identify the MCG $\hat{\Gamma}_{g,n}$ with self-dualities. As the special case they include $SL(2, \mathbb{Z})$ duality for $\mathcal{N}=4$ super Yang-Mills. The full duality which exchanges duality frames is the Moore-Seiberg groupoid which includes the MCG as a “subgroup”. (See [204] for example.) A direct evidence for the full duality is the AGT correspondence mainly for $SU(2)$ case. The other and weaker one for self-dualities is the M-theory construction itself in which the four dimensional physics depends on only the complex moduli of the Seiberg-Witten curve in a given complex structure of a background

except for some cases with free Lagrangians.

hyperKähler manifold. However, in summary, there is little understanding for this except for $SU(2)$ case. We do explain some of these subjects in terms of the well-known aspects of both string theories and field theories. We consider hereafter only A_{N-1} -type *i.e.* $SU(N)$ gauge theories.³⁾

F.1.1 A_1 case

In A_1 case, each internal edge (thin tube) and external edge (puncture) gives a gauge group $SU(2)$ and a flavor group $SU(2)$ respectively and this is all of the rules in A_1 case. In other words, a pair of pants gives a free tri-fundamental chiral multiplet⁴⁾ and a degenerate graph says how coupled these matters are via gauge multiplets corresponding to the tubes between the pants. Assume that all punctures are equivalent but have one mass parameter which is a Cartan of $SU(2)$ -flavor symmetry for each puncture.

$N_c = 2 N_f = 4$ SQCD is a famous example of SCQCD with fundamental “quarks” admitting a non-trivial $SL(2, \mathbb{Z})$ duality and its marginal deformation space of the holomorphic gauge coupling is given as a four-punctured Riemann surface. The outstanding property of this duality is a triality combined in the $Spin(8)$ flavor symmetry,⁵⁾ which maps quarks physics into monopoles one or dyons one. In the above Gaiotto’s framework, this triality is realized as the permutations of the punctures. Since each puncture carry a $SU(2)$ -flavor symmetry, the explicit flavor symmetry read off from the four-punctured Riemann sphere is $SU(2)_A \times SU(2)_B \times SU(2)_C \times SU(2)_D \simeq Spin(4) \times Spin(4)$ and this is the maximal subgroup of $Spin(8)$.

The self-duality stems from the equivalence of all four punctures up to their mass parameters although it is less trivial in terms of the type IIA construction. The famous triality corresponds to the action under the permutation of $SU(2)$ *i.e.* \mathfrak{S}_4 . This exchanges the three 8 dimensional representations of $Spin(8)$:

$$\begin{aligned}
\mathbf{8}_v &= (\mathbf{2}_a \otimes \mathbf{2}_b) \oplus (\mathbf{2}_c \otimes \mathbf{2}_d) \quad \cdots \cdots \text{quark} \\
\mathbf{8}_s &= (\mathbf{2}_a \otimes \mathbf{2}_c) \oplus (\mathbf{2}_b \otimes \mathbf{2}_d) \quad \cdots \cdots \text{monopole} \\
\mathbf{8}_c &= (\mathbf{2}_a \otimes \mathbf{2}_d) \oplus (\mathbf{2}_b \otimes \mathbf{2}_c) \quad \cdots \cdots \text{dyon}
\end{aligned}
\tag{F.1.1}$$

The corresponding geometrical point is shown in Fig. F.3.

We can extend the above discussion to the more complicated gauge theories. The mapping class group of the starting punctured Riemann surface is generated by some local actions on two pairs of pants. Weakening some gauge couplings or thinning the corresponding tubes geometrically, and then applying the $SL(2, \mathbb{Z})$ duality on the four punctured sphere (permutation of punctures), we finally obtain other duality frames.

³⁾At least, we can treat D_N -type *i.e.* SO/USp gauge theories incorporating M-orientifolds. ([205]) Note that USp gauge groups appear even in the set-up of A -type 6d $\mathcal{N}=(2, 0)$ SCFTs.

⁴⁾It has $2^4 = 16$ degrees of freedom in real. The tri-fundamental representation in $SU(2)^3$ gives 8 and the complex value does 2. This is the half of the ordinary hypermultiplet and usually called “half-hypermultiplet”.

⁵⁾The triality is the outermorphism of $Spin(8)$ and the full global symmetry is $SL(2, \mathbb{Z}) \times Spin(8)$.

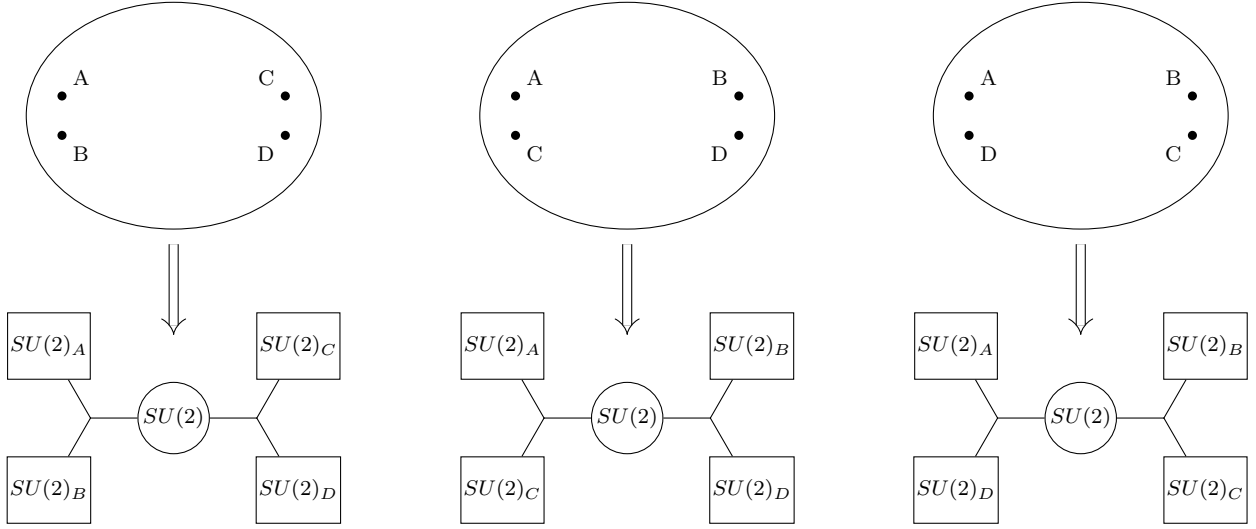


Figure F.3: We can gain three types of $SU(2)$ $N_f = 4$ quivers. These are related by the permutation of punctures. Each puncture has global $SU(2)$ -symmetry and these are also exchanged.

Let us consider $C_{0,6}$ case. This enjoys a non-trivial duality which is not self-dual in the sense that some action can map the original quiver gauge theory into distinct duality frames where some vector multiplets and some hypermultiplets are differently coupled. See Fig. F.4. In this case, there shows up a tri-fundamental half-hypermultiplet coupled to three gauge groups.

The more non-trivial cases are shown in Fig. F.1 and F.2. The former has three $SU(2)$ gauge groups and two hypermultiplets and closed loops stand for the adjoint indices of the matter. The latter does two $SU(2)$ gauge groups and $SU(2) \times SU(2)$ flavor symmetry.

F.1.2 A_2 case

For $N_c = 3$ case, we have a more non-trivial and interesting phenomenon. This theory enjoys only the $\Gamma_0(2)$ duality generated by $\tilde{\tau} \rightarrow \tilde{\tau} + 2, \tilde{\tau} \rightarrow -1/\tilde{\tau}$ where $\tilde{\tau} = \frac{\theta}{\pi} + \frac{8\pi i}{g^2}$ (See later or [206]) and there appears the infinite strongly-coupled point not to map into the weakly-coupled point via it. This can be easily accounted for considering a four punctured sphere whose punctures are categorized as two and two into two groups called simple/minimal and full/maximal punctures. We will explain the kind of punctures in F.3.1. There exist two kind of degenerate limits : See Fig. F.5 and F.6.

Then we obtain two essentially distinct duality frames one of which is well-known SCQCD with six fundamental hypermultiplets. The other is mysterious because there appears a $SU(2)$ gauge group. Decoupling this $SU(2)$ gauge coupling of dual theory, we obtain one free $SU(2)$ fundamental hypermultiplet and non-trivial SCFT named Minahan-

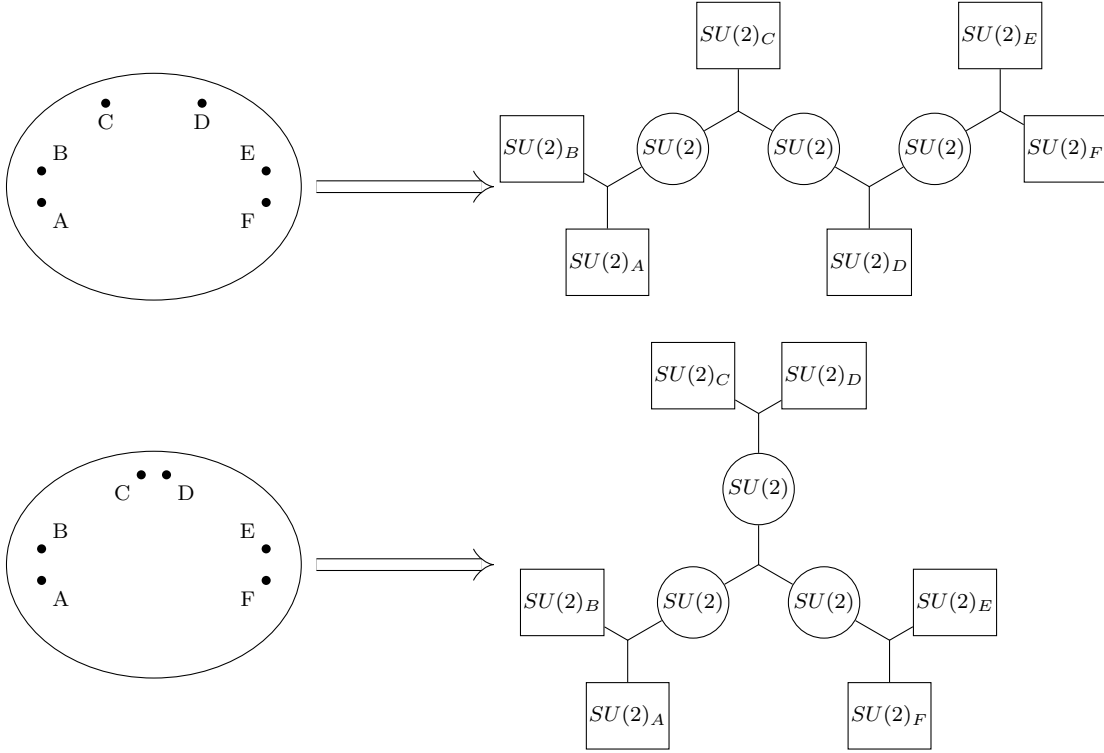


Figure F.4: $SU(2)$ quiver gauge theories with distinct degenerations

Nemeschansky theory or T_3 theory with E_6 flavor symmetry. ⁶⁾ Note that the explicit flavor symmetry seen from the punctures is $SU(3)^3$ which is the maximal subgroup of E_6 . In F.2.2, we will see this duality in terms of the Seiberg-Witten curve (or the Gaiotto curve).

F.2 Gaiotto curve from the Seiberg-Witten curve

Next, we are going to derive and ensure some aspects of the Gaiotto's conjectures and discussions via the Seiberg-Witten curves' analysis. Utilizing the famous Witten's M-theory construction [20], the Seiberg-Witten curve of a linear quiver gauge theory T with n gauge groups and fundamental hypermultiplets gauged under only gauge groups at ends of a quiver is given by

$$F_T(t, v) := \prod_{\ell=1}^N (v - v_\ell^{(\infty)}) t^{n+1} + \sum_{\alpha=1}^n c_\alpha q_\alpha(v) t^{n+1-\alpha} + c_{n+1} \prod_{\ell=1}^N (v - v_\ell^{(0)}) = 0 \quad (\text{F.2.1})$$

where we use a holomorphic coordinate $v := x^4 + ix^5$ and $s := \frac{x^6 + ix^{10}}{R_{10}}$ (R_{10} is the radius of x^{10} -direction) or $t := e^{-s}$ corresponding to the choice of a complex structure in the

⁶⁾See also Fig. F.7 and F.8 later.

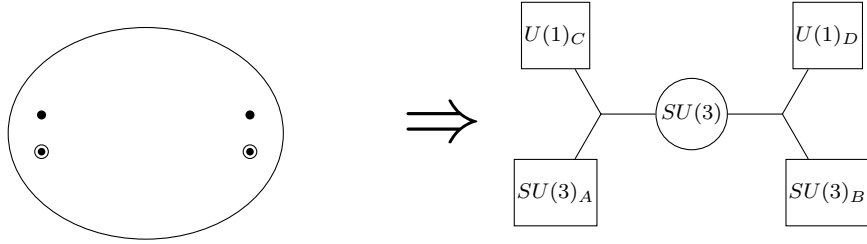


Figure F.5: This is a Gaiotto curve of $N_f = 6$ SCQCD. There are two types of punctures.

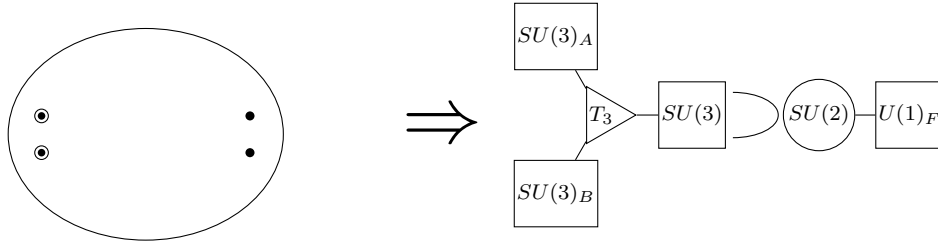


Figure F.6: The same Gaiotto curve gives another duality frame that one $SU(2)$ fundamental hypermultiplet is weakly coupled to a isolated SCFT via a $SU(2)$ gauge field.

flat hyperKähler space \mathbb{R}^4 . $v_\ell^{(\infty)}$ and $v_\ell^{(0)}$ are the positions of the M5-brane at $t = \infty$ and $t = 0$ respectively and correspond to the mass deformations. c_α ($\alpha = 1, \dots, n+1$) are functions of the effective gauge couplings and $q_\alpha(v)$ ($\alpha = 1, \dots, n$) are polynomials of v and the Coulomb branch parameters $\tilde{u}_\ell^{(\alpha)}$ except for $\tilde{u}_1^{(\alpha)}$ given by

$$q_\alpha(v) := v^{k_\alpha} - \sum_{j=1}^{k_\alpha} \tilde{u}_j^{(\alpha)} v^{k_\alpha-j} \quad (\text{F.2.2})$$

where the whole gauge groups are $SU(k_1) \times SU(k_2) \times \dots \times SU(k_n)$. Each $\tilde{u}_j^{(\alpha)}$ ($j \neq 1$) is an expectation value of the j -th order Casimir operator in the Coulomb branch for $SU(k_\alpha)$ and $\tilde{u}_1^{(\alpha)}$ are constants decided by some linear combinations of the mass deformation parameters and vanish for the fully massless case.⁷⁾

The original field-theoretical representation of the curves appearing in [206] which we call “standard” here (following [15]) is introduced later as a remark for the special $C_{0,4}$ case. In this relation, we can see that \tilde{u}_1 is concretely determined by the mass deformations.

Introducing $K := \max\{k_1, k_2, \dots, k_n\}$, (F.2.1) can be written for v 's order

$$F_T(t, v) = \prod_{\alpha} (t - t_\alpha) v^K + \sum_{j=1}^K p_j(t) v^{K-j} = 0 \quad (\text{F.2.3})$$

⁷⁾These u_1 correspond to non-normalizable modes on the deformation space of the complex structure. See also F.2.3.

which we will use later to derive the Gaiotto's form. Notice that c_α are symmetric polynomials of $-t_\alpha$.

Now let us impose the balanced (for D-branes) or conformal (for gauge theories) condition :

$$b_i := -2k_i + k_{i+1} + k_{i-1} = 0 \quad (\text{F.2.4})$$

In terms of IIA brane set-up, this means the force-balanced condition for each NS5-brane because each is forced by D4-branes ending on that from both sides and bends in general except that the forces or the numbers are balanced.⁸⁾ In fact the bending is consistent with the running of the (holomorphic) gauge coupling at 1-loop level. ([20])

Finally, the Seiberg-Witten differential is given by

$$\lambda^{ord} := v \frac{dt}{t} = -v ds \quad (\text{F.2.5})$$

in this case ([207], [208]) but we redefine the Seiberg-Witten differential subsequently. Note that this also differs from the differential for the standard form of the Seiberg-Witten curve in [206] as remarked later.

(F.2.3) can be further written as

$$F_T(t, v') = \prod_{\alpha} (t - t_{\alpha})(v')^K + \sum_{j=2}^K p'_j(t)(v')^{K-j} = 0 \quad (\text{F.2.6})$$

such that the coefficient of v'^{K-1} to vanish. $p'_j(t)$ are not polynomials of t but rational functions allowing the poles at $t = t_{\alpha}$. Then we redefine the new Seiberg-Witten differential as

$$\lambda = \lambda_M := v' \frac{dt}{t} = -v' ds \quad (\text{F.2.7})$$

This redefinition is important for this new formulation but subtle point at the same time.

Mass parameters and residues

The difference between the ordinary one and this new one is the local center of mass.

$$\Delta\lambda = (v' - v) \frac{dt}{t} = -\frac{\bar{V}(t)}{N} \frac{dt}{t} \quad (\text{F.2.8})$$

where

$$\bar{V}(t) := \frac{\sum_{\alpha=0}^{n+1} c_{\alpha} \tilde{V}_{\alpha} t^{n+1-\alpha}}{\prod_{\alpha=1}^{n+1} (t - t_{\alpha})} \quad (\text{F.2.9})$$

⁸⁾We assume that D6-branes are absent or if exist, moved to infinity via branes' creations and annihilations. See F.3.1.

and

$$\tilde{V}_\alpha := \begin{cases} \sum_{\ell=1}^N v_\ell^{(\infty)} & \alpha = 0 \\ \tilde{u}_1^{(\alpha)} & 1 \leq \alpha \leq n \\ \sum_{\ell=1}^N v_\ell^{(0)} & \alpha = n + 1 \end{cases} \quad (\text{F.2.10})$$

The residues of λ can be calculated by those of λ^{ord} . They are given as

$$\text{Res}_{t=0} \lambda^{ord} = -v_1^{(\infty)}, -v_2^{(\infty)}, \dots, -v_N^{(\infty)} \quad (\text{F.2.11})$$

$$\text{Res}_{t=t_\alpha} \lambda^{ord} = \underbrace{0, 0, \dots, 0}_{N-1}, \frac{1}{t_\alpha} \lim_{t \rightarrow t_\alpha} (t - t_\alpha) \bar{V}(t) \quad (\text{F.2.12})$$

$$\text{Res}_{t=\infty} \lambda^{ord} = v_1^{(0)}, v_2^{(0)}, \dots, v_N^{(0)} \quad (\text{F.2.13})$$

noticing that the limits are well-defined because of the definition (F.2.9).

The fact that the sum of residues of λ vanishes helps us to attain

$$\text{Res}_{t=0} \lambda = -\Delta v_1^{(\infty)}, -\Delta v_2^{(\infty)}, \dots, -\Delta v_N^{(\infty)} \quad (\text{F.2.14})$$

$$\text{Res}_{t=t_\alpha} \lambda = \left(\frac{1}{t_\alpha} \lim_{t \rightarrow t_\alpha} (t - t_\alpha) \bar{V}(t) \right) \times \underbrace{\left(-\frac{1}{N}, -\frac{1}{N}, \dots, \frac{N-1}{N} \right)}_{N-1} \quad (\text{F.2.15})$$

$$\text{Res}_{t=\infty} \lambda = \Delta v_1^{(0)}, \Delta v_2^{(0)}, \dots, \Delta v_N^{(0)} \quad (\text{F.2.16})$$

with $\Delta v_\ell^{(0/\infty)} = v_\ell^{(0/\infty)} - \frac{1}{N} V_{(0/\infty)}$.

The overall factors at t_1 , t_{n+1} and t_α ($1 < \alpha < n + 1$) in the second line (F.2.15) correspond to the center of mass V_∞ and V_0 and the mass deformation parameters of the $(\alpha - 1)$ -st bi-fundamental hypermultiplet respectively.

Recalling that the mass parameters belong to the adjoint representation of the flavor symmetry, we can say that there is $SU(N)$ symmetry at $t = 0, \infty$ and $U(1)$ symmetry at the others. Actually, in the weakly-coupled limit of all gauge couplings, t_1 approaches to 0 and the total flavor symmetry $SU(N) \times U(1)$ accord with the flavor symmetry $U(N)$ of the N D4-branes. The redefinition of λ^{ord} to λ corresponds to the decoupling of the diagonal $U(1)$ in $U(N)$. To correctly reproduce the BPS mass formulae, we must redefine the flavor charges assigned to the flavor cycles. Since $\Delta\lambda$ in (F.2.8) are independent of the Coulomb branch parameters, the expectation value of adjoint complex scalar in the $\mathcal{N}=2$ vector multiplet are only shifted by a linear combination of mass parameters. To verify that this redefinition always works well in general case is so difficult problem and we assume that we have another realization of 4d $\mathcal{N}=2$ supersymmetric gauge theories via the M5-brane.⁹⁾

⁹⁾I appreciate the participants in my seminar for the thesis to make me reconsider this subtle point.

There is the more convenient and mostly used form of the Seiberg-Witten curve in terms of a projected curve :

$$x^N = \sum_{i=2}^N \varphi_i(t) x^{N-i} \quad (\text{F.2.17})$$

$$x := \frac{v'}{t} \quad \varphi_i(t) := -\frac{p'_i(t)}{t^i \prod_{\alpha=1}^{n+1} (t - t_\alpha)} \quad (\text{F.2.18})$$

or equivalently

$$\lambda^N = \sum_{i=2}^N \phi_i(t) \lambda^{N-i} \quad \phi_i(t) := \varphi_i(t) dt^{\otimes i} \quad (\text{F.2.19})$$

which is used later.

In the framework of the construction lifting from the type IIA set-up, this projective t -“plane” is always a complex plane or a Riemann sphere. However once we attain this place describing the UV information of 4d $\mathcal{N}=2$ superconformal gauge theories geometrically, it is natural to extend the punctured sphere to a general punctured Riemann surface. This is the Gaiotto curve itself !¹⁰⁾

The Seiberg-Witten curve is a holomorphic curve of $(t, \lambda(t))$ or $(t, x(t))$ and equivalently $\Sigma_{SW} \subset T^{*(1,0)}C$. The relation between the Seiberg-Witten curve Σ_{SW} and the Gaiotto curve $C_{g,n}$ is clear : Σ_{SW} is the N -fold cover of $C_{g,n}$. N values of $\lambda(t)$ corresponds to the positions of the M5-brane along the fiber direction at $t \in C_{g,n}$ and some points in $C_{g,n}$ at which some of λ degenerate is a ramified point in terms of $C_{g,n}$.

Finally, let us see the massless case. In this case the things is so simple that $v' = v$, $\lambda^{ord} = \lambda$ and

$$p'_j(t) = p_j(t) = -\sum_{\alpha=1}^n c_\alpha \tilde{u}_j^{(\alpha)} t^{n+1-\alpha} \quad (\text{F.2.20})$$

and we attain

$$\phi_i(t) = \frac{\sum_{\alpha=1}^n c_\alpha \tilde{u}_i^{(\alpha)} t^{n-\alpha} dt^{\otimes i}}{\prod_{\alpha=1}^{n+1} (t - t_\alpha) t^{i-1}} \quad (\text{F.2.21})$$

Notice that the orders of poles at $t = t_{\alpha=1,2,\dots,n+1}$ are always 1 and those at $t = 0, \infty$ are $i - 1$ for $\phi_i(t)$. These numbers have a close relation to the flavor symmetries at the punctures. It will be discussed about this point in F.3.1.

$SU(N)$ and $C_{0,4}$ case

In this case $K = N$ and $n = 1$, (F.2.1) is

$$F_T(t, v) = \prod_{\ell=1}^N (v - v_\ell^{(\infty)}) t^2 - (1 + q) \left(v^N - \sum_{\ell=1}^N \tilde{u}_\ell v^{N-\ell} \right) t + q \prod_{\ell=1}^N (v - v_\ell^{(0)}) = 0 \quad (\text{F.2.22})$$

¹⁰⁾This curve itself when $\mathbb{C}P^1$ has been considered for a long time as an auxiliary tool.

Here we rescale t to set $c_1 = 1 + q$, $c_2 = q$ where q is a UV holomorphic coupling.¹¹⁾

F.2.1 $N_c = 2$ $N_f = 4$ case

This is the most simple case. The Seiberg-Witten curve (F.2.22) is

$$(v - v_a)(v - v_b)t^2 + (1 + q)(v^2 - \tilde{u}_1 v - \tilde{u}_2)t + q(v - v_c)(v - v_d) = 0 \quad (\text{F.2.23})$$

$$(t - 1)(t - q)v^2 + (-(v_a + v_b)t^2 - (1 + q)\tilde{u}_1 t - (v_c + v_d))v \\ + (v_a v_b t^2 + q v_c v_d - (1 + q)\tilde{u}_2 t) = 0 \quad (\text{F.2.24})$$

and

$$p_0(t)v^2 + p_1(t)v + p_2(t) = 0 \iff x^2 = \varphi_2(t) \quad (\text{F.2.25})$$

$$\text{where } \varphi_2(t) = \frac{p_1^2 - 4p_0 p_2}{4t^2 p_0^2}$$

where $q = t_2/t_1$ and $\tau_{UV} := \frac{1}{2i\pi} \log(q)$. Note that this definition is only valid for $|q| < 1$ if requiring $\Im(\tau_{UV}) > 0$.

If $u_1 = \frac{q}{1+q}(v_a + v_b + v_c + v_d)$, the masses which are associated to each puncture and given by the residue of $\tilde{\lambda}$ are $\pm \frac{v_a \pm v_b}{2}, \pm \frac{v_c \pm v_d}{2}$. These are very $SO(8)$ (adjoint) masses and reproduce quark masses $|\pm m_X + A|$ ($X = a, b, c, d$) where we denote the scalar VEV A to avoid confusing it with the label of puncture a .

In fact,

$$\lambda = v \frac{dt}{t} = \pm \frac{\sqrt{qu_2 dt}}{\sqrt{t(t-1)(t-q)}} \quad (\text{F.2.26})$$

and the behaviour at each puncture is the same. This suggests that the four punctures $t = 0, q, 1, \infty$ are locally equivalent. This is consistent with the discussion F.1.1.

On the other hand, we have room to map the punctures via $SL(2, \mathbb{Z})$ translation on $C_{0,4}$.

$$t \rightarrow \frac{az + b}{cz + d}, \quad x \rightarrow (cz + d)^2 x \quad (\text{F.2.27})$$

We can gain arbitrary positions of punctures z_a, z_b, z_c, z_d but they are subject to a constant cross ratio $q = \frac{z_a z_c}{z_b z_d} \frac{z_d z_c}{z_a z_b}$. This is useful to move freely the punctures to collide each other.

Using the permutation subgroup of the above $SL(2, \mathbb{Z})$ preserving the punctures' positions $0, 1, \infty$, we can map q into $1 - q$ for example. As we see in F.2.3, this corresponds to $\tau_{SW} \rightarrow -\frac{1}{\tau_{SW}}$.

¹¹⁾The relation to the Seiberg-Witten holomorphic (IR) coupling is remarked in F.2.3.

F.2.2 $N_c = 3 N_f = 6$ case

Here, we explain the simplest case of Argyres-Seiberg dualities from the Gaiotto's formulation.

The Seiberg-Witten curve of $N_c = 3 N_f = 6$ SQCD is given by

$$p_0(t)v^3 + p_1(t)v^2 + p_2(t)v + p_3(t) = 0 \iff x^3 = \varphi_2(t)x + \varphi_3(t) \quad (\text{F.2.28})$$

$$\text{where } \varphi_2(t) = \frac{p_1^2 - 3p_0p_2}{3t^2p_0^2} \quad \varphi_3(t) = -\frac{2p_1^3 - 9p_0p_1p_2 + 27p_0^2p_3}{27t^3p_0^3}$$

Especially, $p_0(t) = (t-1)(t-q)$ and all the masses turn off

$$\phi_2(t) = -\frac{(1+q)u_2}{t(t-1)(t-q)} \quad \phi_3(t) = -\frac{(1+q)u_3}{t^2(t-1)(t-q)} \quad (\text{F.2.29})$$

For this curve, we at first take a limit $q \rightarrow 1$ and $u_2 \rightarrow 0$ (the latter corresponds to turning off the mass deformation in coupled $SU(2)$ sector) :

$$x^3 = \frac{-2u_3}{t^2(t-1)^2} \quad (\text{F.2.30})$$

This says that all the three punctures at $t = 0, 1, \infty$ are equivalent (in the meaning that each is a second order pole in $K_C^{\otimes 3}$) and that the puncture at $t = 1$ carry $SU(3)$ flavor symmetry. Then the explicit flavor symmetry is $SU(3) \times SU(3) \times SU(3)$ but enhanced to E_6 as expected. This can be seen via the famous Kodaira's classification of the elliptic singularities with the standard forms of the curves.

For this purpose, we change the variables as

$$w' = \frac{1}{2}u_3v \quad y' = \frac{iu_3}{4}[(t-1) + u_3] \quad u' = \frac{1}{2i}u_3 \quad (\text{F.2.31})$$

Note that this is invertible and preserves the Seiberg-Witten differential up to the (meromorphic) exact 1-form (giving the same physics). The curve (F.2.30) is rewritten as

$$y'^2 = w'^3 - u'^4 \quad (\text{F.2.32})$$

This is the E_6 type elliptic curve or Minahan-Nemeschansky's curve ([147]) in physics. The Gaiotto curve picture is shown in Fig. F.7.

Another point of view corresponds to a collision of the simple punctures. In order to derive it, change the cross ratio using a $SL(2, \mathbb{C})$ transformation $z = \frac{(q-1)t}{q-t}$.¹²⁾

This maps $0, q, 1, \infty$ into $0, \infty, 1, q' = 1 - q$ and x into $\frac{q-1}{z+q-1}x$. Therefore (F.2.28) is rewritten as

$$x^3 = \frac{(2-q')u_2}{z(z-1)(z-q')}x + \frac{-(2-q')q'u_3}{z^2(z-1)(z-q')^2} \quad (\text{F.2.33})$$

¹²⁾We have done the reduction.

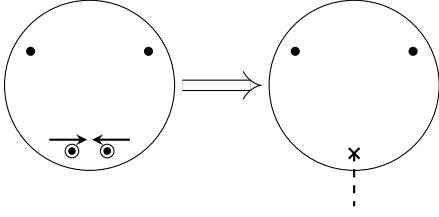


Figure F.7: collision of two simple punctures in A_2

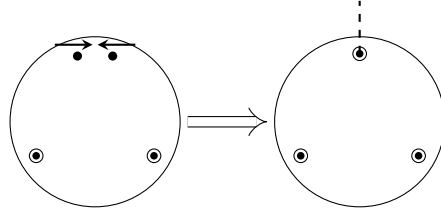


Figure F.8: collision of two full punctures in A_2

In a colliding limit $q' \rightarrow 0$, we have (factoring out x)

$$x^2 = \frac{2u_2}{z^2(z-1)} \quad (\text{F.2.34})$$

This is the very $SU(2)$ $N_f = 4$ curve without masses in the weak coupling limit.(Fig. F.8) Actually we can gain the coupled one setting u_3 be zero in (F.2.33).

Taking the above two observations into consideration, we can guess the special case of Argyres-Seiberg duality :

$$SU(3) \text{ w/ } 6 \cdot (\mathbf{3} \oplus \bar{\mathbf{3}}) \xleftrightarrow[\text{S-dual}]{} SU(2) \text{ w/ } (2 \cdot \mathbf{2} \oplus \text{SCFT}_{E_6}) \quad (\text{F.2.35})$$

F.2.3 Remarks on the relation to the standard Seiberg-Witten curve

Here we discuss the the most simple and important $C_{0,4}$ case about the relation to the original representation of the curves.

The standard forms of the Seiberg-Witten curves in superconformal cases (A_{N-1} -type) are given by [206]

$$y^2 = P(w)^2 - (1 - g(\tau)^2)Q(w) \quad (\text{F.2.36})$$

$$P(w) := \det(w - u) \quad Q(w) := \prod_{I=1}^{2N} (w + g\mu + \mu_I)$$

Here m_I are the mass parameters of $U(2N)$ flavor symmetry, $\mu := \frac{1}{2N} \sum_{I=1}^{2N} m_I$ is the center of mass and $\mu_I := m_I - \mu$ is the relative to it. $g(\tau)$ is a modular function defined as

$$g(\tau) := \frac{\vartheta_4(q)^4 + \vartheta_2(q)^4}{\vartheta_4(q)^4 - \vartheta_2(q)^4} \quad \text{for } q := e^{2\pi i\tau} \quad (\text{F.2.37})$$

which gives the UV coupling $q_{UV} = e^{2\pi i\tau_{UV}}$.¹³⁾

¹³⁾This terminology is the convention too. Both describes the same physics but differ by a finite renormalization.

These standard curves are related to those via M-theory by the following variable transformations

$$t := \frac{1}{1 - g(\tau)} \frac{P(w) - y}{Q_\infty(w)} \quad v := w + (g - 1)\mu \quad v_I := -m_I \quad (\text{F.2.38})$$

and these are one-to-one because the inverse ones exist. The sign difference between v and the mass cancels the minus of $-v'ds$ in (F.2.5).

Here divide the $2N$ hypermultiplets' masses into two groups N and N as

$$Q_\infty(v) := \prod_{i=1}^N (v - v_i^{(\infty)}) \quad Q_0(v) := \prod_{a=1}^N (v - v_a^{(0)}) \quad (\text{F.2.39})$$

Then we attain the M-theoretically constructed curves :

$$Q_\infty(v)t^2 - (1 + q)\tilde{P}(v) + qQ_0(v) = 0 \quad (\text{F.2.40})$$

where $\tilde{P}(v) := P(v - (g - 1)\mu)$. This is why we use the notation \tilde{u} instead of u in (F.2.2) and so on.

Next focus on the Seiberg-Witten differential. Recall that the differential is given by

$$\lambda_{SW} = \frac{w + (g - 1)\mu}{2\pi i} d \log \left(\frac{P(w) - y}{P(w) + y} \right) \quad (\text{F.2.41})$$

$$\lambda_M = v d \log(t) \quad (\text{F.2.42})$$

The relation between two is

$$\lambda_M + \frac{v}{2} d \log \left(\frac{Q_\infty(v)}{Q_0(v)} \right) = \pi i \lambda_{SW} \quad (\text{F.2.43})$$

This says that two are equivalent up to an exact 1-form.

The Seiberg-Witten curve with fundamental hypermultiplets

A string ending on a D4-brane and a D6-brane at the center of a monopole generate a quark in (anti-)fundamental representation. Therefore the Seiberg-Witten curves in Q describe dynamics with hypermultiplets. However, it is complexified and difficult to analyse it on the non-trivial background metric of Q .

We can replace Q by flat \mathbb{R}^4 with a trick. For the purpose, recall that the four dimensional low-energy physics is independent of the Kähler parameters because the curve and Seiberg-Witten differential are determined by only the complex structures. The Kähler parameters of the Taub-NUT space are the center positions of the monopoles and this suggests us to take arbitrary positions. It seems strange because we can get the D6-branes away to the infinity and then the D6-branes give no effect on the four dimensional low-energy physics. The solution to this puzzle is to consider the branes' creation-annihilation process sometimes called *Hanany-Witten effect (transition)*. ([19])

Then we can replace Q by \mathbb{R}^4 with the generated D4-branes. The brane creation-annihilation are dictated by a linking number. This linking number for each D6-brane is defined by

$$(L - R) - \frac{1}{2}(\ell - r) \quad (\text{F.2.44})$$

where $L/R = (\# \text{ of D4-branes in the left/right})$ and $\ell/r = (\# \text{ of NS5-branes in the left/right})$. We can define those of NS5-brane by replacing NS5-branes into D6-branes in the above. Then the Hanany-Witten effect says that the linking numbers are preserved before and after the branes' contact. ¹⁴⁾

Now let us write down the Seiberg-Witten curve taking this into the consideration. Let I_α be the α -th interval between α -th and $(\alpha + 1)$ -st NS5-branes in the type IIA setup. Then introduce

$$J_\alpha(v) := \prod_{x_\ell^6 \in I_\alpha} (v - v_a) \quad J_0(v) := J_{n+1}(v) := 1 \quad (\text{F.2.45})$$

$$g_\alpha(v) := v^{k_\alpha} - \sum_{i=1}^{k_\alpha-1} \tilde{u}_i^{(\alpha)} v^{k_\alpha-i} \quad g_0(v) := g_{n+1}(v) := 1 \quad (\text{F.2.46})$$

for $\alpha = 1, 2, \dots, n$

where x_ℓ^6 is the x^6 -position of ℓ -th D6-brane (ℓ here is not the number of NS5-branes used in the linking number) and $J_\alpha(v)$ and $g_\alpha(v)$ are degree d_α and k_α polynomial of v respectively. With these polynomials,

$$A_\alpha(v) := c_\alpha g_\alpha(v) \prod_{\beta=0}^{\alpha} J_\beta(v)^{\alpha-\beta} \quad \text{for } \alpha = 0, 1, \dots, n, n+1 \quad (\text{F.2.47})$$

where c_α are constant complex numbers associated to the gauge couplings.

Assembling these ingredients, define

$$\hat{q}_\alpha(v) := c_\alpha g_\alpha(v) \prod_{\beta=0}^{\alpha} J_{\beta,R}(v)^{\alpha-\beta} \prod_{\beta=\alpha+1}^{n+1} J_{\beta,L}(v)^{-\alpha+\beta} \quad \text{for } \alpha = 0, 1, \dots, n, n+1 \quad (\text{F.2.48})$$

and finally the complete Seiberg-Witten curve can be written down as

$$F_T(t, v) := \sum_{\alpha=0}^{n+1} \hat{q}_\alpha(v) t^{n+1-\alpha} = 0 \quad (\text{F.2.49})$$

Note that the position along x^4 and x^5 directions of the D4-brane created by the Hanany-Witten effect is fixed by the position of the D6-brane. In fact, there are no other variable complex parameters. See Fig. F.10.

¹⁴⁾I thank S.Sugimoto for telling me a nice and intuitive interpretation in terms of M-theory as follow. Roughly speaking, the moving M5-brane is hooked on the Taub-NUT center and the hooked part of the M5-brane reduces into D4-brane in the type IIA setup. (See [209])

We find that the degrees of v for $\hat{g}_\alpha(v)$ can be all the same for each conformal quiver by appropriately moving the D6-branes to the left or right infinities. This proof and the classification of possible conformal quiver tails will be discussed in F.3.1 for that of conformal punctures.

F.3 Classification of punctures

In this section, we focus on a puncture. This is a boundary condition and restricts the Seiberg-Witten curve or four dimensional low-energy physics. In terms of six dimensional SCFT, this is a codimension two defect which arises from a M5-M5 branes' intersection. Therefore there naturally appear the same tools describing the surface operators in four dimension.

There are two types of puncture, one of which naturally appears in the superconformal quiver gauge theories and is called *regular*. We analyse this type of punctures in detail and the definition will be clear finally. The other type of punctures (not regular) are called *irregular*. These punctures play important roles in the construction of non-conformal quiver gauge theories or AD theories but are not treated in this thesis. (See [15] or [210] for example.)

F.3.1 Regular punctures

In this stage, we can not define regular punctures directly but they are punctures or defects preserving conformal symmetry roughly speaking. Here the punctures constructed from the IIA set-ups lifted to M-theory are called “regular”. It is possible to represent the data (integer sequences) in various equivalent manners.

- the orders of the pole of ϕ at the puncture : $\{p_i\}$ (= Newton polygon P)
- the leading orders of the pole of $\lambda \sim \mathcal{O}((z - z_a)^{\frac{1-q_a}{q_a}})dz : \{q_a\}$
- gauge groups $\prod_a U(k_a) : \{k_a\}$
- flavor groups $S(\prod_a U(d_a)) : \{d_a\}$

We can simply summarize them as a Young diagram Y as explained later and it will be also clear that there exists an one-to-one correspondence between the diagrams and the punctures. Then we have $p(N)$ kinds of regular punctures.¹⁵⁾ Here $p(N)$ denote the number of the partition of N . We will explain this fact by starting from IIA set-up.

Consider one end of a (conformal) quiver gauge theory and assume that it is like the form in Fig. F.9. This is sometimes called a *quiver tail*. ([211]) In this case, we have a

¹⁵⁾As we will see soon, they include a negligible puncture which does not affect the theory and there are $p(N) - 1$ kinds exactly for A -type.

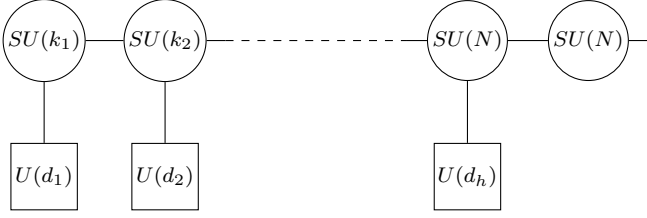


Figure F.9: conformal quiver tail

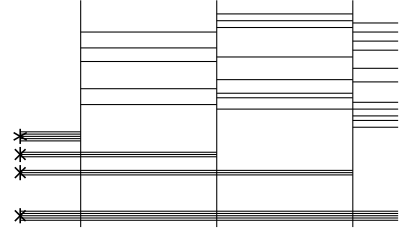


Figure F.10: NS5-D4-D6 systemes

sequent gauge groups and flavor groups for fundamental hypermultiplets and denote those sizes (= rank for U / rank+1 for SU) by $\{k_a\}$ and $\{d_a\}$ ($a = 1, 2, \dots, h$) respectively. h is the length of gauge groups chains and is an arbitrary positive integer. Note that $k_{h-1} \neq k_h = N$ (definition of h) and add $k_0 = d_0 = 0$ and $k_{h+1} = N$, $d_{h+1} = N$ for later convenience. Then define another sequence $\{q_a\}$ as $q_a := k_a - k_{a-1}$.

The conformal quiver condition in $\mathcal{N}=2$ gauge theory says that the one-loop part of the β function should vanish or that is

$$b_a := -2k_a + k_{a+1} + k_{a-1} + d_a = 0 \quad (\text{F.3.1})$$

which is modified from (F.2.4). (F.3.1) says that $d_h > 0$ or $k_{h-1} < k_h$ and that $\{q_a\}$ is non-increasing since $q_{a+1} = q_a - d_a \leq q_a$ using (F.3.1).

We also have a restriction $k_a \geq 2$ because non-vanishing $U(1)$ gauge couplings are not conformal in four dimension and find that

$$q_1 \geq q_2 \geq \dots \geq q_h = d_h > 0 \quad (\text{F.3.2})$$

These assert that $\{k_a\}$ is a strictly increasing sequence starting from k_1 greater than 1. This assertion actually guarantees the first assumption of the tail form.

Now we have a N 's partition $\{q_a\}$ since $\sum_{a=1}^h q_a = k_h - k_0 = N$. The reverse map from a partition to a quiver is trivial except for $N = 1 + 1 + \dots + 1$. It is summarized that the classification of the conformal quiver tails equals to the set of all partitions of N except for a partition like $[1, 1, 1, \dots, 1]$ (all 1).¹⁶⁾ It is conventional and useful to introduce the corresponding Young diagram by Y_q and its transposed by $Y := Y_q^T = [n_1, n_2, \dots, n_s]$. We number boxes in Y by 1 to N such that $k_{a-1} + 1, k_{a-1} + 2, \dots, k_a$ from the left to the right in the a -th row. We also denote the height of i -box in Y by H_i .

For instance, the classified list for the A_5 -type quiver gauge theory is shown in Fig. F.11.

The form of Seiberg-Witten curve

Next we investigate the pole structures of the mass-undeformed Seiberg-Witten curve or the Seiberg-Witten differential. Before doing this analysis, we must prove the fact that

¹⁶⁾The exception type is called “null puncture” but plays no role for A -type.

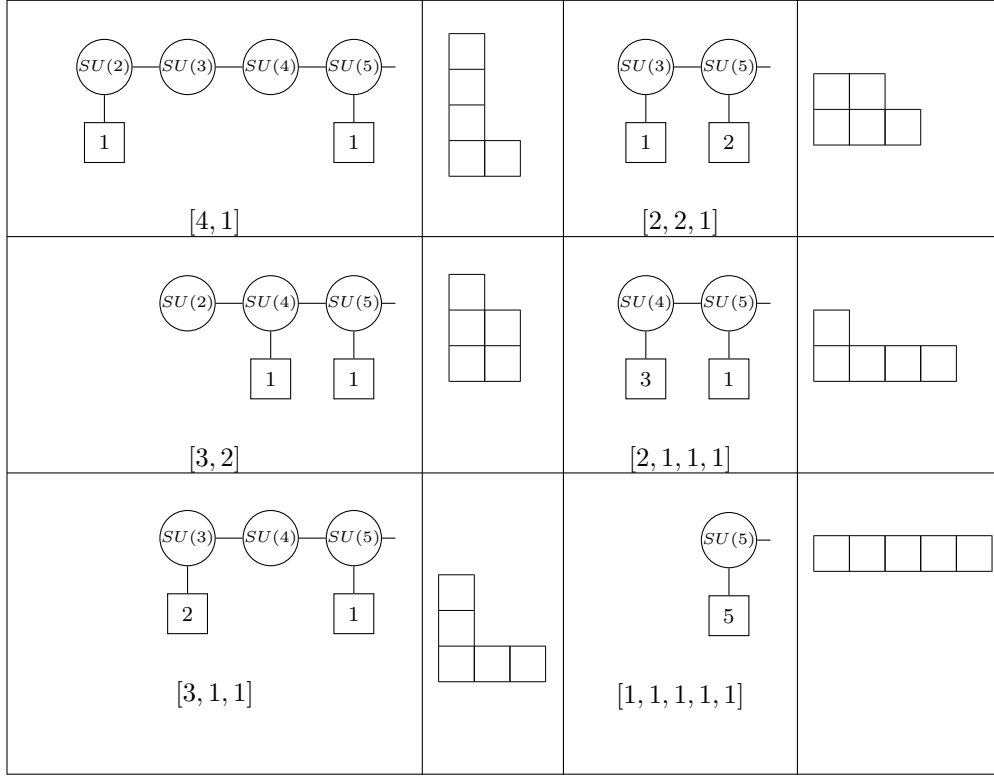


Figure F.11: The classification of all the possible quiver tails and their Young diagrams for A_5 ($SU(6)$) case.

all $\hat{g}_\alpha(v)$ can have the same degree of v if moving the D6-branes appropriately. This is the extension of the last analysis of the quiver tail.

We can see in the same way as before that $\{k_{\alpha+1} - k_\alpha\}_{\alpha=0,1,\dots,n}$ is a non-increasing sequence and we have

$$k_1 \leq k_2 \leq \dots < k_{h_L} = k_{h+1} = \dots = k_{n+1-h_R} = N > \dots \geq k_{n-2} \geq k_{n-1} \geq k_n \quad (\text{F.3.3})$$

Note that when $k_1 = N$ or $k_n = N$, $h_L = 1$ or $h_R = 1$ respectively. Then divide the D6-branes into two groups such that all in I_α ($\alpha \leq h_L$) belong to a group \mathcal{L} and all in I_α ($\alpha \geq h_R$) to another group \mathcal{R} when $h_L < n + 1 - h_R$. For $h_L = n + 1 - h_R =: h$ case, $d_L := N - k_{h-1}$ D6-branes are put into \mathcal{L} and $d_R := N - k_{h+1} = d_h - d_L$ into \mathcal{R} . After moving all the D6-branes to the left infinity if in \mathcal{L} or the right infinity if in \mathcal{R} , we have \hat{k}_α D4-branes in I_α . The previous analysis tells us that

$$\begin{aligned}
 \hat{k}_\alpha &= k_\alpha + \sum_{j=\alpha+1}^{h_L-1} (j - \alpha)d_j + (h_L - \alpha)d_L & \text{for } \alpha = 0, \dots, h_L - 2 \\
 \hat{k}_{h_L-1} &= k_{h_L-1} + d_L \\
 \hat{k}_\alpha &= k_\alpha = N & \text{for } \alpha = h_L, \dots, n + 1 - h_R
 \end{aligned} \quad (\text{F.3.4})$$

$$\begin{aligned}\hat{k}_{n+2-h_R} &= k_{n+2-h_R} + d_R \\ \hat{k}_\alpha &= k_\alpha + \sum_{j=n+2-h_R}^{\alpha-1} (\alpha-j)d_j + (\alpha-h_R)d_R \quad \text{for } \alpha = n+3-h_R, \dots, n+1\end{aligned}$$

For $\hat{q}_\alpha := \hat{k}_\alpha - \hat{k}_{\alpha-1}$,

$$\begin{aligned}\hat{q}_{\alpha+1} - \hat{q}_\alpha &= k_{\alpha+1} + k_{\alpha-1} - 2k_\alpha + d_\alpha = -b_\alpha = 0 \\ &\text{except for } \alpha = h_L = n+1-h_R = h\end{aligned} \tag{F.3.5}$$

$$\begin{aligned}\hat{q}_{h+1} - \hat{q}_h &= \hat{k}_{h+1} + \hat{k}_{h-1} - 2\hat{k}_h = k_{h+1} + k_{h-1} - 2k_h + d_h = -b_h = 0 \\ &\text{for } h_L = n+1-h_R = h\end{aligned} \tag{F.3.6}$$

shows that $\hat{q}_1 = \hat{q}_2 = \dots = \hat{q}_n = \hat{q}_{n+1} = \hat{q}_h = 0$ and $\hat{k}_\alpha = N$ for $\forall \alpha = 0, 1, \dots, n, n+1$ in conclusion.

Pole structures

As a final step we study the behaviour of ϕ_i and λ at a $t = \infty$ pole labelled by Y . As $t \rightarrow \infty$, the Seiberg-Witten curve (F.2.49) gives

$$\prod_{a=0}^{n+1} (t-t_a)v^N + \sum_{i=2}^N (-c_{s_i} \tilde{u}_i^{(s_i)} t^{n+1-s_i} - c_{s_i+1} \tilde{u}_i^{(s_i+1)} t^{n-s_i} - \dots) v^{N-i} = 0 \tag{F.3.7}$$

where we define

$$s_i := \min\{\alpha | k_\alpha \geq i\} \tag{F.3.8}$$

which equals to H_i by definition.

Recalling (F.2.21),

$$\phi_i(t) \rightarrow c_{s_i} u_i^{(s_i)} t^{n+1-s_i} \quad \text{as } t \rightarrow \infty \tag{F.3.9}$$

In the coordinate $z = 1/t$, p_i is defined as

$$\phi_i(z) \rightarrow z^{-p_i} dz^{\otimes i} \quad \text{as } z \rightarrow 0 \quad (t \rightarrow \infty) \tag{F.3.10}$$

and on the other hand (F.3.9) says

$$\phi_i(z) = \frac{p_i(z)}{\prod_a (z-z_a) z^i} dz^{\otimes i} \sim z^{-(n+1-s_i)} z^{n+1} z^{-i} = z^{s_i-i} \tag{F.3.11}$$

Then we obtain the relation between p_i and H_i .

$$p_i = i - s_i = i - H_i \tag{F.3.12}$$

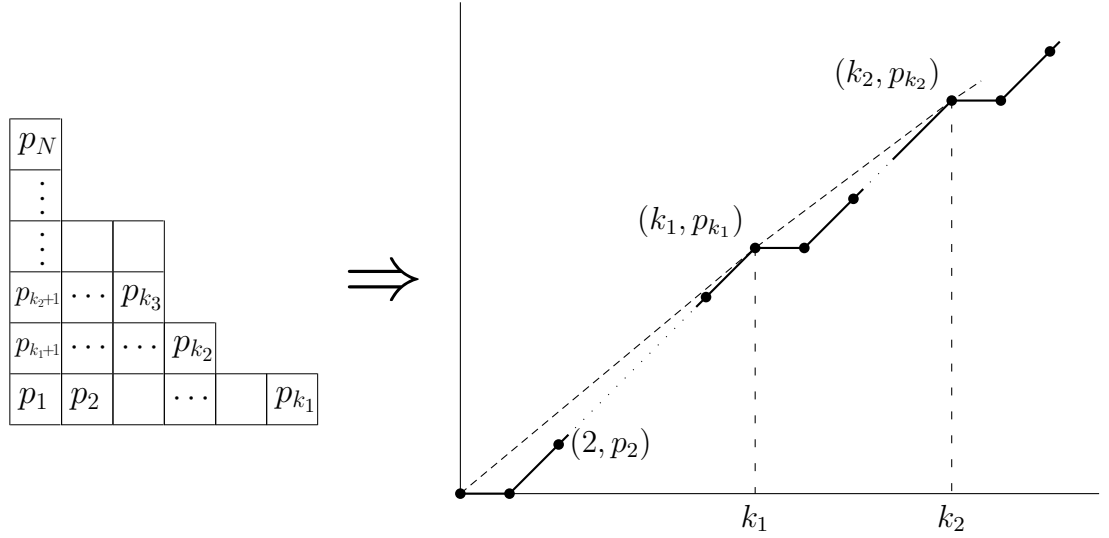


Figure F.12: The numbers $p_i = i - H_i$ assigned to each box of the Young diagram (left) give a Newton polygon (right). The shape of the polygon is restricted such that the slope given by each neighbored two points is either 0 or 1.

This can be determined by the rule shown in Fig. F.12. Note that $p_{i+1} - p_i = 0$ or 1 and then $\{p_i\}$ is a non-decreasing sequence.

The final relation to prove is the singular behaviour of λ or x . If we assume $x \sim z^{-\alpha}$ as $z \rightarrow 0$ then we gain

$$\phi_i(z)\lambda^{N-i} \sim z^{-(p_i+(N-i)\alpha)} \quad \text{as } z \rightarrow 0 \quad (\text{F.3.13})$$

The leading order cancellation suggests

$$\exists a < b \quad p_a + (N - a)\alpha = p_b + (N - b)\alpha \quad (\text{F.3.14})$$

$$p_a + (N - a)\alpha \geq p_i + (N - i)\alpha \quad \text{for } i(\neq a, b) = 0, 1, \dots, N \quad (\text{F.3.15})$$

and this can be rewritten as the condition

$$\frac{p_b - p_a}{b - a} \begin{cases} \geq \frac{p_i - p_a}{i - a} & \text{for } i > a \\ \leq \frac{p_i - p_a}{i - a} & \text{for } i < a \end{cases} \quad (\text{F.3.16})$$

This condition and the non-decrease of $\{p_i\}$ tell us the restriction shown in Fig. F.13 and finally give a Newton polygon shown in Fig. F.12.

The equation (F.3.14) means that the order of the singularity at $z = 0$ in λ is given by the slopes shown in Fig. F.12 because

$$\frac{p_{k_a} - p_{k_{a-1}}}{k_a - k_{a-1}} = \frac{q_a - 1}{q_a} \quad (\text{F.3.17})$$

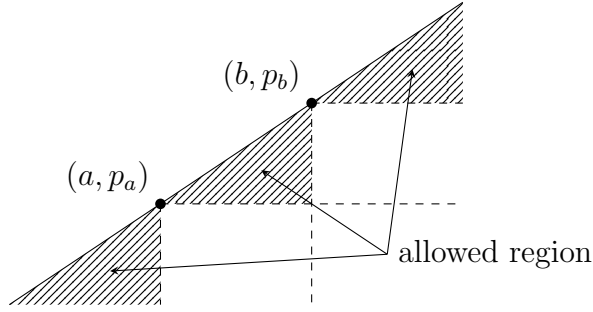


Figure F.13: Given the two points which cause the leading cancellation of $\phi_i \lambda^{N-i}$, the other points are restricted to the shaded areas.

There exist q_a of N solutions with a behaviour $\lambda \sim z^{\frac{1-q_a}{q_a}}$ around $z = 0$.

In summary, we see the previous list to characterize the punctures constructed from the type IIA set-up. To gain the quiver tail from the 6d $\mathcal{N}=(2,0)$ SCFT, we need some $U(1)$ flavor symmetries of each bi-fundamental hypermultiplet and fundamental ones. For the purpose, it is necessary to collide enough number of simple punctures with the generic regular puncture. In fact, the claim that the punctures to collide should be the simple ones is found from the analysis of the Seiberg-Witten curve (F.2.49). This can be also found in terms of the number matching of complex structure moduli parameters and the holomorphic gauge couplings. See Fig. F.16 as the example.

Revisit the definition of regular punctures. We once defined it by the lift from the brane constructions of quiver tails in the type IIA string theory. A clear definition will be introduced in analysing the boundary conditions of the Hitchin system in F.3.2. However, we see that a general puncture satisfying the assumptions gives a conformal quiver tail when we collide enough simple punctures with it and admit some assumptions and justify the former definition.

Assume that the order of each pole in ϕ_i in the massless case is an integer and less than i . The integral condition claims that $\varphi_i(z)$ are single valued functions. Then colliding enough simple punctures to the puncture to take the appropriate weak coupling limit, we can have a degeneration shown in the left of Fig. F.17. Each pair of pants has a simple puncture. For the purpose, let us count the Coulomb dimension for it. This is the number of independent coefficients (complex moduli parameters) of the polynomial lying in the numerator of $\phi_k(z)$. As we know the singular behaviour at each puncture, we can determine the degree of the polynomial. The result is

$$d_k = (p_k^{(0)} + p_k^{(1)} + p_k^{(\infty)}) - (2k - 1) \quad (\text{F.3.18})$$

which is the Riemann-Roch theorem, mathematically speaking. If there is a simple puncture at $z = 0$, $p_k^{(0)} = 1$ and $p_k^{(0)} + p_k^{(1)} + p_k^{(\infty)} \leq 2k - 1$. Then the pair of pants with a simple puncture has no Coulomb moduli and gives just free hypermultiplets coupled to gauge fields because there are no degrees of freedom in the 4d low-energy effective theory. Now returning the starting set-up with a general regular puncture and enough simple ones, we

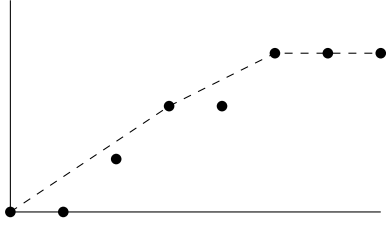


Figure F.14: This is a Newton polygon for $[4, 2, 1]$. The horizontal axis represents the order of the pole in the degree i differential $\phi_i(z)$ and the vertical does p_i . The slopes of the dashed segments correspond to q_s .

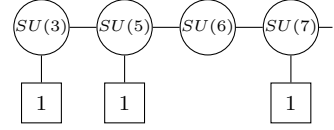


Figure F.15: The quiver tail graph for $[4, 2, 1]$ type. This is conformal.

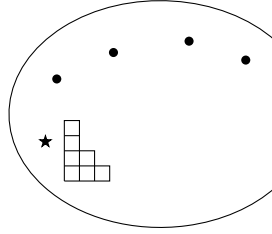


Figure F.16: The punctures for regular one $[4, 2, 1]$ and four simple ones give the above right quiver tail subdiagram if they collides. \star accompanied with a Young diagram has the data about (the flavor symmetry of) the fundamental hypermultiplets without a diagonal $U(1)$ and \bullet 's do the $U(1)$ and (those of) the bi-fundamental ones.

have an ordinary conformal quiver gauge theory if the conformality is unbroken in the process and this must be included in the already obtained classification started from the IIA set-up.

A direct interpretation of Young diagram

Finally, we comment on how to see readily what brane configuration appears in the type IIA with a general puncture labelled by Y and enough many simple punctures. A box in α -th row and ℓ -th column of the Young diagram Y represents a D4-brane connecting the ℓ -th D6-brane and the α -th NS5-brane. Here we label the orders of D6-branes such that the outer D6-branes be the smaller.

This point of view will be useful on considering the mirror dual set-up. When we consider the appropriate T-dual NS5-D3-D5 set-up, the S-duality in type IIB string theory acts on the Young diagram as the transposition. (c.f. [125])

F.3.2 Punctures as the boundary condition of the Hitchin system

The discussion here is based on [131]. The starting point is the Hitchin equation over $C_{g,n}$ (2.2.1).

Consider a general puncture preserving the conformal symmetry at $z = 0$ and see the singular behaviour of the Higgs field :

$$\Phi(z) := \langle \varphi(z) \rangle = \frac{\check{\Phi}}{z} + (\text{regular}) \quad (\text{F.3.19})$$

where $\check{\Phi}$ is an element of $\mathfrak{sl}(N, \mathbb{C})$ and a semisimple (= diagonalizable) element.

$$\check{\Phi} \sim \text{diag}(m_1, m_2, \dots, m_N) \quad \text{satisfying} \quad \sum_{i=1}^N m_i = 0 \quad (\text{F.3.20})$$

Here \sim means that they are equivalent up to conjugacy. Recalling the Seiberg-Witten curve is given by the Hitchin equation, we find out that $\{m_i\}_{i=1,2,\dots,N}$ equal to the residues of λ at $z = 0$ and then just the mass deformation parameters.

What happens in the massless case ? Naively, $\check{\Phi}$ vanishes and there seems to disappear the Seiberg-Witten curve. However $\check{\Phi}$ is an element of $\mathfrak{sl}(N, \mathbb{C})$ in general and not always diagonalizable. Since all the eigenvalues are degenerate to zero in this case, there are all possibilities of the Jordan blocks with only zero eigenvalues. We write the Jordan blocks and Jordan cell as

$$J_{[d_1, d_2, \dots, d_t]} := J_{d_1} \oplus J_{d_2} \oplus \dots \oplus J_{d_t} \quad J_d := \overbrace{\begin{pmatrix} 0 & 1 & 0 & \dots & 0 \\ 0 & 0 & 1 & \dots & 0 \\ \vdots & \ddots & \ddots & \ddots & \vdots \\ \vdots & & & 0 & 1 \\ 0 & 0 & \dots & 0 & 0 \end{pmatrix}}^{d \text{ components}} \quad (\text{F.3.21})$$

and there appears a partition or a Young diagram Y_d again. Therefore it is expected that there exists an one-to-one correspondence between the regular punctures and the types of the Jordan blocks.

The proof is straightforward. It is possible to suppose the regular (non-singular) term in $\Phi(z)$ to be non-zero in general. Then it is enough to represent $\det(\lambda_M - \Phi(z)dz)$ as a polynomial of x for $\lambda_M = xdz$ and read off the singular behaviour of each coefficient function of z when $\check{\Phi} = J_{[d_1, d_2, \dots, d_t]}$ for $d_1 \geq d_2 \geq \dots \geq d_t$. Using the definition of determinant, we can decide the most singular term of z among the terms with a fixed degree of x . Notice that there are no x^{N-1} terms. The most singular term for x^i comes from $(N-i+1, N-i+1)$, $(N-i+2, N-i+2)$, \dots , (N, N) components in the diagonal and the order of the singularity is.

$$\sum_{\alpha=1}^{\beta} (d_{\alpha} - 1) \quad \text{for } \exists \beta \text{ s.t. } \sum_{\alpha=\beta+1}^t d_{\alpha} = i \quad (\text{F.3.22})$$

$$\sum_{\alpha=1}^{\beta+1} (d_\alpha - 1) - \delta_i \quad \text{for } d_\beta > \delta_i := i - \sum_{\alpha=\beta+1}^t d_\alpha > 0 \quad (\text{F.3.23})$$

Actually, these values are given by the rule just remarked in F.3.1 from Young diagram $Y_q = [q_1, q_2, \dots, q_N]$ to $\{p_i\}$ itself.

In summary, we can conclude that the Jordan block type Y_d of $\check{\Phi}(z)$ gives the type of regular puncture for $Y = Y_d^T$ and that the insertions of codimension 2 defects or punctures impose boundary conditions of the Higgs field in the Hitchin system.. The behaviour of the Higgs field at a puncture is also the simple definition of regular punctures. If $\check{\Phi}$ is the more singular than $1/z$ at $z = 0$, we have a ‘‘irregular puncture’’.

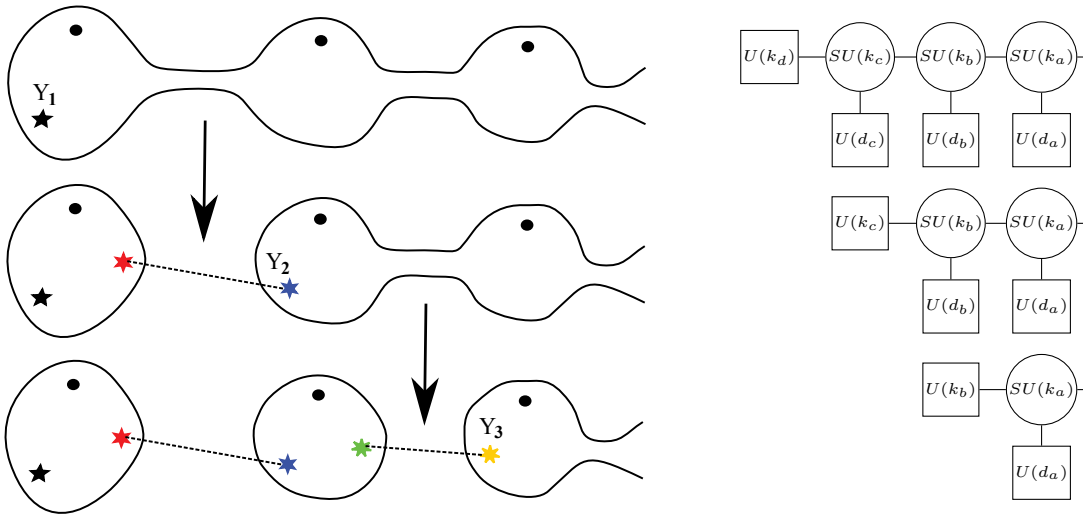


Figure F.17: The degeneration makes new punctures at both edge of the thin tube. The above shows that Y_1 and \bullet (simple) give rise to Y_2 and that Y_2 and \bullet do to Y_3 . (left) The corresponding quivers are changed by decoupling the gauge group at the end one by one. (right)

F.3.3 Operator product expansion of regular puncture defects

We can regard the choice of pants decomposition and its degeneration limit as the operator product expansion (OPE) of punctures in terms of the six dimension SCFT. We assume that the OPE of the punctures or the codimension 2 defects should be determined locally. In other words, the newly generated defect in the OPE is determined if we choose the kinds of colliding punctures.

The most clear case is the OPE of a regular puncture and a simple puncture. See Fig. F.17. The procedure in terms of Young diagram for the regular puncture is shown in Fig. F.18.

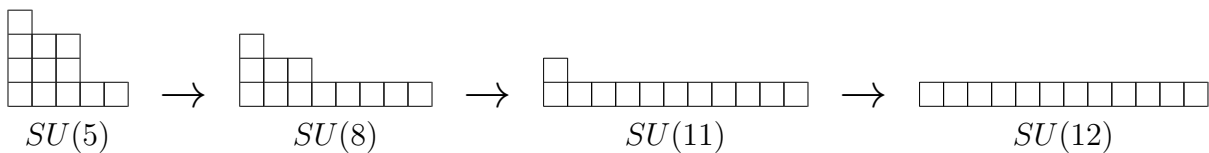


Figure F.18: This is the sequent collisions of simple punctures. The group below each Young diagrams is the gauge group at the end of the quiver tail in each step.

We can analyse what type of puncture appears in the OPE of two general regular punctures as follow. Suppose q is a position of a puncture enough near 0 and the sigular behavior of $\Phi(z)$ both at 0 and at q is

$$\Phi(z) = \frac{\check{\Phi}^{Y_a^T}}{z} + \frac{\check{\Phi}^{Y_b^T}}{z-q} + (\text{regular}) \quad (\text{F.3.24})$$

and we can set $\check{\Phi}^{Y_a^T} = J_a$ and $\check{\Phi}^{Y_b^T} = g^{-1}J_b g$ for some $g \in SL(N, \mathbb{C})$.

The OPE corresponds to the limit $q \rightarrow 0$ and we gain

$$\Phi(z) \longrightarrow \frac{\check{\Phi}^{Y_A} + \check{\Phi}^{Y_b}}{z} + \dots = \frac{J_a + g^{-1}J_b g}{z} + \dots \quad (\text{F.3.25})$$

In general $J_a + g^{-1}J_b g$ has non-zero eigenvalues m'_1, m'_2, \dots, m'_N and is semisimple. This says that the generated puncture in the OPE has a non-zero mass deformation. Therefore we must take the massless limit $m'_1, m'_2, \dots, m'_N \rightarrow 0$. All the eigenvalues vanish and the new type of the puncture is determined.

For example, we can directly check for $N = 3$. Recall that the partition [3] corresponds to the full puncture with $SU(3)$ flavor symmetry and [2, 1] does to the simple puncture with $U(1)$ flavor symmetry. The concrete calculation following the above procedure shows

$$[3] \times [3] = [3] \quad [3] \times [2, 1] = [3] \quad [2, 1] \times [2, 1] = [3] \quad (\text{F.3.26})$$

and this supports Argyres-Seiberg duality discussion.

F.4 Class S construction

We explain why codimension 2 defects are important for class S theories and derive some fundamental properties utilizing string dualities. [212]

The building blocks are called *triskelion*.¹⁷⁾ Especially, the most basic theory is obtained from the N M5-branes wrapped on the sphere with three full punctures ($C_{0,3f}$). This is usually called T_N and non-Lagrangian theory for $N > 2$.¹⁸⁾

¹⁷⁾This is a terminology introduced in [124].

¹⁸⁾For $N = 2$, T_2 is a free hypermultiplet in the trifundamental of $SU(2)^3$ since the simple and the full are same. For $N > 2$, there are some Coulomb branch deformations in spite of non-gauge theory.

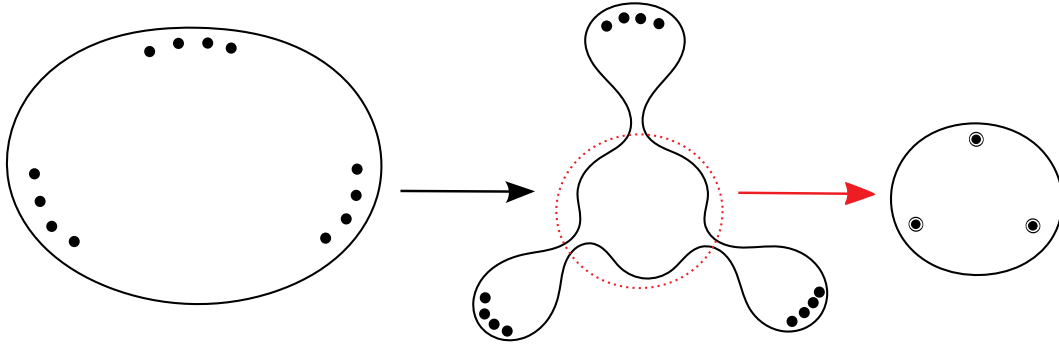


Figure F.19: The example of the procedure for A_4 . The extension to general N is direct. Left : This is a Riemann sphere with 12 simple punctures. Middle : 3 branches of 4 simple punctures are gathered. When 4 simple punctures approach each other, there appears a quiver tail with gauge groups $SU(2) \times SU(3) \times SU(4) \times SU(5) \times SU(4) \times SU(3) \times SU(2)$ and with 1,1 and 2 fundamental hypermultiplets are coupled to left end $SU(2)$, right end $SU(2)$ and $SU(5)$ respectively. In the weak limit, the Riemann sphere gives rise to the quiver shown in fig.F.20. Right : This is a trinion (pairs of pants). The low-energy theory appearing when N M5-branes wrapped on this is usually called T_N .

F.4.1 T_N theory

Here we explain how this T_N theory is obtained from a Riemann surface's configuration with a weakly-coupled Langrangian description. Let us start from the sphere with $3N - 3$ simple punctures which gives a linear quiver gauge theory and then the simple punctures are grouped into three banches with $N - 1$ simple punctures in each banch. Recalling that colliding $N - 1$ simple punctures yields a full puncture from F.3.1 and F.3.3, we can replace each banch by a full puncture.¹⁹⁾ Decoupling the gauge symmetries, we attain the desired trinion with three full punctures. This procedure is also shown in Fig. F.19.

The Seiberg-Witten curve for this T_N theory can be written down recalling the previous discussion in F.3. The behavior at a puncture is known and $\varphi_k \sim \frac{1}{(z - z_a)^{k-1}}$ for the full puncture at z_a . We can set three punctures at $z = 0, 1, \infty$ by the $SL(2, \mathbb{Z})$ transformation. Then we have

$$\phi_k(z) = \frac{P_{k-3}(z)}{z^{k-1}(z-1)^{k-1}} dz^{\otimes k} \quad \text{for } k \geq 3 \quad (\text{F.4.1})$$

where $P_k(z)$ is an order $k - 3$ polynomial of z and each coefficient of z^i gives a Coulomb branch parameter $u_k^{(i)}$ whose scaling dimension is k . The Seiberg-Witten curve is

$$x^N = \sum_{k=3}^N \varphi_k(z) x^{N-k} \quad (\text{F.4.2})$$

¹⁹⁾Here we assume that the kind of the puncture are determined locally.

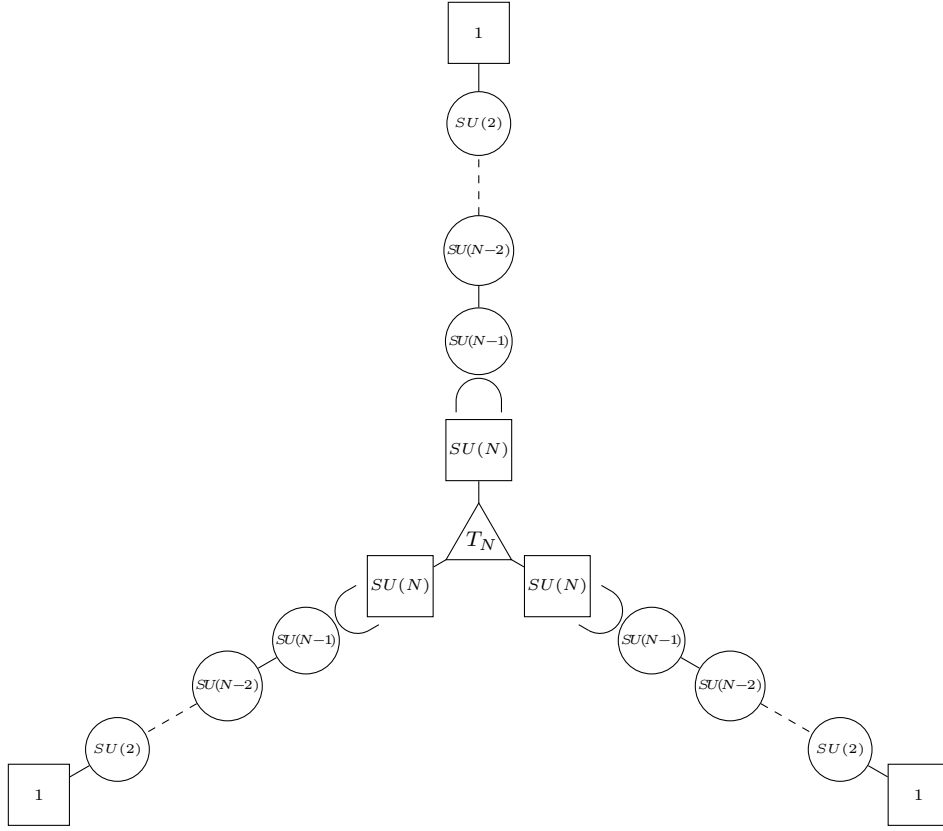


Figure F.20: The triangle quiver gauge theory corresponding to the middle in fig.F.19.

as we have seen before.

The total dimension of the Coulomb branch is

$$\sum_{k=3}^N (k-2) = \frac{(N-1)(N-2)}{2} \quad (\text{F.4.3})$$

We can do the same discussion for any theories (not gauge theories) which can be obtained as the four dimensional low-energy theories from the N coincide M5-branes compactification by a three-punctured sphere $C_{0,3}$ with three codimension two defects labelled by $\{p_i^{(0)}\}$, $\{p_i^{(1)}\}$ and $\{p_i^{(\infty)}\}$. Here $\{p_i^{(z)}\}$ represents the order of the singularity of $\phi_i(z)$ at z . Its Coulomb dimension is already given in (F.3.18). This pair of pants is the triskelion. Then we can construct many kinds of quiver gauge theories by sewing several triskelions. The sewing means gauging some subgroups of flavor symmetries associated to the punctures.

Appendix G

Drukker-Morrison-Okuda's correspondence

In this Appendix, we see that there exists a correspondence between the charges of Wilson-'t Hooft loop operators and the curves on $C_{g,n}$ (genus g Riemann surface with n ($[1^2]$ -type) punctures) for generalized quiver gauge theories. This one-to-one correspondence between the total charge lattice and a certain class of curves on $C_{g,n}$ was mathematically discussed in [25]. Their precise claim is that the Wilson-'t Hooft loop operator classification including flavor 't Hooft loops in the A_1 quiver gauge theory $T_{A_1}^S[C_g(n \cdot [1^2])]$ associated to $C_{g,n}$ is the same as the isotropic classification of the multiple non-(self-)intersecting unoriented curves on the punctured Riemann surface $C_{g,n}$. Using the skein relations, we can decompose any curves into non-self-intersecting loops. No orientation for curves corresponds to the fact $\mathbf{2} \simeq \mathbf{2}^*$. Notice that they just claim that both generate the same modules. The concrete map does not guarantee the precise correspondence but just true for “the highest weight”. See the introduction in Sec. 5.3 for example. Note that all the dyonic loops are pure type in the A_1 quiver gauge theory, that is to say, any dyonic loop can be mapped to a Wilson loop by a duality action *i.e.* a Moore-Seiberg groupoid action. This fact corresponds to the absence of junctions in the language of the 2D geometry on $C_{g,n}$.

We introduce a useful mathematical terminology for this purpose. Consider a set of closed curves over $C_{g,n}$ without any intersection points but permitted to end on punctures. This may be disconnected but all the loops contractible to a point or homotopic to the cycle around a puncture should be removed away from it.¹⁾ We call the isotropic class of the collection of these curves *lamination* on $C_{g,n}$.

G.1 Possible set of loop operators

At first, we classify all the loop operators in the A_1 -type quiver gauge theory associated to a punctured Riemann surface $C_{g,n}$ with a pants decomposition σ . Recalling the classi-

¹⁾Or we consider the equivalent class up to such loops.

fication result for one gauge group (1.2.19), each cuff gives a pair of integers (p_i, q_i) .²⁾ p_i corresponds to an element of $\Lambda_{mw}/\mathcal{W}_{su(2)} \simeq \mathbb{Z}_{\geq 0}$ or a magnetic charge. If $p_i \neq 0$, there remains no Weyl gauge symmetry and q_i is an element of $\Lambda_{wt} \simeq \mathbb{Z}$. If $p_i = 0$, the possible choice of q_i matches with the classification of Wilson loop and is an element of $\Lambda_{wt} \simeq \mathbb{Z}$. There are $2(3g - 3 + n)$ integers because the number of gauge groups is $3g - 3 + n$.

In addition to these, there are another n parameters corresponding to the flavor ('t Hooft) loop which is coupled to the background (dual) gauge field with the associated flavor (magnetic) charge. We label them by p_i where i runs from $3g - 3 + n + 1$ to $3g - 3 + 2n$ because these are the ordinary 't Hooft loops after it is gauged. In summary, each p_i is associated to a cuff ($i = 1, 2, \dots, 3g - 3 + n$) or a puncture ($i = 3g - 3 + n + 1, \dots, 3g - 3 + 2n$). Then we have $6g - 6 + 3n$ parameters. However there is another constraint in these quiver gauge theories : quantization condition. Each free hypermultiplet associated to each trinion gets a phase when it is transported around the Dirac string of loops. When the integers p_a, p_b and p_c represent charges which the hypermultiplet has, the phase factors acting on the tri-fundamental hypermultiplet of $SU(2)$ (See Sec. 2.4.1) are given as

$$(e^{2\pi i p_a (\frac{1}{2}\sigma_3)}, e^{2\pi i p_b (\frac{1}{2}\sigma_3)}, e^{2\pi i p_c (\frac{1}{2}\sigma_3)}) \quad (\text{G.1.1})$$

for each $SU(2)$ symmetry. Therefore, the diagonal components of the 8×8 matrix acting on the free matters are $\exp[\pi i(\pm p_a \pm p_b \pm p_c)]$. Since the gauge transformation must be single-valued, we should impose the constraint³⁾

$$p_a + p_b + p_c \in 2\mathbb{Z} \quad (\text{G.1.2})$$

and then the above 8×8 phase factor matrix become the identity matrix.

In summary, the generalized Wilson-'t Hooft loops which include flavor loops of the quiver theory $T_{A_1}^S[C_g(n \cdot [1^2])]$ are parametrized by $6g - 6 + 3n$ integers with a Weyl reflection identification and the quantization condition.

G.2 Construction of the one-to-one map

Although there are several manners to characterize the lamination, we use the tube-pants decomposition adding tubes between the pairs of pants here because this corresponds to a choice of the duality frames of the $SU(2)$ quiver gauge theory.⁴⁾ Now, the n punctured genus g Riemann surface consists of $3g - 3 + n$ thin tubes and $2g - 2 + n$ pairs of pants. We depict a pair of pants by a disk with two holes as shown in Fig. G.1.

1. Homotopic operation

The lamination is also decomposed according to the pants decomposition. We can keep any windings around the thin tubes on the decomposition. The part of the lamination on

²⁾Here we use the different notation in which the root has length 1.

³⁾The factor 2 before \mathbb{Z} origins from the different notation. See the last footnote.

⁴⁾The viewpoint from the triangulation is remarked in [83] for example.

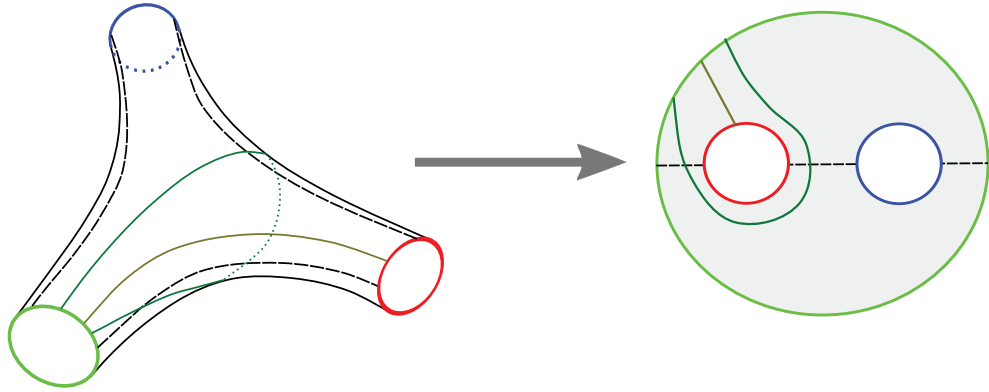


Figure G.1: The pair of pants can be represented as a disk with two holes. If one or two of the cuffs are punctures, we replace the puncture(s) by a hole(s). Notice that there are two regions “upper” side and “lower” side separated by the dashed lines in both representations. It is necessary to map the upper side of the pair of pants into that of the disk.

a pair of pants is the collection of several arcs ending on the boundaries of each pair of pants. Assign a number to each cycle around the thin tube or each puncture in order.

After removing the loops around punctures, each non-trivial arc connecting two boundaries or a common boundary can be always continuously moved to one of the six fundamental arcs shown in Fig. G.2 without no intersections among the arcs. Note that we define the upper side and the lower side on the twice-holed disk separated by dashed lines in Fig. G.2.

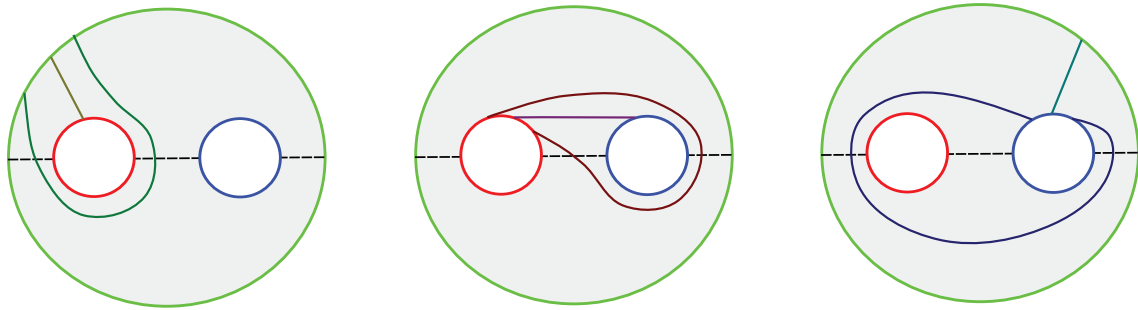


Figure G.2: The six types of building arcs on the pair of pants.

2. Intersection numbers

Denote by P_i the number of endpoints of the arcs on the i -th cuff or the intersecting number of the lamination. This gives a map from the lamination to the $3g - 3 + 2n$ non-negative integers as $p_i = P_i$ where each gauge/flavor group is also naturally labelled by the number assigned to the corresponding tube/puncture.

Next, let us consider the inverse map from three non-negative integers to the lamination. Let us focus on a pair of pants or the disk with two holes and there are three integers P_i, P_j and P_k to each boundary cycle γ_i, γ_j and γ_k respectively. We also define the arc ℓ_{ij} connecting γ_i and γ_j permitting the case $i = j$. Hereafter, $a\ell_A + b\ell_B + \dots$ denotes the collection of non-intersecting arcs on the pair of pants with a arcs ℓ_A , b arcs ℓ_B and such as for \dots part.

Without the loss of generality, we can have two possibilities for the arc construction:

- $P_i > P_j + P_k, P_j \leq P_k + P_i$ and $P_k \leq P_i + P_j$ case : the collection of the arcs is

$$\frac{1}{2}(P_i - P_j - P_k)\ell_{ii} + P_j\ell_{ij} + P_k\ell_{ik} \quad (\text{G.2.1})$$

- $P_i \leq P_j + P_k, P_j \leq P_k + P_i$ and $P_k \leq P_i + P_j$ case : the collection of the arcs is

$$\frac{1}{2}(P_i + P_j - P_k)\ell_{ij} + \frac{1}{2}(P_j + P_k - P_i)\ell_{jk} + \frac{1}{2}(P_k + P_i - P_j)\ell_{ki} \quad (\text{G.2.2})$$

and we gain a lamination on sewing all the pairs of pants to keep the upper part and the lower part without the “twisting” discussed in the following. Finally, by setting P_i to be p_i , the map from laminations to loop operators is completed.

3. Twisting number

We define a twisting number Q_i of arcs by the winding number for the i -th tube. The non-intersecting condition implies that the winding numbers of the several arcs are common. If $P_i = 0$, this is the number of loops which is a non-negative integer $Q_i \geq 0$. Otherwise, we have a sign in addition to how many times they wind. The sign of the twisting number is defined such that the winding in the right direction along the arc gives the positive sign. For the positive twisting number, see arcs in Fig. G.3. This procedure determines

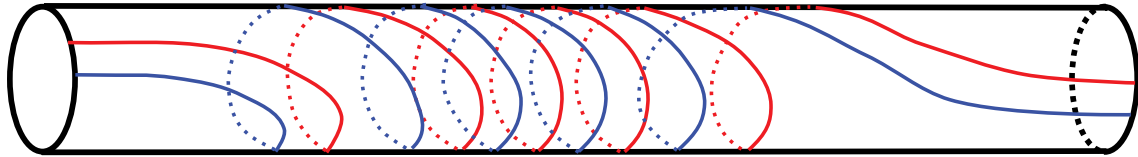


Figure G.3: The winding arcs on a thin tube with a common positive twisting number 5.

$3g - 3 + n$ integers for the lamination. The inverse construction is trivial by the definition.

Combining the equality $Q_i = q_i$ with the previous results $P_i = p_i$, we finally have the desired map.

Bibliography

- [1] M. E. Peskin and D. V. Schroeder, *An Introduction to Quantum Field Theory; 1995 ed.* Westview, Boulder, CO, 1995. Includes exercises.
- [2] S. Weinberg, *The Quantum Theory of Fields: Modern applications. 2.* No. Vol.I in Quantum theory of fields. Cambridge University Press, 2001.
- [3] S. Weinberg, *The Quantum Theory of Fields.* No. Vol.II in The Quantum Theory of Fields 3 Volume Hardback Set. Cambridge University Press, 1995.
- [4] P. Francesco, P. Mathieu, and D. Sénéchal, *Conformal Field Theory.* Graduate Texts in Contemporary Physics. Springer New York, 2012.
- [5] D. Simmons-Duffin, *TASI Lectures on the Conformal Bootstrap*, 1602.07982.
- [6] S. Rychkov, *EPFL Lectures on Conformal Field Theory in $D=3$ Dimensions*, 1601.05000.
- [7] N. Arkani-Hamed, F. Cachazo, and J. Kaplan, *What is the Simplest Quantum Field Theory?*, *JHEP* **09** (2010) 016, [0808.1446].
- [8] F. Cachazo, P. Svrcek, and E. Witten, *MHV vertices and tree amplitudes in gauge theory*, *JHEP* **09** (2004) 006, [hep-th/0403047].
- [9] R. Britto, F. Cachazo, B. Feng, and E. Witten, *Direct proof of tree-level recursion relation in Yang-Mills theory*, *Phys. Rev. Lett.* **94** (2005) 181602, [hep-th/0501052].
- [10] N. Arkani-Hamed, J. L. Bourjaily, F. Cachazo, A. B. Goncharov, A. Postnikov, and J. Trnka, *Scattering Amplitudes and the Positive Grassmannian*, 1212.5605.
- [11] S. J. Parke and T. R. Taylor, *An Amplitude for n Gluon Scattering*, *Phys. Rev. Lett.* **56** (1986) 2459.
- [12] P. Deligne, P. Etingof, D. S. Freed, L. C. Jeffrey, D. Kazhdan, J. W. Morgan, D. R. Morrison, and W. Edward, *Quantum Fields and Strings: A Course for Mathematicians Vol.I and Vol.II.* American Mathematical Soc., 1999.

- [13] J. M. Maldacena, *The Large N limit of superconformal field theories and supergravity*, *Int. J. Theor. Phys.* **38** (1999) 1113–1133, [hep-th/9711200]. [Adv. Theor. Math. Phys.2,231(1998)].
- [14] D. Gaiotto, *$N=2$ dualities*, *JHEP* **1208** (2012) 034, [0904.2715].
- [15] D. Gaiotto, G. W. Moore, and A. Neitzke, *Wall-crossing, Hitchin Systems, and the WKB Approximation*, 0907.3987.
- [16] Y. Tachikawa, *$N=2$ supersymmetric dynamics for pedestrians*, in *Lecture Notes in Physics, vol. 890, 2014*, vol. 890, p. 2014, 2013. 1312.2684.
- [17] L. F. Alday, D. Gaiotto, and Y. Tachikawa, *Liouville Correlation Functions from Four-dimensional Gauge Theories*, *Lett.Math.Phys.* **91** (2010) 167–197, [0906.3219].
- [18] A. Gadde, E. Pomoni, L. Rastelli, and S. S. Razamat, *S -Duality and 2D Topological QFT*, *JHEP* **1003** (2010) 032, [0910.2225].
- [19] A. Hanany and E. Witten, *Type IIB superstrings, BPS monopoles, and three-dimensional gauge dynamics*, *Nucl.Phys.* **B492** (1997) 152–190, [hep-th/9611230].
- [20] E. Witten, *Solutions of four-dimensional field theories via M theory*, *Nucl.Phys.* **B500** (1997) 3–42, [hep-th/9703166].
- [21] C. Montonen and D. I. Olive, *Magnetic Monopoles as Gauge Particles?*, *Phys.Lett.* **B72** (1977) 117.
- [22] C. Vafa, *Geometric origin of Montonen-Olive duality*, *Adv.Theor.Math.Phys.* **1** (1998) 158–166, [hep-th/9707131].
- [23] K. G. Wilson, *Confinement of Quarks*, *Phys.Rev.* **D10** (1974) 2445–2459.
- [24] J. Polchinski, *Tasi lectures on D-branes*, in *Fields, strings and duality. Proceedings, Summer School, Theoretical Advanced Study Institute in Elementary Particle Physics, TASI'96, Boulder, USA, June 2-28, 1996*, pp. 293–356, 1996. hep-th/9611050.
- [25] N. Drukker, D. R. Morrison, and T. Okuda, *Loop operators and S -duality from curves on Riemann surfaces*, *JHEP* **0909** (2009) 031, [0907.2593].
- [26] L. F. Alday, D. Gaiotto, S. Gukov, Y. Tachikawa, and H. Verlinde, *Loop and surface operators in $N=2$ gauge theory and Liouville modular geometry*, *JHEP* **1001** (2010) 113, [0909.0945].
- [27] N. Drukker, J. Gomis, T. Okuda, and J. Teschner, *Gauge Theory Loop Operators and Liouville Theory*, *JHEP* **1002** (2010) 057, [0909.1105].

- [28] N. Drukker, D. Gaiotto, and J. Gomis, *The Virtue of Defects in 4D Gauge Theories and 2D CFTs*, *JHEP* **1106** (2011) 025, [1003.1112].
- [29] V. Pestun, *Localization of gauge theory on a four-sphere and supersymmetric Wilson loops*, *Commun.Math.Phys.* **313** (2012) 71–129, [0712.2824].
- [30] N. Hama and K. Hosomichi, *Seiberg-Witten Theories on Ellipsoids*, *JHEP* **1209** (2012) 033, [1206.6359].
- [31] J. Kinney, J. M. Maldacena, S. Minwalla, and S. Raju, *An Index for 4 dimensional super conformal theories*, *Commun. Math. Phys.* **275** (2007) 209–254, [hep-th/0510251].
- [32] C. Romelsberger, *Counting chiral primaries in $N = 1$, $d=4$ superconformal field theories*, *Nucl. Phys.* **B747** (2006) 329–353, [hep-th/0510060].
- [33] D. Gaiotto, *Asymptotically free $\mathcal{N} = 2$ theories and irregular conformal blocks*, *J. Phys. Conf. Ser.* **462** (2013), no. 1 012014, [0908.0307].
- [34] D. Gaiotto and J. Teschner, *Irregular singularities in Liouville theory and Argyres-Douglas type gauge theories, I*, *JHEP* **12** (2012) 050, [1203.1052].
- [35] M. Buican and T. Nishinaka, *On the superconformal index of Argyres–Douglas theories*, *J. Phys.* **A49** (2016), no. 1 015401, [1505.05884].
- [36] C. Cordova and S.-H. Shao, *Schur Indices, BPS Particles, and Argyres-Douglas Theories*, *JHEP* **01** (2016) 040, [1506.00265].
- [37] J. Song, *Superconformal indices of generalized Argyres-Douglas theories from 2d TQFT*, *JHEP* **02** (2016) 045, [1509.06730].
- [38] N. Wyllard, *A_{N-1} Conformal Toda Field Theory Correlation Functions from Conformal $\mathcal{N} = 2$ $SU(N)$ Quiver Gauge Theories*, *JHEP* **11** (2009) 002, [0907.2189].
- [39] A. Gadde, L. Rastelli, S. S. Razamat, and W. Yan, *The 4D Superconformal Index from Q -Deformed 2D Yang-Mills*, *Phys.Rev.Lett.* **106** (2011) 241602, [1104.3850].
- [40] A. Gadde, L. Rastelli, S. S. Razamat, and W. Yan, *Gauge Theories and Macdonald Polynomials*, *Commun.Math.Phys.* **319** (2013) 147–193, [1110.3740].
- [41] P. C. Argyres and N. Seiberg, *S -duality in $N=2$ supersymmetric gauge theories*, *JHEP* **0712** (2007) 088, [0711.0054].
- [42] G. 't Hooft, *On the Phase Transition Towards Permanent Quark Confinement*, *Nucl.Phys.* **B138** (1978) 1.

- [43] J. M. Maldacena, *Wilson loops in large N field theories*, *Phys. Rev. Lett.* **80** (1998) 4859–4862, [[hep-th/9803002](#)].
- [44] A. Kapustin, *Wilson- 't Hooft operators in four-dimensional gauge theories and S-duality*, *Phys.Rev.* **D74** (2006) 025005, [[hep-th/0501015](#)].
- [45] A. Kapustin and E. Witten, *Electric-Magnetic Duality And The Geometric Langlands Program*, *Commun.Num.Theor.Phys.* **1** (2007) 1–236, [[hep-th/0604151](#)].
- [46] J. Gomis, T. Okuda, and V. Pestun, *Exact Results for 't Hooft Loops in Gauge Theories on S^4* , *JHEP* **1205** (2012) 141, [[1105.2568](#)].
- [47] T. Dimofte, D. Gaiotto, and S. Gukov, *3-Manifolds and 3D Indices*, [1112.5179](#).
- [48] D. Gang, E. Koh, and K. Lee, *Line Operator Index on $S^1 \times S^3$* , *JHEP* **1205** (2012) 007, [[1201.5539](#)].
- [49] Y. Ito, T. Okuda, and M. Taki, *Line operators on $S^1 \times R^3$ and quantization of the Hitchin moduli space*, *JHEP* **1204** (2012) 010, [[1111.4221](#)].
- [50] S. Gukov and E. Witten, *Gauge Theory, Ramification, And The Geometric Langlands Program*, [hep-th/0612073](#).
- [51] S. Gukov and E. Witten, *Rigid Surface Operators*, *Adv.Theor.Math.Phys.* **14** (2010) [0804.1561].
- [52] Y. Nakayama, *4D and 2D superconformal index with surface operator*, *JHEP* **08** (2011) 084, [[1105.4883](#)].
- [53] D. Gaiotto, *Surface Operators in $N = 2$ 4d Gauge Theories*, *JHEP* **1211** (2012) 090, [[0911.1316](#)].
- [54] N. Doroud, J. Gomis, B. Le Floch, and S. Lee, *Exact Results in $D=2$ Supersymmetric Gauge Theories*, *JHEP* **05** (2013) 093, [[1206.2606](#)].
- [55] A. Gadde and S. Gukov, *2d Index and Surface operators*, *JHEP* **03** (2014) 080, [[1305.0266](#)].
- [56] S. Gukov, *Surface Operators*, [1412.7127](#).
- [57] J. Polchinski, *Introduction to cosmic F- and D-strings*, in *String theory: From gauge interactions to cosmology. Proceedings, NATO Advanced Study Institute, Cargese, France, June 7-19, 2004*, pp. 229–253, 2004. [hep-th/0412244](#).
- [58] L. F. Alday and Y. Tachikawa, *Affine $SL(2)$ conformal blocks from 4d gauge theories*, *Lett. Math. Phys.* **94** (2010) 87–114, [[1005.4469](#)].

- [59] C. Kozcaz, S. Pasquetti, F. Passerini, and N. Wyllard, *Affine $sl(N)$ conformal blocks from $N=2$ $SU(N)$ gauge theories*, *JHEP* **01** (2011) 045, [1008.1412].
- [60] Y. Tachikawa, *On W -algebras and the symmetries of defects of 6d $N=(2,0)$ theory*, *JHEP* **03** (2011) 043, [1102.0076].
- [61] E. Frenkel, S. Gukov, and J. Teschner, *Surface Operators and Separation of Variables*, *JHEP* **01** (2016) 179, [1506.07508].
- [62] D. Xie, *Higher laminations, webs and $N=2$ line operators*, 1304.2390.
- [63] D. Xie, *Aspects of line operators of class S theories*, 1312.3371.
- [64] I. Coman, M. Gabella, and J. Teschner, *Line operators in theories of class S , quantized moduli space of flat connections, and Toda field theory*, *JHEP* **10** (2015) 143, [1505.05898].
- [65] E. P. Verlinde, *Fusion Rules and Modular Transformations in 2D Conformal Field Theory*, *Nucl.Phys.* **B300** (1988) 360.
- [66] F. Passerini, *Gauge Theory Wilson Loops and Conformal Toda Field Theory*, *JHEP* **1003** (2010) 125, [1003.1151].
- [67] J. Gomis and B. Le Floch, *'t Hooft Operators in Gauge Theory from Toda CFT*, *JHEP* **1111** (2011) 114, [1008.4139].
- [68] M. Bullimore, *Defect Networks and Supersymmetric Loop Operators*, 1312.5001.
- [69] A. A. Migdal, *Recursion Equations in Gauge Theories*, *Sov. Phys. JETP* **42** (1975) 413. [Zh. Eksp. Teor. Fiz.69,810(1975)].
- [70] E. Witten, *Gauge Theories and Integrable Lattice Models*, *Nucl.Phys.* **B322** (1989) 629.
- [71] E. Witten, *Gauge Theories, Vertex Models and Quantum Groups*, *Nucl. Phys.* **B330** (1990) 285.
- [72] S. Cordes, G. W. Moore, and S. Ramgoolam, *Lectures on 2-d Yang-Mills theory, equivariant cohomology and topological field theories*, *Nucl. Phys. Proc. Suppl.* **41** (1995) 184–244, [hep-th/9411210].
- [73] E. Buffenoir and P. Roche, *Two-Dimensional Lattice Gauge Theory Based on a Quantum Group*, *Commun.Math.Phys.* **170** (1995) 669–698, [hep-th/9405126].
- [74] M. Aganagic, H. Ooguri, N. Saulina, and C. Vafa, *Black Holes, Q -Deformed 2D Yang-Mills, and Non-Perturbative Topological Strings*, *Nucl.Phys.* **B715** (2005) 304–348, [hep-th/0411280].

- [75] Y. Tachikawa and N. Watanabe, *On skein relations in class S theories*, *JHEP* **06** (2015) 186, [1504.00121].
- [76] J. Gomis and B. Le Floch, *M2-brane surface operators and gauge theory dualities in Toda*, 1407.1852.
- [77] D. Gaiotto, L. Rastelli, and S. S. Razamat, *Bootstrapping the superconformal index with surface defects*, *JHEP* **01** (2013) 022, [1207.3577].
- [78] L. F. Alday, M. Bullimore, M. Fluder, and L. Hollands, *Surface Defects, the Superconformal Index and Q-Deformed Yang-Mills*, *JHEP* **1310** (2013) 018, [1303.4460].
- [79] M. Bullimore, M. Fluder, L. Hollands, and P. Richmond, *The superconformal index and an elliptic algebra of surface defects*, *JHEP* **10** (2014) 62, [1401.3379].
- [80] L. F. Alday, M. Bullimore, and M. Fluder, *On S-duality of the Superconformal Index on Lens Spaces and 2d TQFT*, *JHEP* **05** (2013) 122, [1301.7486].
- [81] S. S. Razamat and M. Yamazaki, *S-duality and the N=2 Lens Space Index*, *JHEP* **10** (2013) 048, [1306.1543].
- [82] D. Gaiotto, G. W. Moore, and A. Neitzke, *Wall-Crossing in Coupled 2d-4d Systems*, 1103.2598.
- [83] D. Gaiotto, G. W. Moore, and A. Neitzke, *Framed BPS States*, 1006.0146.
- [84] E. Witten, *Quantum Field Theory and the Jones Polynomial*, *Commun. Math. Phys.* **121** (1989) 351–399.
- [85] E. Witten, *Quantization of Chern-Simons Gauge Theory With Complex Gauge Group*, *Commun. Math. Phys.* **137** (1991) 29–66.
- [86] J.-F. Wu and Y. Zhou, *From Liouville to Chern-Simons, Alternative Realization of Wilson Loop Operators in AGT Duality*, 0911.1922.
- [87] D. Gaiotto, *Open Verlinde line operators*, 1404.0332.
- [88] S. de Haro, *Chern-Simons theory, 2d Yang-Mills, and Lie algebra wanderers*, *Nucl. Phys.* **B730** (2005) 312–351, [hep-th/0412110].
- [89] R. J. Szabo and M. Tierz, *q-deformations of two-dimensional Yang-Mills theory: Classification, categorification and refinement*, *Nucl. Phys.* **B876** (2013) 234–308, [1305.1580].
- [90] N. Watanabe, *Wilson punctured network defects in 2D q-deformed Yang-Mills theory*, *JHEP* **12** (2016) 063, [1603.02939].

- [91] N. Watanabe, *Schur indices with class S line operators from networks and further skein relations*, 1701.04090.
- [92] N. Drukker, T. Okuda, and F. Passerini, *Exact results for vortex loop operators in 3d supersymmetric theories*, *JHEP* **07** (2014) 137, [1211.3409].
- [93] H.-C. Kim, *Line defects and 5d instanton partition functions*, *JHEP* **03** (2016) 199, [1601.06841].
- [94] D. Gaiotto and E. Witten, *Supersymmetric Boundary Conditions in $N=4$ Super Yang-Mills Theory*, *J.Statist.Phys.* **135** (2009) 789–855, [0804.2902].
- [95] D. Gaiotto and E. Witten, *S -Duality of Boundary Conditions In $N=4$ Super Yang-Mills Theory*, *Adv. Theor. Math. Phys.* **13** (2009) 721, [0807.3720].
- [96] K. Hosomichi, S. Lee, and J. Park, *AGT on the S -duality Wall*, *JHEP* **12** (2010) 079, [1009.0340].
- [97] S. Gukov and A. Kapustin, *Topological Quantum Field Theory, Nonlocal Operators, and Gapped Phases of Gauge Theories*, 1307.4793.
- [98] A. Kapustin and N. Seiberg, *Coupling a QFT to a TQFT and Duality*, *JHEP* **04** (2014) 001, [1401.0740].
- [99] J. Gomis and F. Passerini, *Holographic Wilson Loops*, *JHEP* **08** (2006) 074, [hep-th/0604007].
- [100] J. Gomis and F. Passerini, *Wilson Loops as $D3$ -Branes*, *JHEP* **01** (2007) 097, [hep-th/0612022].
- [101] D. Gaiotto, S. Gukov, and N. Seiberg, *Surface Defects and Resolvents*, *JHEP* **09** (2013) 070, [1307.2578].
- [102] Y. Ito and Y. Yoshida, *Superconformal index with surface defects for class S_k* , 1606.01653.
- [103] J. Gomis, B. Le Floch, Y. Pan, and W. Peelaers, *Intersecting Surface Defects and Two-Dimensional CFT*, 1610.03501.
- [104] B. Assel and J. Gomis, *Mirror Symmetry And Loop Operators*, *JHEP* **11** (2015) 055, [1506.01718].
- [105] D. Gaiotto and H.-C. Kim, *Surface defects and instanton partition functions*, *JHEP* **10** (2016) 012, [1412.2781].
- [106] M. Bullimore, H.-C. Kim, and P. Koroteev, *Defects and Quantum Seiberg-Witten Geometry*, *JHEP* **05** (2015) 095, [1412.6081].

- [107] F. Nieri, S. Pasquetti, and F. Passerini, *3d and 5d Gauge Theory Partition Functions as q -deformed CFT Correlators*, *Lett. Math. Phys.* **105** (2015), no. 1 109–148, [1303.2626].
- [108] M. Bullimore and H.-C. Kim, *The Superconformal Index of the $(2,0)$ Theory with Defects*, *JHEP* **05** (2015) 048, [1412.3872].
- [109] A. Hanany and K. Hori, *Branes and $N=2$ theories in two-dimensions*, *Nucl. Phys.* **B513** (1998) 119–174, [hep-th/9707192].
- [110] J. L. Cardy, *Boundary conformal field theory*, hep-th/0411189.
- [111] V. B. Petkova and J. B. Zuber, *Generalized twisted partition functions*, *Phys. Lett.* **B504** (2001) 157–164, [hep-th/0011021].
- [112] M. Billò, V. Gonçalves, E. Lauria, and M. Meineri, *Defects in conformal field theory*, *JHEP* **04** (2016) 091, [1601.02883].
- [113] A. Gadde, *Conformal constraints on defects*, 1602.06354.
- [114] J. Erickson, G. Semenoff, and K. Zarembo, *Wilson loops in $N=4$ supersymmetric Yang-Mills theory*, *Nucl.Phys.* **B582** (2000) 155–175, [hep-th/0003055].
- [115] O. Aharony, N. Seiberg, and Y. Tachikawa, *Reading between the lines of four-dimensional gauge theories*, *JHEP* **08** (2013) 115, [1305.0318].
- [116] P. Goddard, J. Nuyts, and D. I. Olive, *Gauge Theories and Magnetic Charge*, *Nucl.Phys.* **B125** (1977) 1.
- [117] K. Zarembo, *Supersymmetric Wilson loops*, *Nucl.Phys.* **B643** (2002) 157–171, [hep-th/0205160].
- [118] E. Witten, *On S duality in Abelian gauge theory*, *Selecta Math.* **1** (1995) 383, [hep-th/9505186].
- [119] M. Henningson, *Wilson-’t Hooft operators and the theta angle*, *JHEP* **0605** (2006) 065, [hep-th/0603188].
- [120] D. Nanopoulos and D. Xie, *$N=2$ SU Quiver with USP Ends or SU Ends with Antisymmetric Matter*, *JHEP* **08** (2009) 108, [0907.1651].
- [121] O. Chacaltana, J. Distler, and Y. Tachikawa, *Gaiotto duality for the twisted A_{2N-1} series*, *JHEP* **05** (2015) 075, [1212.3952].
- [122] N. Seiberg and E. Witten, *Gauge dynamics and compactification to three-dimensions*, hep-th/9607163.
- [123] K. A. Intriligator and N. Seiberg, *Mirror symmetry in three-dimensional gauge theories*, *Phys.Lett.* **B387** (1996) 513–519, [hep-th/9607207].

- [124] F. Benini, Y. Tachikawa, and D. Xie, *Mirrors of 3d Sicilian theories*, *JHEP* **1009** (2010) 063, [1007.0992].
- [125] O. Chacaltana, J. Distler, and Y. Tachikawa, *Nilpotent orbits and codimension-two defects of 6d $N=(2,0)$ theories*, *Int.J.Mod.Phys.* **A28** (2013) 1340006, [1203.2930].
- [126] J. Polchinski, *String theory*, vol. 1, 2 of *Cambridge Monographs on Mathematical Physics*. Cambridge University Press, 1998.
- [127] N. Hitchin, *The self-duality equations on a riemann surface*, *Proc.London Math.Soc.(3)* **55** (1987), no. 1 59–126.
- [128] T. Kawano and N. Matsumiya, *5D SYM on 3D Sphere and 2D YM*, *Phys. Lett.* **B716** (2012) 450–453, [1206.5966].
- [129] Y. Fukuda, T. Kawano, and N. Matsumiya, *5D SYM and 2D q -Deformed YM*, *Nucl. Phys.* **B869** (2013) 493–522, [1210.2855].
- [130] C. Closset, T. T. Dumitrescu, G. Festuccia, and Z. Komargodski, *The Geometry of Supersymmetric Partition Functions*, *JHEP* **01** (2014) 124, [1309.5876].
- [131] D. Nanopoulos and D. Xie, *Hitchin Equation, Singularity, and $N=2$ Superconformal Field Theories*, *JHEP* **1003** (2010) 043, [0911.1990].
- [132] A. Kapustin and S. Sethi, *The Higgs branch of impurity theories*, *Adv. Theor. Math. Phys.* **2** (1998) 571–591, [hep-th/9804027].
- [133] E. Corrigan and P. Goddard, *Construction of instanton and monopole solutions and reciprocity*, *Annals of Physics* **154** (Apr., 1984) 253–279.
- [134] N. J. Hitchin, A. Karlhede, U. Lindstrom, and M. Rocek, *Hyperkahler Metrics and Supersymmetry*, *Commun. Math. Phys.* **108** (1987) 535.
- [135] D. Collingwood and W. McGovern, *Nilpotent Orbits In Semisimple Lie Algebra: An Introduction*. Mathematics series. Taylor & Francis, 1993.
- [136] P. B. Kronheimer, *A hyper-Kählerian structure on coadjoint orbits of a semisimple complex group*, *J. London Math. Soc. (2)* **42** (1990), no. 2 193–208.
- [137] O. Chacaltana and J. Distler, *Tinkertoys for Gaiotto Duality*, *JHEP* **1011** (2010) 099, [1008.5203].
- [138] A. Gadde, S. S. Razamat, and B. Willett, *“Lagrangian” for a Non-Lagrangian Field Theory with $\mathcal{N} = 2$ Supersymmetry*, *Phys. Rev. Lett.* **115** (2015), no. 17 171604, [1505.05834].
- [139] F. Benini, Y. Tachikawa, and B. Wecht, *Sicilian gauge theories and $N=1$ dualities*, *JHEP* **01** (2010) 088, [0909.1327].

- [140] C. Beem, M. Lemos, P. Liendo, W. Peelaers, L. Rastelli, and B. C. van Rees, *Infinite Chiral Symmetry in Four Dimensions*, *Commun. Math. Phys.* **336** (2015), no. 3 1359–1433, [1312.5344].
- [141] D. Anselmi, J. Erlich, D. Z. Freedman, and A. A. Johansen, *Positivity constraints on anomalies in supersymmetric gauge theories*, *Phys. Rev.* **D57** (1998) 7570–7588, [hep-th/9711035].
- [142] Y. Tachikawa, *A review of the T_N theory and its cousins*, *PTEP* **2015** (2015), no. 11 11B102, [1504.01481].
- [143] J. A. de Azcárraga and J. M. Izquierdo, *Lie Groups, Lie Algebras, Cohomology and Some Applications in Physics*, vol. 1 of *Series on Cambridge Monographs on Mathematical Physics*. Cambridge University Press, 1998.
- [144] E. Witten, *An $SU(2)$ anomaly*, *Physics Letters B* **117** (Nov., 1982) 324–328.
- [145] D. Gaiotto, A. Neitzke, and Y. Tachikawa, *Argyres-Seiberg duality and the Higgs branch*, *Commun. Math. Phys.* **294** (2010) 389–410, [0810.4541].
- [146] F. Benini, S. Benvenuti, and Y. Tachikawa, *Webs of five-branes and $N=2$ superconformal field theories*, *JHEP* **0909** (2009) 052, [0906.0359].
- [147] J. A. Minahan and D. Nemeschansky, *An $N=2$ superconformal fixed point with $E(6)$ global symmetry*, *Nucl.Phys.* **B482** (1996) 142–152, [hep-th/9608047].
- [148] M. R. Gaberdiel and B. Zwiebach, *Exceptional groups from open strings*, *Nucl. Phys.* **B518** (1998) 151–172, [hep-th/9709013].
- [149] D. Gaiotto, G. W. Moore, and Y. Tachikawa, *On 6d $\mathcal{N}=(2,0)$ theory compactified on a Riemann surface with finite area*, *PTEP* **2013** (2013) 013B03, [1110.2657].
- [150] S. Cecotti, J. Song, C. Vafa, and W. Yan, *Superconformal Index, BPS Monodromy and Chiral Algebras*, 1511.01516.
- [151] C. Cordova, D. Gaiotto, and S.-H. Shao, *Infrared Computations of Defect Schur Indices*, *JHEP* **11** (2016) 106, [1606.08429].
- [152] D. Cassani and D. Martelli, *Supersymmetry on curved spaces and superconformal anomalies*, *JHEP* **10** (2013) 025, [1307.6567].
- [153] B. Assel, D. Cassani, and D. Martelli, *Localization on Hopf surfaces*, *JHEP* **08** (2014) 123, [1405.5144].
- [154] B. Assel, D. Cassani, L. Di Pietro, Z. Komargodski, J. Lorenzen, and D. Martelli, *The Casimir Energy in Curved Space and its Supersymmetric Counterpart*, *JHEP* **07** (2015) 043, [1503.05537].

- [155] N. Bobev, M. Bullimore, and H.-C. Kim, *Supersymmetric Casimir Energy and the Anomaly Polynomial*, *JHEP* **09** (2015) 142, [1507.08553].
- [156] M. Sugiura, *Conjugate classes of Cartan subalgebras in real semi-simple Lie algebras*, *J. Math. Soc. Japan* **11** (1959) 374–434.
- [157] D. Green, Z. Komargodski, N. Seiberg, Y. Tachikawa, and B. Wecht, *Exactly Marginal Deformations and Global Symmetries*, *JHEP* **06** (2010) 106, [1005.3546].
- [158] S. Gukov, D. Pei, W. Yan, and K. Ye, *Equivariant Verlinde algebra from superconformal index and Argyres-Seiberg duality*, 1605.06528.
- [159] F. A. Dolan and H. Osborn, *On short and semi-short representations for four-dimensional superconformal symmetry*, *Annals Phys.* **307** (2003) 41–89, [hep-th/0209056].
- [160] D. Gaiotto and S. S. Razamat, *Exceptional Indices*, *JHEP* **05** (2012) 145, [1203.5517].
- [161] O. Aharony, J. Marsano, S. Minwalla, K. Papadodimas, and M. Van Raamsdonk, *The Hagedorn - deconfinement phase transition in weakly coupled large N gauge theories*, *Adv. Theor. Math. Phys.* **8** (2004) 603–696, [hep-th/0310285]. [161(2003)].
- [162] M. Lemos, W. Peelaers, and L. Rastelli, *The superconformal index of class S theories of type D* , *JHEP* **05** (2014) 120, [1212.1271].
- [163] A. Gadde, L. Rastelli, S. S. Razamat, and W. Yan, *The Superconformal Index of the E_6 SCFT*, *JHEP* **08** (2010) 107, [1003.4244].
- [164] A. Y. Alekseev, H. Grosse, and V. Schomerus, *Combinatorial Quantization of the Hamiltonian Chern-Simons Theory*, *Commun.Math.Phys.* **172** (1995) 317–358, [hep-th/9403066].
- [165] S. de Haro, *A Note on knot invariants and q -deformed 2-D Yang-Mills*, *Phys. Lett.* **B634** (2006) 78–83, [hep-th/0509167].
- [166] D. Gaiotto, A. Kapustin, N. Seiberg, and B. Willett, *Generalized Global Symmetries*, *JHEP* **02** (2015) 172, [1412.5148].
- [167] G. Kuperberg, *Spiders for rank 2 Lie algebras*, *Comm. Math. Phys.* **180** (1996), no. 1 109–151, [q-alg/9712003].
- [168] H. Murakami, T. Ohtsuki, and S. Yamada, *Homfly polynomial via an invariant of colored plane graphs*, *Enseign. Math. (2)* **44** (1998), no. 3-4 325–360.

- [169] C. Gómez, M. Ruiz-Altaba, and G. Sierra, *Quantum groups in two-dimensional physics*. Cambridge Monographs on Mathematical Physics. Cambridge University Press, Cambridge, 1996.
- [170] T. Dimofte, D. Gaiotto, and S. Gukov, *Gauge Theories Labelled by Three-Manifolds*, *Commun. Math. Phys.* **325** (2014) 367–419, [1108.4389].
- [171] T. Okuda, *Line Operators in Supersymmetric Gauge Theories and the 2D-4D Relation*, 1412.7126.
- [172] S. Gukov, *Surface Operators*, 1412.7127.
- [173] M.-J. Jeong and D. Kim, *The quantum $sl(n, \mathbb{C})$ representation theory and its applications*, *J. Korean Math. Soc.* **49** (2012), no. 5 993–1015, [math/0506403].
- [174] S. Cautis, J. Kamnitzer, and S. Morrison, *Webs and quantum skew Howe duality*, *Math. Ann.* **360** (2014), no. 1-2 351–390, [1210.6437].
- [175] A. Chirvasitu and M. Tucker-Simmons, *Remarks on quantum symmetric algebras*, *Journal of Algebra* **397** (2014) 589 – 608, [1206.1614].
- [176] Y. Tachikawa, *On the 6d origin of discrete additional data of 4d gauge theories*, *JHEP* **05** (2014) 020, [1309.0697].
- [177] I. H. Kauffman, *Knots and Physics*, vol. 1 of *Series on Knots and Everything*. World Scientific, 1991.
- [178] G. E. Andrews, R. J. Baxter, and P. J. Forrester, *Eight-vertex SOS model and generalized Rogers-Ramanujan-type identities*, *J.Stat.Phys.* **35** (1984) 193–266.
- [179] P. Di Francesco and J. B. Zuber, *$SU(N)$ Lattice Integrable Models Associated With Graphs*, *Nucl. Phys.* **B338** (1990) 602–646.
- [180] V. Pasquier, *Two-dimensional critical systems labelled by Dynkin diagrams*, *Nucl. Phys.* **B285** (1987) 162–172.
- [181] K. Costello, *Integrable lattice models from four-dimensional field theories*, *Proc. Symp. Pure Math.* **88** (2014) 3–24, [1308.0370].
- [182] N. Saulina, *A Note on Wilson-’t Hooft Operators*, *Nucl.Phys.* **B857** (2012) 153–171, [1110.3354].
- [183] R. Moraru and N. Saulina, *OPE of Wilson-’t Hooft operators in $N=4$ and $N=2$ SYM with gauge group $G=PSU(3)$* , 1206.6896.
- [184] A. Hanany and K. D. Kennaway, *Dimer Models and Toric Diagrams*, hep-th/0503149.

- [185] S. Franco, A. Hanany, K. D. Kennaway, D. Vegh, and B. Wecht, *Brane Dimers and Quiver Gauge Theories*, *JHEP* **01** (2006) 096, [hep-th/0504110].
- [186] A. Hanany, D. Orlando, and S. Reffert, *Sublattice Counting and Orbifolds*, *JHEP* **1006** (2010) 051, [1002.2981].
- [187] A. Neitzke, *Hitchin Systems in $\mathcal{N} = 2$ Field Theory*, in *New Dualities of Supersymmetric Gauge Theories* (J. Teschner, ed.), pp. 53–77. 2016. 1412.7120.
- [188] C. Córdova and A. Neitzke, *Line Defects, Tropicalization, and Multi-Centered Quiver Quantum Mechanics*, *JHEP* **09** (2014) 099, [1308.6829].
- [189] K. Hori and M. Romo, *Exact Results In Two-Dimensional (2,2) Supersymmetric Gauge Theories With Boundary*, 1308.2438.
- [190] D. Honda and T. Okuda, *Exact results for boundaries and domain walls in 2d supersymmetric theories*, *JHEP* **09** (2015) 140, [1308.2217].
- [191] S. Sugishita and S. Terashima, *Exact Results in Supersymmetric Field Theories on Manifolds with Boundaries*, *JHEP* **11** (2013) 021, [1308.1973].
- [192] D. Gang, N. Kim, M. Romo, and M. Yamazaki, *Aspects of Defects in 3d-3d Correspondence*, 1510.05011.
- [193] S. Chun, S. Gukov, and D. Rognenkamp, *Junctions of surface operators and categorification of quantum groups*, 1507.06318.
- [194] J. Bourdier, N. Drukker, and J. Felix, *The exact Schur index of $\mathcal{N} = 4$ SYM*, *JHEP* **11** (2015) 210, [1507.08659].
- [195] M. Gabella, *Quantum Holonomies from Spectral Networks and Framed BPS States*, 1603.05258.
- [196] J. Teschner, *Supersymmetric gauge theories, quantisation of moduli spaces of flat connections, and Liouville theory*, 1412.7140.
- [197] J. Teschner and G. S. Vartanov, *Supersymmetric gauge theories, quantization of $\mathcal{M}_{\text{flat}}$, and conformal field theory*, *Adv. Theor. Math. Phys.* **19** (2015) 1–135, [1302.3778].
- [198] M. Lemos, W. Peelaers, and L. Rastelli, *The superconformal index of class S theories of type D*, *JHEP* **05** (2014) 120, [1212.1271].
- [199] O. Chacaltana, J. Distler, and A. Trimm, *Tinkertoys for the Z_3 -twisted D_4 Theory*, 1601.02077.
- [200] L. Frappat, P. Sorba, and A. Sciarrino, *Dictionary on Lie superalgebras*, hep-th/9607161.

- [201] A. A. Belavin, A. M. Polyakov, and A. B. Zamolodchikov, *Infinite Conformal Symmetry in Two-Dimensional Quantum Field Theory*, *Nucl. Phys.* **B241** (1984) 333–380.
- [202] R. Baston and M. Eastwood, *The Penrose Transform: Its Interaction with Representation Theory*. Dover Books on Mathematics. Dover Publications, 2016.
- [203] H. Wang, *Closed manifolds with homogeneous complex structure*, *Ann.J.Math.* **76** (1956) 1 – 32.
- [204] J. Teschner, *From Liouville theory to the quantum geometry of Riemann surfaces*, [hep-th/0308031](#).
- [205] Y. Tachikawa, *Six-dimensional $D(N)$ theory and four-dimensional SO - USp quivers*, *JHEP* **0907** (2009) 067, [[0905.4074](#)].
- [206] P. C. Argyres, M. R. Plesser, and A. D. Shapere, *The Coulomb phase of $N=2$ supersymmetric QCD*, *Phys.Rev.Lett.* **75** (1995) 1699–1702, [[hep-th/9505100](#)].
- [207] M. Henningson and P. Yi, *Four-dimensional BPS spectra via M theory*, *Phys.Rev.* **D57** (1998) 1291–1298, [[hep-th/9707251](#)].
- [208] A. Fayyazuddin and M. Spaliński, *The Seiberg-Witten differential from M theory*, *Nucl.Phys.* **B508** (1997) 219–228, [[hep-th/9706087](#)].
- [209] T. Nakatsu, K. Ohta, T. Yokono, and Y. Yoshida, *A Proof of brane creation via M theory*, *Mod.Phys.Lett.* **A13** (1998) 293–302, [[hep-th/9711117](#)].
- [210] D. Nanopoulos and D. Xie, *Hitchin Equation, Irregular Singularity, and $N = 2$ Asymptotical Free Theories*, [1005.1350](#).
- [211] N. Drukker and F. Passerini, *(de)Tails of Toda CFT*, *JHEP* **1104** (2011) 106, [[1012.1352](#)].
- [212] Y. Tachikawa, *On W -algebras and the symmetries of defects of 6d $N=(2,0)$ theory*, *JHEP* **1103** (2011) 043, [[1102.0076](#)].